

NIST NCSTAR 1-5F

Federal Building and Fire Safety Investigation of the
World Trade Center Disaster

Computer Simulation of the Fires in the World Trade Center Towers

Kevin B. McGrattan

Charles Bouldin

Glenn P. Forney

NIST NCSTAR 1-5F

Federal Building and Fire Safety Investigation of the World Trade Center Disaster

Computer Simulation of the Fires in the World Trade Center Towers

Kevin B. McGrattan
Charles Bouldin
Glenn P. Forney
*Building and Fire Research Laboratory
National Institute of Standards and Technology*

September 2005



U.S. Department of Commerce
Carlos M. Gutierrez, Secretary

Technology Administration
Michelle O'Neill, Acting Under Secretary for Technology

National Institute of Standards and Technology
William Jeffrey, Director

Disclaimer No. 1

Certain commercial entities, equipment, products, or materials are identified in this document in order to describe a procedure or concept adequately or to trace the history of the procedures and practices used. Such identification is not intended to imply recommendation, endorsement, or implication that the entities, products, materials, or equipment are necessarily the best available for the purpose. Nor does such identification imply a finding of fault or negligence by the National Institute of Standards and Technology.

Disclaimer No. 2

The policy of NIST is to use the International System of Units (metric units) in all publications. In this document, however, units are presented in metric units or the inch-pound system, whichever is prevalent in the discipline.

Disclaimer No. 3

Pursuant to section 7 of the National Construction Safety Team Act, the NIST Director has determined that certain evidence received by NIST in the course of this investigation is "voluntarily provided safety-related information" that is "not directly related to the building failure being investigated" and that "disclosure of that information would inhibit the voluntary provision of that type of information" (15 USC 7306c).

In addition, a substantial portion of the evidence collected by NIST in the course of the investigation has been provided to NIST under nondisclosure agreements.

Disclaimer No. 4

NIST takes no position as to whether the design or construction of a WTC building was compliant with any code since, due to the destruction of the WTC buildings, NIST could not verify the actual (or as-built) construction, the properties and condition of the materials used, or changes to the original construction made over the life of the buildings. In addition, NIST could not verify the interpretations of codes used by applicable authorities in determining compliance when implementing building codes. Where an investigation report states whether a system was designed or installed as required by a code *provision*, NIST has documentary or anecdotal evidence indicating whether the requirement was met, or NIST has independently conducted tests or analyses indicating whether the requirement was met.

Use in Legal Proceedings

No part of any report resulting from a NIST investigation into a structural failure or from an investigation under the National Construction Safety Team Act may be used in any suit or action for damages arising out of any matter mentioned in such report (15 USC 281a; as amended by P.L. 107-231).

**National Institute of Standards and Technology National Construction Safety Team Act Report 1-5F
Natl. Inst. Stand. Technol. Natl. Constr. Sfty. Tm. Act Rpt. 1-5F, 164 pages (September 2005)
CODEN: NSPUE2**

U.S. GOVERNMENT PRINTING OFFICE
WASHINGTON: 2005

For sale by the Superintendent of Documents, U.S. Government Printing Office
Internet: bookstore.gpo.gov — Phone: (202) 512-1800 — Fax: (202) 512-2250
Mail: Stop SSOP, Washington, DC 20402-0001

ABSTRACT

This report presents the results of numerical simulations of the fires in World Trade Center (WTC) 1 and WTC 2 on September 11, 2001. The calculations were performed with the National Institute of Standards and Technology (NIST) Fire Dynamics Simulator, a computational fluid dynamics model that describes the flow of smoke and hot gases from a fire. Before performing the simulations, the model was validated by comparing its predictions with measurements from a series of large scale fire experiments performed at NIST. The model also was enhanced to better describe the pyrolysis of charring fuels, like wood; and the computer program was re-configured to run on multiple processors. Input data for the simulations of WTC 1 and WTC 2 consisted of descriptions of the properties of typical office furnishings and jet fuel, floor layouts, exterior damage, and interior damage estimates. Results of the simulations were compared with visual observations. Predicted temperatures and gas concentrations were subsequently used to analyze the temperatures within steel trusses and columns.

Keywords: Fire Dynamics Simulator, fire simulation, World Trade Center.

This page intentionally left blank.

TABLE OF CONTENTS

Abstract	iii
List of Figures	ix
List of Tables	xiii
List of Acronyms and Abbreviations	xv
Metric Conversion Table	xvii
Preface	xix
Acknowledgments.....	xxix
Executive Summary	xxxix
Chapter 1	
Introduction	1
1.1 Report Overview	1
1.2 References.....	3
Chapter 2	
Fire Dynamics Simulator.....	5
2.1 Model Description	5
2.1.1 Name and History.....	5
2.1.2 Type of Model.....	5
2.1.3 Model Developers	5
2.1.4 Model Uses.....	6
2.1.5 Model Results.....	6
2.1.6 Relevant Publications	7
2.1.7 Governing Equations, Assumptions, and Numerics.....	8
2.1.8 Limitations of the Model.....	9
2.1.9 Input Data Required to Run the Model	11
2.1.10 Property Data.....	11
2.2 Scenarios for Which FDS Has Been Evaluated.....	11
2.2.1 Description of Scenarios or Phenomenon of Interest	12
2.2.2 List of Quantities Predicted by FDS upon which Evaluation Is Based	12
2.2.3 Degree of Accuracy Required for Each Output Quantity.....	13
2.3 Model Improvements for the WTC Investigation.....	14
2.3.1 Charring Pyrolysis Model.....	14

2.3.2	Parallel Processing	14
2.4	References.....	16
Chapter 3		
Model Accuracy Assessment – Steady Fires		19
3.1	Overview.....	19
3.2	Description of the Experiments	19
3.3	Results.....	21
3.3.1	Comparison of Gas Temperature.....	21
3.3.2	Comparison of Heat Fluxes to Targets	21
3.3.3	Surface Temperatures.....	22
3.3.4	Comparison of Gas Species Concentrations.....	23
3.3.5	Comparison of Inlet and Outlet Velocity	23
3.4	Model Accuracy.....	24
3.5	Model Sensitivity.....	26
3.5.1	Grid Size.....	26
3.5.2	Compartment Geometry	28
3.5.3	Heat Release Rate.....	28
3.5.4	Thermal Radiation.....	29
3.5.5	Wall Materials	29
3.5.6	Smoke Production	29
3.6	Summary.....	30
3.7	References.....	31
Chapter 4		
Model Accuracy Assessment – Workstation Fires		33
4.1	Overview.....	33
4.2	Description of the Workstation Components.....	33
4.3	Description of the Multiple Workstation Simulations	37
4.4	Results and Discussion	39
4.5	Summary.....	42
4.6	References.....	43
Chapter 5		
Model Input Parameters		45
5.1	Overview.....	45
5.2	Parameter Sensitivity Analysis	46

5.3 Numerical Grid	47
5.4 Floor Layouts and Combustible Load.....	49
5.5 Exterior Damage	52
5.6 Interior Damage	53
5.7 Ignition Scenario.....	55
5.8 Summary.....	56
5.9 References.....	58
Chapter 6	
Simulations of the Fires in WTC 1 and WTC 2	59
6.1 Overview.....	59
6.2 Simulation of WTC 1, Case A	61
6.2.1 Floor 92, Case A.....	62
6.2.2 Floor 93, Case A.....	64
6.2.3 Floor 94, Case A.....	66
6.2.4 Floor 95, Case A.....	68
6.2.5 Floor 96, Case A.....	70
6.2.6 Floor 97, Case A.....	72
6.2.7 Floor 98, Case A.....	74
6.2.8 Floor 99, Case A.....	76
6.3 Simulation of WTC 1, Case B	78
6.4 Simulation of WTC 2, Case C	87
6.4.1 Floor 78, Case C.....	88
6.4.2 Floor 79, Case C.....	90
6.4.3 Floor 80, Case C.....	92
6.4.4 Floor 81, Case C.....	94
6.4.5 Floor 82, Case C.....	96
6.4.6 Floor 83, Case C.....	98
6.5 Simulation of WTC 2, Case D	100
6.6 Discussion.....	107
6.6.1 Fire Spread	107
6.6.2 Fire Temperatures.....	109
6.6.3 Global Heat Release Rates	111
6.7 Data Transfer	113
6.8 References.....	113

Chapter 7	
Summary of Technical Results	115
Appendix A	
Floor Plans	117

LIST OF FIGURES

Figure P-1.	The eight projects in the federal building and fire safety investigation of the WTC disaster.	xxi
Figure 3-1.	Centerline gas temperatures in a spray burner test.....	20
Figure 3-2.	Comparison of gas temperatures, Test 5.....	21
Figure 3-3.	Heat fluxes to column and floor, Test 5.....	22
Figure 3-4.	Comparison of ceiling surface and inner temperatures, Test 5.....	23
Figure 3-5.	Comparison of oxygen and carbon dioxide concentrations, Test 5.	23
Figure 3-6.	Comparison of gas velocities at the inlet and outlet, Test 5.....	24
Figure 3-7.	Coarse grid prediction of intake side temperatures for Test 5.	28
Figure 4-1.	Typical office workstation.	35
Figure 4-2.	Single office workstation burning at peak intensity.....	35
Figure 4-3.	Heat release rates for the single workstation fire experiments.....	37
Figure 4-4.	Geometry of the multiple workstation simulations.....	38
Figure 4-5.	Disassembled workstation burned in Test 5.....	38
Figure 4-6.	Multiple workstation fire experiment.	40
Figure 4-7.	Coarse grid simulation of a multiple workstation experiment.	40
Figure 4-8.	Heat release rates for multiple workstation experiments.	41
Figure 4-9.	Upper layer temperatures at 4 locations, Test 1.....	42
Figure 5-1.	Eight floor model of WTC 1.....	48
Figure 5-2.	A work area in the WTC.....	50
Figure 5-3.	Plan view of the 97th floor of WTC 1.	50
Figure 5-4.	Modeled interior layout.....	51
Figure 5-5.	Damage to north face of WTC 1 just after impact.	53
Figure 5-6.	Damage estimates for 96th floor, WTC 1, and 80th floor, WTC 2.....	54
Figure 6-1.	Predicted upper layer temperature 15 min past impact, WTC 1, floor 94.	60
Figure 6-2.	North face of WTC 1 with fires seen just inside northeast corner of floor 92.....	62
Figure 6-3.	Upper layer temperatures of WTC 1, floor 92.....	63
Figure 6-4.	North face of WTC 1 at the onset of collapse.....	64

Figure 6-5. Upper layer temperatures of WTC 1, floor 93..... 65

Figure 6-6. East face of WTC 1 at 8:59 a.m. showing fires on the 94th floor..... 66

Figure 6-7. Upper layer temperatures of WTC 1, floor 94..... 67

Figure 6-8. West face of WTC 1 shortly before collapse..... 68

Figure 6-9. Upper layer temperature of WTC 1, floor 95..... 69

Figure 6-10. West side of south face of WTC 1, 15 min past impact..... 70

Figure 6-11. Upper layer temperature of WTC 1, floor 96..... 71

Figure 6-12. North face of WTC 1 at 8:55 a.m..... 72

Figure 6-13. Upper layer temperatures of WTC 1, floor 97..... 73

Figure 6-14. East face of WTC 1 at 9:55 a.m..... 74

Figure 6-15. Upper layer temperatures of WTC 1, floor 98..... 75

Figure 6-16. South face of WTC 1 burning, with WTC 2 in the foreground..... 76

Figure 6-17. Upper layer temperature of WTC 1, floor 99..... 77

Figure 6-18. Simulation of WTC 1, floor 92, Case B, upper layer temperatures..... 79

Figure 6-19. Simulation of WTC 1, floor 93, Case B, upper layer temperatures..... 80

Figure 6-20. Simulation of WTC 1, floor 94, Case B, upper layer temperatures..... 81

Figure 6-21. Simulation of WTC 1, floor 95, Case B, upper layer temperatures..... 82

Figure 6-22. Simulation of WTC 1, floor 96, Case B, upper layer temperatures..... 83

Figure 6-23. Simulation of WTC 1, floor 97, Case B, upper layer temperatures..... 84

Figure 6-24. Simulation of WTC 1, floor 98, Case B, upper layer temperatures..... 85

Figure 6-25. Simulation of WTC 1, floor 99, Case B, upper layer temperatures..... 86

Figure 6-26. East face of WTC 2 at 9:26 a.m., 23 min after impact..... 88

Figure 6-27. Upper layer temperatures of WTC 2, floor 78..... 89

Figure 6-28. North face of WTC 2, with the fire on the 79th floor shown at center..... 90

Figure 6-29. Upper layer temperatures of WTC 2, floor 79..... 91

Figure 6-30. East side of north face, WTC 2, at 9:58 a.m., just before collapse..... 92

Figure 6-31. Upper layer temperatures of WTC 2, floor 80..... 93

Figure 6-32. Northeast corner of WTC 2..... 94

Figure 6-33. Upper layer temperatures of WTC 2, floor 81..... 95

Figure 6-34. Impact area of south face of WTC 2..... 96

Figure 6-35. Upper layer temperatures of WTC 2, floor 82..... 97

Figure 6-36. North face of WTC 2 at 9:29 a.m., 26 min after impact..... 98

Figure 6-37. Upper layer temperatures of WTC 2, floor 83..... 99

Figure 6-38. Simulation of WTC 2, floor 78, Case D, upper layer temperatures..... 101

Figure 6-39. Simulation of WTC 2, floor 79, Case D, upper layer temperatures..... 102

Figure 6-40. Simulation of WTC 2, floor 80, Case D, upper layer temperatures.....	103
Figure 6-41. Simulation of WTC 2, floor 81, Case D, upper layer temperatures.....	104
Figure 6-42. Simulation of WTC 2, floor 82, Case D, upper layer temperatures.....	105
Figure 6-43. Simulation of WTC 2, floor 83, Case D, upper layer temperatures.....	106
Figure 6-44. Simulated fire movement, floors 94 and 97, WTC 1.....	108
Figure 6-45. Aerial view of the south face of WTC 1 shortly before collapse.....	109
Figure 6-46. Predicted upper layer temperatures at various locations on the 97th floor.....	110
Figure 6-47. Predicted heat release rates for fires in WTC 1 and WTC 2.....	111
Figure 6-48. Energy budget for WTC 1 fire simulation, Case A.....	112

This page intentionally left blank.

LIST OF TABLES

Table P-1.	Federal building and fire safety investigation of the WTC disaster.....	xx
Table P-2.	Public meetings and briefings of the WTC Investigation.	xxiii
Table 5-1.	Parameters for orthogonal design of input parameters.	46
Table 5-2.	Parameter combinations for orthogonal design.....	46
Table 5-3.	Jet fuel distribution, WTC 1.....	56
Table 5-4.	Jet fuel distribution, WTC 2.....	56
Table 5-5.	Summary of major input parameters for FDS fire simulations.....	57

This page intentionally left blank.

LIST OF ACRONYMS AND ABBREVIATIONS

Acronyms

ASTM	ASTM International
BFRL	Building and Fire Research Laboratory
BPS	Building Performance Study
CAD	computer-aided design
CFD	computational fluid dynamics
CPU	central processing unit
DNS	Direct Numerical Simulation
DTAP	dissemination and technical assistance program
FDS	Fire Dynamics Simulator
FEMA	Federal Emergency Management Agency
FFT	Fast Fourier Transform
FSI	Fire-Structure Interface
GCR	Grant/Contract Report
HRR	heat release rate
HVAC	heating, ventilating, and air conditioning
IAFSS	International Association of Fire Safety Science
LES	Large Eddy Simulation
MPI	Message Passing Interface
NFPA	National Fire Protection Association
NIST	National Institute of Standards and Technology
PANYNJ	Port Authority of New York and New Jersey
R&D	research and development
RTE	Radiation Transport Equation
SEAoNY	Structural Engineers Association of New York
SFPE	Society of Fire Protection Engineers
UL	Underwriters Laboratories
USC	United States Code
WTC	World Trade Center

WTC 1	World Trade Center 1 (North Tower)
WTC 2	World Trade Center 2 (South Tower)
WTC 7	World Trade Center 7

Abbreviations

°C	degrees Celsius
µm	micrometer
cm	centimeter
ft	foot
gal	gallon
GW	gigawatt
h	hour
in.	inch
J	joule
K	kelvin
kg	kilogram
kJ	kilojoule
kW	kilowatt
L	liter
lb	pound
m	meter
m ²	square meter
m ³	cubic meter
min	minute
MJ	megajoule
MW	megawatt
s	second
W	watt

METRIC CONVERSION TABLE

To convert from	to	Multiply by
-----------------	----	-------------

AREA AND SECOND MOMENT OF AREA

square foot (ft ²)	square meter (m ²)	9.290 304 E-02
square inch (in. ²)	square meter (m ²)	6.4516 E-04
square inch (in. ²)	square centimeter (cm ²)	6.4516 E+00
square yard (yd ²)	square meter (m ²)	8.361 274 E-01

ENERGY (includes WORK)

kilowatt hour (kW · h)	joule (J)	3.6 E+06
quad (1015 BtuIT)	joule (J)	1.055 056 E+18
therm (U.S.)	joule (J)	1.054 804 E+08
ton of TNT (energy equivalent)	joule (J)	4.184 E+09
watt hour (W · h)	joule (J)	3.6 E+03
watt second (W · s)	joule (J)	1.0 E+00

HEAT FLOW RATE

calorieth per minute (calth/min)	watt (W)	6.973 333 E-02
calorieth per second (calth/s)	watt (W)	4.184 E+00
kilocalorieth per minute (kcalth/min)	watt (W)	6.973 333 E+01
kilocalorieth per second (kcalth/s)	watt (W)	4.184 E+03

LENGTH

foot (ft)	meter (m)	3.048 E-01
inch (in)	meter (m)	2.54 E-02
inch (in.)	centimeter (cm)	2.54 E+00
micron (m)	meter (m)	1.0 E-06
yard (yd)	meter (m)	9.144 E-01

MASS DIVIDED BY LENGTH

pound per foot (lb/ft)	kilogram per meter (kg/m)	1.488 164 E+00
pound per inch (lb/in.)	kilogram per meter (kg/m)	1.785 797 E+01
pound per yard (lb/yd)	kilogram per meter (kg/m)	4.960 546 E-01

To convert from	to	Multiply by
TEMPERATURE		
degree Celsius (°C)	kelvin (K)	$T/K = t/^{\circ}C + 273.15$
degree centigrade	degree Celsius (°C)	$t/^{\circ}C \approx t / \text{deg. cent.}$
degree Fahrenheit (°F)	degree Celsius (°C)	$t/^{\circ}C = (t/^{\circ}F - 32)/1.8$
degree Fahrenheit (°F)	kelvin (K)	$T/K = (t/^{\circ}F + 459.67)/1.8$
kelvin (K)	degree Celsius (°C)	$t/^{\circ}C = T/K - 273.15$
TEMPERATURE INTERVAL		
degree Celsius (°C)	kelvin (K)	1.0 E+00
degree centigrade	degree Celsius (°C)	1.0 E+00
degree Fahrenheit (°F)	degree Celsius (°C)	5.555 556 E-01
degree Fahrenheit (°F)	kelvin (K)	5.555 556 E-01
degree Rankine (°R)	kelvin (K)	5.555 556 E-01
VELOCITY (includes SPEED)		
foot per second (ft/s)	meter per second (m/s)	3.048 E-01
inch per second (in./s)	meter per second (m/s)	2.54 E-02
kilometer per hour (km/h)	meter per second (m/s)	2.777 778 E-01
mile per hour (mi/h)	kilometer per hour (km/h)	1.609 344 E+00
mile per minute (mi/min)	meter per second (m/s)	2.682 24 E+01
VOLUME (includes CAPACITY)		
cubic foot (ft ³)	cubic meter (m ³)	2.831 685 E-02
cubic inch (in. ³)	cubic meter (m ³)	1.638 706 E-05
cubic yard (yd ³)	cubic meter (m ³)	7.645 549 E-01
gallon (U.S.) (gal)	cubic meter (m ³)	3.785 412 E-03
gallon (U.S.) (gal)	liter (L)	3.785 412 E+00
liter (L)	cubic meter (m ³)	1.0 E-03
ounce (U.S. fluid) (fl oz)	cubic meter (m ³)	2.957 353 E-05
ounce (U.S. fluid) (fl oz)	milliliter (mL)	2.957 353 E+01

PREFACE

Genesis of This Investigation

Immediately following the terrorist attack on the World Trade Center (WTC) on September 11, 2001, the Federal Emergency Management Agency (FEMA) and the American Society of Civil Engineers began planning a building performance study of the disaster. The week of October 7, as soon as the rescue and search efforts ceased, the Building Performance Study Team went to the site and began its assessment. This was to be a brief effort, as the study team consisted of experts who largely volunteered their time away from their other professional commitments. The Building Performance Study Team issued its report in May 2002, fulfilling its goal “to determine probable failure mechanisms and to identify areas of future investigation that could lead to practical measures for improving the damage resistance of buildings against such unforeseen events.”

On August 21, 2002, with funding from the U.S. Congress through FEMA, the National Institute of Standards and Technology (NIST) announced its building and fire safety investigation of the WTC disaster. On October 1, 2002, the National Construction Safety Team Act (Public Law 107-231), was signed into law. The NIST WTC Investigation was conducted under the authority of the National Construction Safety Team Act.

The goals of the investigation of the WTC disaster were:

- To investigate the building construction, the materials used, and the technical conditions that contributed to the outcome of the WTC disaster.
- To serve as the basis for:
 - Improvements in the way buildings are designed, constructed, maintained, and used;
 - Improved tools and guidance for industry and safety officials;
 - Recommended revisions to current codes, standards, and practices; and
 - Improved public safety.

The specific objectives were:

1. Determine why and how WTC 1 and WTC 2 collapsed following the initial impacts of the aircraft and why and how WTC 7 collapsed;
2. Determine why the injuries and fatalities were so high or low depending on location, including all technical aspects of fire protection, occupant behavior, evacuation, and emergency response;
3. Determine what procedures and practices were used in the design, construction, operation, and maintenance of WTC 1, 2, and 7; and
4. Identify, as specifically as possible, areas in current building and fire codes, standards, and practices that warrant revision.

NIST is a nonregulatory agency of the U.S. Department of Commerce's Technology Administration. The purpose of NIST investigations is to improve the safety and structural integrity of buildings in the United States, and the focus is on fact finding. NIST investigative teams are authorized to assess building performance and emergency response and evacuation procedures in the wake of any building failure that has resulted in substantial loss of life or that posed significant potential of substantial loss of life. NIST does not have the statutory authority to make findings of fault nor negligence by individuals or organizations. Further, no part of any report resulting from a NIST investigation into a building failure or from an investigation under the National Construction Safety Team Act may be used in any suit or action for damages arising out of any matter mentioned in such report (15 USC 281a, as amended by Public Law 107-231).

Organization of the Investigation

The National Construction Safety Team for this Investigation, appointed by the then NIST Director, Dr. Arden L. Bement, Jr., was led by Dr. S. Shyam Sunder. Dr. William L. Grosshandler served as Associate Lead Investigator, Mr. Stephen A. Cauffman served as Program Manager for Administration, and Mr. Harold E. Nelson served on the team as a private sector expert. The Investigation included eight interdependent projects whose leaders comprised the remainder of the team. A detailed description of each of these eight projects is available at <http://wtc.nist.gov>. The purpose of each project is summarized in Table P-1, and the key interdependencies among the projects are illustrated in Fig. P-1.

Table P-1. Federal building and fire safety investigation of the WTC disaster.

Technical Area and Project Leader	Project Purpose
Analysis of Building and Fire Codes and Practices; Project Leaders: Dr. H. S. Lew and Mr. Richard W. Bukowski	Document and analyze the code provisions, procedures, and practices used in the design, construction, operation, and maintenance of the structural, passive fire protection, and emergency access and evacuation systems of WTC 1, 2, and 7.
Baseline Structural Performance and Aircraft Impact Damage Analysis; Project Leader: Dr. Fahim H. Sadek	Analyze the baseline performance of WTC 1 and WTC 2 under design, service, and abnormal loads, and aircraft impact damage on the structural, fire protection, and egress systems.
Mechanical and Metallurgical Analysis of Structural Steel; Project Leader: Dr. Frank W. Gayle	Determine and analyze the mechanical and metallurgical properties and quality of steel, weldments, and connections from steel recovered from WTC 1, 2, and 7.
Investigation of Active Fire Protection Systems; Project Leader: Dr. David D. Evans; Dr. William Grosshandler	Investigate the performance of the active fire protection systems in WTC 1, 2, and 7 and their role in fire control, emergency response, and fate of occupants and responders.
Reconstruction of Thermal and Tenability Environment; Project Leader: Dr. Richard G. Gann	Reconstruct the time-evolving temperature, thermal environment, and smoke movement in WTC 1, 2, and 7 for use in evaluating the structural performance of the buildings and behavior and fate of occupants and responders.
Structural Fire Response and Collapse Analysis; Project Leaders: Dr. John L. Gross and Dr. Therese P. McAllister	Analyze the response of the WTC towers to fires with and without aircraft damage, the response of WTC 7 in fires, the performance of composite steel-trussed floor systems, and determine the most probable structural collapse sequence for WTC 1, 2, and 7.
Occupant Behavior, Egress, and Emergency Communications; Project Leader: Mr. Jason D. Averill	Analyze the behavior and fate of occupants and responders, both those who survived and those who did not, and the performance of the evacuation system.
Emergency Response Technologies and Guidelines; Project Leader: Mr. J. Randall Lawson	Document the activities of the emergency responders from the time of the terrorist attacks on WTC 1 and WTC 2 until the collapse of WTC 7, including practices followed and technologies used.

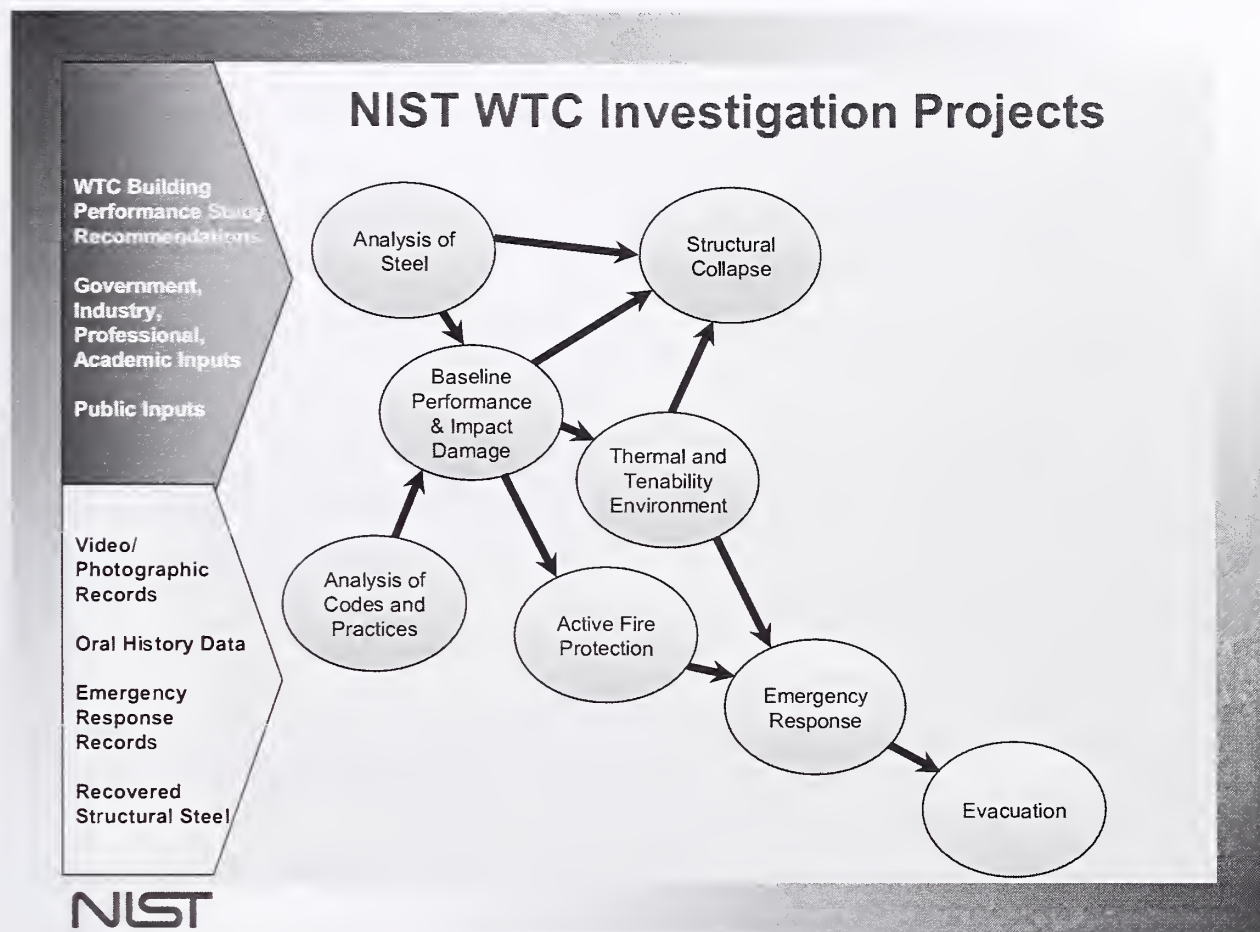


Figure P-1. The eight projects in the federal building and fire safety investigation of the WTC disaster.

National Construction Safety Team Advisory Committee

The NIST Director also established an advisory committee as mandated under the National Construction Safety Team Act. The initial members of the committee were appointed following a public solicitation. These were:

- Paul Fitzgerald, Executive Vice President (retired) FM Global, National Construction Safety Team Advisory Committee Chair
- John Barsom, President, Barsom Consulting, Ltd.
- John Bryan, Professor Emeritus, University of Maryland
- David Collins, President, The Preview Group, Inc.
- Glenn Corbett, Professor, John Jay College of Criminal Justice
- Philip DiNenno, President, Hughes Associates, Inc.

- Robert Hanson, Professor Emeritus, University of Michigan
- Charles Thornton, Co-Chairman and Managing Principal, The Thornton-Tomasetti Group, Inc.
- Kathleen Tierney, Director, Natural Hazards Research and Applications Information Center, University of Colorado at Boulder
- Forman Williams, Director, Center for Energy Research, University of California at San Diego

This National Construction Safety Team Advisory Committee provided technical advice during the Investigation and commentary on drafts of the Investigation reports prior to their public release. NIST has benefited from the work of many people in the preparation of these reports, including the National Construction Safety Team Advisory Committee. The content of the reports and recommendations, however, are solely the responsibility of NIST.

Public Outreach

During the course of this Investigation, NIST held public briefings and meetings (listed in Table P-2) to solicit input from the public, present preliminary findings, and obtain comments on the direction and progress of the Investigation from the public and the Advisory Committee.

NIST maintained a publicly accessible Web site during this Investigation at <http://wtc.nist.gov>. The site contained extensive information on the background and progress of the Investigation.

NIST's WTC Public-Private Response Plan

The collapse of the WTC buildings has led to broad reexamination of how tall buildings are designed, constructed, maintained, and used, especially with regard to major events such as fires, natural disasters, and terrorist attacks. Reflecting the enhanced interest in effecting necessary change, NIST, with support from Congress and the Administration, has put in place a program, the goal of which is to develop and implement the standards, technology, and practices needed for cost-effective improvements to the safety and security of buildings and building occupants, including evacuation, emergency response procedures, and threat mitigation.

The strategy to meet this goal is a three-part NIST-led public-private response program that includes:

- A federal building and fire safety investigation to study the most probable factors that contributed to post-aircraft impact collapse of the WTC towers and the 47-story WTC 7 building, and the associated evacuation and emergency response experience.
- A research and development (R&D) program to (a) facilitate the implementation of recommendations resulting from the WTC Investigation, and (b) provide the technical basis for cost-effective improvements to national building and fire codes, standards, and practices that enhance the safety of buildings, their occupants, and emergency responders.

Table P-2. Public meetings and briefings of the WTC Investigation.

Date	Location	Principal Agenda
June 24, 2002	New York City, NY	Public meeting: Public comments on the <i>Draft Plan</i> for the pending WTC Investigation.
August 21, 2002	Gaithersburg, MD	Media briefing announcing the formal start of the Investigation.
December 9, 2002	Washington, DC	Media briefing on release of the <i>Public Update</i> and NIST request for photographs and videos.
April 8, 2003	New York City, NY	Joint public forum with Columbia University on first-person interviews.
April 29–30, 2003	Gaithersburg, MD	NCST Advisory Committee meeting on plan for and progress on WTC Investigation with a public comment session.
May 7, 2003	New York City, NY	Media briefing on release of <i>May 2003 Progress Report</i> .
August 26–27, 2003	Gaithersburg, MD	NCST Advisory Committee meeting on status of the WTC investigation with a public comment session.
September 17, 2003	New York City, NY	Media and public briefing on initiation of first-person data collection projects.
December 2–3, 2003	Gaithersburg, MD	NCST Advisory Committee meeting on status and initial results and release of the <i>Public Update</i> with a public comment session.
February 12, 2004	New York City, NY	Public meeting on progress and preliminary findings with public comments on issues to be considered in formulating final recommendations.
June 18, 2004	New York City, NY	Media/public briefing on release of <i>June 2004 Progress Report</i> .
June 22–23, 2004	Gaithersburg, MD	NCST Advisory Committee meeting on the status of and preliminary findings from the WTC Investigation with a public comment session.
August 24, 2004	Northbrook, IL	Public viewing of standard fire resistance test of WTC floor system at Underwriters Laboratories, Inc.
October 19–20, 2004	Gaithersburg, MD	NCST Advisory Committee meeting on status and near complete set of preliminary findings with a public comment session.
November 22, 2004	Gaithersburg, MD	NCST Advisory Committee discussion on draft annual report to Congress, a public comment session, and a closed session to discuss pre-draft recommendations for WTC Investigation.
April 5, 2005	New York City, NY	Media and public briefing on release of the probable collapse sequence for the WTC towers and draft reports for the projects on codes and practices, evacuation, and emergency response.
June 23, 2005	New York City, NY	Media and public briefing on release of all draft reports for the WTC towers and draft recommendations for public comment.
September 12–13, 2005	Gaithersburg, MD	NCST Advisory Committee meeting on disposition of public comments and update to draft reports for the WTC towers.
September 13–15, 2005	Gaithersburg, MD	WTC Technical Conference for stakeholders and technical community for dissemination of findings and recommendations and opportunity for public to make technical comments.

- A dissemination and technical assistance program (DTAP) to (a) engage leaders of the construction and building community in ensuring timely adoption and widespread use of proposed changes to practices, standards, and codes resulting from the WTC Investigation and the R&D program, and (b) provide practical guidance and tools to better prepare facility owners, contractors, architects, engineers, emergency responders, and regulatory authorities to respond to future disasters.

The desired outcomes are to make buildings, occupants, and first responders safer in future disaster events.

National Construction Safety Team Reports on the WTC Investigation

A final report on the collapse of the WTC towers is being issued as NIST NCSTAR 1. A companion report on the collapse of WTC 7 is being issued as NIST NCSTAR 1A. The present report is one of a set that provides more detailed documentation of the Investigation findings and the means by which these technical results were achieved. As such, it is part of the archival record of this Investigation. The titles of the full set of Investigation publications are:

NIST (National Institute of Standards and Technology). 2005. *Federal Building and Fire Safety Investigation of the World Trade Center Disaster: Final Report on the Collapse of the World Trade Center Towers*. NIST NCSTAR 1. Gaithersburg, MD, September.

NIST (National Institute of Standards and Technology). 2006. *Federal Building and Fire Safety Investigation of the World Trade Center Disaster: Final Report on the Collapse of World Trade Center 7*. NIST NCSTAR 1A. Gaithersburg, MD.

Lew, H. S., R. W. Bukowski, and N. J. Carino. 2005. *Federal Building and Fire Safety Investigation of the World Trade Center Disaster: Design, Construction, and Maintenance of Structural and Life Safety Systems*. NIST NCSTAR 1-1. National Institute of Standards and Technology. Gaithersburg, MD, September.

Fanella, D. A., A. T. Derecho, and S. K. Ghosh. 2005. *Federal Building and Fire Safety Investigation of the World Trade Center Disaster: Design and Construction of Structural Systems*. NIST NCSTAR 1-1A. National Institute of Standards and Technology. Gaithersburg, MD, September.

Ghosh, S. K., and X. Liang. 2005. *Federal Building and Fire Safety Investigation of the World Trade Center Disaster: Comparison of Building Code Structural Requirements*. NIST NCSTAR 1-1B. National Institute of Standards and Technology. Gaithersburg, MD, September.

Fanella, D. A., A. T. Derecho, and S. K. Ghosh. 2005. *Federal Building and Fire Safety Investigation of the World Trade Center Disaster: Maintenance and Modifications to Structural Systems*. NIST NCSTAR 1-1C. National Institute of Standards and Technology. Gaithersburg, MD, September.

Grill, R. A., and D. A. Johnson. 2005. *Federal Building and Fire Safety Investigation of the World Trade Center Disaster: Fire Protection and Life Safety Provisions Applied to the Design and Construction of World Trade Center 1, 2, and 7 and Post-Construction Provisions Applied after Occupancy*. NIST NCSTAR 1-1D. National Institute of Standards and Technology. Gaithersburg, MD, September.

Razza, J. C., and R. A. Grill. 2005. *Federal Building and Fire Safety Investigation of the World Trade Center Disaster: Comparison of Codes, Standards, and Practices in Use at the Time of the Design and Construction of World Trade Center 1, 2, and 7*. NIST NCSTAR 1-1E. National Institute of Standards and Technology. Gaithersburg, MD, September.

Grill, R. A., D. A. Johnson, and D. A. Fanella. 2005. *Federal Building and Fire Safety Investigation of the World Trade Center Disaster: Comparison of the 1968 and Current (2003) New*

York City Building Code Provisions. NIST NCSTAR 1-1F. National Institute of Standards and Technology. Gaithersburg, MD, September.

Grill, R. A., and D. A. Johnson. 2005. *Federal Building and Fire Safety Investigation of the World Trade Center Disaster: Amendments to the Fire Protection and Life Safety Provisions of the New York City Building Code by Local Laws Adopted While World Trade Center 1, 2, and 7 Were in Use*. NIST NCSTAR 1-1G. National Institute of Standards and Technology. Gaithersburg, MD, September.

Grill, R. A., and D. A. Johnson. 2005. *Federal Building and Fire Safety Investigation of the World Trade Center Disaster: Post-Construction Modifications to Fire Protection and Life Safety Systems of World Trade Center 1 and 2*. NIST NCSTAR 1-1H. National Institute of Standards and Technology. Gaithersburg, MD, September.

Grill, R. A., D. A. Johnson, and D. A. Fanella. 2005. *Federal Building and Fire Safety Investigation of the World Trade Center Disaster: Post-Construction Modifications to Fire Protection, Life Safety, and Structural Systems of World Trade Center 7*. NIST NCSTAR 1-1I. National Institute of Standards and Technology. Gaithersburg, MD, September.

Grill, R. A., and D. A. Johnson. 2005. *Federal Building and Fire Safety Investigation of the World Trade Center Disaster: Design, Installation, and Operation of Fuel System for Emergency Power in World Trade Center 7*. NIST NCSTAR 1-1J. National Institute of Standards and Technology. Gaithersburg, MD, September.

Sadek, F. 2005. *Federal Building and Fire Safety Investigation of the World Trade Center Disaster: Baseline Structural Performance and Aircraft Impact Damage Analysis of the World Trade Center Towers*. NIST NCSTAR 1-2. National Institute of Standards and Technology. Gaithersburg, MD, September.

Faschan, W. J., and R. B. Garlock. 2005. *Federal Building and Fire Safety Investigation of the World Trade Center Disaster: Reference Structural Models and Baseline Performance Analysis of the World Trade Center Towers*. NIST NCSTAR 1-2A. National Institute of Standards and Technology. Gaithersburg, MD, September.

Kirkpatrick, S. W., R. T. Bocchieri, F. Sadek, R. A. MacNeill, S. Holmes, B. D. Peterson, R. W. Cilke, C. Navarro. 2005. *Federal Building and Fire Safety Investigation of the World Trade Center Disaster: Analysis of Aircraft Impacts into the World Trade Center Towers*, NIST NCSTAR 1-2B. National Institute of Standards and Technology. Gaithersburg, MD, September.

Gayle, F. W., R. J. Fields, W. E. Luecke, S. W. Banovic, T. Foecke, C. N. McCowan, T. A. Siewert, and J. D. McColskey. 2005. *Federal Building and Fire Safety Investigation of the World Trade Center Disaster: Mechanical and Metallurgical Analysis of Structural Steel*. NIST NCSTAR 1-3. National Institute of Standards and Technology. Gaithersburg, MD, September.

Luecke, W. E., T. A. Siewert, and F. W. Gayle. 2005. *Federal Building and Fire Safety Investigation of the World Trade Center Disaster: Contemporaneous Structural Steel Specifications*. NIST Special Publication 1-3A. National Institute of Standards and Technology. Gaithersburg, MD, September.

Banovic, S. W. 2005. *Federal Building and Fire Safety Investigation of the World Trade Center Disaster: Steel Inventory and Identification*. NIST NCSTAR 1-3B. National Institute of Standards and Technology. Gaithersburg, MD, September.

Banovic, S. W., and T. Foecke. 2005. *Federal Building and Fire Safety Investigation of the World Trade Center Disaster: Damage and Failure Modes of Structural Steel Components*. NIST NCSTAR 1-3C. National Institute of Standards and Technology. Gaithersburg, MD, September.

Luecke, W. E., J. D. McColskey, C. N. McCowan, S. W. Banovic, R. J. Fields, T. Foecke, T. A. Siewert, and F. W. Gayle. 2005. *Federal Building and Fire Safety Investigation of the World Trade Center Disaster: Mechanical Properties of Structural Steels*. NIST NCSTAR 1-3D. National Institute of Standards and Technology. Gaithersburg, MD, September.

Banovic, S. W., C. N. McCowan, and W. E. Luecke. 2005. *Federal Building and Fire Safety Investigation of the World Trade Center Disaster: Physical Properties of Structural Steels*. NIST NCSTAR 1-3E. National Institute of Standards and Technology. Gaithersburg, MD, September.

Evans, D. D., R. D. Peacock, E. D. Kuligowski, W. S. Dols, and W. L. Grosshandler. 2005. *Federal Building and Fire Safety Investigation of the World Trade Center Disaster: Active Fire Protection Systems*. NIST NCSTAR 1-4. National Institute of Standards and Technology. Gaithersburg, MD, September.

Kuligowski, E. D., D. D. Evans, and R. D. Peacock. 2005. *Federal Building and Fire Safety Investigation of the World Trade Center Disaster: Post-Construction Fires Prior to September 11, 2001*. NIST NCSTAR 1-4A. National Institute of Standards and Technology. Gaithersburg, MD, September.

Hopkins, M., J. Schoenrock, and E. Budnick. 2005. *Federal Building and Fire Safety Investigation of the World Trade Center Disaster: Fire Suppression Systems*. NIST NCSTAR 1-4B. National Institute of Standards and Technology. Gaithersburg, MD, September.

Keough, R. J., and R. A. Grill. 2005. *Federal Building and Fire Safety Investigation of the World Trade Center Disaster: Fire Alarm Systems*. NIST NCSTAR 1-4C. National Institute of Standards and Technology. Gaithersburg, MD, September.

Ferreira, M. J., and S. M. Strege. 2005. *Federal Building and Fire Safety Investigation of the World Trade Center Disaster: Smoke Management Systems*. NIST NCSTAR 1-4D. National Institute of Standards and Technology. Gaithersburg, MD, September.

Gann, R. G., A. Hamins, K. B. McGrattan, G. W. Mulholland, H. E. Nelson, T. J. Ohlemiller, W. M. Pitts, and K. R. Prasad. 2005. *Federal Building and Fire Safety Investigation of the World Trade Center Disaster: Reconstruction of the Fires in the World Trade Center Towers*. NIST NCSTAR 1-5. National Institute of Standards and Technology. Gaithersburg, MD, September.

Pitts, W. M., K. M. Butler, and V. Junker. 2005. *Federal Building and Fire Safety Investigation of the World Trade Center Disaster: Visual Evidence, Damage Estimates, and Timeline Analysis*. NIST NCSTAR 1-5A. National Institute of Standards and Technology. Gaithersburg, MD, September.

Hamins, A., A. Maranghides, K. B. McGrattan, E. Johnsson, T. J. Ohlemiller, M. Donnelly, J. Yang, G. Mulholland, K. R. Prasad, S. Kukuck, R. Anleitner and T. McAllister. 2005. *Federal Building and Fire Safety Investigation of the World Trade Center Disaster: Experiments and Modeling of Structural Steel Elements Exposed to Fire*. NIST NCSTAR 1-5B. National Institute of Standards and Technology. Gaithersburg, MD, September.

Ohlemiller, T. J., G. W. Mulholland, A. Maranghides, J. J. Filliben, and R. G. Gann. 2005. *Federal Building and Fire Safety Investigation of the World Trade Center Disaster: Fire Tests of Single Office Workstations*. NIST NCSTAR 1-5C. National Institute of Standards and Technology. Gaithersburg, MD, September.

Gann, R. G., M. A. Riley, J. M. Repp, A. S. Whittaker, A. M. Reinhorn, and P. A. Hough. 2005. *Federal Building and Fire Safety Investigation of the World Trade Center Disaster: Reaction of Ceiling Tile Systems to Shocks*. NIST NCSTAR 1-5D. National Institute of Standards and Technology. Gaithersburg, MD, September.

Hamins, A., A. Maranghides, K. B. McGrattan, T. J. Ohlemiller, and R. Anleitner. 2005. *Federal Building and Fire Safety Investigation of the World Trade Center Disaster: Experiments and Modeling of Multiple Workstations Burning in a Compartment*. NIST NCSTAR 1-5E. National Institute of Standards and Technology. Gaithersburg, MD, September.

McGrattan, K. B., C. Bouldin, and G. Forney. 2005. *Federal Building and Fire Safety Investigation of the World Trade Center Disaster: Computer Simulation of the Fires in the World Trade Center Towers*. NIST NCSTAR 1-5F. National Institute of Standards and Technology. Gaithersburg, MD, September.

Prasad, K. R., and H. R. Baum. 2005. *Federal Building and Fire Safety Investigation of the World Trade Center Disaster: Fire Structure Interface and Thermal Response of the World Trade Center Towers*. NIST NCSTAR 1-5G. National Institute of Standards and Technology. Gaithersburg, MD, September.

Gross, J. L., and T. McAllister. 2005. *Federal Building and Fire Safety Investigation of the World Trade Center Disaster: Structural Fire Response and Probable Collapse Sequence of the World Trade Center Towers*. NIST NCSTAR 1-6. National Institute of Standards and Technology. Gaithersburg, MD, September.

Carino, N. J., M. A. Starnes, J. L. Gross, J. C. Yang, S. Kukuck, K. R. Prasad, and R. W. Bukowski. 2005. *Federal Building and Fire Safety Investigation of the World Trade Center Disaster: Passive Fire Protection*. NIST NCSTAR 1-6A. National Institute of Standards and Technology. Gaithersburg, MD, September.

Gross, J., F. Hervey, M. Izydorek, J. Mammoser, and J. Treadway. 2005. *Federal Building and Fire Safety Investigation of the World Trade Center Disaster: Fire Resistance Tests of Floor Truss Systems*. NIST NCSTAR 1-6B. National Institute of Standards and Technology. Gaithersburg, MD, September.

Zarghamee, M. S., S. Bolourchi, D. W. Eggers, Ö. O. Erbay, F. W. Kan, Y. Kitane, A. A. Liepins, M. Mudlock, W. I. Naguib, R. P. Ojdrovic, A. T. Sarawit, P. R. Barrett, J. L. Gross, and

T. P. McAllister. 2005. *Federal Building and Fire Safety Investigation of the World Trade Center Disaster: Component, Connection, and Subsystem Structural Analysis*. NIST NCSTAR 1-6C. National Institute of Standards and Technology. Gaithersburg, MD, September.

Zarghamee, M. S., Y. Kitane, Ö. O. Erbay, T. P. McAllister, and J. L. Gross. 2005. *Federal Building and Fire Safety Investigation of the World Trade Center Disaster: Global Structural Analysis of the Response of the World Trade Center Towers to Impact Damage and Fire*. NIST NCSTAR 1-6D. National Institute of Standards and Technology. Gaithersburg, MD, September.

McAllister, T., R. W. Bukowski, R. G. Gann, J. L. Gross, K. B. McGrattan, H. E. Nelson, L. Phan, W. M. Pitts, K. R. Prasad, F. Sadek. 2006. *Federal Building and Fire Safety Investigation of the World Trade Center Disaster: Structural Fire Response and Probable Collapse Sequence of World Trade Center 7*. (Provisional). NIST NCSTAR 1-6E. National Institute of Standards and Technology. Gaithersburg, MD.

Gilsanz, R., V. Arbitrio, C. Anders, D. Chlebus, K. Ezzeldin, W. Guo, P. Moloncy, A. Montalva, J. Oh, K. Rubenacker. 2006. *Federal Building and Fire Safety Investigation of the World Trade Center Disaster: Structural Analysis of the Response of World Trade Center 7 to Debris Damage and Fire*. (Provisional). NIST NCSTAR 1-6F. National Institute of Standards and Technology. Gaithersburg, MD.

Kim, W. 2006. *Federal Building and Fire Safety Investigation of the World Trade Center Disaster: Analysis of September 11, 2001, Seismogram Data*. (Provisional). NIST NCSTAR 1-6G. National Institute of Standards and Technology. Gaithersburg, MD.

Nelson, K. 2006. *Federal Building and Fire Safety Investigation of the World Trade Center Disaster: The Con Ed Substation in World Trade Center 7*. (Provisional). NIST NCSTAR 1-6H. National Institute of Standards and Technology. Gaithersburg, MD.

Averill, J. D., D. S. Mileti, R. D. Peacock, E. D. Kuligowski, N. Groner, G. Proulx, P. A. Reneke, and H. E. Nelson. 2005. *Federal Building and Fire Safety Investigation of the World Trade Center Disaster: Occupant Behavior, Egress, and Emergency Communication*. NIST NCSTAR 1-7. National Institute of Standards and Technology. Gaithersburg, MD, September.

Fahy, R., and G. Proulx. 2005. *Federal Building and Fire Safety Investigation of the World Trade Center Disaster: Analysis of Published Accounts of the World Trade Center Evacuation*. NIST NCSTAR 1-7A. National Institute of Standards and Technology. Gaithersburg, MD, September.

Zmud, J. 2005. *Federal Building and Fire Safety Investigation of the World Trade Center Disaster: Technical Documentation for Survey Administration*. NIST NCSTAR 1-7B. National Institute of Standards and Technology. Gaithersburg, MD, September.

Lawson, J. R., and R. L. Vettori. 2005. *Federal Building and Fire Safety Investigation of the World Trade Center Disaster: The Emergency Response Operations*. NIST NCSTAR 1-8. National Institute of Standards and Technology. Gaithersburg, MD, September.

ACKNOWLEDGMENTS

Special thanks is given to the following individuals for their assistance in the fire modeling effort:

Elisa Baker and Johnathan Demarest of the National Institute of Standards and Technology (NIST) produced computer-aided design files based on floor layouts of World Trade Center (WTC) 1 and WTC 2. They also assisted in producing some of the figures contained in the report.

Jonathan Barnett, a member of the Federal Emergency Management Agency/Building Performance Study Team, provided useful comments about the fire dynamics within the buildings.

James Filliben of NIST assisted in developing an orthogonal design for the selection of appropriate input parameters.

Jason Floyd of Hughes Associates helped to develop the combustion model within the Fire Dynamics Simulator (FDS) and provided a description.

The impact calculations were performed by Applied Research Associates of Albuquerque, New Mexico.

Anthony Hamins, Alexander Maranghides, George Mulholland, and Tom Ohlemiller, all of NIST, conducted the spray burner and workstation experiments that provided input information and validation for FDS.

Simo Hostikka and colleagues at VTT Technical Research Centre of Finland developed and tested the charring model within FDS.

Harold Nelson, consultant, provided information and advice concerning past analyses of WTC 1 and WTC 2.

Bill Pitts of NIST provided floor by floor descriptions of the evolving fires near the exterior façade of WTC 1 and WTC 2 and assisted in the comparison of the simulations with the visual observations.

Kuldeep Prasad and Howard Baum of NIST developed the interface used to transfer output from the FDS into the finite element analysis software, ANSYS. Dr. Prasad also developed the multiblock construct within FDS, paving the way for parallel processing.

Ronald Rehm of NIST performed some initial simulations of the fires and provided early estimates of their heat release rates.

Wayne Schletter, a survivor of WTC 2, provided information about the layout of floors 79 through 82.

Ian Thomas of Victoria University of Australia shared the results of compartment fire experiments that were qualitatively similar to those of the WTC.

This page intentionally left blank.

EXECUTIVE SUMMARY

This report presents the results of numerical simulations of the fires in World Trade Center (WTC) 1 and WTC 2 on September 11, 2001. The calculations were performed with the National Institute of Standards and Technology (NIST) Fire Dynamics Simulator (FDS), a computational fluid dynamics model that describes the flow of smoke and hot gases from a fire. The fire model was second in a chain of four simulations performed in an effort to reconstruct the airplane impact, fire, thermal penetration into the structural members, and collapse.

The fire modeling work consisted of two main parts, model development and fire reconstruction. The model development involved substantial improvement of the numerical algorithm, plus validation against large-scale experiments. To accommodate the very large calculations needed to study fires burning simultaneously over six to eight floors of the towers, the model had to be re-written to allow it to be run on multiple processors. The technique, known as Message Passing Interface, enables FDS to assign different parts of the computational domain to separate computers linked by a high-speed network. Ultimately, calculations using as few as 6 and as many as 48 processors were performed on several different computing clusters at NIST.

The next step in the development process was to validate FDS against large scale fire experiments performed at NIST. The initial series of large scale experiments tested the model's ability to reproduce the thermal environment within a large compartment with a well-controlled, specified fire. Measurements were made of gas and surface temperatures, heat flux, gas concentration, and gas velocity. The experiments also served as a test bed to develop the interface between FDS and the commercial finite element model ANSYS. The latter model was used to predict the temperature of the structural members as a function of time. The transfer of the results from the fire model to the finite element model is referred to as the Fire-Structure Interface.

The next stage in the validation process was to develop the necessary pyrolysis models to describe the burning of wooden and plastic office furniture. The most important improvement was to better describe the pyrolysis of charring fuels, like wood, and the new routine was tested against cone calorimeter tests of various materials pulled from a typical office workstation. Next, single office workstations in various states were burned under an exhaust-collecting hood to measure their heat release rate. Following these experiments, a second series of compartment fire experiments was conducted in which three loaded office workstations were burned together within a compartment designed to mimic a representative section of WTC 1 or WTC 2.

During the model development, simulations of the fires within WTC 1 and WTC 2 were systematically improved as better information on the damage, window breakage, floor plans and initial conditions became available from other parts of the Investigation. Input data for the simulations of WTC 1 and WTC 2 consisted of descriptions of typical office furnishings and jet fuel, floor layouts, exterior damage, and interior damage estimates. Ultimately, results of the simulations were compared with visual observations to check for consistency. Predicted temperatures and gas concentrations were subsequently

used to analyze the temperatures within steel trusses and columns. This latter work is described in NIST NCSTAR 1-5G.¹

¹ This reference is to a companion document from this Investigation. A list of these documents appears in the Preface to this report.

Chapter 1

INTRODUCTION

1.1 REPORT OVERVIEW

In the months following the terrorist attacks on the World Trade Center (WTC) and the Pentagon, there was an active debate in the fire protection engineering community about the fires that erupted following the impact of the aircraft on the buildings. Because fires of this magnitude in these types of buildings are rare, there was a wide spectrum of opinion about the fire temperatures and their effects on the structural steel. There were thousands of photographs and videotapes taken by police and fire department personnel, plus hundreds of on-lookers, that showed fires erupting from individual broken windows in a manner not unfamiliar to most people who watch video footage of house fires on the local evening news. The fires burning near the windows of WTC 1 and WTC 2 were not necessarily hotter than those of any house fire. What was different about the WTC was the basic layout of the floors. Many experiments have been performed over the past 30 years in which temperature measurements have been made of fires engulfing compartments typical of a residence, but far fewer for the larger, open-plan office spaces typical of the WTC towers. Each floor of WTC 1 and WTC 2 was about 4,000 m² (approximately 1 acre) in area, but only 3.6 m high, floor slab to floor slab. The behavior of the fire at the exterior windows was well documented, but the behavior of the fires deep within the buildings was not, nor was there an extensive experimental history of this type of fire to guide the Investigation. The study was complicated by the lack of information about the damage to the building core where elevator shafts, stairwells and ventilation ducts were ruptured by the aircraft debris. At the exterior, oxygen needed for combustion was readily available through the broken windows. In the interior, it was not clear how much oxygen was available nor from where it originated.

To reconstruct the fire behavior in WTC 1 and WTC 2, a computer model designed specifically to study fire was used as part of the Investigation. Over the past 25 years, the National Institute of Standards and Technology (NIST) has developed several computer fire models used by fire protection engineers to assess the impact of fire on a building (Wright 2003). These models have become more and more detailed as computers have become faster and cheaper. The earliest models were essentially correlations of existing fire test data, followed later by relatively simple computer programs that solved mass and energy conservation equations for entire rooms or compartments. These models came to be known as “zone models” because they divided buildings into rooms, and each room into well-mixed upper and lower zones. The concept of conserving mass and energy in “zones” was extended to the point where each room could be divided into thousands or potentially millions of zones or “cells.” Adding the momentum conservation equation to that of mass and energy yielded what is known as a computational fluid dynamics (CFD) model. Such models have been used for many purposes, including designing jet aircraft and predicting the weather. The results of a CFD model yield a very detailed picture of the movement of fluids (either gases or liquids) as a function of time. A CFD fire model predicts the movement of hot gases from a fire as they spread throughout a building. In the case of the WTC Investigation these calculations provided estimates of the temperature of the smoke and hot gases surrounding the structural elements, information needed to assess the weakening of the steel over the course of a few hours.

The simulation of the fires within the WTC was the second in a chain of four major modeling efforts undertaken to explain why WTC 1, 2 and 7 collapsed. The first was a detailed reconstruction of the impact of the two airplanes on WTC 1 and WTC 2, resulting in estimates of structural damage and the redistribution of jet fuel and building contents (NIST NCSTAR 1-2¹). These latter results were used as initial conditions for the fire simulations. The results of the fire simulations, essentially the gas temperatures throughout the relevant floors as a function of time, were then used as boundary conditions for a detailed analysis of the thermal penetration of the structural steel and concrete (NIST NCSTAR 1-5G). Finally, the estimated structural damage from the impact study and the thermal history of the structural steel and concrete were incorporated into a global structural analysis that identified the most likely collapse mechanism of each building (NIST NCSTAR 1-6E). Descriptions of these models can be found in companion reports.

The fire model used in the WTC Investigation is known as the NIST Fire Dynamics Simulator (FDS). A detailed description of the model is given in Chapter 2. In September 2001, FDS had only been released for about a year and a half. Although its actual development went back much further in time, a number of improvements had to be made to make the model capable of handling the simulation of multiple fires spread over half a dozen floors of two buildings. The most important of these improvements was to make the model run in parallel, that is, to use more than one computer to work on the calculation. Because the floors in WTC 1 and WTC 2 were very similar in overall dimension, it was possible to compute the solution of the governing equations for each floor on separate computers, periodically exchanging information to describe the movement of smoke and hot gases between floors. Other enhancements to the model were made to better describe the variety of office furnishings and other combustible materials found throughout the buildings. Details of this work are described in Chapters 3 and 4.

The development of any computer model requires a complementary experimental program to provide the physical properties of the various materials described within it, and to furnish large scale test data with which to compare model predictions. The first set of experiments involved a liquid fuel spray burner that generated a fixed amount of energy in a compartment with various targets and obstructions, like columns, trusses and other steel objects (NIST NCSTAR 1-5B). The height of the compartment was chosen to be the same as that of the floors in WTC 1 and WTC 2. These experiments were designed to assess the accuracy of the model, its sensitivity to changes in various input parameters, and the heat transfer between the hot gases and solid surfaces. The next set of experiments consisted of open burns of single office workstations set under a large calorimeter. The purpose of these burns was to measure the heat output from a typical set of furnishings found throughout the WTC (NIST NCSTAR 1-5C). These measurements were compared with the model predictions, and the material properties were adjusted to calibrate the model, that is, to improve agreement with experiment. The third set of experiments, conducted within a larger compartment than was used in the first series, examined the behavior of three office workstations burning under conditions similar to those near the broken windows of WTC 1 and WTC 2 (NIST NCSTAR 1-5E). These experiments were designed to test the model's ability to characterize the burning behavior of real furnishings under conditions typical of the WTC fires.

While the model was being developed and the experiments conducted, the simulations of WTC 1 and WTC 2 began to take shape. From the months just after September 2001, until August 2004, a

¹ This reference is to one of the companion documents from this Investigation. A list of these documents appears in the Preface to this report.

progression of calculations unfolded that became more detailed and comprehensive in scope as more information about the interior and exterior damage, window breakage, furnishings, and floor plans was obtained (NIST NCSTAR 1-5A). Along the way, it became apparent which parameters had a significant impact on the final results, and which did not. For example, the exact distribution of the jet fuel, something virtually impossible to predict, did not influence the calculations in any significant way. The pattern of window breakage, however, was of tremendous importance. Chapters 5 and 6 describe the parameters needed by the numerical model and the results of the simulations as compared to the visual evidence.

1.2 REFERENCES

Wright, R.N. 2003. Building and Fire Research at NBS/NIST 1975-2000. NIST BSS 179. National Institute of Standards and Technology, Gaithersburg, MD, December.

This page intentionally left blank.

Chapter 2

FIRE DYNAMICS SIMULATOR

2.1 MODEL DESCRIPTION

The Fire Dynamics Simulator (FDS) is a computational fluid dynamics (CFD) model developed and maintained by the National Institute of Standards and Technology (NIST) Building and Fire Research Laboratory (BFRL) for the purpose of predicting the heat and mass transfer resulting from a fire. This chapter contains information about the model, its development, and its use in fire protection engineering. Most of the information has been extracted from the FDS Technical Reference Guide (McGrattan 2004) and supplemented with information relevant to the World Trade Center (WTC) Investigation. A comprehensive description of the governing equations and numerical algorithms used to solve them can be found in the Technical Reference Guide. The format of this chapter follows that of ASTM International (ASTM) E 1355, "Standard Guide for Evaluating the Predictive Capability of Deterministic Fire Models" (2004).

2.1.1 Name and History

FDS is a computer program that solves the governing equations of fluid dynamics with a particular emphasis on fire and smoke transport. Smokeview is a companion program that produces images and animations of the FDS calculations. Version 1 of FDS/Smokeview was publicly released in February 2000, version 2 in December 2001, and version 3 in November 2002. The present version of FDS/Smokeview is 4, released in July 2004. Changes in the version number correspond to major changes in the physical model or input parameters. For minor changes and bug fixes, incremental versions are released, referenced according to fractions of the integer version number.

The simulations of the WTC fires described in this report were performed with FDS 4.0.

2.1.2 Type of Model

FDS is a CFD model of fire-driven fluid flow. The model solves numerically a form of the Navier-Stokes equations appropriate for low-speed, thermally-driven flow with an emphasis on smoke and heat transport from fires. The partial derivatives of the conservation equations of mass, momentum and energy are approximated as finite differences, and the solution is updated in time on a three-dimensional, rectilinear grid. Thermal radiation is computed using a finite volume technique on the same grid as the flow solver. Lagrangian particles are used to simulate smoke movement and sprinkler discharge.

2.1.3 Model Developers

FDS was developed and is currently maintained by the Fire Research Division in BFRL at NIST. A substantial contribution to the development of the model was made by VTT Building and Transport in Finland.

2.1.4 Model Uses

Throughout its development, FDS has been aimed at solving practical fire problems in fire protection engineering, while at the same time providing a tool to study fundamental fire dynamics and combustion. FDS can be used to model the following phenomena:

- Low speed transport of heat and combustion products from fire
- Radiative and convective heat transfer between the gas and solid surfaces
- Pyrolysis
- Flame spread and fire growth
- Sprinkler, heat detector, and smoke detector activation
- Sprinkler sprays and suppression by water

Although FDS was designed specifically for fire simulations, it can be used for other low-speed fluid flow simulations that do not necessarily include fire or thermal effects. To date, about half of the applications of the model have been for design of smoke control systems and sprinkler/detector activation studies. The other half consist of residential and industrial fire reconstructions.

2.1.5 Model Results

FDS computes the temperature, density, pressure, velocity and chemical composition within each numerical grid cell at each discrete time step. There are typically hundreds of thousands to several million grid cells and thousands to hundreds of thousands of time steps. In addition, FDS computes at solid surfaces the temperature, heat flux, mass loss rate, and various other quantities. The user must carefully select what data to save, much like one would do in designing an actual experiment. Even though only a small fraction of the computed information can be saved, the output typically consists of fairly large data files. Typical output quantities for the gas phase include:

- Gas temperature
- Gas velocity
- Gas species concentration (water vapor, CO₂, CO, N₂)
- Smoke concentration and visibility estimates
- Pressure
- Heat release rate per unit volume
- Mixture fraction (or air/fuel ratio)
- Gas density

- Water droplet mass per unit volume

On solid surfaces, FDS predicts additional quantities associated with the energy balance between gas and solid phase, including:

- Surface and interior temperature
- Heat flux, both radiative and convective
- Burning rate
- Water droplet mass per unit area

Global quantities recorded by the program include:

- Total heat release rate (HRR)
- Sprinkler and detector activation times
- Mass and energy fluxes through openings or solids

Time histories of various quantities at a single point in space or global quantities like the fire's HRR are saved in simple, comma-delimited text files that can be plotted using a spreadsheet program. However, most field or surface data are visualized with a program called Smokeview, a tool specifically designed to analyze data generated by FDS. FDS and Smokeview are used in concert to model and visualize fire phenomena. Smokeview performs this visualization by presenting animated tracer particle flow, animated contour slices of computed gas variables and animated surface data. Smokeview also presents contours and vector plots of static data anywhere within a scene at a fixed time.

A complete list of FDS output quantities and formats is given in McGrattan and Forney (2004). Details on the use of Smokeview are found in Forney (2004).

2.1.6 Relevant Publications

Each version of FDS and Smokeview are documented by three separate publications – the FDS Technical Reference Guide (McGrattan 2004), the FDS User's Guide (McGrattan and Forney 2004), and the Smokeview User's Guide (Forney 2004). The User's Guides only describe the mechanics of using the computer programs. The Technical Reference Guide provides the theory and algorithm details, plus a description of the verification and validation studies. There are numerous sources that describe various parts of the model. The basic set of equations solved in FDS were formulated by Rehm and Baum in the *Journal of Research of the National Bureau of Standards* (Rehm and Baum 1978). The basic hydrodynamic algorithm evolved at NIST through the 1980s and 1990s, incorporating fairly well-known numerical schemes that are documented in books by Anderson, Tannehill and Pletcher (1984), Peyret and Taylor (1983), and Ferziger and Peric (1999). This last book provides a good description of the large eddy simulation technique and provides references to many current publications on the subject. Numerical techniques appropriate for combustion systems are described by Oran and Boris (1987). The mixture fraction combustion model is described in a review article by Bilger (1989). Basic heat transfer theory is

provided by Holman (1989) and Incropera and De Witt (1996). Thermal radiation is described in Siegel and Howell (2002). Much of the current knowledge of fire science and engineering is found in the *SFPE Handbook of Fire Protection Engineering* (DiNenno 2002). Popular textbooks in fire protection engineering include those by Drysdale (2002), Quintiere (1998), and Karlsson and Quintiere (2000).

On-going research in fire and combustion is documented in several periodicals and conference proceedings. The International Association of Fire Safety Science (IAFSS) organizes a conference every two years, the proceedings of which are frequently referenced by fire researchers. Interscience Communications, a London-based publisher of several fire-related journals, hosts a conference known as Interflam roughly every three years in the United Kingdom. The Combustion Institute hosts an international symposium on combustion every two years, and in addition to the proceedings of this symposium, the organization publishes its own journal *Combustion and Flame*. The papers appearing in the IAFSS conference proceedings, the Combustion Symposium proceedings, and *Combustion and Flame* are all peer-reviewed, while those appearing in the Interflam proceedings are selected based on the submission of a short abstract. Both the Society for Fire Protection Engineers and the National Fire Protection Association publish peer-reviewed technical journals entitled the *Journal of Fire Protection Engineering* and *Fire Technology*. Other often-cited, peer-reviewed technical journals include the *Fire Safety Journal*, *Fire and Materials*, *Combustion Science and Technology*, *Combustion Theory and Modeling* and the *Journal of Heat Transfer*.

Research at NIST is documented in various ways beyond contributions made by staff to external journals and conferences. NIST publishes several forms of internal reports, special publications, and its own journal called the *Journal of Research of NIST*. An internal report, referred to as a NISTIR, is a convenient means to disseminate information, especially when the quantity of data exceeds what could normally be accepted by a journal. Often a NISTIR is streamlined and published externally, with the NISTIR serving as a more complete record of the work performed. Previous versions of the FDS Technical Reference Guide and User's Guide were published as NISTIRs. The current FDS and Smokeview manuals are being published as NIST Special Publications, distinguished from NISTIRs by the fact that they are permanently archived. Work performed by an outside person or organization working under a NIST grant or contract is published in the form of a NIST Grant/Contract Report. All work performed by the staff of the Building and Fire Research Laboratory at NIST beyond 1993 is permanently stored in electronic form and made freely available via the Internet and yearly released compact disks.

2.1.7 Governing Equations, Assumptions, and Numerics

Following is a brief description of the major components of FDS. Detailed information regarding the assumptions and governing equations associated with the model is provided in McGrattan (2004).

Hydrodynamic Model: FDS solves numerically a form of the Navier-Stokes equations appropriate for low speed, thermally-driven flow with an emphasis on smoke and heat transport from fires. The core algorithm is an explicit predictor-corrector scheme, second order accurate in space and time. Turbulence is treated by means of the Smagorinsky (1963) form of Large Eddy Simulation (LES). It is possible to perform a Direct Numerical Simulation if the underlying numerical grid is fine enough. LES is the default mode of operation and was used for the WTC simulations.

Combustion Model: For most applications, FDS uses a mixture fraction combustion model. The mixture fraction is a conserved scalar quantity that is defined as the fraction of gas at a given point in the flow field that originated as fuel. The model assumes that combustion is mixing-controlled, and that the reaction of fuel and oxygen is infinitely fast. The mass fractions of all of the major reactants and products can be derived from the mixture fraction by means of “state relations,” empirical expressions arrived at by a combination of simplified analysis and measurement.

Radiation Transport: Radiative heat transfer is included in the model via the solution of the radiation transport equation for a non-scattering gray gas. In a limited number of cases, a wide band model can be used in place of the gray gas model. The radiation equation is solved using a technique similar to a finite volume method for convective transport, thus the name given to it is the Finite Volume Method. Using approximately 100 discrete angles, the finite volume solver requires about 15 percent of the total central processing unit (CPU) time of a calculation, a modest cost given the complexity of radiation heat transfer. Water and fuel droplets can absorb thermal radiation, and the absorption coefficients are based on Mie theory. This capability was exercised in the WTC simulations to describe the combustion of jet fuel.

Geometry: FDS approximates the governing equations on one or more rectilinear grids. The user prescribes rectangular obstructions that are forced to conform with the underlying grid (Prasad et al. 2000).

Boundary Conditions: All solid surfaces are assigned thermal boundary conditions, plus information about the burning behavior of the material. Usually, material properties are stored in a database and invoked by name. Heat and mass transfer to and from solid surfaces is usually handled with empirical correlations.

Sprinklers and Detectors: The activation of sprinklers and heat and smoke detectors are modeled using fairly simple correlations based on thermal inertia in the case of sprinklers and heat detectors, and the lag in smoke transport through smoke detectors. Sprinkler sprays are modeled by Lagrangian particles that represent a sampling of the water droplets ejected from the sprinkler. No smoke detectors were used in the WTC simulations, but sprinklers were used as a means to simulate the initial dispersion of jet fuel droplets.

2.1.8 Limitations of the Model

Although FDS can address most fire scenarios, there are limitations in all of its various algorithms. Some of the more prominent limitations of the model are listed here. More specific limitations are discussed as part of the description of the governing equations in McGrattan (2004).

Low Speed Flow Assumption: The use of FDS is limited to low-speed¹ flow with an emphasis on smoke and heat transport from fires. This assumption rules out using the model for any scenario involving flow speeds approaching the speed of sound, such as explosions, choke flow at nozzles, and detonations. FDS was used to simulate the fireballs created by the sudden ignition of jet fuel following the airplane crashes in the WTC towers, but the flow speeds did not violate the basic low speed assumptions (Rehm et al. 2002).

¹ Mach numbers less than about 0.3.

Rectilinear Geometry: The efficiency of FDS is due to the simplicity of its rectilinear numerical grid and the use of fast, direct solvers for the pressure field. This can be a limitation in some situations where certain geometric features do not conform to the rectangular grid, although most building components do. There are techniques in FDS to lessen the effect of “sawtooth” obstructions used to represent nonrectangular objects, but these cannot be expected to produce good results if, for example, the intent of the calculation is to study boundary layer effects. For most practical large-scale simulations, the increased grid resolution afforded by the fast pressure solver offsets the approximation of a curved boundary by small rectangular grid cells. For the WTC simulations, every geometric feature was assumed to be rectangular.

Fire Growth and Spread: Because the model was originally designed to analyze large industrial fires, it can be used reliably when the HRR of the fire is specified and the transport of heat and exhaust products is the principal aim of the simulation. In these cases, the model predicts flow velocities and temperatures to an accuracy within 5 percent to 20 percent of experimental measurements, depending on the resolution of the numerical grid.² However, for fire scenarios where the heat release rate is *predicted* rather than *prescribed*, the uncertainty of the model is higher. There are several reasons for this: (1) properties of real materials and real fuels are often unknown or difficult to obtain, (2) the physical processes of combustion, radiation and solid phase heat transfer are more complicated than their mathematical representations in FDS, (3) the results of calculations are sensitive to both the numerical and physical parameters. *The experimental work that is documented in Chapter 4 was performed specifically to address these concerns.*

Combustion: For most applications, FDS uses a mixture fraction combustion model. The mixture fraction is a conserved scalar quantity that is defined as the fraction of gas at a given point in the flow field that originated as fuel. The model assumes that combustion is mixing-controlled, and that the reaction of fuel and oxygen is infinitely fast, regardless of the temperature. For large-scale, well-ventilated fires, this is a good assumption. However, if a fire is in an under-ventilated compartment, or if a suppression agent like water mist or CO₂ is introduced, fuel and oxygen may mix but may not burn. Also, a shear layer with high strain rate separating the fuel stream from an oxygen supply can prevent combustion from taking place. The physical mechanisms underlying these phenomena are complex, and even simplified models still rely on an accurate prediction of the flame temperature and local strain rate. Sub-grid scale modeling of gas phase suppression and extinction is still an area of active research in the combustion community. Until reliable models can be developed for building-scale fire simulations, simple empirical rules can be used that prevent burning from taking place when the atmosphere immediately surrounding the fire cannot sustain the combustion. The validation experiments described in Chapter 4 were conducted to address concerns about the model’s ability to simulate oxygen-limited fires.

Radiation: Radiative heat transfer is included in the model via the solution of the radiation transport equation for a non-scattering gray gas, and in some limited cases using a wide band model. The equation is solved using a technique similar to finite volume methods for convective transport, thus the name given to it is the Finite Volume Method. There are several limitations of the model. First, the absorption coefficient for the smoke-laden gas is a complex function of its composition and temperature. Because of the simplified combustion model, the chemical composition of the smokey gases, especially the soot content, can effect both the absorption and emission of thermal radiation. Second, the radiation transport

² It is extremely rare to find measurements of local velocities and/or temperatures from fire experiments that have reported error estimates that are less than 5 percent. Thus, the most accurate calculations using FDS do not introduce significantly greater errors in these quantities than the vast majority of fire experiments.

is discretized via approximately 100 solid angles. For targets far away from a localized source of radiation, like a growing fire, the discretization can lead to a non-uniform distribution of the radiant energy. This can be seen in the visualization of surface temperatures, where “hot spots” show the effect of the finite number of solid angles. The problem can be lessened by the inclusion of more solid angles, but at a price of longer computing times. In most cases, the radiative flux to far-field targets is not as important as those in the near-field, where coverage by the default number of angles is much better.

The validation experiments described in Chapter 3 addressed concerns about the radiation solver, the composition of exhaust gases, and the accuracy of heat flux predictions to solid objects.

2.1.9 Input Data Required to Run the Model

All of the input parameters required by FDS to describe a particular scenario are conveyed via one or two text files created by the user. These files contain information about the numerical grid, ambient environment, building geometry, material properties, combustion kinetics, and desired output quantities. The numerical grid is one or more rectilinear meshes with (usually) uniform cells. All geometric features of the scenario have to conform to this numerical grid. Objects smaller than a single grid cell are either approximated as a single cell or rejected. The building geometry is input as a series of rectangular obstructions. Materials are defined by their thermal conductivity, specific heat, density, thickness, and burning behavior. There are various ways that this information is conveyed, depending on the desired level of detail. A significant part of the FDS input file directs the code to output various quantities in various ways. Much like in an actual experiment, the user must decide before the calculation begins what information to save. There is no way to recover information after the calculation is over if it was not requested at the start. A complete description of the input parameters required by FDS can be found in McGrattan and Forney (2004).

2.1.10 Property Data

Any simulation of a real fire scenario involves prescribing material properties for the walls, floor, ceiling, and furnishings. FDS treats all of these objects as homogeneous solids, thus the physical parameters for many real objects can only be viewed as approximations to the actual properties. Describing these materials in the input file is the single most challenging task for the user. Thermal properties such as thermal conductivity, specific heat, density, and thickness can be found in various handbooks, or in manufacturers literature, or from bench-scale measurements. More difficult is the burning behavior at different heat fluxes. Even though entire books are devoted to the subject (Babrauskas 2003), it is still difficult to find information on a particular item. For the WTC simulations, various common materials found in the WTC were tested using a variety of apparatus (NIST NCSTAR 1-5C).

2.2 SCENARIOS FOR WHICH FDS HAS BEEN EVALUATED

This section provides a description of the scenarios or phenomena of interest that have been included in past efforts to evaluate FDS. Because FDS is used both for research and for practical applications, there were some routines within the model that had not been comprehensively validated at the start of the Investigation. Experimental efforts to validate FDS for the WTC simulations are described in Chapters 3 and 4.

2.2.1 Description of Scenarios or Phenomenon of Interest

FDS is suited for a wide range of thermally-driven fluid flow scenarios, including fire, both in the open (e.g. unconfined fire plumes) as well as within the built environment. To date, about half of the applications of FDS have been for design, and half for forensic reconstruction. Design applications typically involve an existing building or a building under design. A so-called “design fire” is prescribed either by a regulatory authority or by the engineers performing the analysis. Because the fire’s heat release rate is known, the role of the model is to predict the transport of heat and combustion products throughout the room or rooms of interest. Ventilation equipment is often included in the simulation, like fans, blowers, exhaust hoods, heating, ventilating, and air conditioning ducts, smoke management systems, etc. Sprinkler and heat and smoke detector activation are also of interest. The effect of the sprinkler spray on the fire is usually less of interest since the fire is prescribed rather than predicted. Detailed descriptions of the contents of the building are usually not necessary because these items are not assumed to be burning, and even if they are, the burning rate will be fixed, not predicted. Sometimes, it is necessary to predict the heat flux from the fire to a nearby “target,” and even though the target may heat up to some prescribed ignition temperature, the subsequent spread of the fire usually goes beyond the scope of the analysis because of the uncertainty inherent in object to object fire spread.

Forensic reconstructions require the model to simulate an actual fire based on information that is collected after the event, such as eye witness accounts, unburned materials, burn signatures, etc. The purpose of the simulation is to connect a sequence of discrete observations with a continuous description of the fire dynamics. Usually, reconstructions involve more gas/solid phase interaction because virtually all objects in a given room are potentially ignitable, especially when flashover occurs. Thus, there is much more emphasis on such phenomena as heat transfer to surfaces, pyrolysis, flame spread, and suppression. In general, forensic reconstructions are more challenging simulations to perform because they require more detailed information about the room contents, and there is much greater uncertainty in the total heat release rate as the fire spreads from object to object.

Validation studies of FDS to date have focussed more on design applications than reconstructions. The reason is that design applications usually involve prescribed fires and demand a minimum of thermophysical properties of real materials. Transport of smoke and heat is the primary focus, and measurements can be limited to well-placed thermocouples, a few heat flux gauges, gas samplers, etc. Phenomena of importance in forensic reconstructions, like second item ignition, flame spread, vitiation effects and extinction, are more difficult to model and more difficult to study with well-controlled experiments. Uncertainties in material properties and measurements, as well as simplifying assumptions in the model, often force the comparison between model and measurement to be qualitative at best. Nevertheless, current validation efforts, including those conducted for the Investigation, are moving in the direction of these more difficult issues.

2.2.2 List of Quantities Predicted by FDS upon which Evaluation Is Based

An FDS simulation predicts the thermal environment of the entire volume of interest by computing thermodynamic quantities in each grid cell of the computational mesh. The number of quantities predicted by the model is greater than the number of quantities that are typically measured in validation experiments. Following is a list of quantities predicted in each computational cell by the model that are

typically compared to experimental measurement. The order of the items on the list emphasize their relative importance in most validation studies.

- Gas temperature
- Gas velocity
- Major gas species concentrations (CO₂, CO, O₂)
- Smoke concentration/obscuration
- Pressure

On solid surfaces, FDS predictions of the following are typically compared with measurements:

- Surface temperature (and sometimes back surface temperature)
- Total heat flux (radiative plus convective)
- Burning (or mass loss) rate

In addition to these point measurements, model and experimental predictions of global quantities, such as heat release rate and the flux of mass and energy through openings or walls in the compartment, are often compared. These global quantities can be used to assess the overall energy budget, confirming energy conservation in the model, and helping to assess systematic uncertainty in the experiments.

2.2.3 Degree of Accuracy Required for Each Output Quantity

The degree of accuracy for each output variable required by the user is highly dependent on the technical issues associated with the analysis. The user must ask: How accurate does the analysis have to be to answer the technical question posed? Thus, a generalized definition of the accuracy required for each quantity with no regard as to the specifics of a particular analysis is not practical and would be limited in its usefulness. Returning to the earlier definitions of “design” and “reconstruction,” design applications typically are more accurate because the heat release rate is prescribed rather than predicted, and the initial and boundary conditions are far better characterized. Mathematically, a design calculation is an example of a “well-posed” problem in which the solution of the governing equations is advanced in time starting from a known set of initial conditions and constrained by a known set of boundary conditions. The accuracy of the results is a function of the fidelity of the numerical solution, which is mainly dependent on the size of the computational grid. Validation efforts to date involving well-characterized geometries and prescribed fires have shown that FDS predictions vary from being within experimental uncertainty to being about 20 percent different than measurements of temperature, heat flux, gas concentration, etc. (McGrattan 2004).

A reconstruction is an example of an “ill-posed” problem because the outcome is known whereas the initial and boundary conditions are not. There is no single, unique solution to the problem, that is, it is possible to simulate numerous fires that produce the given outcome. There is no right or wrong answer, but rather a small set of plausible fire scenarios that are consistent with the collected evidence. These

simulations are then used to demonstrate why the fire behaved as it did based on the current understanding of fire physics incorporated in the model.

2.3 MODEL IMPROVEMENTS FOR THE WTC INVESTIGATION

The description of FDS above points out various limitations in the model. At the start of the WTC Investigation, it was understood that FDS would need several improvements to its physical and numerical algorithms, plus large scale validation experiments to assess the accuracy of the improved model. Following is a brief description of the two most important improvements made to FDS for the Investigation. The validation work is described in Chapters 3 and 4.

2.3.1 Charring Pyrolysis Model

The temperature of solid objects is calculated in FDS via a one dimensional solution of a heat transfer equation for either a thermally-thin or thermally-thick solid. At the interface between solid and gas, mass and energy balances are imposed where radiative and convective heat transfer from the gas heats the solid internally until a prescribed pyrolysis temperature is achieved, at which point fuel gas is generated and burning results. Originally, the pyrolysis of the solid was assumed to occur at the surface where the energy flux from the gas was roughly proportional to the energy needed to gasify the solid. A solid object which burns at the surface is often referred to as a “thermoplastic.” This model is still included in FDS, but a second pyrolysis model has been implemented that accounts for char-forming solids like wood where the degradation of the material does not occur at the surface but rather in the interior.

The heat transfer and pyrolysis inside the charring material are modeled using a simplified version of the one dimensional model of Atreya (1980), which was further developed by Ritchie et al. (1997). It describes the evaporation of moisture and the degradation of virgin wood to gaseous fuel and char. The volatile gases are instantaneously released into the gas. The selection of the proper material properties and the pyrolysis rate coefficients is difficult. Most of the thermal properties have been taken from previous work (Di Blasi 1998; Fredlund 1988; Novozhilov et al. 1996; Parker 1989), but the applicability of these data to the various wooden furnishings in the WTC was uncertain and hence subjected to a parameter sensitivity analysis that is described in Chapter 4.

2.3.2 Parallel Processing

Modeling large fires is computationally intensive, both in terms of CPU time and memory. Motivated by the need to model the large WTC fires in detail, FDS has been modified to make use of parallel processing. Up to this point, FDS has been limited to calculations small enough to run on a single CPU and to fit into the memory of a common desktop personal computer. The WTC study is an example of a large-scale fire modeling problem that would have been impossible to undertake without the use of parallel processing.

In terms of parallelization, many details of the fire model are not important. The approach taken to run FDS on a cluster of machines can be applied to virtually any CFD code, in particular those that involve three spatial dimensions and time. In such cases, the computational demand is well represented by the product of the number of computational grid cells and the number of time steps taken to advance the solution of the governing equations in time. For example, if the computational grid consists of one million

cells and the simulation requires ten thousand time steps, the demand is 10^{10} cell-cycles. The overall demand includes both a memory requirement and CPU time. The memory requirement is a function of the number of grid cells, and the CPU time is a function of number of time steps.

For very large building fire simulations, the computing constraint is both the large volume and the long simulation time. It was determined that single processor systems would require nearly 60 days to run a single WTC fire simulation, which was prohibitive, given that many trial simulations were required. Even worse, the simulation is large in the static sense as well, requiring 6 GB to 12 GB of memory, well over the 4 GB address space of 32 bit processors. Because of this, the current calculations are not only impractical on single processor systems, they are impossible on any 32 bit processor. A 64 bit processor system may theoretically handle the static memory requirements of a large simulation, but the run times for large calculations remain prohibitive.

To assess the computational requirements in detail, FDS was analyzed to determine what parts of the program required the bulk of the CPU time. These profiling tests showed that the compute-intensive parts of FDS are not well-localized. This is because most CFD codes repeatedly compute finite-difference approximations for the roughly half dozen partial differential equations. Therefore, parallel programming constructs added to the various routines would involve non-localized changes to the source code in modules that are part of the physics model. Furthermore, this low-level parallelism does nothing to solve the memory address space limitation. Finally, this type of parallel processing leads to frequent, small bursts of communication that demand extra overhead.

Because the computational load is distributed throughout much of the source code, an alternative approach to parallelization was taken. A feature common of many CFD codes is multi-block or multi-mesh structure in which more than one structured grid is used in the calculation (Pankajakshan 1996; Gropp 1999). This feature is exploited by simply assigning the data and computation for each block on a different processor. This has advantages and some limitations. The advantages are (1) a natural and scalable extension of the existing code, (2) the amount of data communication is kept to a minimum, since communication is limited to overlap information, rather than the data for full blocks, (3) source code changes are localized in small communication routines, and (4) development is fairly fast. The disadvantages to the multi-block approach are (1) equal distribution of work across processors (load balancing) depends on using blocks of comparable computational complexity (same number of cell-cycles in each block), (2) the level of parallelism and the speed up of the calculation is limited to the number of spatial blocks that can be used in the calculation. These limitations are not severe in many cases, including the large building fires discussed in this report.

To maintain a scalable, portable code, Message Passing Interface (MPI) was used. This is a standard, well-documented system of implementing parallel processing, that can work with shared memory, distributed memory, or combinations of those architectures (Gropp 1999). The goal in using MPI was to produce a code that, except for the requirement of the MPI library, is as portable and standardized as the sequential version that is widely used in the fire protection engineering community.

The most widely used MPI constructs in FDS are non-blocking Send/Receive messages that exchange temperature, density, velocity, pressure and various other quantities. The information exchanged is needed at mesh boundaries, so the overall communication time relative to total CPU time is on the order of a few percent. The term "non-blocking" means that information is passed from machine to machine

while the calculation continues. This is important when there are potentially dozens of overlapping meshes exchanging information with each other.

The parallel version of FDS has been designed to run on a cluster of conventional computers under any operating system that supports MPI. In a parallel processing cluster, the design follows from trading off between fewer, faster processors, or more, slower processors, and how much to spend optimizing network speed, at the cost of fewer computational nodes. In the case of FDS, it was clear at the outset that the code required fast communication and it quickly became clear that the level of initial parallelism was of the order of 10 processors, not hundreds. To optimize communication speed, the network was internally connected using gigabit ethernet. Faster, lower latency communication hardware was available, but it was found that gigabit ethernet is a good compromise between speed, low cost and compatibility with standard Linux distributions. Faster networking hardware may be added later. The final consideration was to allow the cluster to be dual use, so it could operate as a “farm” running many long single processor runs, or as an MPI cluster. For the WTC Investigation, it was used both ways, with single floors running separately on single processors, and multiple floors running in parallel.

2.4 REFERENCES

- American Society for Testing and Materials, 2004. *ASTME 1355-04*. Standard Guide for Evaluating the Predictive Capabilities of Deterministic Fire Models. West Conshohocken, PA.
- Anderson, D.A., J.C. Tannehill, and R.H. Pletcher. 1984. *Computational Fluid Mechanics and Heat Transfer*. Hemisphere Publishing Corporation, Philadelphia, PA.
- Atreya, A. 1984. Pyrolysis, Ignition and Fire Spread on Horizontal Surfaces of Wood. National Bureau of Standards. Report NBS-GCR-83-449, Gaithersburg, MD.
- Babrauskas, V. 2003. *Ignition Handbook*. Fire Science Publishers, Issaquah, Washington USA, 1st edition, Co-published by the Society of Fire Protection Engineers.
- Bilger, R.W. 1989. Turbulent Diffusion Flames. *Annual Review of Fluid Mechanics*, vol. 21.
- Di Blasi, C. 1998. Physico-chemical processes occurring inside a degrading two-dimensional anisotropic porous medium. *International Journal of Heat and Mass Transfer*. Vol. 41.
- DiNenno, P.J., editor. 2002. *SFPE Handbook of Fire Protection Engineering*. National Fire Protection Association, Quincy, MA, 3rd edition.
- Drysdale, D. 2002. *An Introduction to Fire Dynamics*. John Wiley and Sons, New York, 2nd edition.
- Ferziger, J.H. and M. Peric. 1999. *Computational Methods for Fluid Dynamics*. Springer-Verlag, Berlin, 2nd edition.
- Forney, G.P. and K.B. McGrattan. 2004. User’s Guide for Smokeview Version 4. NIST Special Publication 1017, National Institute of Standards and Technology, Gaithersburg, MD, July.

- Fredlund, B. 1988. A Model for Heat and Mass Transfer in Timber Structures During Fire, A theoretical, numerical and experimental study. Report LUTVDG (TVBB-1003), Department of Fire Safety Engineering, Lund University, Sweden.
- Gropp, W., E. Lusk and A. Skjellum. 1999. *Using MPI: Portable Parallel Programming with the Message-Passing Interface*. 2nd Ed. MIT Press, Cambridge, MA.
- Holman, J.P. 1989. *Heat Transfer*. McGraw-Hill, New York, 5th edition.
- Incropera, F.P. and D.P. De Witt. 1996. *Fundamentals of Heat and Mass Transfer*. John Wiley and Sons, New York. 4th edition.
- Karlsson, B. and J. Quintiere. 2000. *Enclosure Fire Dynamics*, CRC Press, New York.
- McGrattan, K., Ed. 2004. *Fire Dynamics Simulator (Version 4) Technical Reference Guide*. National Institute of Standards and Technology, NIST Special Publication 1018, Gaithersburg, MD, September.
- McGrattan, K. and G.P. Forney. 2004. *Fire Dynamics Simulator (Version 4) User's Guide*. National Institute of Standards and Technology, NIST Special Publication 1019, Gaithersburg, MD, July.
- Novozhilov, V., B. Moghtaderi, D.F. Fletcher and J.H. Kent. 1996. Computational Fluid Dynamics Modelling of Wood Combustion. *Fire Safety Journal*, vol. 27.
- Oran, E.S. and J.P. Boris. 1987. *Numerical Simulation of Reactive Flow*. Elsevier Science Publishing Company, New York.
- Pankajakshan, R. and W.R. Briley. 1996. Parallel Solution of Viscous Incompressible Flow on Multi-Block Structured Grids Using MPI, in *Parallel Computational Fluid Dynamics - Implementations and Results Using Parallel Computers*, Eds S. Taylor, A. Ecer, J. Periaux, and N. Satofuca, Elsevier Science, B. V., Amsterdam.
- Parker, W. J. 1989. Prediction of the Heat Release Rate of Douglas Fir. *Fire Safety Science-- Proceedings of the 2nd International Symposium*. International Association of Fire Safety Science.
- Peyret, R. and T.D. Taylor. 1983. *Computational Methods for Fluid Flow*. Springer-Verlag, New York.
- Prasad, K., G. Patnaik, and K. Kailasanath. 2000. Advanced Simulation Tool for Improved Damage Assessment (1) A Multiblock Technique for Simulating Fire and Smoke Transport in Large Complex Enclosures. US Naval Research Laboratory, NRL/MR/6140—00—8428.
- Quintiere, J.G. 1998. *Principles of Fire Behavior*. Delmar Publishers, Albany, New York.
- Rehm, R.G. and H.R. Baum. 1978. The Equations of Motion for Thermally Driven, Buoyant Flows. *Journal of Research of the NBS*, vol. 83.

- Rehm, R.G., W.A. Pitts, H.R. Baum, D.D. Evans, K. Prasad, K.B. McGrattan and G.P. Forney. 2002. *Initial Model for Fires in the World Trade Center*. NISTIR 6879. National Institute of Standards and Technology, Gaithersburg, MD, May.
- Ritchie, S. J., K. D. Steckler, A. Hamins, T. G. Cleary, J. C. Yang, T. Kashiwagi. 1997. Effect of Sample Size on the Heat Release Rate of Charring Materials. Hasemi, Y. (ed.) *Fire Safety Science -- Proceedings of the Fifth International Symposium*. International Association of Fire Safety Science.
- Siegel, R. and J. Howell. 1992. *Thermal Radiation Heat Transfer (3rd ed.)* Hemisphere Publishing Corp. Philadelphia, PA.
- Smagorinsky, J. 1963. General Circulation Experiments with the Primitive Equations. I. The Basic Experiment. *Monthly Weather Review*, vol. 91.

Chapter 3

MODEL ACCURACY ASSESSMENT – STEADY FIRES

3.1 OVERVIEW

The first set of experiments conducted as part of the World Trade Center (WTC) Investigation was designed to assess the accuracy of the fire model's predictions for scenarios in which the heat release rate (HRR) of the fire was prescribed. It was necessary to assess the basic transport algorithms within the model with calculations where the source of mass and energy was known before embarking on more complicated simulations of entire furnished compartments burning. These experiments are described in the next chapter.

In the initial experiments, the fire itself was relatively well characterized, and the heat release rate was measured and prescribed as a model input. The compartment was heavily instrumented so that all of the energy from the fire could be accounted for and reported in terms of conductive losses to walls, convective flux through openings, etc. With the large number of measurements, it was possible to go beyond the traditional point by point comparison and discover why the model either over-predicted or under-predicted a given measurement. It was possible to compare the transport of energy, starting with the combustion of fuel, and ending with effluent exiting into a large hood. Based on these integrated quantities, discrepancies in heat flux and gas concentration predictions could be tied to errors in the overall energy budget, allowing for an assessment of the accuracy of various components within the model.

3.2 DESCRIPTION OF THE EXPERIMENTS

A complete description of the spray fire experiments is found in NIST NCSTAR 1-5B. The description given here is intended to highlight the details required for the numerical predictions of the experiments.

Simulations of the experiments with the Fire Dynamics Simulator (FDS) were performed before testing began to guide the design of the compartment and also to provide a baseline set of "blind" predictions. The geometry of the compartment was relatively simple. The overall enclosure was rectangular, as were the vents and most of the obstructions. A uniform numerical grid made up of 10 cm cubes was chosen based on the observation that the ratio of the fire's characteristic diameter, D^* , to the size of a grid cell, δx , is an indicator of the degree of resolution achieved by the simulation.¹ In short, the greater the ratio $D^*/\delta x$, the more the fire dynamics are resolved directly, and the more accurate the simulation. Past experience has shown that a ratio of 10 produces favorable results at a moderate computational cost (McGrattan et al. 2003).

¹ D^* is given by the expression $(\dot{Q}/\rho_\infty c_p T_\infty \sqrt{g})^{2/5}$, where \dot{Q} is the heat release rate of the fire, and the subscript ∞ refers to ambient values of density and temperature, respectively.

Figure 3–1 is a snapshot of a simulation showing the major geometric features of the compartment, the fire, and an instantaneous temperature profile along the vertical centerline plane. The compartment walls and ceiling were made of 2.54 cm (1 in.) thick Marinite I, a product of BNZ Materials, Inc. The manufacturer provided the thermal properties of the material used in the calculation. The density was 737 kg/m^3 , conductivity 0.12 W/m/K . The specific heat ranged from $1,172 \text{ J/kg/K}$ at $93 \text{ }^\circ\text{C}$ to $1,423 \text{ J/kg/K}$ at $425 \text{ }^\circ\text{C}$.

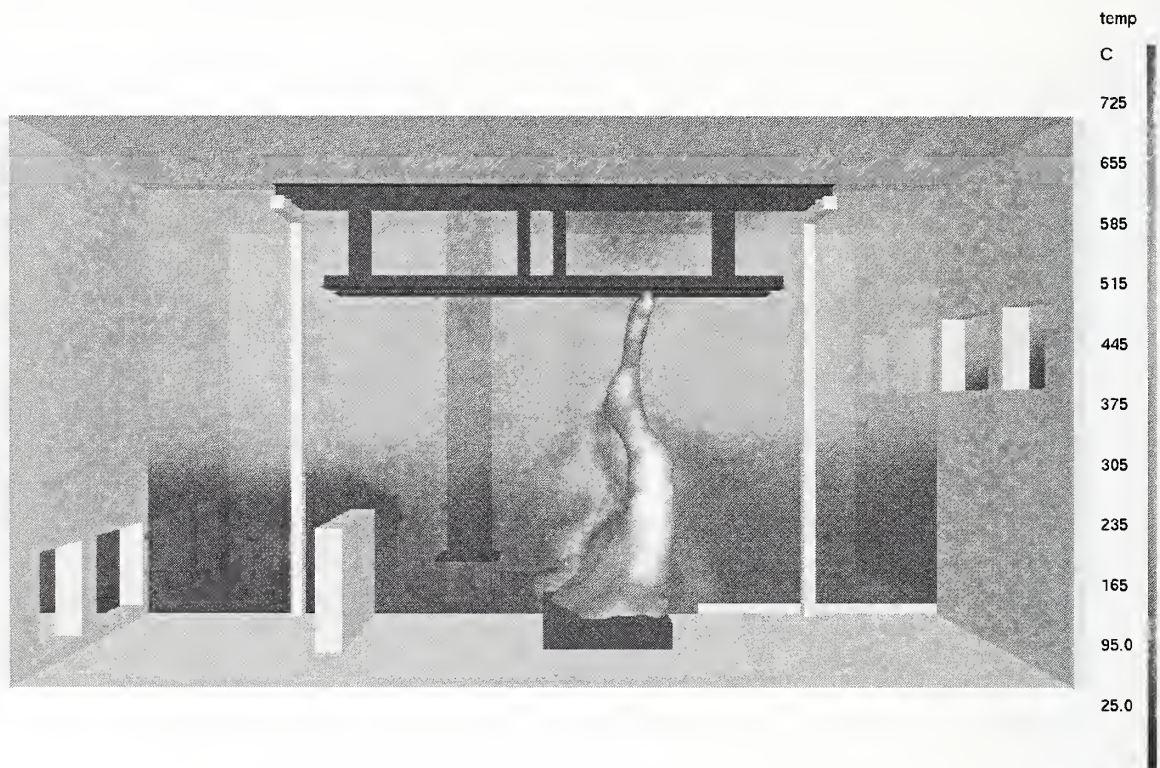


Figure 3–1. Centerline gas temperatures in a spray burner test.

The steel used to construct the column and truss flanges was 0.64 cm ($1/4 \text{ in.}$) thick. The density of the steel was assumed to be $7,860 \text{ kg/m}^3$; its specific heat 450 J/kg/K (NIST NCSTAR 1-3E). The steel was assumed in the FDS model to be thermally-thin; thus, no thermal conductivity was used. Note that FDS performed a simple one-dimensional calculation of the steel temperature to be used as a boundary condition in the calculation. More detailed calculations of the steel and concrete temperatures were done using another model (NIST NCSTAR 1-5G).

Two fuels were used in the tests. The properties of the fuels were obtained from measurements made on a series of unconfined burns (Hamins, Maranghides and Mulholland 2003). The first fuel was a blend of heptane isomers (C_7H_{16}). Its soot yield was set at a constant 1.5 percent. The version of FDS used in the Investigation did not adjust the soot yield based on compartment ventilation or combustion efficiency. The second fuel was a mixture (40 percent/ 60 percent by volume) of toluene, C_7H_8 , and heptanes. Because FDS only considers the burning of a single hydrocarbon fuel, the mixture was taken to be C_7H_{12} with a soot yield of 11.2 percent. The radiative fraction for the heptane blend was 0.44; for the heptane/toluene mixture it was 0.39. The FDS Technical Reference Guide (McGrattan 2004) contains a discussion of how these parameters are interpreted in the simulations.

The heat release rate of the simulated burner was set to that which was measured in the experiments. No attempt was made to model the spray burner. Rather, it was assumed that the liquid fuel evaporated from the steel pan at a prescribed rate.

3.3 RESULTS

Six experiments were performed and the complete results can be found in NIST NCSTAR 1-5B. Tests 5 and 6 were replicates; thus, FDS simulations were performed for Tests 1 through 5. Only the results of Test 5 (using heptane as fuel) are shown here because it was the longest test and most representative of the duration of the WTC fires. The performance of the model for the other tests was very similar to that of Test 5. In Sections 3.4 and 3.5 the accuracy of the predictions and sensitivity of the input parameters are discussed.

3.3.1 Comparison of Gas Temperature

Upper and lower layer gas temperatures were measured in the experiments, using both aspirated and bare-bead thermocouples. For the purpose of model validation, the aspirated thermocouples were preferable because they greatly reduced the influence of external thermal radiation. Two vertical arrays of thermocouples were used, one on the inlet (west) side, near the centerline, and one on the outlet (east) side. Figure 3–2 displays the time histories of both measured and predicted compartment gas temperatures. The outlet or “exhaust” side of the compartment was hotter than the inlet side. The model was able to differentiate the hot side from the slightly cooler side.

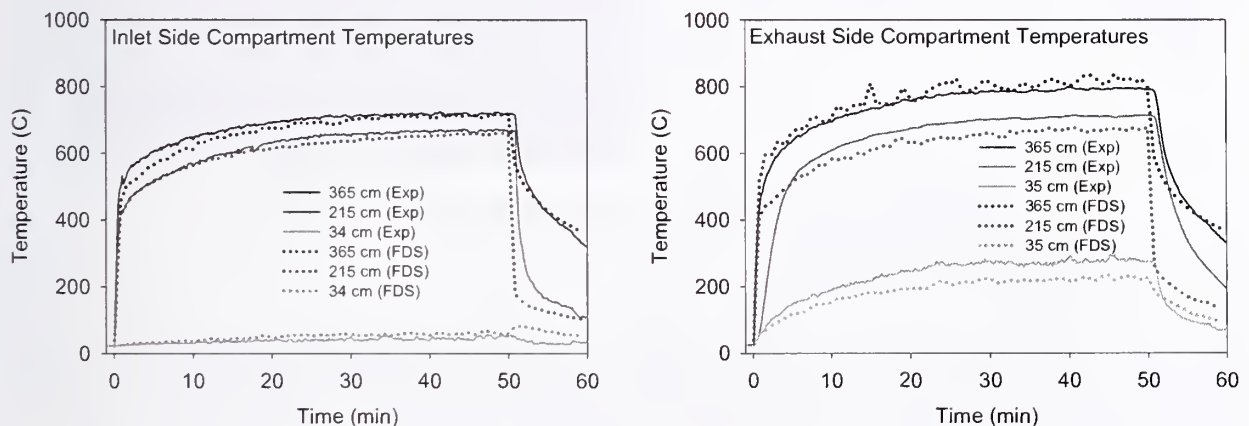


Figure 3–2. Comparison of gas temperatures, Test 5.

3.3.2 Comparison of Heat Fluxes to Targets

Heat flux gauges were positioned at various locations in both the upper and lower layers. Measured and predicted heat fluxes to the upper and lower section of the column, facing both towards and away from the fire, are shown in Fig. 3–3. Also shown are the heat fluxes to two floor targets roughly half a meter from the fire pan. These targets showed the greatest error in heat flux, probably because of their proximity to the fire. The overall distribution of energy throughout the compartment was handled properly by the

model as evidenced by the gas temperatures and heat fluxes to objects further away. However, from the picture included at right, the heat flux pattern near the pan was difficult to capture exactly.

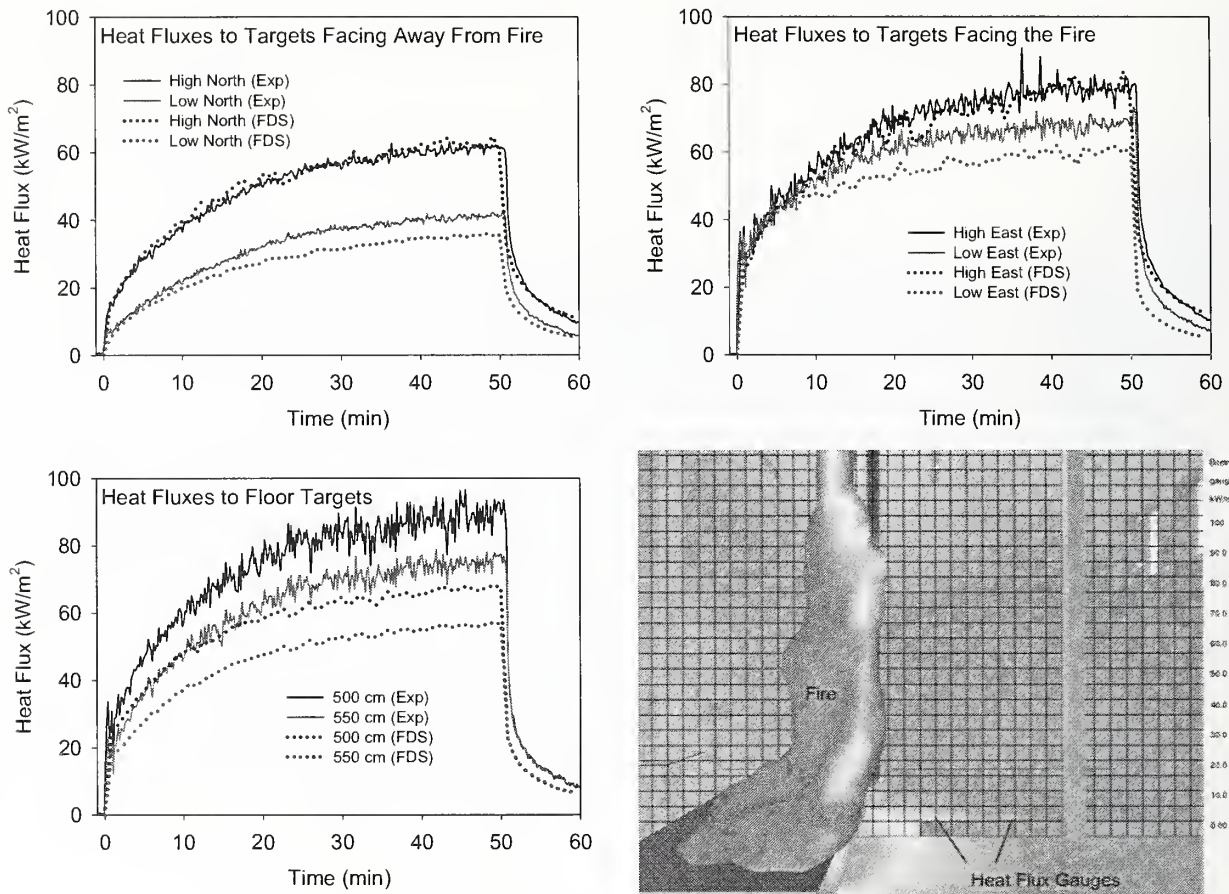


Figure 3–3. Heat fluxes to column and floor, Test 5.

3.3.3 Surface Temperatures

Bare-bead thermocouples were attached to the ceiling, walls and other objects within the compartment. In addition, several thermocouples were sandwiched between the two sheets of marinite that made up the outer wall. These thermocouples were used to test the model's prediction of conductive losses through the walls, an important component of the accounting of the overall energy budget. Ceiling surface temperatures and the corresponding inner temperatures are shown in Fig. 3–4. The three points chosen for comparison are along the centerline of the compartment – one directly over the fire (399 cm from inlet wall), one half a meter east of the fire (456 cm) and one out of the fire plume (612 cm). The model over-predicted the ceiling surface temperatures directly above the fire. There were two possible reasons for this: first, the thermal properties of the compartment lining (Marinite) were only known up to 500 °C. Second, the fire plume was observed to tilt more towards the south wall than was predicted by the simulation. Thus the plume impingement point on the ceiling was different. In any event, the inner surface temperature predictions were insensitive to the surface over-prediction, and the surface temperature predictions elsewhere in the compartment were in good agreement with measurement because there was no issue of fire impingement.

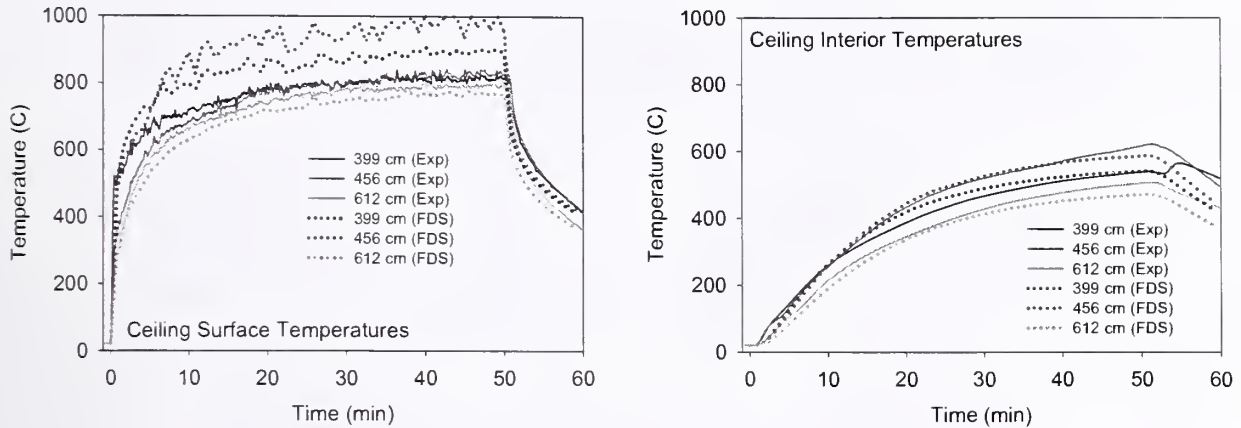


Figure 3-4. Comparison of ceiling surface and inner temperatures, Test 5.

3.3.4 Comparison of Gas Species Concentrations

FDS uses a mixture fraction combustion model, meaning that all gas species within the compartment are assumed to be functions of a single scalar variable. FDS solves only one transport equation for this variable and reports gas concentrations at any given point at any given time by extracting its value from a pre-computed “look-up table.” For the major species, like carbon dioxide and oxygen, the predictions are essentially an indicator of how well FDS is predicting the bulk transport of combustion products throughout the space. For minor species, like carbon monoxide, the version of FDS did not account for changes in combustion efficiency, relying only on a fixed yield of CO from the combustion product. In reality, the generation rate of CO changes depending on the ventilation conditions in the compartment. Figure 3-5 presents comparisons of the oxygen and carbon dioxide concentrations for Test 5.

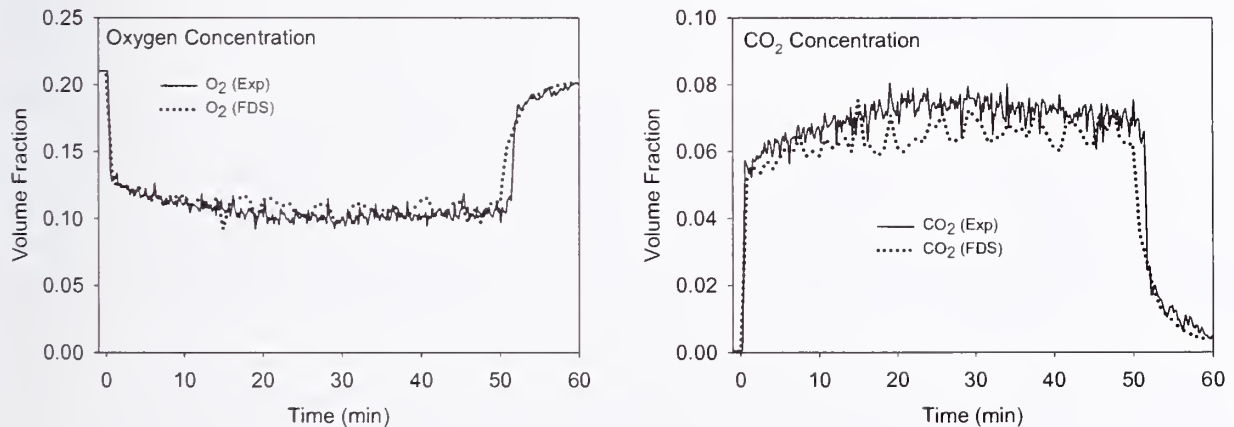


Figure 3-5. Comparison of oxygen and carbon dioxide concentrations, Test 5.

3.3.5 Comparison of Inlet and Outlet Velocity

Velocity probes were placed in both the inlet and outlet windows. Comparisons of experimental measurement and model prediction for Test 5 are shown in Fig. 3-6. The measurement labeled “Top” was

located 10 cm below the top of the window, just south of the compartment centerline. The “Middle” was slightly above the midpoint of the window. The “Bottom” was 15 cm above the base of the window.

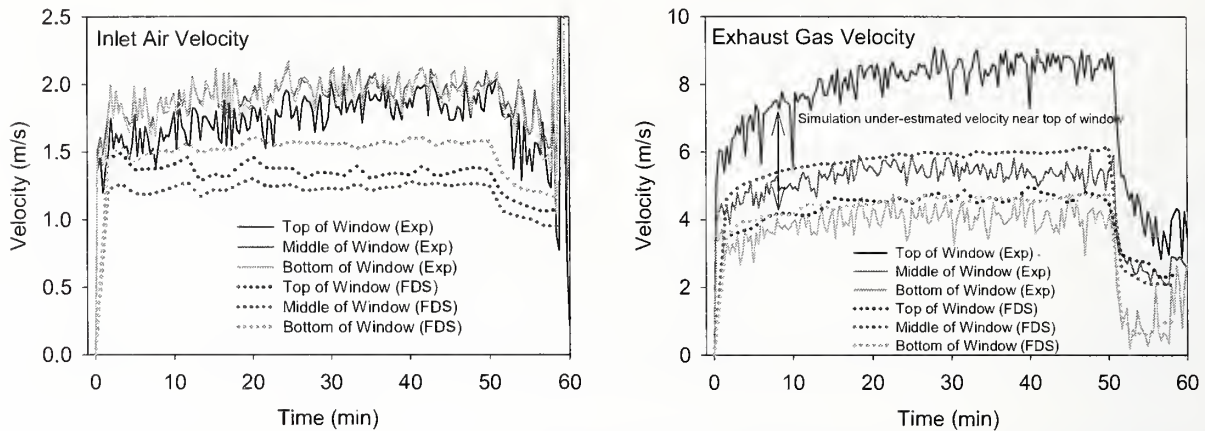


Figure 3–6. Comparison of gas velocities at the inlet and outlet, Test 5.

Measurements and predictions of gas velocity were difficult for this experiment. The measurements were made with bi-directional probes which were sensitive to placement and angular displacement (more details in NIST NCSTAR 1-5B). The predictions were difficult because the window was spanned only by seven cells in the vertical direction on the 10 cm grid. Although bulk flows of gases were predicted well by the model as evidenced by the temperatures and major gas species predictions, the detailed flow profile, especially at the exhaust outlet, could not be replicated. The greatest error was in the “Top” prediction of the exhaust flow. Here, hot gases exited the compartment by slipping under the soffit via a fairly narrow jet. This jet was spanned by at most two grid cells, and thus smeared out by the model.

3.4 MODEL ACCURACY

Overall, the agreement between the numerical predictions and the measurements was within experimental uncertainty for measurement locations not in the immediate vicinity of the fire (> 1 m). Near field comparisons (< 1 m) yielded differences that could not be attributed solely to experimental uncertainty. The good agreement in the far-field was due to the fact that the model predicted the upper layer temperature in most cases to within a few percentage points of the experiment. The heat flux to the walls and objects within the upper layer was dependent on the upper layer temperature according to $q = \epsilon \sigma T^4$, where T is the temperature, σ is the Stefan-Boltzmann constant and ϵ is the emissivity of the gas. From the measurements of the gas temperature and the heat fluxes in the upper layer, it appeared that the emissivity was nearly 1. This is a useful result because it tied the upper layer temperature to the heat flux to structural elements in the upper layer. Of course, all the measurement locations needed to be examined to determine where it could be assumed that the emissivity was effectively unity.

To better quantify the accuracy of the predictions, start with the measurement and prediction of the upper layer gas temperatures. An accurate prediction of compartment temperature depends on an accurate prescription of the heat release rate (HRR) of the fire. According to an empirical correlation by McCaffrey, Quintiere and Harkleroad (Walton and Thomas 2003), the rise in the upper layer gas temperature ΔT_g in a compartment is related to the overall HRR by the relation

$$\Delta T_g = 6.85 \left(\frac{Q^2}{A_0 \sqrt{H_0} h_k A_T} \right)^{1/3} \quad (3-1)$$

where:

Q = Heat Release Rate (KW)

A_0 = area of openings (m²)

H_0 = height of openings (m)

$h_k = k / \delta$; k = thermal conductivity of walls (kW/m/K); δ = wall thickness (m)

A_T = total area of compartment surfaces (m²)

What is of importance here is the fact that the temperature rise is proportional to the HRR raised to the 2/3 power. The reported uncertainty in the heat release rate measurement was 5 percent (one standard deviation). The 5 percent uncertainty in the HRR corresponds to a $2/3 \times 5\% = 3.3\%$ uncertainty in the temperature rise. For upper layer temperatures of approximately 600 °C, this translates to roughly ± 20 °C. The difference in upper layer temperatures for all the experiments ranged from 5 °C to 20 °C, consistent with the uncertainty estimate of the HRR. Even though there were uncertainties in the measurement of the temperature itself, the discrepancy between measurement and prediction can be accounted for solely in terms of the uncertainty in the HRR measurement.

The measured heat flux onto surfaces in the upper layer was nearly equal to σT^4 where $\sigma = 5.67 \times 10^{-11}$ kW/m²/K⁴ and T was the measured gas temperature in degrees K. In other words, the emissivity of the upper layer gases was nearly 1, not surprising given the high level of soot. Given the uncertainty in the upper layer temperature rise of 3.3 percent, the uncertainty in *absolute* temperature at 600 °C was 2.3 percent, leading to an estimate for the uncertainty in heat flux of $4 \times 2.3\% = 9.2\%$. For most of the tests, the difference between measurement and prediction was within 10 percent, confirming that the accuracy of the model output was within experimental uncertainty.

Figure 3–3 shows a comparison of heat flux measurements and predictions to two targets on the floor of the compartment. Because the targets were not within the upper layer, the simple σT^4 estimate of the heat flux no longer applied, and the assessment of experimental uncertainty was more difficult because it could not be traced back directly to the uncertainty in the HRR. Nevertheless, in most cases, the difference between measurement and prediction was within 10 percent. In cases where the difference was larger, as in Tests 4 and 5, it is possible that the model did not capture the near-field influence of the fire itself. One of the floor targets was near the fire pan, and subtle differences between the real and simulated fire dynamics could have had a substantial impact on the heat flux to a nearby target.

The accuracy of the ceiling surface temperatures was a function of the distance away from the plume impingement point. Predictions of surface temperatures at points outside of a circle of roughly 1 m radius agreed with measurements to about 5 percent. Predictions within the plume impingement zone were in greater disagreement with experiment, about 20 percent. This was not surprising since the point of plume impingement changes throughout the test. Although the experiments were designed to be symmetric along

the centerline of the compartment, the inclusion of the column and instrumentation tunnels on one side of the compartment apparently caused the flow in the compartment to be asymmetric, and the fire was observed to lean towards the trusses, which were positioned south of the centerline (foreground of Fig. 3-1). The simulation captured the asymmetry as well, but it did not appear to be as pronounced as in the experiment. As a result, the ceiling surface temperature predictions above the fire were noticeably higher than the experiment because the actual impingement point of the plume was not instrumented.

The comparison of oxygen and carbon dioxide prediction and measurement at one sampling point (Fig. 3-5) indicated that FDS modeled the bulk transport of gases well. In the first three tests, the CO₂ prediction was indistinguishable from the experiment, and the oxygen predictions differed from the measurements by about 5 percent. In the simulation, both oxygen and CO₂ were tied to the mixture fraction, a single scalar for which FDS solves a transport equation. The prediction of CO was not expected to agree with the experiment since it was assumed in the model that its yield was constant. In reality, the yield of CO changed over the course of the experiments, increasing as the room filled with combustion products.

The comparison of inlet and outlet velocities revealed that the model predicted well the mass flow of air into the compartment, but it could not resolve the details of the outlet velocity profile due to the coarseness of the numerical grid. The model used 10 cm grid cells, meaning that the outlet window was spanned by seven cells in the vertical direction. Whereas the inlet velocity was fairly uniform over the height of the window, the outlet velocity varied by at least 3 m/s from top to bottom. Plus, the position of the probes relative to the depth of the opening was important because the probes were designed to measure the velocity within a certain range of angular displacement.

3.5 MODEL SENSITIVITY

In the discussion above, it was shown that predicted upper layer temperatures and heat fluxes were within the uncertainty range of the experiment. For this exercise it was assumed that the uncertainty in the experimental results was based largely on the uncertainty of the heat release rate measurement. Thus, it was shown how *sensitive* the upper layer temperature and heat flux measurements were to the heat release rate. In the numerical simulations there were dozens of user-prescribed input parameters. It was difficult to assess the sensitivity of each of these parameters except by numerical experiment; that is, running the model with small changes to the base parameters to see what effect these have on the predictions.

There are two types of input parameters: numerical and physical. Physical parameters describe the wall materials, fuel properties, reaction stoichiometry, etc. Numerical parameters describe how the calculation is to be performed. Following is a description of the various parameters and their effect on the results, starting with the numerical parameters.

3.5.1 Grid Size

The most important numerical parameters are the number of grid cells in each coordinate direction. Computational fluid dynamics (CFD) models solve an approximate form of the conservation equations of mass, momentum and energy. The error associated with the discretization of partial derivatives on a discrete grid is a function of the size of the grid cells and the type of differencing used. FDS uses second-order accurate approximations of both the temporal and spatial derivatives of the Navier-Stokes

equations, meaning that the discretization error is proportional to the square of the cell size. In other words, reducing the grid cell size by a factor of 2 reduces the discretization error by a factor of 4. However, it also increases the computing time by a factor of 16 (a factor of 2 for the temporal and each spatial dimension). Clearly, there is a point of diminishing returns as one refines the numerical mesh. Determining what size grid cell to use in any given calculation is known as a *grid sensitivity study*.

The simulations of the spray burner experiments were performed on a grid whose cells were 10 cm cubes. However, the simulations of the fires in the WTC were performed with grid cells of dimension 0.5 m by 0.5 m by 0.4 m high. Suppose this more coarse mesh were used to simulate the spray burner experiments. An obvious problem was that many of the obstructions in the test compartment could not be resolved on a half meter grid, especially the small windows on either side of the space. A remedy for the problem was to maintain in the coarse calculations as many geometrical features as possible. For example, the exit windows in the coarse calculation had approximately the same total area and soffit height as in the refined calculations. The trusses, bars and column were removed from the coarse calculation, but the barrier in front of the fire remained. Figure 3–7 presents a comparison of the predicted temperatures from the coarse calculation of Test 5 with the experimental measurements (compare with Fig. 3–2). The results were encouraging, although it should be emphasized that as a rule coarsening a numerical grid to the extent done here will not yield such good results.² The reason for the good agreement is that in the experiment, a very stable, uniform layer of hot gases was established in the upper layer of the compartment over the course of an hour. Given a fixed HRR and a comparable convective flux of energy through the windows, energy conservation dictated that the compartment temperatures should have been comparable between calculation and experiment. Even two-zone lumped parameter models that are often used in fire protection engineering would be expected to yield a good prediction in this case due to the uniformity of the upper and lower layers within the compartment. In a stably stratified compartment with fairly uniform upper and lower layer, both a CFD model and zone model will make similar predictions of temperature because both assume conservation of mass and energy. The behavior of the flow field as predicted by the momentum conservation equation was not as important *in this case*, so long as the enthalpy flow through the compartment windows was captured by both the fine and coarse meshes. However, the prediction of the temperature and heat flux to various objects in the compartment near the fire plume were subject to more uncertainty than suggested by the results shown because the flow dynamics were greatly simplified by the coarse mesh. This was less of a concern for the simulations done as part of the WTC Investigation because the heat flux to the structural members was computed using the upper layer temperature field. Indeed, the FDS simulations of the WTC fires did not include the floor trusses because these objects could not be resolved on the coarse grid.

² The simulation of the hour-long experiment on the coarse grid required only a half hour of computing time on a Pentium 4, 240 MHz personal computer.

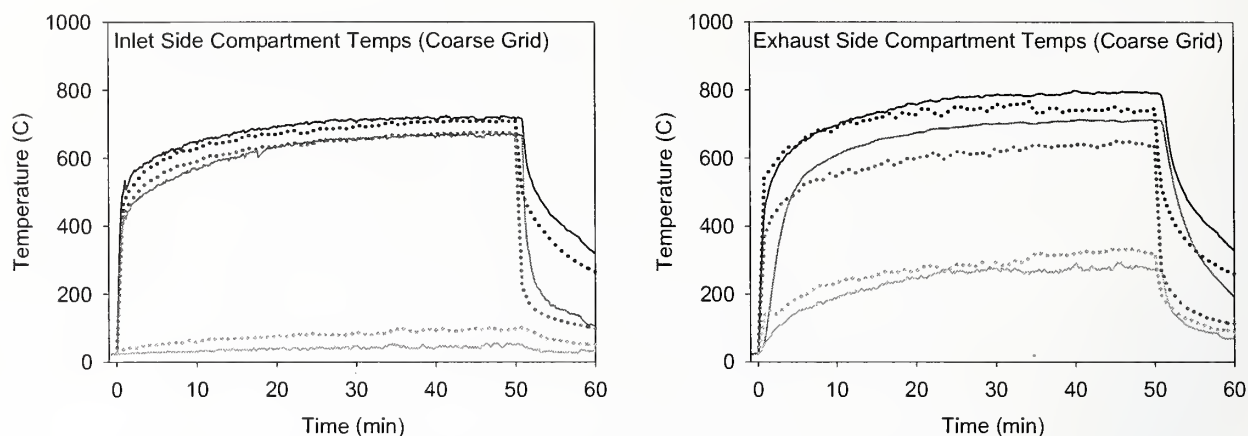


Figure 3–7. Coarse grid prediction of intake side temperatures for Test 5.

3.5.2 Compartment Geometry

Beyond the numerical grid, there were numerous physical parameters prescribed to simulate the experiments, including the physical dimensions of the compartment and the objects within. Because one of the objectives of the experiments was model validation, the geometry was very simple. With a 10 cm numerical grid, the compartment was modeled to an accuracy of ± 5 cm, and there were no detectable differences in results based on small adjustments made to objects to fit the nearest grid cell. With the 50 cm grid, however, there were significant differences in the results if proper attention was not paid to adjusting the windows to maintain the area and soffit height. A 20 cm shift in the height of the top of the window led to a change in the hot upper layer depth of the same amount, resulting in changes of upper layer temperature on the order of 100 °C. Based on these findings, the cell size for the WTC simulations was selected to maintain the window area and height. The external columns of WTC 1 and WTC 2 were spaced by the designers 40 in. (1.016 m) apart. The horizontal dimensions of the grid cells used were 50 cm, yielding an alternating pattern of solid column, window, column, window, etc.

3.5.3 Heat Release Rate

As important as the compartment geometry was the total HRR from the fire. According to the correlation given in Eq. 3–1, the upper layer temperature is proportional to the HRR raised to the $2/3$ power. This means that a 10 percent increase in the HRR will lead to a $2/3 \times 10 = 6.7$ % increase in relative temperature. It is important to note that the MQH correlation is based on fire test data with temperatures not exceeding 600 °C. In the exercise carried out here, the upper layer temperature was about 750 °C. Nevertheless, it was useful to test the correlation. The simulation of Test 5 was re-run using a 10 percent increase in the measured HRR. The result was a 9 percent increase in the upper layer temperature. Although larger than the theoretical increase, the increase seen in the simulation was not unexpected, given the simplifications made to derive Eq. 3–1 and the fact that it is not necessarily valid for higher temperatures. The important idea is that upper layer temperature is nearly proportional to the HRR, reinforcing a widely accepted principle of fire protection engineering.

3.5.4 Thermal Radiation

Along with the HRR, another parameter of importance to fire models is the radiative loss from the fire. Room-scale fires typically radiate about 1/3 of their energy, with the other 2/3 of the energy rising to form the smoke plume. Often the radiative loss fraction is a user input to fire models because a prediction of it requires a fairly detailed model of the combustion processes. FDS uses a partial approach to the problem. Based on the predicted fire temperature and chemical composition, it computes the source term in the radiative transport equation, thus predicting the radiative loss from the fire. However, since the temperature and chemical composition within the fire are subject to uncertainty due to the coarseness of the numerical grid, the algorithm will use a user-prescribed radiative loss fraction instead of its own prediction if that prediction is lower than what the user believes it ought to be. In short, the user has the power to over-ride the FDS prediction if he thinks it is warranted. To ensure that the results of the simulations were not sensitive to the user-prescribed radiative loss fraction, several simulations were performed with prescribed loss fractions between 0.3 and 0.4. There was no discernable difference in the results. Again, this is not always the case. Compartment geometry is important, particularly the ceiling height. Also, in these tests, the hot upper layer was as important a radiator as the fire. The prescribed loss fraction only pertained to the fire. The radiative heat transfer within the hot upper layer was not prescribed, but rather computed based on the local temperature, soot volume fraction and species concentration.

3.5.5 Wall Materials

Other physical parameters prescribed by the user included the thermal properties of the wall material. In this case, the walls were lined with a 2.5 cm (1 in.) layer of calcium silicate board (tradename: Marinite I). The manufacturer provided the thermal properties of the material, including the thermal conductivity. To determine the sensitivity of the model to this parameter, a simulation was performed with the thermal conductivity doubled from its listed value of 0.12 W/m/K to 0.24 W/m/K. The predicted upper layer temperatures of Test 5, the hour-long 3 MW fire, decreased only 4 percent due to the doubling of the conductivity. This suggested that these simulations were not especially sensitive to the thermal properties of the wall materials, *although this is not always true*. In this case, of the 3 MW of energy generated in the compartment by the fire, more than half flowed out the windows, either as thermal radiation or hot gases. The increase in conductivity meant more energy was being conducted through the walls, but since the walls conducted a small amount of the total energy, the increased loss did not affect the overall compartment temperature appreciably. If the compartment were of different dimension, aspect ratio, or ventilation, the thermal conductivity might have played more of a role.

3.5.6 Smoke Production

Parameters associated with the combustion process were also tested. The smoke yields of the heptane and heptane/toluene mixture were obtained during free burns of the two fuels. The smoke yield is the fraction of fuel mass that is converted into soot via the combustion process. In a ventilation-limited fire, the soot yield will usually increase due to the decrease in combustion efficiency. What effect can the increased soot yield have on the temperature predictions? The soot yield for the heptane fires was measured to be 0.014. Increasing this value to 0.10 produced a 1 percent increase in the upper layer temperature prediction. The reason for this was that the upper layer was nearly optically thick, that is, the emissivity of

the smoke was already nearly 1. Adding more soot to the layer only blackened what was already essentially black. The radiative heat transfer within the layer and to external targets was not affected.

3.6 SUMMARY

The purpose of the spray fire experiments and simulations was to quantify the uncertainty of FDS for a fire scenario in which the fire and compartment were very well characterized. Using a well-established correlation between the compartment temperature and the heat release rate of the fire, it was possible to propagate the uncertainty in the measurement of the heat release rate to the measurement of the upper layer temperature and then finally to the measurement of the heat flux to the walls and structural members. The FDS predictions fell within the uncertainty bounds of the gas temperatures, which implied that the model was accurate to within 10 percent of the measurements of upper and lower layer temperatures. This is important because in the analysis of the WTC fires, FDS was used to predict the gas temperatures in the vicinity of the floor trusses, and these temperatures were transferred, via the Fire-Structure Interface (FSI), to a detailed model of the thermal response of the structural components (trusses, columns, floor slabs).

FDS predictions of heat flux and solid surface temperatures *were not* transferred to the solid phase thermal model via the FSI, but nevertheless these calculations were important in the fire simulations as the surface temperatures provided thermal boundary conditions for the gas phase calculation. Heat fluxes to, and temperatures of, solid surfaces greater than about 1 m from the fire were predicted to within experimental uncertainty (10 percent). Ceiling surface temperature predictions above the fire were within 20 percent of the measurements, as were heat flux predictions to points on the floor near the fire. The greater uncertainty in near-field predictions was due to a combination of limited spatial resolution of the numerical grid, simplification of the combustion and radiation processes, and differences between model and actual burner geometries. For example, the steel pan into which the fuel was sprayed deformed during the tests due to the extreme temperatures, possibly causing a larger shift in the plume centerline than was predicted in the simulation. These types of errors were not expected to adversely affect the outcome of the WTC calculations because the fires were spread over a wide area and the thermal gradients were not as large as in the single fire compartment tests.

In addition to checking the accuracy of the model, the experiments also served as a means to check the sensitivity of the model to changes in input parameters, both numerical and physical. One of the most important parameters prescribed by the model user is the size of the numerical grid. Simulations of all the tests were performed with grid cells 10 cm by 10 cm by 10 cm, and the results were reported here. Several tests were also simulated using a coarse grid 50 cm by 50 cm by 40 cm, the same as was used to perform the simulations of the WTC fires. The upper layer temperature predictions did not differ appreciably from those of the fine grid simulation, supporting the use of the coarse grid in the WTC simulations. Changes in various other physical parameters, like the thermal conductivity, also did not significantly change the results. This was important because the initial and boundary conditions in the WTC simulations were far less certain than those of these experiments.

3.7 REFERENCES

- Hamins, A., A. Maranghides and G. Mulholland. 2003. The Global Combustion Behavior of 1 MW to 3 MW Hydrocarbon Spray Fires Burning in an Open Environment. NISTIR 7013. National Institute of Standards and Technology, Gaithersburg, MD, June.
- McGrattan, K., J. Floyd, G. Forney, H. Baum and S. Hostikka. 2003. Improved Radiation and Combustion Routines for a Large Eddy Simulation Fire Model. *Fire Safety Science -- Proceedings of the Seventh International Symposium*. International Association for Fire Safety Science.
- Walton, W.D. and P.H. Thomas. 2003. Estimating Temperatures in Compartment Fires. *Fire Protection Handbook, 3rd Ed.* National Fire Protection Association, Quincy, MA.

This page intentionally left blank.

Chapter 4

MODEL ACCURACY ASSESSMENT – WORKSTATION FIRES

4.1 OVERVIEW

Following the completion of the initial spray fire experiments, the experimental program concentrated on the thermal properties of the office furnishings that constituted the bulk of the combustible fuel within the World Trade Center (WTC) buildings under study. Several types of office workstations typical of those used in WTC 1 and WTC 2 were purchased at area office supply stores. The thermal properties of the major materials making up the workstations were derived from cone calorimeter experiments (NIST NCSTAR 1-5C). These properties were input into the Fire Dynamics Simulator (FDS), which was used to simulate experiments in which single office workstations were burned in the open under a hood that was used to measure the heat release rate. The thermal and combustion properties of the workstation components were adjusted slightly so that the model prediction of the heat release rate would match the experiment. The adjustment was necessary because some of the material samples burned in the cone calorimeter displayed different behavior than in the full-scale tests. For example, the plastic laminate of the desktop separated from the wooden pressboard in the cone because the sample size was only 10 cm.

Following the single office workstation burns, the model was used to predict the heat release rates from a series of experiments in which three workstations of various conditions were burned within a large enclosure. The purpose of this exercise was to improve confidence that FDS could simulate the dynamics of a fire in settings similar to WTC 1, 2, and 7.

4.2 DESCRIPTION OF THE WORKSTATION COMPONENTS

A detailed description of the various materials making up the office workstation is given in NIST NCSTAR 1-5C. Briefly, cone calorimeter experiments at three different heat fluxes were performed for the carpet, desk (wood), computer monitor, chair, privacy panel, and stacked paper. For the simulations of the WTC fires, only the carpet, desk and privacy panel data was used directly. The carpet and privacy panel were modeled as thermoplastics, that is, the burning rate was assumed to be proportional to the heat flux from the surrounding gases. The desk was modeled as a charring solid in which a pyrolysis front was assumed to propagate through the material, leaving a layer of char behind that insulated the material and reduced the burning rate. Details of the pyrolysis models can be found in the FDS Technical Reference Guide (McGrattan 2004).

The thermal properties of the wood of the desktop and its char were taken from both the calorimeter experiments and the work of Ritchie et al. (1997). The desk was 2.8 cm thick with density 450 kg/m^3 , specific heat 1.2 kJ/kg/K at $20 \text{ }^\circ\text{C}$ and 1.6 kJ/kg/K at $900 \text{ }^\circ\text{C}$, conductivity 0.13 W/m/K at $20 \text{ }^\circ\text{C}$ and 0.16 W/m/K at $900 \text{ }^\circ\text{C}$. The ignition temperature was $360 \text{ }^\circ\text{C}$, and the heat of combustion was $14,000 \text{ kJ/kg} \pm 800 \text{ kJ/kg}$. Its total available energy content was estimated to be $210 \text{ MJ/m}^2 \pm 50 \text{ MJ/m}^2$.

The carpet was modeled as a thermoplastic, meaning the burning rate was assumed to be proportional to the heat flux from the surrounding gases. Its density was 750 kg/m^3 , specific heat 4.5 kJ/kg/K ,

conductivity 0.16 W/m/K, ignition temperature 290 °C, thickness 6 mm, heat of vaporization 2,000 kJ/kg, heat of combustion 22,300 kJ/kg \pm 600 kJ/kg. Its total available energy content was 61 MJ/m² \pm 2 MJ/m².

The privacy panel was modeled as a thermally-thin thermoplastic. The product of specific heat, thickness and density was 0.73 kJ/m²/K. Its surface density was 0.25 kg/m², ignition temperature 380 °C, heat of vaporization 6,000 kJ/kg, heat of combustion 30,000 kJ/kg \pm 500 kJ/kg. Its total available energy content was 6.0 MJ/m² \pm 1.3 MJ/m².

The compartment walls and ceiling were made of three layers of 1.27 cm (0.5 in.) thick Marinite I, a product of BNZ Materials, Inc. (<http://www.bnzmaterials.com>). The manufacturer provided the thermal properties of the material used in the calculation. The density was 737 kg/m³, conductivity 0.12 W/m/K. The specific heat ranged from 1.2 kJ/kg/K at 93 °C to 1.4 kJ/kg/K at 425 °C.

In the simulations of the fires within the WTC, the chair, computer, paper, and other miscellaneous items within the workstation were modeled as a composite material by lumping their mass together into large “boxes” and distributing them throughout the workstation. It is common practice in fire protection engineering to use surrogate materials for fire experiments, and this practice has been extended to numerical modeling. Over the years, simple, well-characterized combustibles have been developed that are representative of more complicated commercial products. For example, wood cribs are often used to represent ordinary combustibles found in residential or light industrial settings. Paper cartons with various amounts of plastic within are also used as surrogates for a wide range of retail commodities. One in particular is called the FMRC (Factory Mutual Research Corporation) Standard Plastic Commodity, or more commonly, Group A Plastic. This test fuel is often used in sprinkler approval testing at Factory Mutual and Underwriters Laboratories in the United States, and similar test fuels have been developed in Europe. In the late 1990s, FDS was used to simulate large scale rack storage fires to determine the effectiveness of the combined use of sprinklers, roof vents and draft curtains (curtain boards). As part of this effort, a considerable amount of work was done to characterize the thermal properties of Group A Plastic (Hamins and McGrattan 2003). Because Group A Plastic has been shown to be fairly representative of fires fueled by a mixture of paper (cellulosic materials) and plastic, and because it has been used in numerous FDS simulations, it was decided to model the miscellaneous contents of the office workstations with a fuel similar to Group A Plastic. Blind predictions of the single open workstation burns were made using the material properties obtained during the sprinkler/roof vent study, and then these properties were adjusted to match the results of the experiments. Thus, the single workstation burns served to *calibrate* the model. They were not intended as *validation* experiments. Figures 4–1 and 4–2 show a typical office workstation before and during a burn.



Source: NIST.

Figure 4–1. Typical office workstation.



Source: NIST.

Figure 4–2. Single office workstation burning at peak intensity.

The surrogate fuel, to be referred to as “miscellaneous combustibles,” was modeled as a homogenous solid whose density was 172 kg/m^3 . The paper carton was treated as a thermally-thin material whose density \times specific heat \times thickness was $1.0 \text{ kJ/m}^2/\text{K}$. Its ignition temperature was set to $370 \text{ }^\circ\text{C}$, and the heat of combustion was $30,000 \text{ kJ/kg}$. When the local surface temperature increased above the ignition temperature, it was assumed that this area of the object’s surface would begin burning and reach a heat release rate of 450 kW/m^2 in roughly 1 min. Note that this fuel package was similar, but not the same, as Group A Plastic.¹ The density was increased to account for the total mass of the miscellaneous combustible items within the workstation. Also note that unlike the desk, partition and carpet, the “miscellaneous combustibles” were simply given a burning rate rather than a heat of vaporization, meaning that these objects were assumed to burn at the given rate regardless of the heat flux upon them. The reason for this was that it was not possible to predict the burning rate using the heat feedback approach because the geometry of the real combustibles was too complex to predict directly the response of the materials to the thermal insult. By collecting all the scattered items into idealized boxes, the geometry of the combustibles was greatly simplified, and as a result the burning behavior had to be simplified as well.

Several open burns of single workstations were performed as part of the WTC Investigation. These burns served to check that the assumptions made in modeling the workstation with the simplified fuel packages would produce reasonable results. Figure 4–3 shows a comparison of the heat release rates (HRR) of four workstation fires with the FDS predictions (clockwise from upper left: undamaged workstation, undamaged workstation with ceiling tiles partially covering the desktop and floor, workstation sprayed with jet fuel and covered with obstructions, workstation sprayed with jet fuel). Note that the peak HRR in some of the simulations occurred sooner than in the experiments. In the experiments, the time to peak HRR was strongly influenced by the melting of the chair plastic onto the carpet. This level of detail was not captured in the numerical model, especially given the fact that the chair had been lumped together with various other combustible items. What was important was the fact that the model and experimental HRR curves had the same basic form, peak HRR, and duration. When inputting the simulated workstations into the calculations for WTC 1, 2, and 7, the discrepancies in HRR seen in the experiments were outweighed by the uncertainty in the exact combustible content of the various building tenants. In fact, it would have been possible to further refine or “tune” the properties of the simulated workstations to better match the experiments, but this would have been a waste of time and resources since the workstations were merely convenient surrogates for a variety of other combustible furnishings found throughout the buildings. Indeed, sensitivity studies revealed that the total mass loading of combustibles was more important than its composition. More discussion of this issue is included in Chapter 5.

¹ To account for the lower burning rate of damaged furnishings, the heat release rate of the surrogate was lowered from 450 kW/m^2 to 300 kW/m^2 . To increase or decrease the overall combustible load of an entire floor, the density of the surrogate fuel was adjusted accordingly.

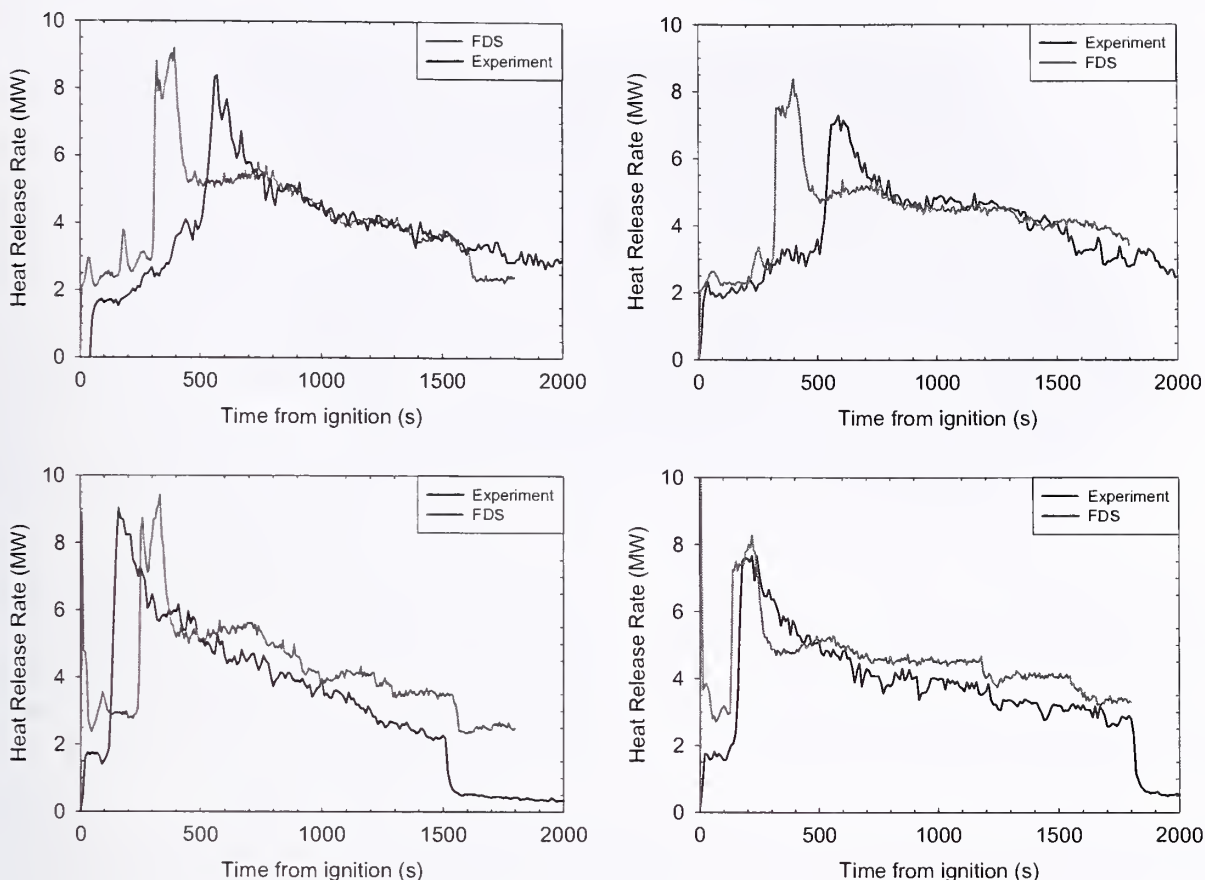


Figure 4–3. Heat release rates for the single workstation fire experiments.

4.3 DESCRIPTION OF THE MULTIPLE WORKSTATION SIMULATIONS

The following is a brief discussion of the experiments involving multiple office workstations burning within an enclosure. A complete description of the experiments is given in NIST NCSTAR 1-5E.

The geometry of the compartment was relatively simple. The overall enclosure was rectangular, as were the vents and most of the obstructions. Numerical grids of 25 and 50 cm cells were used to model the fires. The purpose of the grid variation was to ensure that the model was not sensitive to the change in grid cell size. Typically, enclosures of this size are modeled using 10 cm grid cells. However, for the simulations of WTC 1, 2, and 7, a 50 cm by 50 cm by 40 cm grid was used. The purpose of simulating the experiments at 25 and 50 cm was to test if the model produced significantly different results with grid cells of different sizes.

Figure 4–4 is a snapshot of a simulation showing the fire and the major geometric features of the compartment for the simulations. Note that the objects representing “miscellaneous combustibles” were placed roughly where the computer monitor, chair and paper were located. A 2 MW burner was placed either near the windows of the compartment overlooking Workstation 1 in Tests 1, 2, and 3, or towards the rear of the compartment overlooking Workstation 2 in Tests 4, 5, and 6.

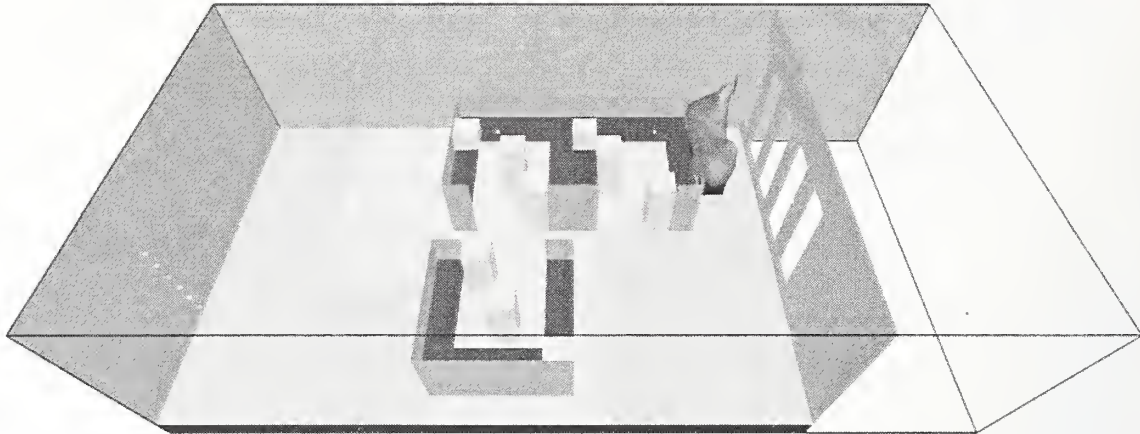


Figure 4–4. Geometry of the multiple workstation simulations.

In Tests 3, 5, and 6 Jet A fuel was poured over the workstations and surrounding carpet. To simulate this in the model, spray nozzles were positioned over the center of each workstation, 2 m above the floor. These nozzles are normally used to simulate water sprinklers, but in this case, the water was replaced by a liquid having similar properties to Jet A. The nozzles were activated for 2 s, in which time the equivalent amount of liquid as in the tests was ejected and spread over the furnishings.

In Test 5, Workstations 1 and 2 were disassembled prior to the burn, and the contents were piled on top of the respective load cells (see Fig. 4–5). To model this scenario, the burning rate of the collective fuel packages was reduced by one half to account for the decrease in burning area of the fuel pile. The choice of one half was based on the test results because no free burns of damaged workstations had been performed. Thus, Test 5 was not a prediction, but rather, a crude calibration.



Source: NIST.

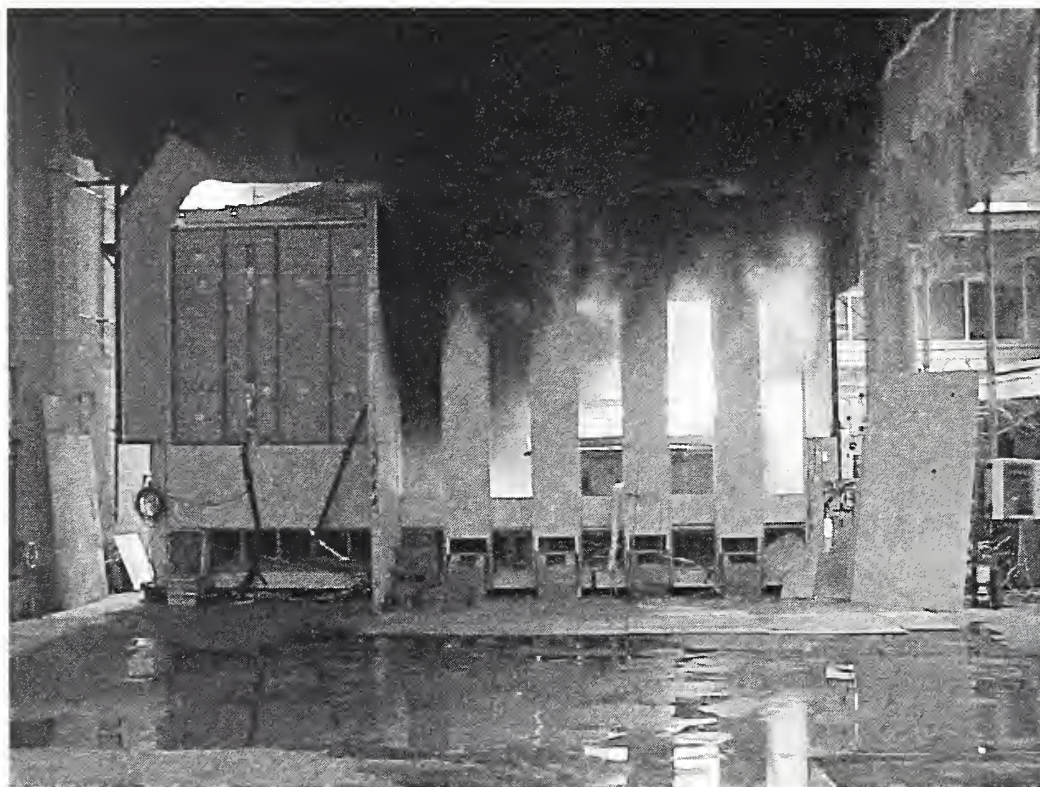
Figure 4–5. Disassembled workstation burned in Test 5.

4.4 RESULTS AND DISCUSSION

Six experiments were performed within the compartment, of which five were simulated because Tests 1 and 2 were replicate tests. Figures 4–6 and 4–7 show pictures of an actual test and a corresponding simulation. Both the heat release rate and the compartment temperatures were compared. Figure 4–8 displays comparison plots of measured and predicted heat release rates. Figure 4–9 displays the upper layer temperature for Test 1 at four locations (clockwise from upper left: near window, between workstations, behind workstations, rear wall). The measured and predicted temperatures for all the tests were similar to those shown in Fig. 4–9. Peak temperatures near the compartment opening were about 1,000 °C, decreasing to 800 °C at the very back of the compartment. The trend was captured in the simulations. The decrease in temperature was important because in the simulations of the WTC fires, the only basis of comparison was the visual observations of fires around the exterior of the buildings. It was important to demonstrate that the model not only predicted accurately the temperature near the windows, but also the decrease in temperature as a function of distance from the windows. The temperature predictions for the other tests were similar and are included in NIST NCSTAR 1-5E.

The heat release rate and temperature predictions shown in Figs. 4–8 and 4–9 were made using a 50 cm by 50 cm by 40 cm grid, the same as was used for the final WTC calculations. Results were similar with the 25 cm by 25 cm by 20 cm grid. The reason for the agreement was that the burning rate of the workstation assemblies was largely a function of the heat feedback from the hot upper layer. Given that the peak upper layer temperatures were similar in each case, the burning rates were similar. Note that the grid independence demonstrated in both the spray burner and the workstation fire simulations is not guaranteed for all applications of the fire model. Indeed, the simulation of small fires (relative to the overall compartment size) demands a much finer grid than the one used in the WTC Investigation because of the model's tendency to smear out steep gradients on coarse grids. However, if the fires are large enough to form a relatively uniform layer over an appreciable expanse of the compartment ceiling, the model is far less sensitive to the size of the grid cells so long as there are enough of them spanning the uniform regions. This was the case for all of the WTC simulations.

The model also captured the major features of the individual tests. For example, Tests 1 and 4 were similar in design except for the burner location. In Test 1, the burner was near the windows; in Test 4, it was near the rear of the compartment. The peak heat release rate was reached in about 15 min in Test 1, whereas it was reached in about 10 min in Test 4. The model showed a similar trend. The faster growth of Test 4 was probably due to the fact that the compartment heated up more quickly with the fire deep inside rather than near the windows, leading to more rapid spread of the fire across the pre-heated furnishings. Even though ceiling tiles were distributed over the desk and carpet in Test 4, this did not seem to have a noticeable effect on the growth, or at the very least, the burner position seemed to have a far greater role in explaining the difference between Tests 1 and 4.



Source: NIST.

Figure 4–6. Multiple workstation fire experiment.

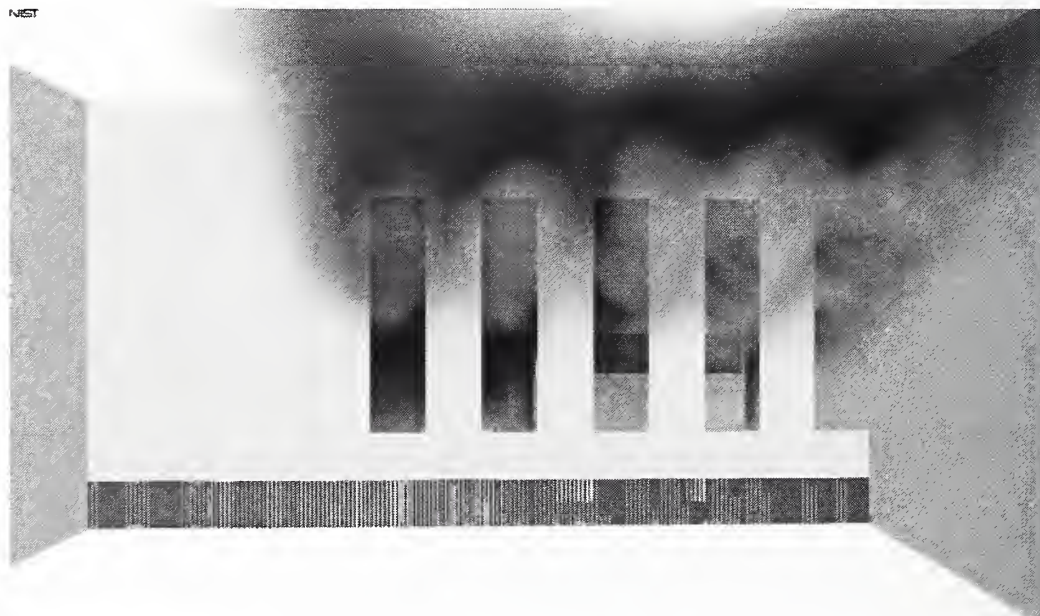


Figure 4–7. Coarse grid simulation of a multiple workstation experiment.

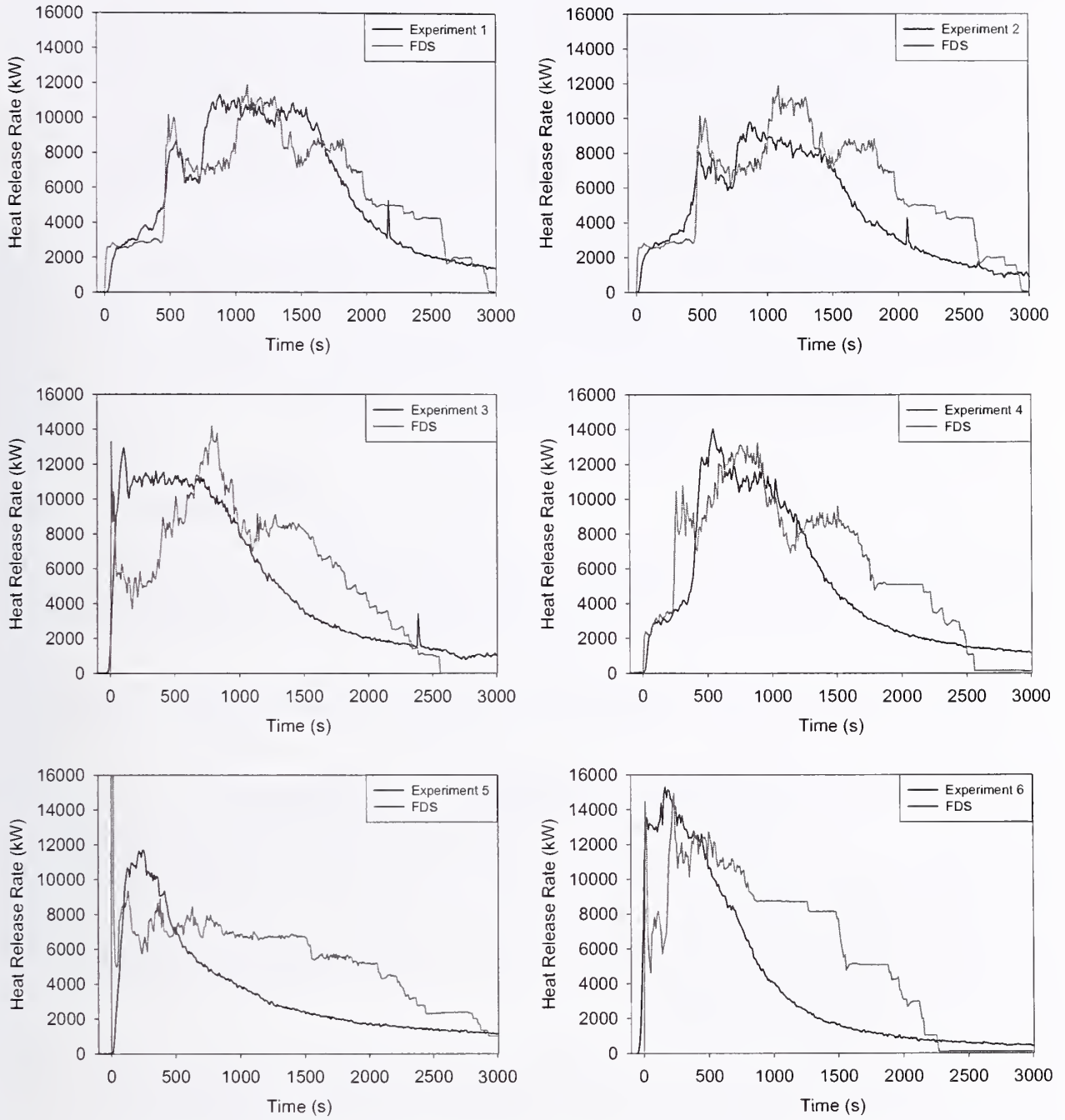


Figure 4–8. Heat release rates for multiple workstation experiments.

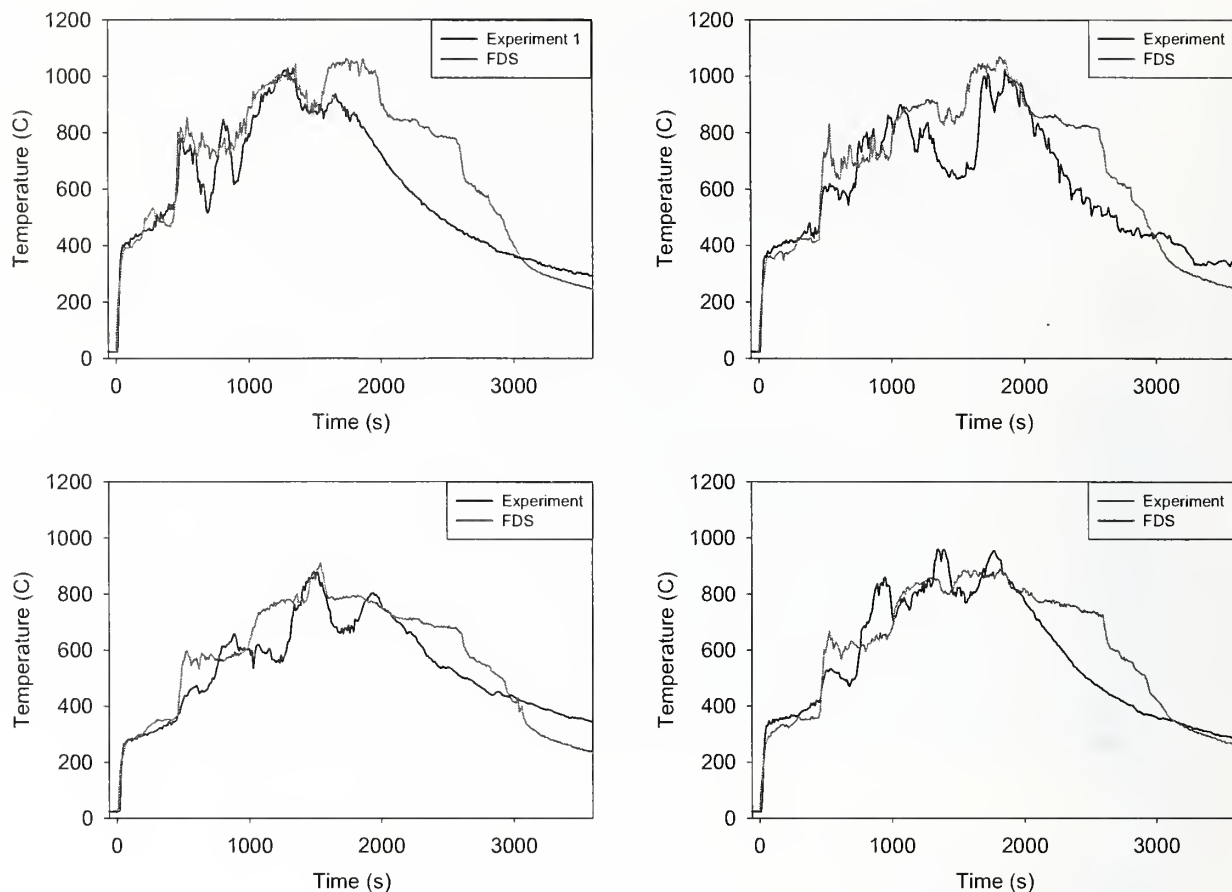


Figure 4–9. Upper layer temperatures at 4 locations, Test 1.

The predicted time histories of HRR for Tests 3, 5, and 6 showed a spike at the start of the simulations. This was due to the fact that FDS used a mixture fraction, or “mixed is burnt,” combustion model where vaporized fuel burned immediately upon mixing with the oxygen in the air. This spike was not seen in the experimental data since the fuel was absorbed more readily by the furnishings and, thus, required more time to burn. The jet fuel significantly decreased the time to peak HRR, and this effect was captured by the model following the initial spurious spike.

The most difficult test to model was Test 5, in which two of the workstations were disassembled and left in a pile. There were no free burns of this type of “rubble pile,” so the model parameters were altered in this case by reducing the burning rate of the fuel from 450 kW/m^2 to 300 kW/m^2 while maintaining the same fuel mass. From the results, it was evident that this was an over-simplification, but the National Institute of Standards and Technology (NIST) decided not to explore the issue further. As will be discussed later, the burning rate of “rubble” was one of the parameters for which sensitivity analyses were performed.

4.5 SUMMARY

From a modeling perspective, the objective of the simulations of the single and multiple workstation fires was to develop a simplified representation of the office furnishings found throughout the WTC, and then

demonstrate that the fire model was capable of reproducing the thermal environment of a compartment filled with these furnishings. Because of the magnitude of the simulations of the building fires, the model of the workstation had to be fairly simple. However, because of the many uncertainties in the initial conditions of the fire simulations, the lack of detail in the model was not considered to be a problem. The model fires had similar growth patterns, peak heat release rates, decay patterns, and compartment temperatures. All agreed with measurements to within about 20 percent, an accuracy that was sufficient given the uncertainty in the state of the building and its furnishings following the impact of the airplanes.

The office workstation was considered a surrogate for a wide variety of furnishings found throughout the WTC. It would have been impossible to analyze and burn every item known to have been in the buildings, and even if it were possible to study more than just the workstation, the model would have still demanded that the items be represented in the form of simplified combinations of paper, wood and plastic materials. As will be discussed in the next chapter, the properties of the idealized office workstation were subjected to a sensitivity analysis to account for both the model inaccuracies and the narrow selection of test specimens.

4.6 REFERENCES

- Hamins, A., and K.B. McGrattan. 2003. Reduced-Scale Experiments on the Water Suppression of a Rack-Storage Commodity Fire for Calibration of a CFD Fire Model. *Fire Safety Science: Proceedings of the Seventh International Symposium*. International Association for Fire Safety Science.
- McGrattan, K. 2005. Fire Dynamics Simulator (Version 4), Technical Reference Guide. NIST Special Publication 1018. National Institute of Standards and Technology, Gaithersburg, MD, September.
- Ritchie, S.J., K.D. Steckler, A. Hamins, T.G. Cleary, J.C. Yang, and T. Kashiwagi. 1997. The Effect of Sample Size on the Heat Release Rate of Charring Materials. *Fire Safety Science: Proceedings of the Fifth International Symposium*. International Association for Fire Safety Science.

This page intentionally left blank.

Chapter 5

MODEL INPUT PARAMETERS

5.1 OVERVIEW

This chapter describes how the numerical simulations of the fires within World Trade Center (WTC) 1 and WTC 2 were designed. The process of selecting both the numerical and physical parameters for the Fire Dynamics Simulator (FDS) was carried out as the model was undergoing the development and validation that was documented in the previous chapters.

The size and complexity of the fire simulations for the WTC disaster were unprecedented. Most simulations performed with FDS in the years prior to 2001 were limited to a few rooms in a house, or a limited expanse of office or industrial space. Most simulated only a few minutes of time, sufficient to determine the course of the fire, an activation of a sprinkler or detector, etc. Rarely was the survival of the structure itself an issue, as the longer simulation times were often impractical on ordinary desktop computers. Calculations for the WTC Investigation required a considerable amount of time to gradually build in the tremendous amount of information needed to describe the building geometry, materials and the timeline of events like the window breakage. It was not clear from the outset what level of detail would be required to produce useful results. The word “detail” refers both to the physical parameters, like the thermal properties of the materials, and to the numerical parameters, like the size of the computational grid used to approximate the governing equations.

In the months following the attacks on the WTC, calculations were performed with early versions of FDS to determine what improvements would be needed to better describe the fire behavior. Several calculations were performed to study the initial fireballs and the rising smoke plumes (Rehm et al. 2002). The results were useful in providing estimates of jet fuel consumed and overall heat release rates, and also in laying the groundwork for future improvements.

Over the next two years, both the physical and numerical routines within FDS were improved, with the WTC calculations as the focus. These model developments were discussed in Chapter 2. The experiments that were described in Chapters 3 and 4 confirmed that the physical model adequately described the observed fire behavior and guided the development of simplified representations of the hundreds of materials commonly found in any office setting. Indeed, the results of the validation studies confirmed that the accuracy of the model would not be the limiting factor in simulating the fires.

Coinciding with the model development and accuracy assessment, a series of increasingly complex simulations of the WTC fires were performed as more information was made available about the floor layouts, the external damage, the furnishings, the aircraft contents, and other data required by the model. To guide the selection of input parameters, a sensitivity study was undertaken to determine which of the many parameters had the greatest effect on the results of the simulations. This study, known as an “orthogonal design” will be described next, followed by a description of the parameters identified by the study to be the most important.

5.2 PARAMETER SENSITIVITY ANALYSIS

Given the large number of parameters needed to define the initial and boundary conditions of the WTC fire simulations, it was not possible to perform a comprehensive sensitivity analysis to determine the effect on the results of the many input parameters. To narrow down the parameter set to only those few with the greatest effect on the result, an orthogonal design technique was used. An orthogonal design is a method by which an experiment whose outcome is determined by a finite set of parameters is conducted numerous times with different combinations of the parameters to assess the sensitivity of the result to each. For the WTC simulations, five parameters were chosen for the study (see Table 5–1). These five parameters were thought to have a significant influence on the results based on the results of simulations done to that point in the Investigation. Two of the parameters (Fuel Spill and Combustible Load) were related to the amount of fuel available; three (Core Walls, Shaft Velocity, Oxygen Concentration) were related to the oxygen supply.

Table 5–1. Parameters for orthogonal design of input parameters.

Parameter	- Estimate	Mid-Range	+ Estimate
P1. Jet Fuel Spilled on a Single Floor (L)	1,200	2,100	3,000
P2. Combustible Load (kg/m ²)	17	25	34
P3. Core Walls Broken (%)	0	25	50
P4. Air Velocity in Shafts (m/s)	2	6	10
P5. Oxygen Concentration of Air in Shafts (%)	15	18	21

For each of the five parameters, a single value was chosen as a preliminary estimate, and then a lower and higher value was chosen, so-called + and – estimates. The values chosen for each parameter were based on estimates from very early in the Investigation. The intent of the exercise was not necessarily to determine the best values for each, but rather to assess the influence each had on the final result. In all, nine single floor simulations were performed, with the combinations of parameters shown in Table 5–2. The combinations of parameters were intended to be an optimum sampling of all possible combinations. Conventional sensitivity analyses only test one parameter at a time, even though such an approach is not the most efficient way to explore the entire parameter space.

Table 5–2. Parameter combinations for orthogonal design.

	P1	P2	P3	P4	P5
Test 1	-	-	-	+	+
Test 2	+	-	-	-	-
Test 3	-	+	-	-	-
Test 4	+	+	-	+	-
Test 5	-	-	+	+	-
Test 6	+	-	+	-	+
Test 7	-	+	+	-	-
Test 8	-	+	+	-	-
Test 9	0	0	0	0	0

Of the five parameters chosen for the study, two were seen to have the most significant effect on the results.¹ Of these two, Combustible Load was the most important, followed by the damage to the core walls. The Combustible Load influenced the duration of the fires, more so than their intensity. In fact, simulations using the low (–) to mid-range (0) estimates of the Combustible Load produced results consistent with the visual evidence of the fire behavior in WTC 1 that was available at the time the study was done.

The amount of damage to the core also affected the results of the fire simulations in a noticeable way, but it was not possible to say which of the core damage estimates was better or worse. Because the core damage was to be provided by the impact analysis (NIST NCSTAR 1-2), there was no need to pursue the matter further at that time. Ultimately, the impact analysis was to provide a range of damage estimates that were to be input into the fire simulations.

It is important to emphasize that the parameter sensitivity study was not undertaken to select the values of the parameters for the final simulations, but rather to identify which of the parameters to vary. The fact that the low and mid-range values of the Combustible Load used in the study led to results consistent with observations was merely fortuitous. The values chosen were based on some very early estimates made by Port Authority engineers and eventually corroborated by other sources (NIST NCSTAR 1-5C). The values of the other parameters were altered significantly in the final WTC calculations, but their relative degree of sensitivity was not expected to change.

5.3 NUMERICAL GRID

The simulations of WTC 1 included eight floors of the building, 92 through 99. In WTC 2, six floors were included, 78 through 83. These floors were chosen based on observations of the damage to the exterior and the fire activity. The chosen floors did not encompass all of the fire activity. For example, a significant fire was observed on the west face of the 104th floor of WTC 1. There were several reasons for restricting the fire simulations to eight and six floors. First, the structural analysis was limited to the same number of floors. These floors had the most severe structural damage from the impacts and were where the collapses were most likely initiated. Second, the floors chosen had the most severe fires, according to the visual evidence. It would not have been possible to predict with the model how the fires might have spread to parts of the buildings that were not in the immediate vicinity of the impact floors. Third, the simulations of eight and six floors demanded between five and ten days of central processing unit (CPU) time on various parallel computing clusters maintained at the National Institute of Standards and Technology (NIST). The number of CPUs used for a given simulation ranged from 8 to 48. The fire simulations were part of a chain of four major modeling efforts that had to be run serially—the impact analysis, the fire simulations, the thermal analysis of the structural steel, and finally the mechanical analysis of the collapse sequence. Each link in the chain required input from its predecessor, and provided data for its successor. Given that each component in the chain required roughly the same amount of time as the fire simulations, the entire process required about two months. The sensitivity analysis was performed by staggering the component calculations so that several analyses were underway at any given time.

¹ This assessment was made solely from the inspection of contour plots of upper layer temperature predictions by various members of the NIST staff.

The relatively simple layout of each floor in WTC 1 and WTC 2 was exploited by the parallel version of FDS. Each processor was assigned a whole, half or quarter of a single floor. Communication between floors was limited to holes in the floor slabs created by elevator or ventilation shafts, stairwells both inside and outside the building core, and damage due to the impact of the airplane. These holes accounted for less than 10 percent of the total slab area; thus, communication between computers was not a significant time factor in the parallel computations. Figure 5–1 displays the eight floor model of WTC 1, showing the computational mesh and the arrangement of the different grid blocks.

NIST

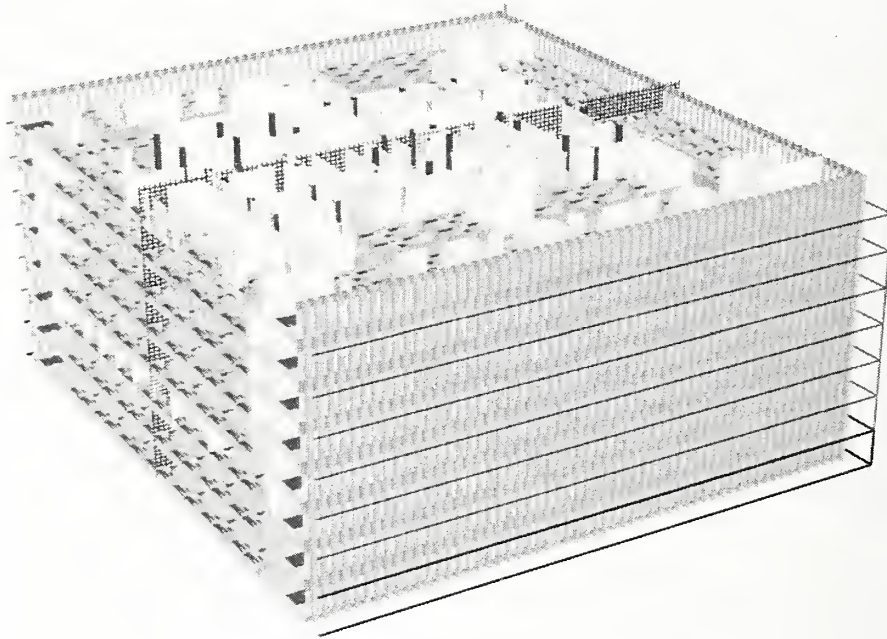


Figure 5–1. Eight floor model of WTC 1.

The windows in WTC 1 and WTC 2 were nominally spaced 40 in. apart. To simplify the numerical description of the building, it was decided to approximate the window spacing as exactly 1 m (39.4 in.). In addition, the external columns plus their aluminum cladding was assumed to be 0.5 m (19.7 in.). The slab-to-slab floor spacing was assumed to be 3.6 m (11.8 ft). Because of these approximations, a uniform numerical mesh consisting of cells whose dimensions were 0.5 m by 0.5 m by 0.4 m was used. The beveled corners of the towers were simplified in the analysis. In the model, each tower face consisted of 58 windows, 61 columns, and two 0.5 m spacers next to each corner column. In the real tower geometry, these spacers formed the bevel.

The numerical grid for each floor of WTC 1 and WTC 2 was of dimension 128 cells by 128 cells by 9 cells (64 m by 64 m by 3.6 m). The 128 cells in the horizontal directions allowed for several meters of simulation outside of the external walls. The calculations were run in parallel, thus each floor was assigned to a different processor. The floor slabs, core walls, and workstations were approximated as thin obstructions. This meant that the objects were considered to have no thickness in the flow calculation, but the objects were assumed to have thickness for the gas to solid phase heat transfer calculation.

Penetrations in the floor slabs representing elevator shafts and heating, ventilating, and air conditioning (HVAC) ducts were created in the model by adding a simple construct to FDS known as a “hole.” Each floor slab was defined as a single obstruction spanning the entire floor area of the building, and openings

for vertical shafts were added by “punching” rectangular holes in the appropriate locations. This construct greatly simplified the task of assembling the input files.

5.4 FLOOR LAYOUTS AND COMBUSTIBLE LOAD

Once the spatial resolution of the numerical grid was decided upon, architectural drawings were needed at a level of detail consistent with the underlying numerical grid. Because of the relative coarseness of the grid and the uncertainty in the damage caused by the aircraft, extremely detailed drawings were not needed, at least for the fire modeling. Information about the layout of the relevant floors was obtained from architectural drawings provided by the occupants. For floors where information was not available, the geometry of a nearby floor or a floor of similar use was substituted, supplemented by information provided by Port Authority of New York and New Jersey (PANYNJ or Port Authority) engineers or occupants.

In WTC 1, floors 92 through 100 were occupied by the firm Marsh & McLennan and had recently undergone renovations. Detailed architectural drawings of all the relevant floors were provided and are included in the Appendix. These drawings were converted into two dimensional Computer Aided Design (CAD) files, and a simple computer program was written to read the CAD files and extract wall dimensions to be input into FDS.

The layouts of the modeled floors in WTC 2 (except floor 78) were not available to the Investigation. However, representatives of the Port Authority and several occupants of the relevant floors provided verbal descriptions of floors 79 through 82. The layout of these floors was similar to those of WTC 1, with the exception of more elevator shafts and more compartmentalization outside of the core area. The layouts of floors 78 through 83 that were assumed for the purpose of the fire modeling are included in the Appendix.

The furnishings in most of the open areas of WTC 1 and WTC 2 were assumed to have consisted of office workstations similar to those burned at NIST. Figure 5–2 shows a typical office environment in the WTC. Each workstation purchased as part of the Investigation contained about 250 kg of combustible material, mostly a mix of paper and plastic (NIST NCSTAR 1-5C). In the numerical simulations, the modeled workstations were distributed on each floor as shown in Figs. 5–3 and 5–4. Notice that the simplified workstations developed during the single and multiple workstation burns were distributed uniformly throughout the work areas exterior to the building core, but not to the point of describing each individual office or work area in detail. Such an effort would not have been warranted given the uncertainty of the furniture layout on September 11, 2001, and also the effect of the airplane impact. Only because corner offices or conference rooms were typically found on each floor was the uniform distribution of workstations changed slightly to include crude mock-ups of large tables and chairs in these areas.

Figure 5–4 shows how the major elements of each floor were arranged in the model. The combustible items consisted of the carpet, desks, privacy panels, and the “miscellaneous combustibles.” To represent damaged furnishings (“rubble”) and aircraft debris, the burning rate of the “miscellaneous combustibles” was reduced from 450 kW/m² to 300 kW/m². The distribution of the rubble was a variable in the final simulations, but the overall strategy used to distinguish rubble from undamaged furnishings was as



Source: Reproduced with permission of The Port Authority of New York and New Jersey.

Figure 5–2. A work area in the WTC.

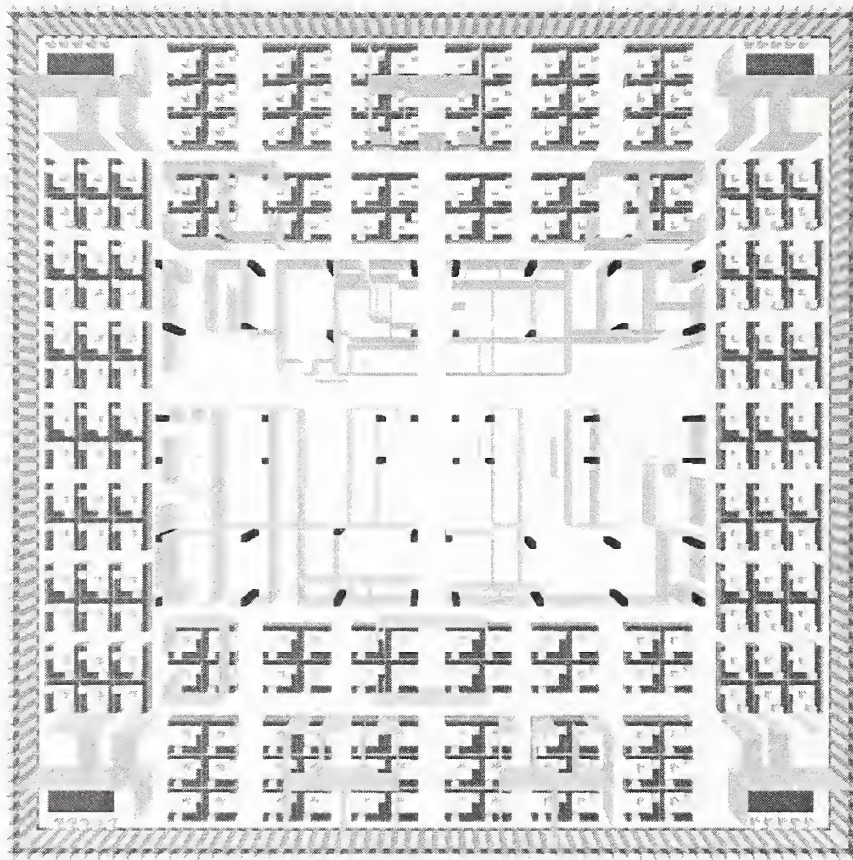


Figure 5–3. Plan view of the 97th floor of WTC 1.

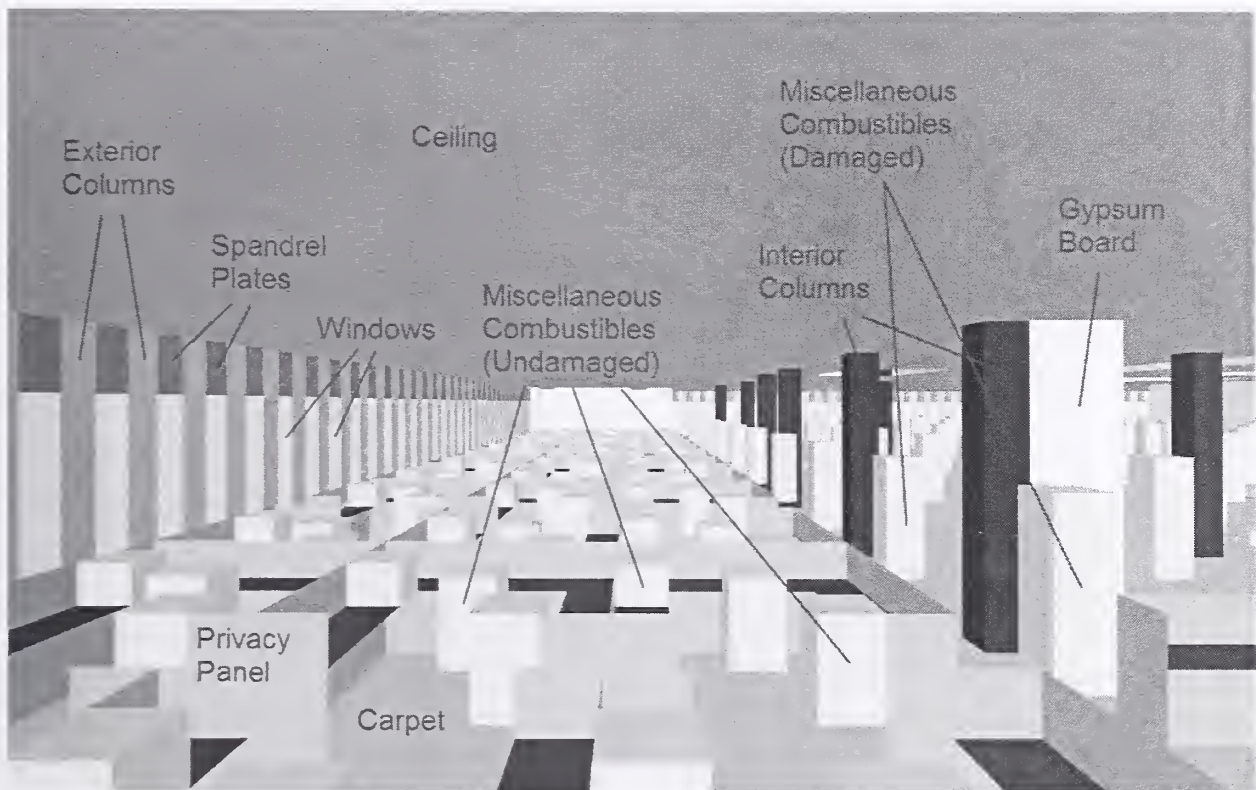


Figure 5-4. Modeled interior layout.

follows: the impact analysis (NIST NCSTAR 1-2) provided estimates of where the heaviest damage occurred. The combustible mass contained within these areas was redistributed over the swath cut by the airplane, an area roughly one third of the entire floor area, extending through the center of WTC 1 from the north to the south face, and through the east side of WTC 2 from the center of the south face to the northeast corner. This strategy conserved the overall combustible load, but shifted it away from the impact area to mimic the “plowing” effect of the airplane debris. At the same time, the rubble burned at a reduced rate to account for the fact that the collapsed furnishings had less exposed surface area. In the model, the geometry of the damaged workstations was not altered; the burning rate was meant to account for the change in the geometry.

Outside of the core area, the combustible load was approximately 20 kg/m^2 (4 lb/ft^2) (NIST NCSTAR 1-5). The core area contained elevator and heating, ventilating, and air conditioning (HVAC) shafts, stairwells, storage rooms, toilets, and various other support facilities. It was unclear what the combustible load was in the various core areas. As a first approximation, the carpet that was assumed to be spread over the entire floor was extended into the core area, not necessarily because the core was carpeted but to represent whatever other combustible objects were to be found there.

Debris from the aircraft was distributed to those parts of each building through which the aircraft was assumed to have penetrated (NIST NCSTAR 1-5). The debris was assumed to have the same properties as the “miscellaneous combustibles” used to model the contents of the individual office workstations, except the debris was assigned a lower burning rate. No attempt was made to factor in the possible combustion of the aluminum airframe because the model only accepts a single fuel. The total mass of the airplane contents ($12,100 \text{ kg}$ for WTC 1 and $12,500$ for WTC 2) was distributed over a wide swath of the impact

floors (95 and 96 in WTC 1, 80 and 81 in WTC 2). The width of these areas was varied as part of the sensitivity analysis. Details of the assumed distributions for WTC 1 and WTC 2 are included in Chapter 6.

The walls and ceiling of each floor were assumed to be non-combustible. It was assumed that the ceiling tiles had mostly fallen out upon impact of the aircraft, exposing the underside of the floor slab (NIST NCSTAR 1-5D). The fallen ceiling tiles were not explicitly modeled. Their effect on the burning rates of the furnishings was accounted for as a result of the calibration and validation work performed as part of the single and multiple workstation fire experiments described in Chapter 4. The underside of the exposed floor slab was assigned the properties of concrete: thermal conductivity 1.0 W/m/K, density 2,000 kg/m³, specific heat 0.88 kJ/kg/K (Quintiere 1998). Although the floor slab actually consisted of a metal deck topped with a concrete slab, for the purposes of modeling the gas temperatures, the thermal properties of the entire floor slab were assumed to be that of concrete. The interior walls were assumed to have the properties of gypsum board (thermal conductivity 0.5 W/m/K, density 1,440 kg/m³, specific heat 0.84 kJ/kg/K). The exterior wall was assumed to be made up of windows (0.76 W/m/K, 2,700 kg/m³, 0.84 kJ/kg/K) or insulated steel columns/spandrel plates with the same properties as the gypsum board. The results were insensitive to the choice of the properties of the various materials. Their role in the model was merely to furnish reasonable boundary conditions for the gas phase calculation. The detailed calculation of the thermal penetration of the structural elements was performed separately using the Fire-Structure Interface developed by Prasad and Baum (NIST NCSTAR 1-5G), and the commercial finite-element software package ANSYS.

5.5 EXTERIOR DAMAGE

A very important component of the fire simulations was the damage to the exterior of the buildings, both from the airplane impacts and from the heat of the fires breaking windows. Broken windows provided air to the fires burning inside the building. Fresh air that was drawn from lower floors by the draft or “chimney effect” also provided oxygen to the fires burning deep within the buildings, but there was much less certainty in the flow of air through the core compared to the flow of air through the broken windows. As a result, the simulations were conducted using the exterior damage provided by the photographs and videotapes. There were no attempts to predict window breakage with the model, nor was there any effort to assess the sensitivity of the calculations to exterior damage. Exterior damage was input directly into the model. In contrast, internal damage to core walls was varied to assess its influence on the results.

In the fire model, unbroken windows were assumed to be thin obstructions, impenetrable to air flow and thermal radiation.² When the simulation reached a pre-set break time, the obstruction was simply removed at which point air flow and thermal radiation were no longer impeded. The flow of air and smoke through a window was governed by the momentum conservation equation. It was not based on any empirical “orifice flow” correlation. Broken external columns were removed in the same way as broken windows. Figure 5-5 shows the observed damage to and fires on the north face of WTC 1 just after impact. The schematic diagram shows column damage, window breakage (black), and fires of varying severity (orange, yellow), based on examination of a large number of photographs and videos (NIST NCSTAR 1-5A).

² The plate glass was assumed to be 0.5 cm thick with a thermal conductivity of 0.76 W/m/K, specific heat 0.84 kJ/kg/K, and density 2,700 kg/m³ (Quintiere 1998).

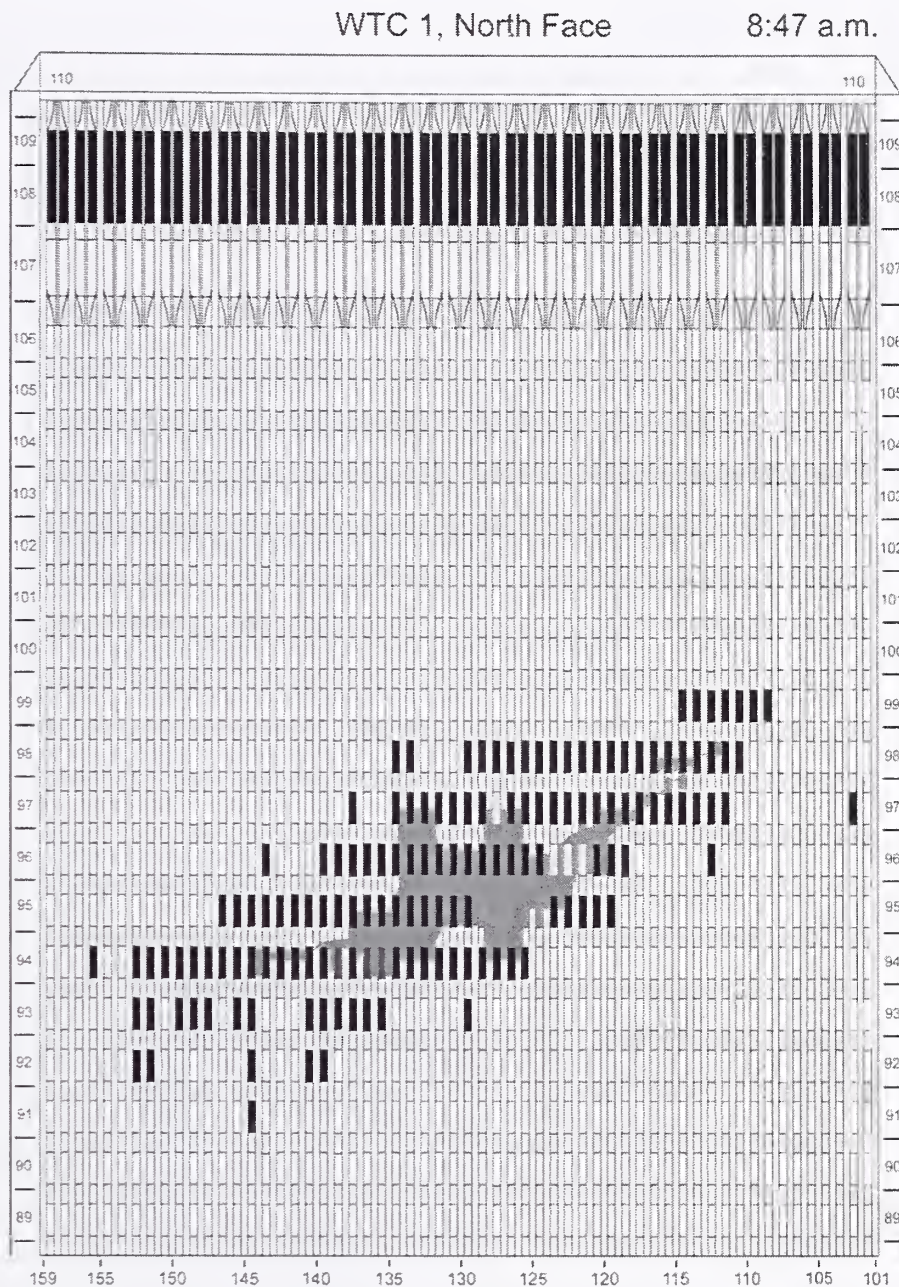


Figure 5-5. Damage to north face of WTC 1 just after impact.

5.6 INTERIOR DAMAGE

The damage caused by the airplanes crashing into the buildings was estimated from calculations consisting of detailed models of both the aircraft and the buildings' major structural elements (NIST NCSTAR 1-2). Because the impact analysis was designed primarily to estimate the damage to the concrete floor slab, interior columns and steel trusses, the predicted extent of the heavy damage to the trusses was used as an indicator of where walls would have been completely destroyed. Figure 5-6 contains layouts of the 96th floor of WTC 1 and the 80th floor of WTC 2, showing estimates of the damaged areas. A complete collection of damage estimates for all the relevant floors is contained in

Severe Floor Damage
Fireproofing (SFRM) and partitions □

Floor system structural damage □

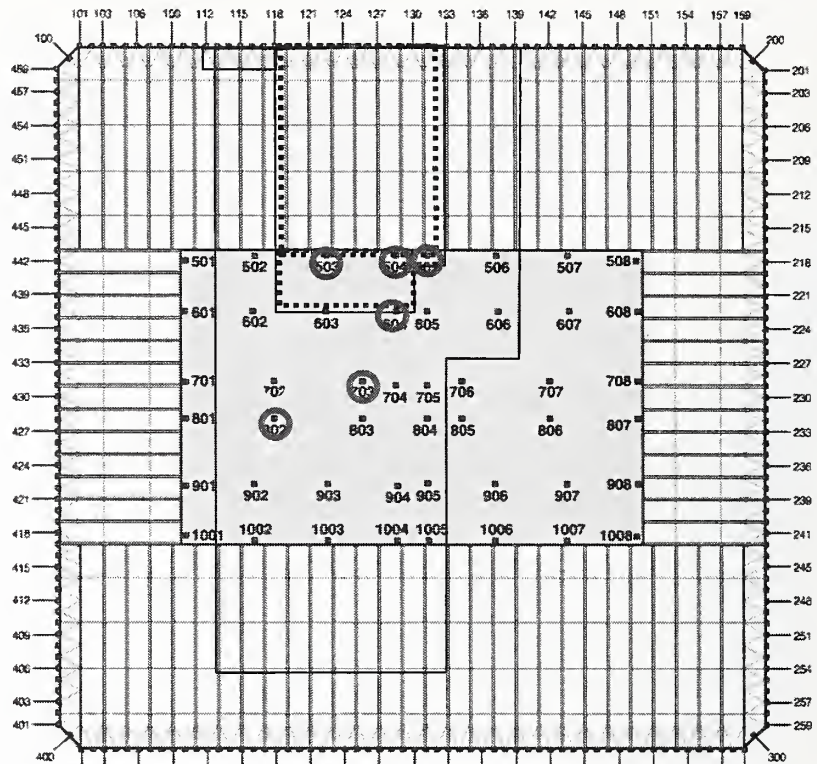
Floor system removed □

Column Damage

Severed ○

Heavy Damage ○

Moderate ○



Severe Floor Damage
Fireproofing (SFRM) and partitions □

Floor system structural damage □

Floor system removed □

Column Damage

Severed ○

Heavy Damage ○

Moderate ○

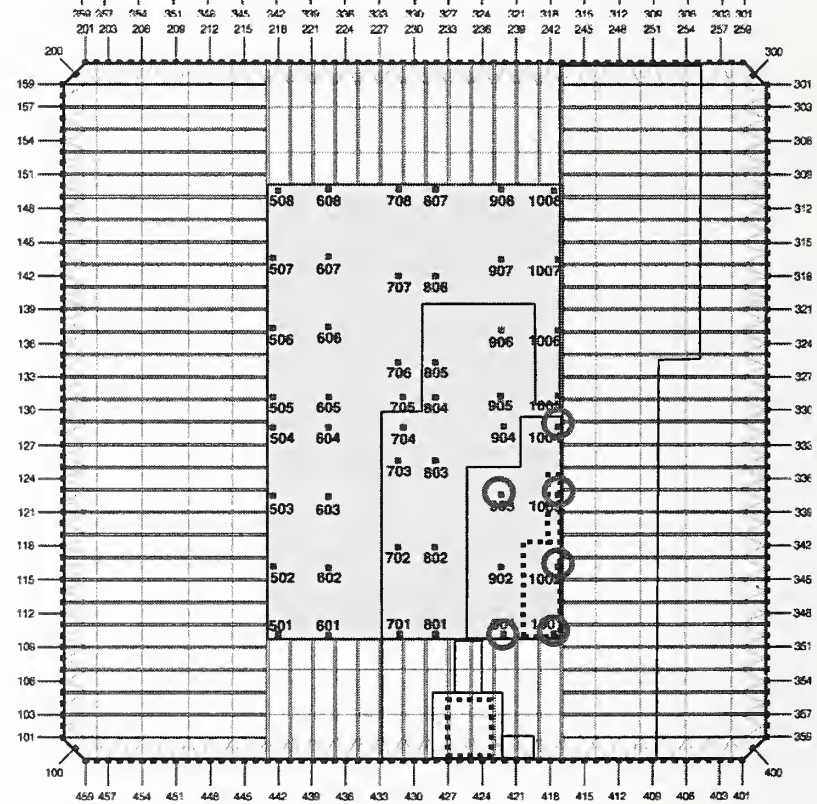


Figure 5–6. Damage estimates for 96th floor, WTC 1, and 80th floor, WTC 2.

NIST NCSTAR 1-2. Furnishings in the impact areas were partly moved along the path of the aircraft, and the remaining combustible mass was assumed to consist of the aircraft contents plus the remaining fraction of the original furnishings. This debris was assigned the properties of “rubble,” based on estimates made during the multiple workstation fire experiments (Chapter 4). In brief, rubble had the same mass but roughly half the burning rate of the undamaged furnishings. Both the burning properties of the rubble and the extent of the migration of furnishings along the path of the aircraft were considered parameters with high uncertainty and were chosen as part of a small set of parameters that were varied as part of the sensitivity study.

Another consideration for the FDS simulations was the representation of damaged walls, especially those surrounding the vertical shafts in the core. The impact analyses could only provide a rough estimate of the extent of serious damage to “soft” building contents, like walls and furnishings, because these calculations were primarily aimed at estimating the damage to load bearing structural components. The “brittleness” of the walls and furnishings was difficult to characterize. Consequently, further interpretation of the impact results was needed for the prescription of damage to walls in the fire model. It had been noticed in prior fire simulations that the complete removal of walls surrounding vertical shafts decreased the depth of the layer of hot smoke surrounding the structural steel in the core area. If the upper portions of the walls surrounding the shafts were left intact, the depth of the hot layer would be sustained at least as far below the ceiling as the unbroken section of wall. With little evidence to support either approach, it was decided that the inclusion or omission of a “soffit” surrounding the core shafts would be a parameter to vary in the final fire simulations. The soffit consisted of the gypsum plank wall board that was assumed to have remained in place after impact. This soffit, when included, extended from the concrete ceiling slab to a height of 1.2 m (4 ft) below the ceiling, and it was applied for every wall in the core area that was assumed to have been heavily damaged by the aircraft.

5.7 IGNITION SCENARIO

The multiple office workstation fire experiments that were discussed in Chapter 4 demonstrated that jet fuel significantly increased the growth rate of the fires, but did not significantly increase the peak heat release rate or the peak compartment temperatures. Although the distribution of the jet fuel from the airplanes that crashed into WTC 1 and WTC 2 was not known, there were numerous reports from survivors that the odor of jet fuel was pervasive throughout the building, including the lobby, and that jet fuel was seen dripping from the ceiling on floors just below the impact area (NIST NCSTAR 1-7). Thus, for the purpose of modeling, the fires in WTC 1 and WTC 2 were assumed to have been ignited over a wide area by the jet fuel ejected from ruptured fuel tanks aboard the airplanes. To reproduce this in the fire model, simulated spray nozzles, normally used to model conventional fire sprinklers, were modified to spray droplets of liquid with the properties of Jet A fuel rather than water. The composition of Jet A varies, but its thermal properties were similar to JP-4 and JP-5, whose properties were obtained from the SFPE Handbook (DiNenno 2003). For the calculation, the following properties were used: boiling temperature 98 °C, latent heat of vaporization 316 kJ/kg, specific heat 2.25 kJ/kg/K, density 800 kg/m³, and heat of combustion 43,000 kJ/kg. The initial burning of the fuel droplets within the model was rapid, and several numerical experiments showed that the overall simulations were not sensitive to either the properties of the jet fuel or the fuel distribution.

The simulated spray nozzles were situated to cover an area on each floor roughly comparable to the area of heavy wall damage predicted by the impact calculations (NIST NCSTAR 1-2). Each nozzle ejected jet

fuel at a rate of 158 L/min (42 gal/min) for 30 s via droplets with a median volumetric diameter of 500 μm . These numbers were chosen so that the fuel would be distributed uniformly over the designated area of each floor. Given the “mixed is burnt” assumption in the fire model, the atomized fuel ignited instantly, created large fires over wide areas of the affected floors, and quickly heated up combustible furnishings to their ignition temperature. Tables 5–3 and 5–4 present the predicted fuel distributions from the impact analysis. Of the total amount of fuel distributed to each floor, only 40 percent was used in the simulations. The reasoning behind this estimate followed that of the Federal Emergency Management Agency (FEMA) study (McAllister 2002). It has been estimated by various forms of analysis (Zalosh 1995; Baum and Rehm 2002) that roughly 20 percent of the jet fuel was consumed in the fireballs that were observed outside of the buildings within seconds of impact. The authors of the FEMA report suggested that half of the fuel not consumed in the fireballs could have flowed away, presumably down the elevator shafts and stairwells based on eyewitness accounts. Some additional discussion of the fireballs may be found in NIST NCSTAR 1-5A.

Table 5–3. Jet fuel distribution, WTC 1.

Floor	Liters	Gallons
92	739	195
93	1,531	405
94	8,864	2,342
95	7,216	1,906
96	7,500	1,982
97	5,853	1,546
98	909	240
99	256	68

Table 5–4. Jet fuel distribution, WTC 2.

Floor	Liters	Gallons
78	3,125	826
79	7,841	2,072
80	3,069	811
81	7,556	1,996
82	5,681	1,500
83	795	210

The jet fuel consumption estimate put forth by the FEMA team was used in the model because (1) no evidence or analysis emerged that significantly altered the FEMA estimate, and (2) the simulations were insensitive to both the amount and the distribution of the jet fuel. Sensitivity studies showed that the amount of fuel spilled in the simulation only influenced the results of the first few minutes; the long-term behavior of the simulated fires was unaffected.

5.8 SUMMARY

This chapter has described how the numerous input parameters for the fire model were chosen. Hundreds of calculations of varying sizes, from partial floors to multiple floors, were performed to assess the

sensitivity of the model to the various parameters. In the final analyses that are described in Chapter 6, two simulations were performed for each building, denoted by Case A and Case B for WTC 1 and Case C and Case D for WTC 2. Each model in the four model chain (impact → fire → thermal penetration → collapse) was run twice for each building. The results were intended to span the range of probable outcomes, given the uncertainty in the damage to the interiors of the buildings. For the fire simulations, the degree to which the internal conditions were varied differed for WTC 1 and WTC 2. Details are provided in Chapter 6 as the results of the simulations are presented.

Table 5-5 summarizes the most important input parameters/assumptions for the FDS simulations of WTC 1 and WTC 2. Although all of these parameters were exercised during the model development phase of the Investigation, only some were varied as part of the final analysis. These parameters are listed first in Table 5-5, and they describe both the amount and condition of the combustibles and the air supply to the core resulting from the damage to the walls of the vertical shafts. The parameters for the simulations of WTC 1 and WTC 2 were similar, but not exactly the same. This was because the choice of parameters for Cases B and D came as a result of examining the output of Cases A and C. For example, after completing the Case A simulation of WTC 1, some assumptions were modified to achieve higher temperatures in the core area. More of the aircraft debris and damaged furnishings were confined to the core area, and soffits were added to the damaged walls to trap more heat in the upper layer of the core area in Case B. The assumptions made for all Cases fell within the range of uncertainty resulting from the impact analyses; the objective of the parameter changes was to generate results that would span as much as possible the set of probable outcomes given the range of plausible initial and boundary conditions.

Table 5-5. Summary of major input parameters for FDS fire simulations.

<i>Parameters Varied for the Final Analyses of WTC 1 (Cases A and B)</i>	
Combustible Load	20 kg/m ² for Case A; 25 kg/m ² for Case B
Condition of Furnishings	Undamaged except in Impact Area
Extent of Debris Field	Wide in Case A; Restricted to core in Case B
Condition of Walls in Impact Area	Totally removed in Case A; Soffits added in Case B
<i>Parameters Varied for the Final Analyses of WTC 2 (Cases C and D)</i>	
Combustible Load	20 kg/m ² for Cases C and D
Condition of Furnishings	Rubble throughout for both cases
Extent of Debris Field	Concentrated in NE Corner in Case C More uniformly distributed in Case D
Condition of Walls in Impact Area	Soffits added in Case C and D
<i>Parameter Varied as a Result of the Impact Analysis</i>	
Core Damage	Impact Study (NIST NCSTAR 1-2)
<i>Parameters that were not Varied in the Final Analyses</i>	
Number of Floors	Eight for WTC 1, six for WTC 2
Amount of Jet Fuel Remaining after Fireballs	40 % of total
Jet Fuel Properties	Section 5.7
Window Breakage	NIST NCSTAR 1-5A
Airplane Combustible Mass	12,100 kg for WTC 1, 12,500 kg for WTC 2
Properties/Geometry of Furnishings	Chapter 4

The next category of parameters listed in Table 5–5 are those that resulted from the impact analyses (NIST NCSTAR 1-2). The main objective of the impact analyses was to predict the damage to the columns, trusses and floor slab, but estimates of the damage to walls and furnishings were also made and used in the fire modeling. Floor by floor diagrams of the damaged areas predicted as part of the impact analyses are included in NIST NCSTAR 1-2.

Finally, the last category of parameters listed in Table 5–5 contains those parameters that were not varied in the final FDS simulations. These parameters were either judged to be very reliable, like the Window Breakage, or relatively insensitive to the final results, like the Core Leakage or Amount of Jet Fuel Remaining after the Fireballs.

The input files for the computer model contained about 20,000 input records, almost all of which were merely the elements of the office workstations, repeated hundreds of times per floor. The geometry of the workstations was not varied. Only the density and burning rate of the “miscellaneous combustibles” contained within were varied to account for variations in the overall combustible load or the condition of the furnishings.

5.9 REFERENCES

- Baum, H.R. and R.G. Rehm. 2002. A Simple Model of the World Trade Center Fireball Dynamics. *Proceedings of the Twenty-Ninth (International) Symposium on Combustion*. Combustion Institute, Pittsburgh, PA.
- DiNenno, P.J. (ed.). 2003. *SFPE Handbook of Fire Protection Engineering*. The National Fire Protection Association, Quincy, MA.
- McAllister, T., ed. 2002. *World Trade Center Building Performance Study: Data Collection, Preliminary Observations, and Recommendations*. FEMA 403. Federal Emergency Management Agency. Washington, DC, May.
- Quintiere, J.G. 1998. *Principles of Fire Behavior*. Delmar Publishers, New York.
- Rehm, R.G., W.A. Pitts, H.R. Baum, D.D. Evans, K. Prasad, K.B. McGrattan and G.P. Forney. 2002. *Initial Model for Fires in the World Trade Center*. NISTIR 6879. National Institute of Standards and Technology, Gaithersburg, MD, May.
- Zalosh, R.G. 1995. “Explosion Protection,” *SFPE Handbook of Fire Protection Engineering*, 2nd edition, Quincy, MA.

Chapter 6

SIMULATIONS OF THE FIRES IN WTC 1 AND WTC 2

6.1 OVERVIEW

The aim of the fire simulations for World Trade Center (WTC) 1 and WTC 2 was to replicate the major features of the fires given the limited knowledge of the impact damage and interior contents, while exploiting as much as possible the visible evidence contained within the thousands of photographs and videotapes shot on September 11, 2001. The major features replicated included the rate of spread of the fires, the duration of fire activity in a given location, the thermal insult to the structural elements, and the overall burn time for each of the affected floors.

Throughout the Investigation, hundreds of preliminary calculations were performed to study the fire behavior. The simulations addressed fires on multiple floors, single floors, or parts of a floor. The objective of these preliminary simulations was to (1) assess the sensitivity of the many input parameters, (2) test the robustness of the numerical model during its development, and (3) gain insight. After the development phase, two final simulations for each building were performed to span the plausible range of influential parameters, like the combustible loading and the damage to the interior core. These two simulations, denoted as Cases A and B for WTC 1 and Cases C and D for WTC 2, used initial conditions provided by the impact analysis (NIST NCSTAR 1-2), and the results were passed on to the Fire-Structure Interface (FSI) model to predict the temperature evolution of the structural steel and concrete (NIST NCSTAR 1-5G). The results of the FSI calculations were then passed on to the structural analysis team to predict the actual collapse sequence (NIST NCSTAR 1-6E). Each of these four major modeling efforts (impact → fire → thermal penetration → collapse) consisted of two simulations for each building. The parameters that were varied were chosen based on two criteria: (1) they were shown to have a significant impact on the final results, and (2) they had a high degree of uncertainty. The outcomes of the two analyses were intended to provide probable bounds on what actually happened as it is impossible to know for sure given the evidence available.

Of the fire-related parameters studied, the distribution and condition of the furnishings and the damage to the core walls/shafts had the greatest influence on the model outcome (see Chapter 5). All of the parameters not associated with either of these conditions were prescribed based on the best available estimates.

The observed fire activity around the building exterior served as a yardstick to assess the fidelity of the fire model. The spread rate of the fire and the duration of fire activity in a given area of a given floor were indicators that the simulations were capturing the major features of the fires. To a limited extent, phone calls from trapped occupants in WTC 1 (NIST NCSTAR 1-7) were used to guide the design of boundary conditions at the lower and upper limits of the floors included in the simulation, but most of the information used as input and used to assess fidelity was gleaned from the thousands of photographs and videotapes taken by eyewitnesses.

To compare the results of the fire simulations with the visual evidence, contour plots of the gas temperature 0.4 m below the floor slab were superimposed on profiles of the observed fire activity for

each floor at 15 min intervals (NIST NCSTAR 1-5A). An example is given in Figure 6–1. The stripes surrounding the image represent a summary of the visual observations, with the black stripes representing broken windows, the orange stripes external flaming, and the yellow stripes fires that were seen inside the building. Fires deeper than a few meters inside the building could not be seen because of the smoke obscuration and the viewing angle. The red regions of the contour maps represent numerical prediction of temperatures in the neighborhood of 1,000 °C, typical of a fully-engulfing compartment fire. Such temperatures were measured during the multiple workstation experiments when the workstations were burning near their peak heat release rate and flames extended outside of the test compartment.

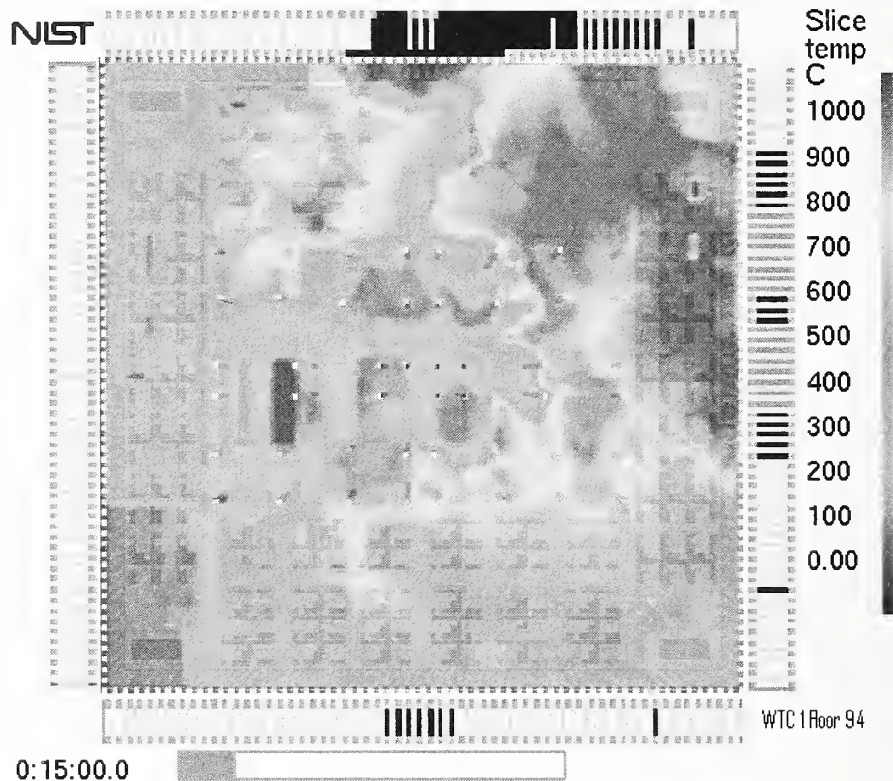


Figure 6–1. Predicted upper layer temperature 15 min past impact, WTC 1, floor 94.

Note that only the window breaking times were prescribed in the fire model. The observed fire activity gleaned from the photographs and videos was not a model input, thus one should not expect a one to one correspondence between predicted high temperatures and observed fire activity. Indeed, in Fig. 6–1, the model predicted significant burning in the northeast corner of floor 94, but the visual evidence only indicated fire activity on the east face, not the north, at that particular instant in time. The fact that no model could ever predict exactly what occurred is the basis for the sensitivity studies conducted throughout the Investigation.

It had been suggested early in the Investigation to perform the fire simulations with the fires “prescribed” at their observed locations, and also to stop the calculations periodically to make various adjustments. Neither step was taken, mainly because the intent of the simulations was to predict the behavior of the fires deep within the buildings. Exterior sightings provided some clues, but it would not have been possible to extrapolate the observed fire activity into the buildings’ interiors. **Consequently, the simulated fires described in this chapter were of comparable character to the actual ones, but they**

did not reproduce all of the observed fire activity because of the uncertainty in the initial and boundary conditions of the calculations. Where there were discrepancies between prediction and reality, consider the following:

- The interior damage and jet fuel distribution were very crudely approximated from the impact analysis, which focused on “hard” (columns, trusses, floor slabs) rather than “soft” (walls, furniture, airplane contents) targets.
- The jet fuel distribution on floors that were not directly impacted by the airplane was very difficult to prescribe because it had to be assumed that the fuel leaked through damaged floor slabs, poured down vertical shafts, or was propelled by the initial fire balls.
- The furniture in the model was distributed uniformly throughout each floor, or it was crudely “plowed” away from the impact area. In reality, some parts of the floors were more heavily loaded with combustibles than others. This assumption affected the dwell time of the simulated fires. The observed fires lingered longer in areas with a relatively heavy fuel loading, and swept more quickly through areas with a light loading.
- All office doors were assumed open in the simulations even though many would have been closed because the buildings were only partially occupied at the time of the attacks. There were often significant differences between prediction and reality in regard to the fires’ penetration into compartmentalized areas of various floors.

6.2 SIMULATION OF WTC 1, CASE A

The Case A simulation of the fires in WTC 1 used the damage estimates of the Case A impact analysis as initial conditions (see NIST NCSTAR 1-2 for floor by floor layouts of estimated damage). From Table 5-5, the combustible load on each floor was assumed to be 20 kg/m^2 , and the workstations were assumed to be intact except in the immediate path of the aircraft. In Case A the mass of displaced furnishings was shifted from north to south. This was done by removing all furnishings within 10 m of the north face in areas designated by the impact analysis to have been heavily damaged. The equivalent mass of these furnishings was redistributed over a wide area (40 m wide all the way to the south face in Case A), and its properties were changed to that of “rubble” (see Chapter 4 for a description of “rubble”). Both the damaged furnishings and the aircraft debris were assumed to have the same properties (“miscellaneous combustibles” with a lower burning rate of 300 kW/m^2 rather than the 450 kW/m^2 that was assigned to the contents of the undamaged workstations). Similar assumptions about the debris field were made in Case B, although the extent of the debris field was limited to the core area.

For the Case A simulation, the walls surrounding the vertical shafts were completely removed in areas designated by the impact analysis as heavily damaged. This assumption was changed for the Case B simulation, where a 1.2 m soffit was left intact on all walls designated as heavily damaged by the impact analysis.

Note that the results of the simulation as compared to observations on the following pages are shown every 15 min, with the exception of the last frame, which is shown at the time of collapse, 1 h 42 min past impact.

6.2.1 Floor 92, Case A

Figure 6–3 presents the simulated and observed fire activity on the 92nd floor of WTC 1. Initially, the observed fire activity was confined to the northeast quadrant, and eventually it spread to the northwest and south central parts of the floor. Plans of the 92nd floor reveal several partitions that may have prevented more rapid spreading; in particular, there appeared to be some type of partition separating the east side of the floor from the north side because the fires did not appear in the northwest quadrant until about 15 min prior to collapse (see Fig. 6–4). Figure 6–2 shows fire activity in the northeast corner just prior to collapse.

Several windows on the south face broke out after about 45 min, and eventually fires were seen extending from several windows in the center of the south face about 15 min before collapse.

In the simulation (Fig. 6–3), no damage was assumed for this floor other than window breakage. The fires were ignited in the northeast corner using jet fuel, the amount of which was predicted in the impact analysis (NIST NCSTAR 1-2). Initially, the simulated fires burned the contents of the northeast corner, sustained by oxygen from numerous broken windows. By roughly 45 min after impact, the contents of the northeast corner were consumed, and the simulated fires moved south along the east face and west along the north side of the interior core. There was a partition in the model that blocked the fires from spreading directly to the north face. Eventually, the simulated fires arrived at the north face about 15 min sooner than was observed. The fire that moved toward the south end of the east face was stopped in the simulation by a partition. The actual fire apparently stopped somewhat further than it did in the model, based on the last observed window break, but it was not clear what caused the fire to stop where it did. The simulated fires never reached the south face because of various walls that obstructed their spread.



Figure 6–2. North face of WTC 1 with fires seen just inside northeast corner of floor 92.

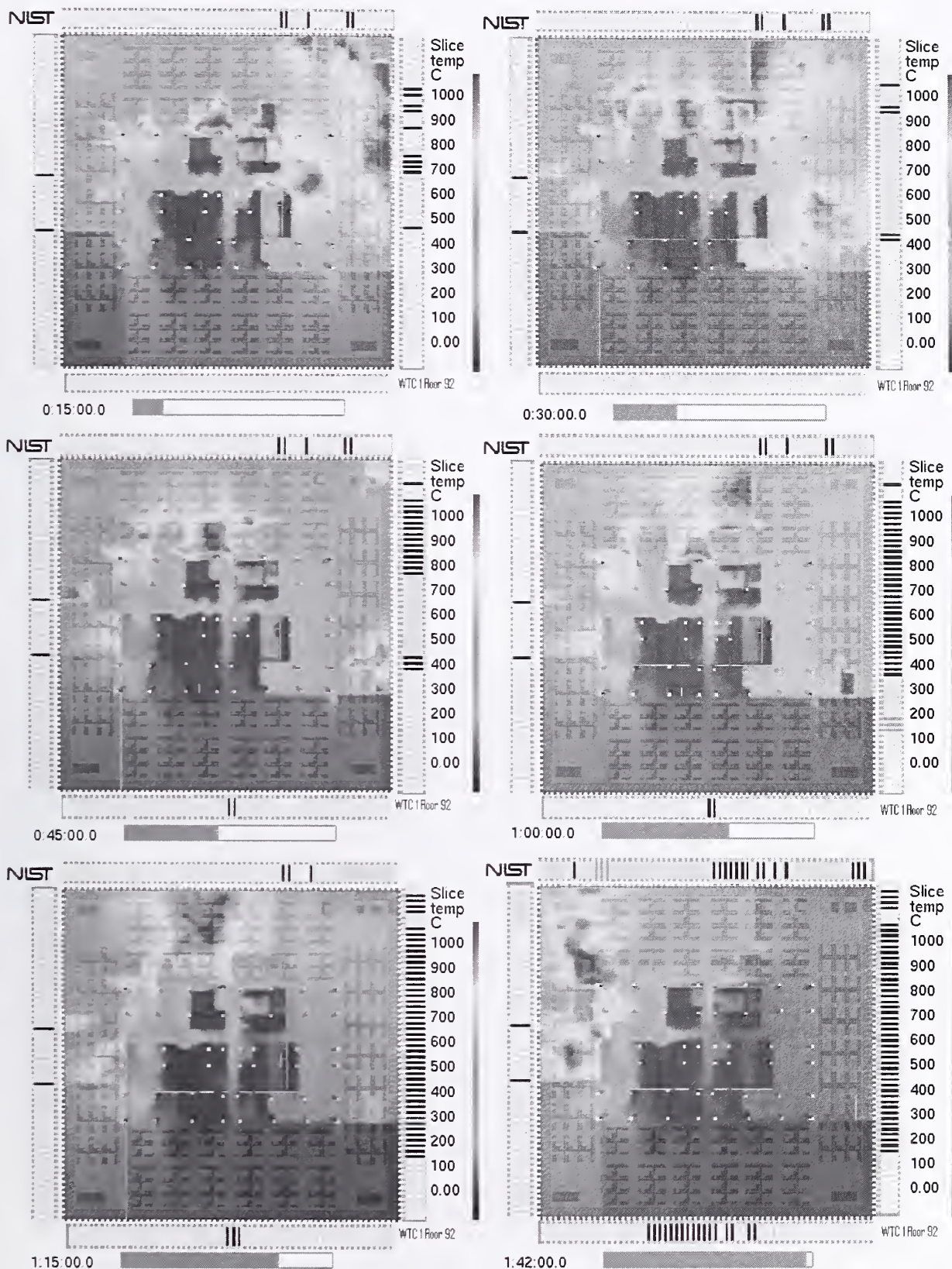


Figure 6-3. Upper layer temperatures of WTC 1, floor 92.

6.2.2 Floor 93, Case A

The 93rd floor was directly below the heavily damaged 94th floor. As with floor 92, the observed fires on the 93rd floor were initially confined to the northeast quadrant, but unlike 92, there was little observed fire activity near the windows on other parts of the floor. In the last 10 min, roughly 20 windows broke out on the west side of the north face and the south side of the east face, due either to internal spread of the fire or an overall build-up in the temperature of the gases of the upper layer. There was no dramatic increase in fire activity near the end as there was on 92, at least not near the windows (see Fig. 6–4).

In the simulation (Fig. 6–5), fires were ignited along a path that roughly followed that of the left wing of the airplane that smashed into the east side of the north face of the 94th floor. Based on the results of the impact study, it was assumed that damage to the floor slab between 93 and 94 allowed jet fuel to drip down and ignite fires on 93. The simulated fires burned out the northeast quadrant in about 30 min. This was consistent with observations, except in regard to a sudden flare-up of fire 45 min after impact in the northeast corner. It was unclear what caused the flare-up as the floor plan showed no office there. The simulated fires consumed all the combustibles in this part of the building and had moved on after 45 min. This westward and southward movement of fire was not observed. However, in the simulation, there were enough broken windows and combustibles to support the gradual migration of the fires around the periphery. Thus, the simulation of the fires on floor 93 over-predicted their intensity near the exterior. The only evidence that the real fires may have spread to other parts of the floor was the observed window breakage in the last 10 min.

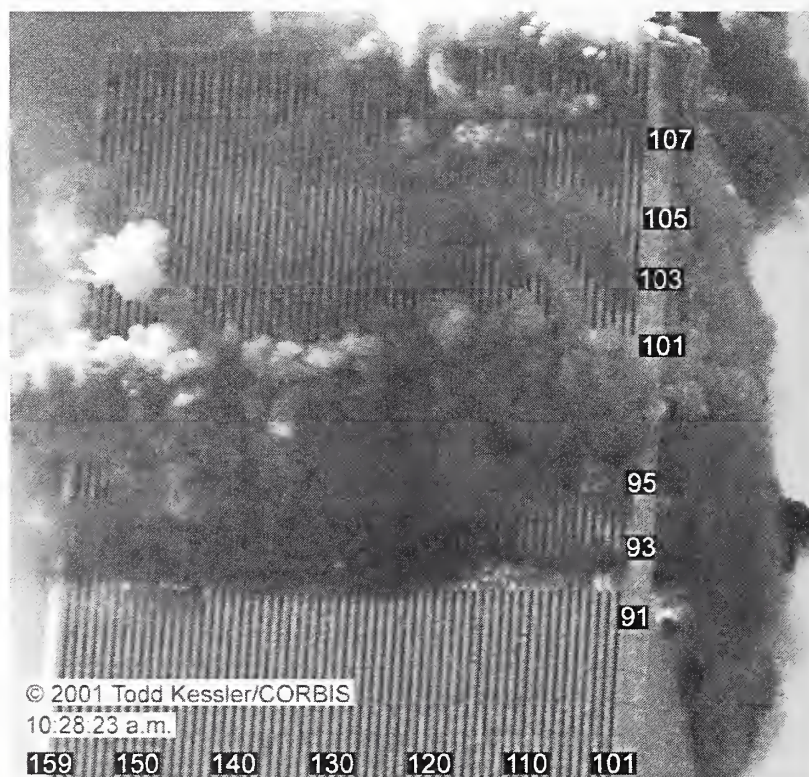


Figure 6–4. North face of WTC 1 at the onset of collapse.

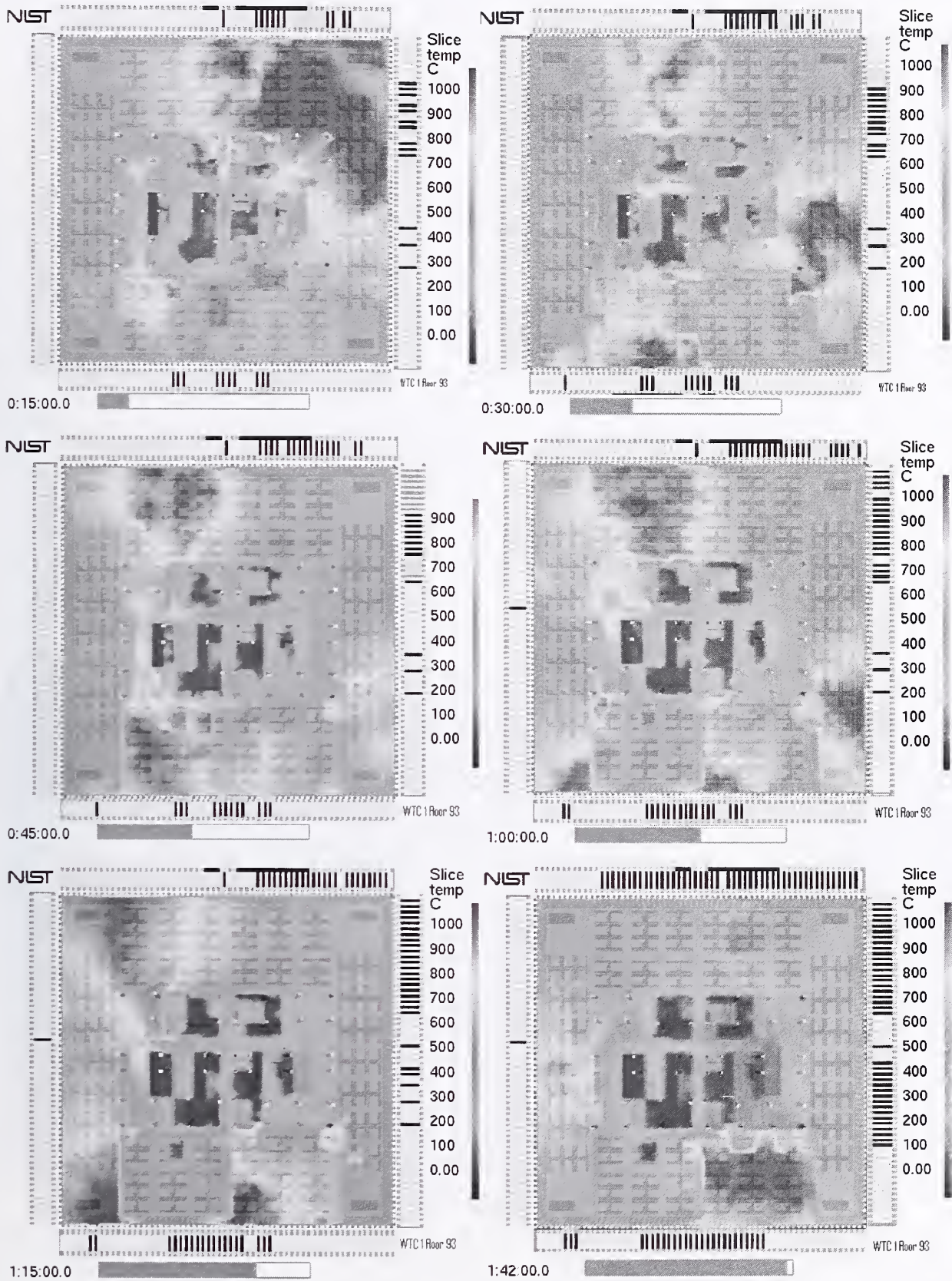


Figure 6–5. Upper layer temperatures of WTC 1, floor 93.

6.2.3 Floor 94, Case A

Floor 94 was directly impacted by the left wing of the airplane, and a substantial amount of jet fuel was spread throughout the east side of the floor. Initially, severe fires were observed on the east face (Fig. 6–6) and then steadily spread around the floor, with the heaviest activity in the end being in the southwest quadrant.

The simulation (Fig. 6–7) captured the movement of the fires reasonably well. The simulated fires burned vigorously in the northeast quadrant for the first 30 min. Then for the next 30 min, the fires moved at roughly the same rate as the real fires toward the southeast and northwest corners. The match in spread rate can be attributed to the prescription within the model of the actual window breakage pattern. In reality, window breakage was caused by the build-up of heat from nearby fires which often were seen to flare up due to the increased supply of oxygen from the newly broken windows. This phenomenon was captured in the simulation, although it is unlikely that the model would have been capable of replicating the exact window breakage pattern. Thus, the actual window breakage guided the simulated fire spread. In addition, the decrease in observed fire activity in the wake of the fire “front” is replicated in the simulation. This was largely due to the prescription of the combustible load. Had the prescribed mass of furnishings in the model been significantly greater than the actual load, the simulated fires would have remained in areas that were observed to have “burned out” far longer than they did. The duration of high temperatures ($\approx 1,000$ °C) is largely a function of the density of combustibles in any particular place. The more furniture to burn, the longer the fires remain.

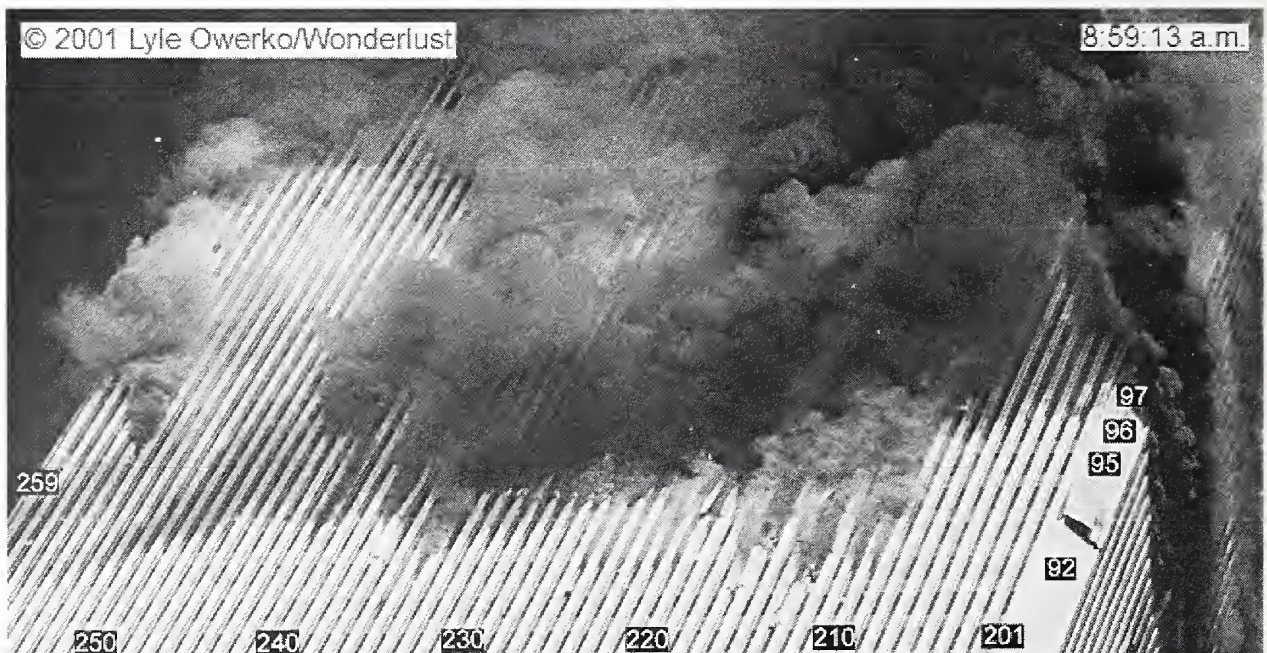


Figure 6–6. East face of WTC 1 at 8:59 a.m. showing fires on the 94th floor.

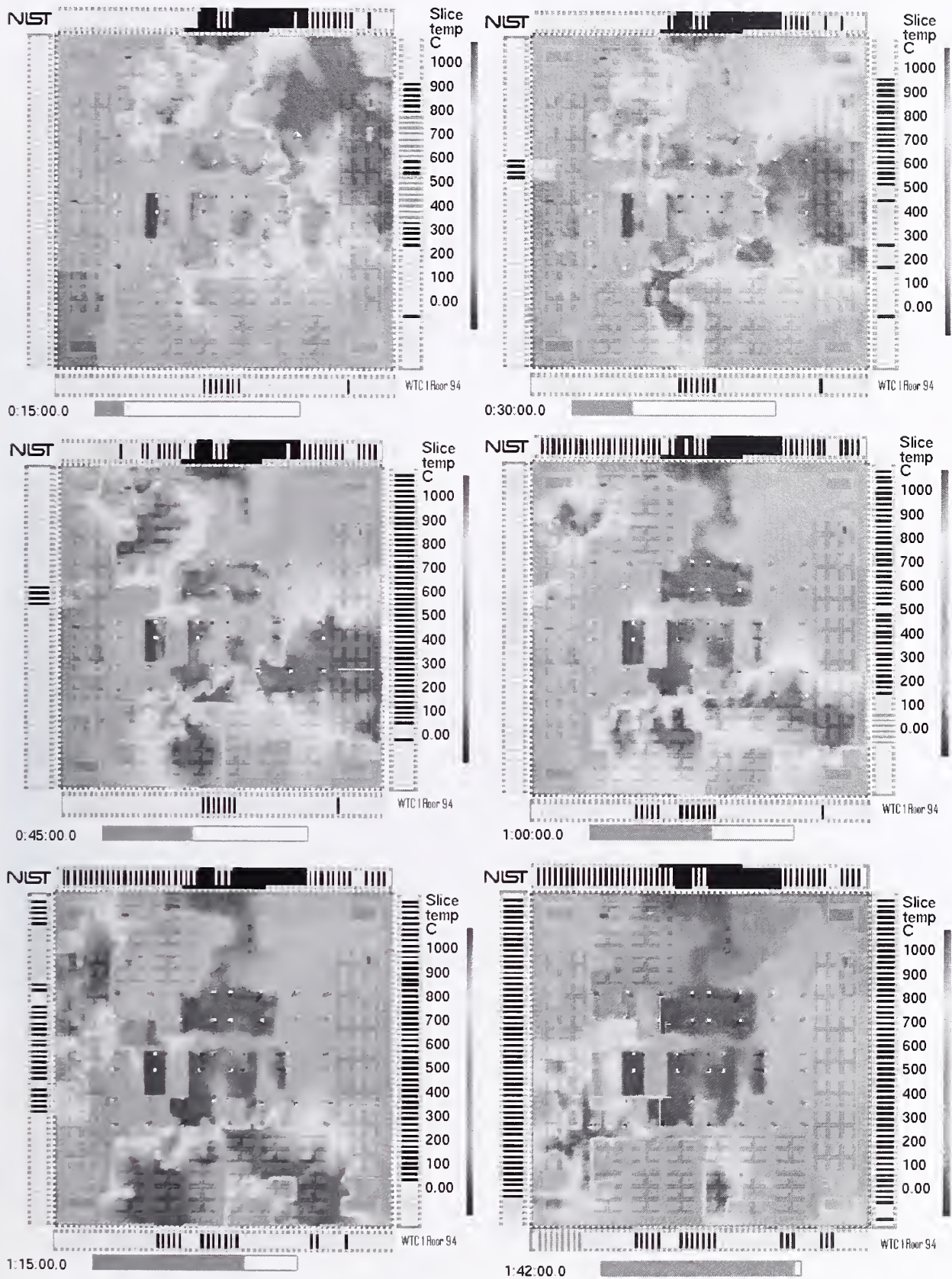


Figure 6-7. Upper layer temperatures of WTC 1, floor 94.

6.2.4 Floor 95, Case A

Floor 95 was directly hit by the fuselage of the aircraft, roughly in the center of the north face. Damage to the west, east and south sides of the building on this floor was modest, and relatively small fires were observed initially on the east and south faces. The most notable fire activity occurred along an extensive part of the west face in the last 15 min (Fig. 6–8).

The simulated fires (Fig. 6–9) were delayed from reaching the east face for about 30 min due to various partitions on the east side of the floor. Fires were predicted along the west face at various times, even though the actual fires did not appear there until the last 15 min. Elsewhere, the simulated fires responded mainly to the opening of windows. There was substantial fire activity predicted in the building core due to the extensive damage predicted by the impact analysis (NIST NCSTAR 1-2). The simulations suggested that air rising through the core mixed with the oxygen-starved fuel gases that were accumulating on this floor because of the relatively light exterior damage away from the impact zone. Because there was no evidence to confirm or deny the existence of vigorous fire activity within the core, the extent of the damage to the core was a parameter identified early in the Investigation as a prime candidate for a sensitivity study.

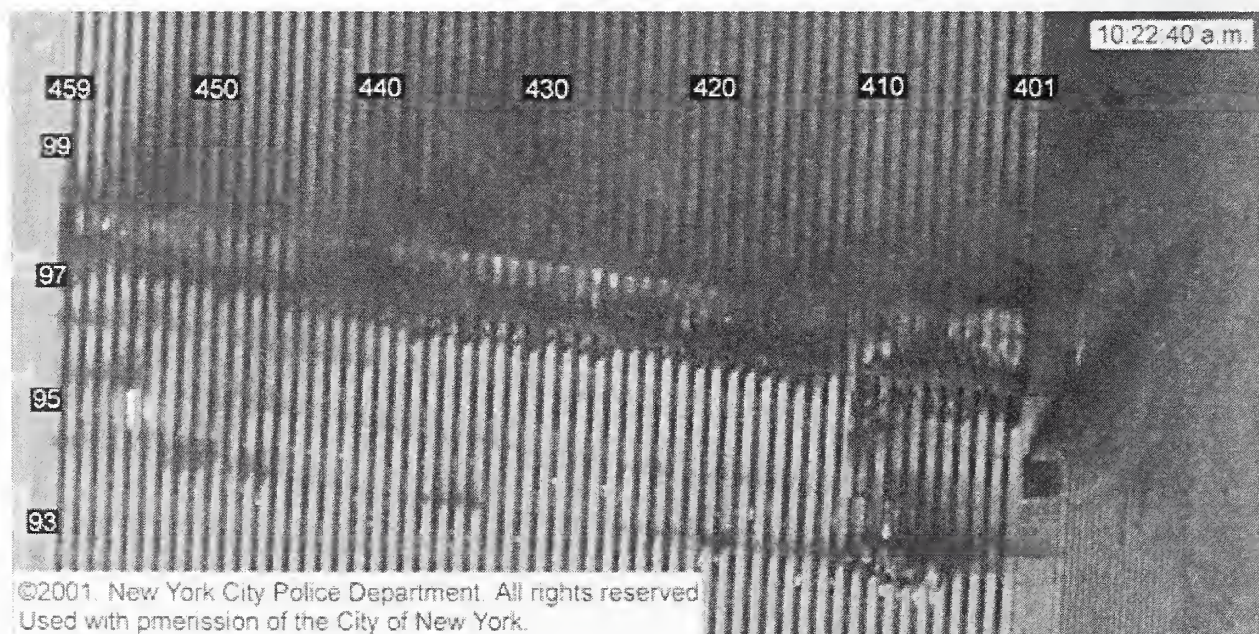


Figure 6–8. West face of WTC 1 shortly before collapse.

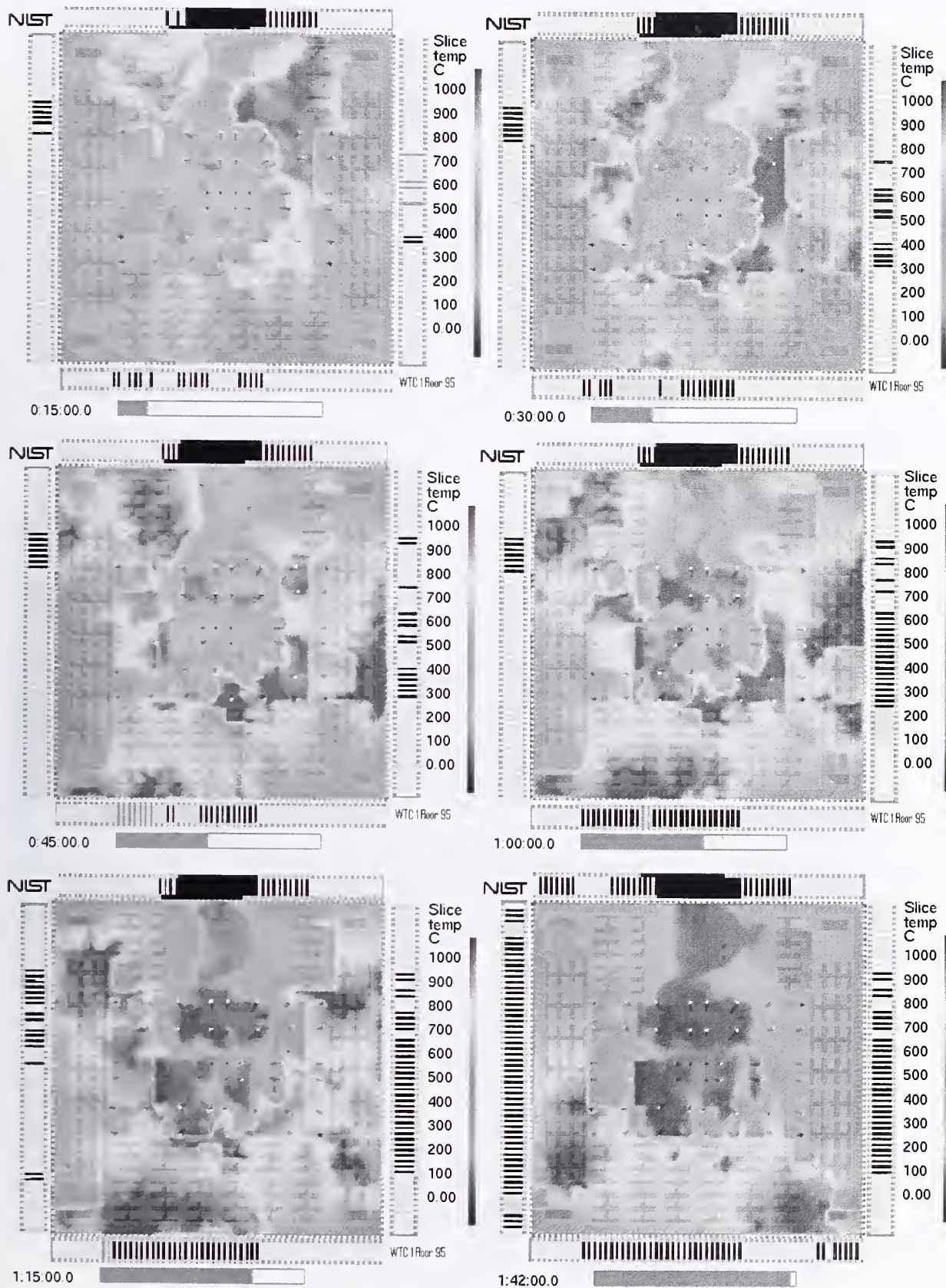


Figure 6-9. Upper layer temperature of WTC 1, floor 95.

6.2.5 Floor 96, Case A

Floor 96 was directly impacted by the airplane, with damage throughout the core. Fires were observed 15 min after impact on the east side of the north face and west side of the south face (Fig. 6–10), corresponding to where aircraft debris exited the building. The fires were observed to be burning vigorously on the east face 20 min after impact, and progressed steadily toward the south. Eventually, the fires arrived at the southeast corner of the floor within about 20 min of collapse. The fires did not spread rapidly west to east along the south face, presumably because of offices and conference rooms located in the south central part of the floor. As on Floor 95, small fires were observed along the west face prior to collapse.

The simulations (Fig. 6–11) mimicked the movement of fire along the east face of the floor, but overestimated the extent of the fire on the west face during the first 45 min. The visual observations suggested that the fire on the west face originated in the south, not the impact area. The simulation suggested a more symmetrical spread of fire along the east and west faces, originating in the impact area. The delayed movement of the fires along the south face was captured in the model because of the inclusion of office walls.

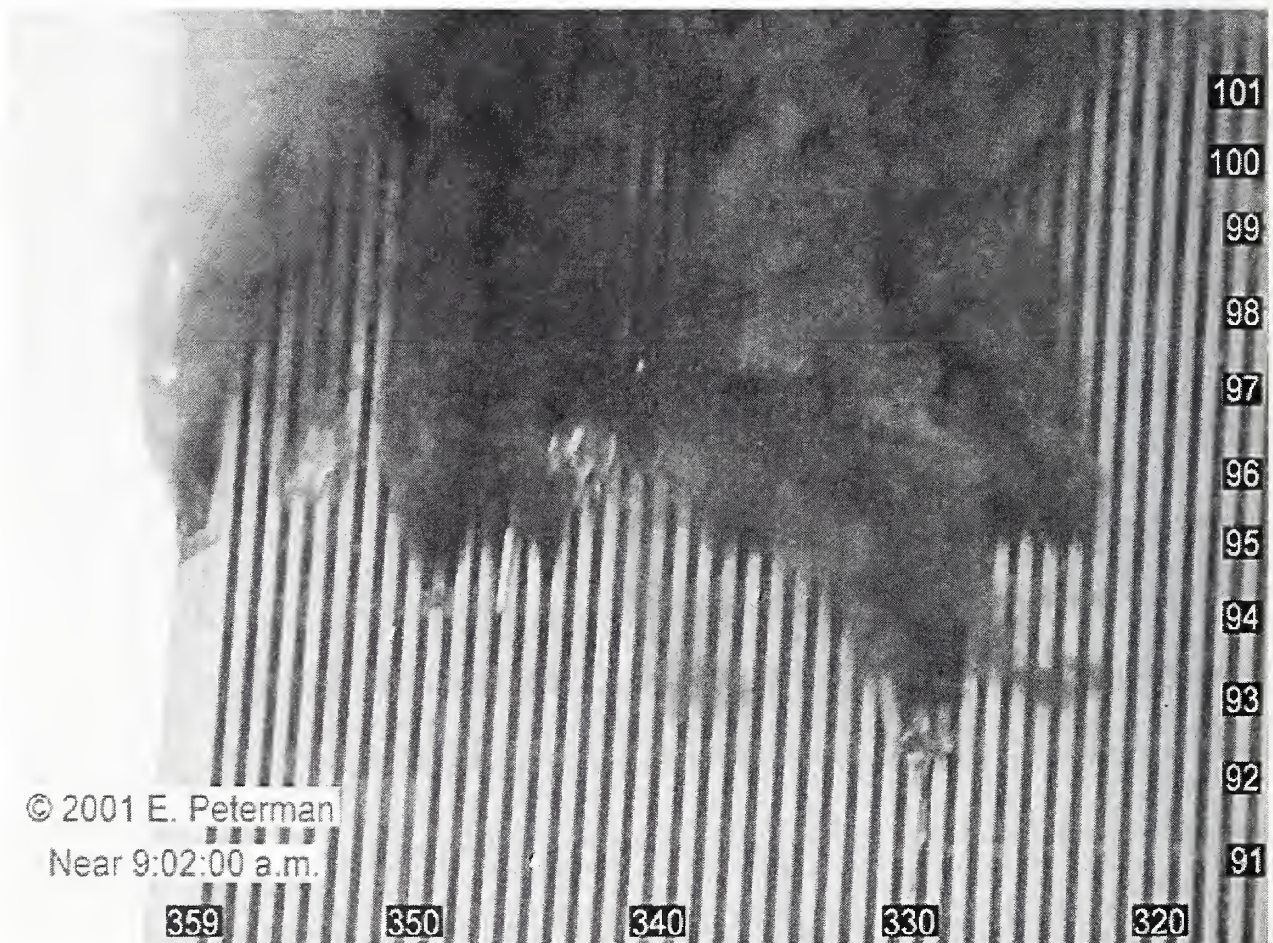


Figure 6–10. West side of south face of WTC 1, 15 min past impact.

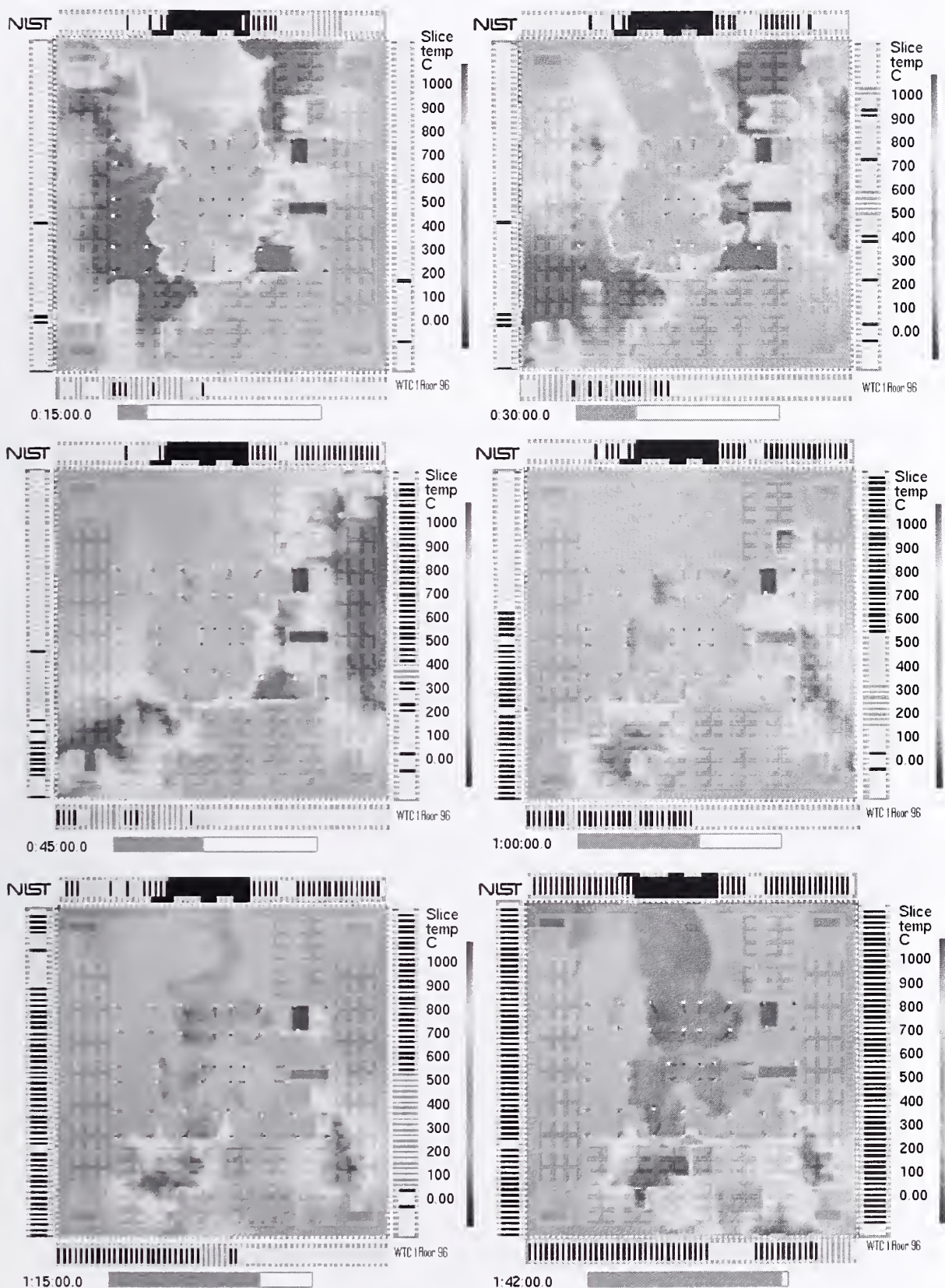


Figure 6–11. Upper layer temperature of WTC 1, floor 96.

6.2.6 Floor 97, Case A

Floor 97 was impacted by the right wing of the airplane. The observed fire activity during the first 15 min was extensive, involving substantial areas on the north (Fig. 6–12), west and east faces. Fire spread steadily southward along the east face, but erupted more rapidly on the west and south faces. Ultimately, the east, west and south face fires converged on the southeast corner, where there was very vigorous burning just prior to collapse.

For the simulation (Fig. 6–13), initial damage was estimated to be confined to the west half of the building core on this floor. The simulated fires followed the observed paths well, probably due to the fact that the floor plan was fairly open and the window breakage pattern more predictable than it was on other floors with more geometric complexity. The simulated fires arrived in the southeast corner at roughly the same time as the observed fires.

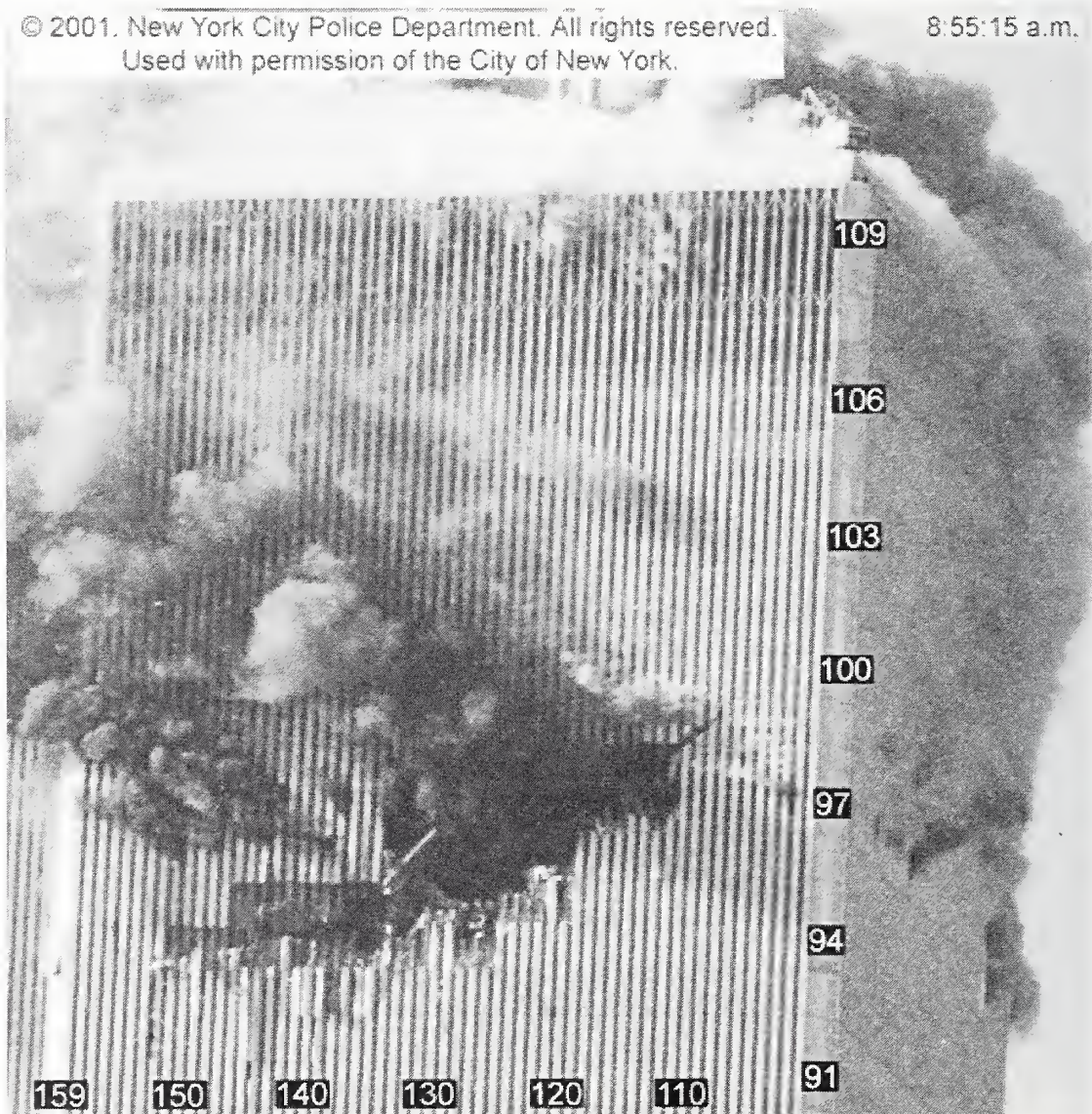


Figure 6–12. North face of WTC 1 at 8:55 a.m.

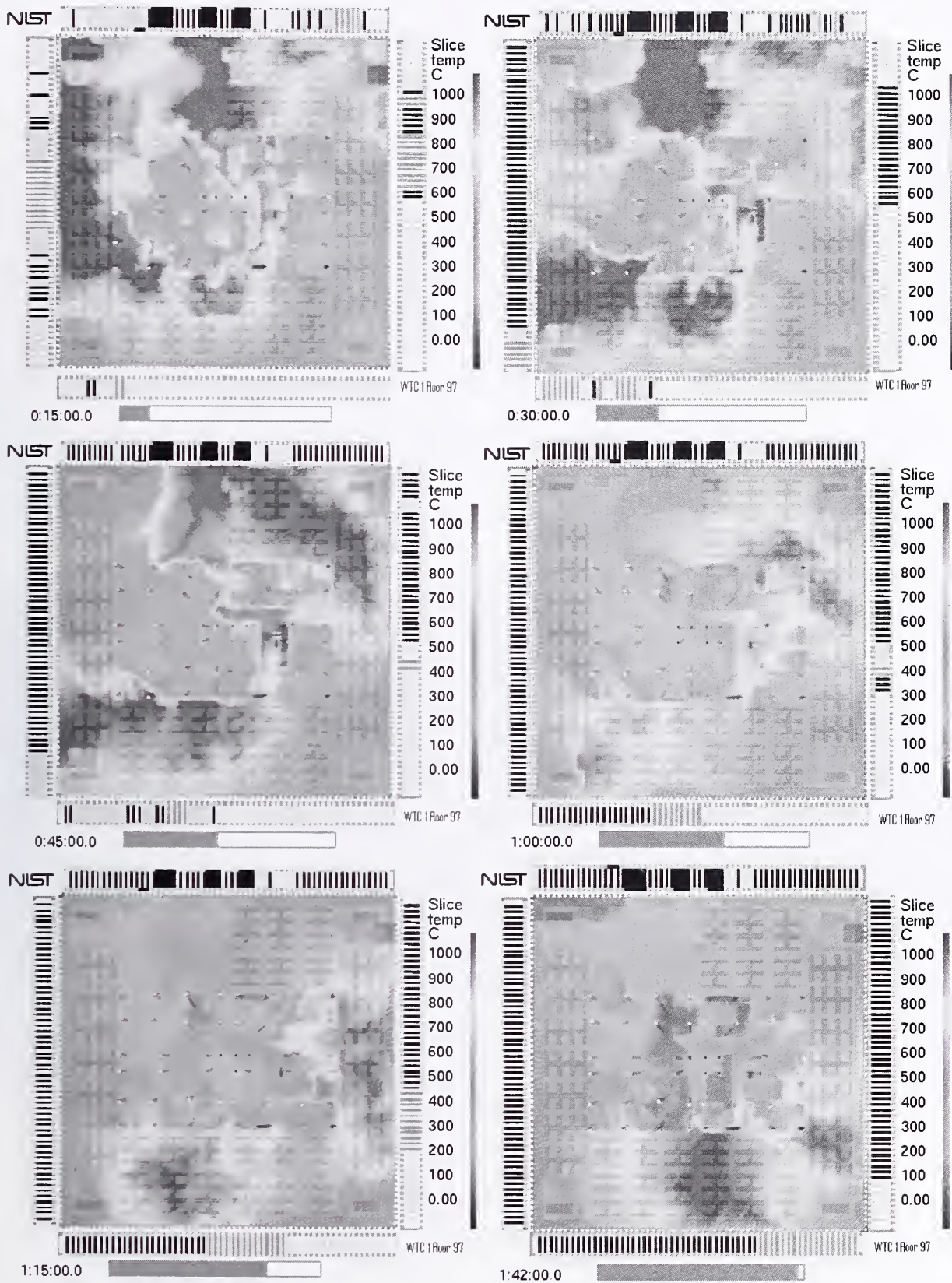


Figure 6-13. Upper layer temperatures of WTC 1, floor 97.

6.2.7 Floor 98, Case A

Floor 98 was struck by the right tip of the airplane wing and suffered minor damage according to the impact analysis and the visual observations. Fires did not appear for at least 40 min, but then they grew rapidly on the west, south and east sides (Fig. 6–14). The most vigorous observed fire activity occurred along the east side of the south face and the south side of the east face in the minutes prior to collapse (refer to Fig. 6–45).

The simulation (Fig. 6–15) showed modest fire activity in the first 30 min, due to the small amount of jet fuel distributed on the floor and the limited openings in the exterior and core. As large numbers of windows broke out, the simulated fires grew, following the observed patterns that eventually brought the heart of the fire to the southeast corner.

The observed fire behavior on the 98th floor was considerably different than that on the 97th. Wide areas on the west, north and east sides were observed burning after 40 min on the 98th floor, whereas on the 97th, the observed fires developed early and progressed along more distinguishable fronts. The simulations appeared to mimic the behavior of the 97th better than the 98th floor, most likely a result of the tendency of the mixture fraction combustion model within FDS to form “fronts” separating fuel-rich from fuel-lean parts of the floor.

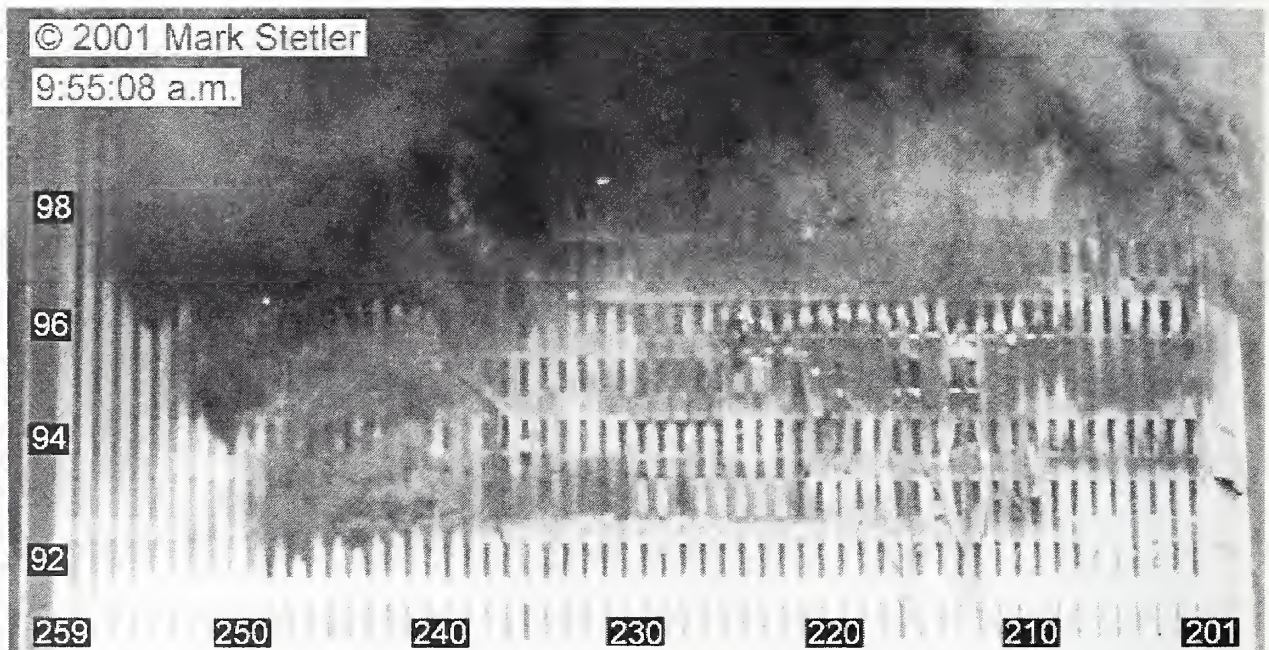


Figure 6–14. East face of WTC 1 at 9:55 a.m.

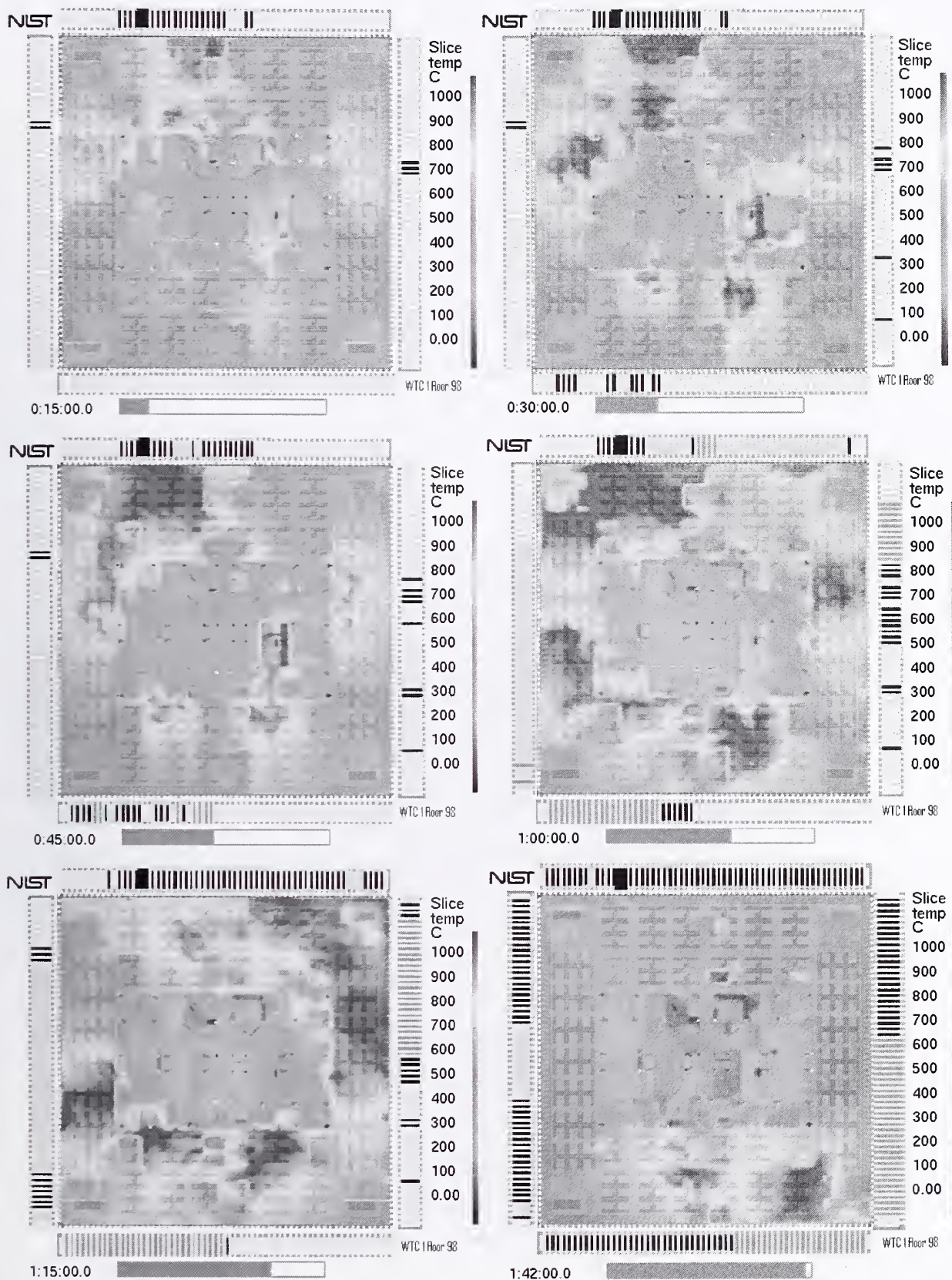


Figure 6-15. Upper layer temperatures of WTC 1, floor 98.

6.2.8 Floor 99, Case A

Floor 99 was only impacted by the right wing tip of the airplane, and the initial observed damage to the exterior was light. There was little window breakage between impact and collapse, but some fires broke out on the south face and could be observed through the smoke rising from fires on lower floors (Fig. 6–16).

The simulated fire activity (Fig. 6–17) did not show any discernable trends and did not provide any clues as to the observed fire activity on the south face. Some jet fuel was initially distributed in the northwest quadrant based on the results of the impact study (NIST NCSTAR 1-2), but with few window openings and no assumed core damage, the simulations behaved as one would expect of an oxygen-limited fire.

One point of interest is the high temperatures in some of the elevator shafts. It has been speculated that the fires observed on the west face of the 104th floor either were started just after impact due to the fuel gases that were pushed into the vertical shafts by the sudden ignition of atomized jet fuel, or the fires were started as a result of the accumulation of fuel rich gases in the core shafts over the course of the 100 min. The presence of fire in the shafts on the 99th floor in the simulation provides some support for the latter hypothesis, but no simulations were performed for floors higher than the 99th.



Figure 6–16. South face of WTC 1 burning, with WTC 2 in the foreground.

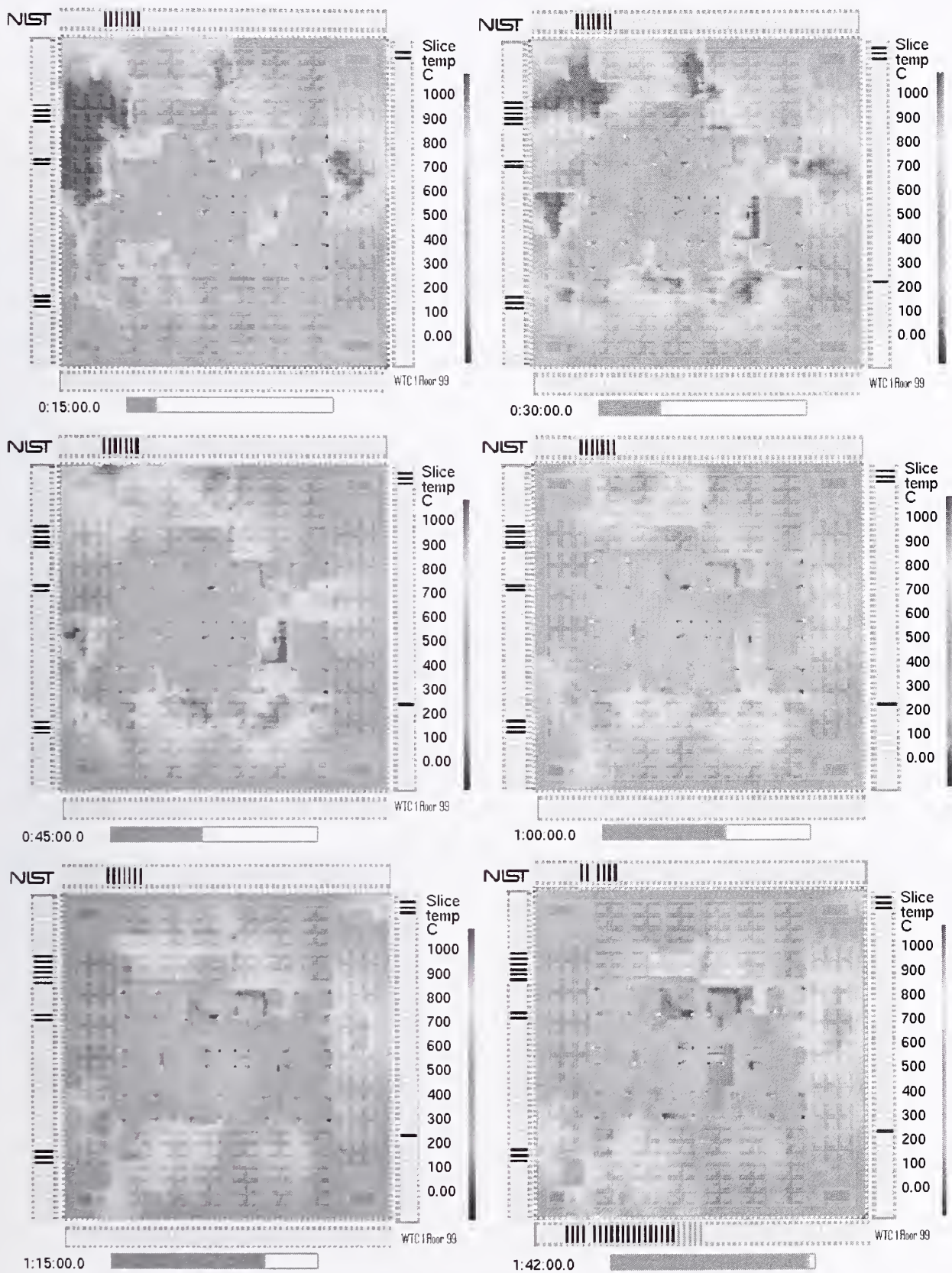


Figure 6–17. Upper layer temperature of WTC 1, floor 99.

6.3 SIMULATION OF WTC 1, CASE B

Following the completion of the Case A simulation of WTC 1, the simulation was re-run with changes made to several important parameters in order to assess the sensitivity of the calculation to changes in model input. For WTC 1, the changes made were designed to create a “more severe” fire.

1. The combustible load was increased from 20 kg/m² (4 lb/ft²) to 25 kg/m² (5 lb/ft²).
2. The walls surrounding vertical shafts in the core were not completely removed. The sections of the walls near the ceiling (1.2 m) were left intact to trap hot gases near the structural members.
3. The aircraft debris was concentrated in the core area, adding to the combustible load surrounding the core columns.

The intent of these changes was to span the probable range of gas temperatures in the core area by considering a more severe case. The Case A simulation showed that the model was replicating the basic fire behavior at the building exterior, but there was no way to confirm the behavior deep within the building. The addition of extra combustibles and the change in geometry to more effectively trap hot gases were designed to increase the duration of the fires in the core area, and also to increase the temperatures by deepening the upper layer with the addition of a soffit. In Case A, the areas of the core identified in the impact study to have sustained major damage had all of the walls removed, completely opening up vertical shafts. This allowed more oxygen to reach the fires from lower floors, but it also allowed the hot gases to escape to higher floors. By opening the walls only part way, the oxygen was allowed to reach the fires, but the hot gases were trapped in the upper layer.

The results of the Case B simulation of WTC 1 are included on the following pages (Figs. 6–18 through 6–25). In general, the results were similar to Case A because the fires in WTC 1 were limited by the supply of air from the exterior windows. As the window breakage pattern was not changed in Case B, the extra combustibles within the building did not contribute to a larger fire, but they did delay the spread slightly because the fires were sustained longer in any given location due to the increase in combustible load.

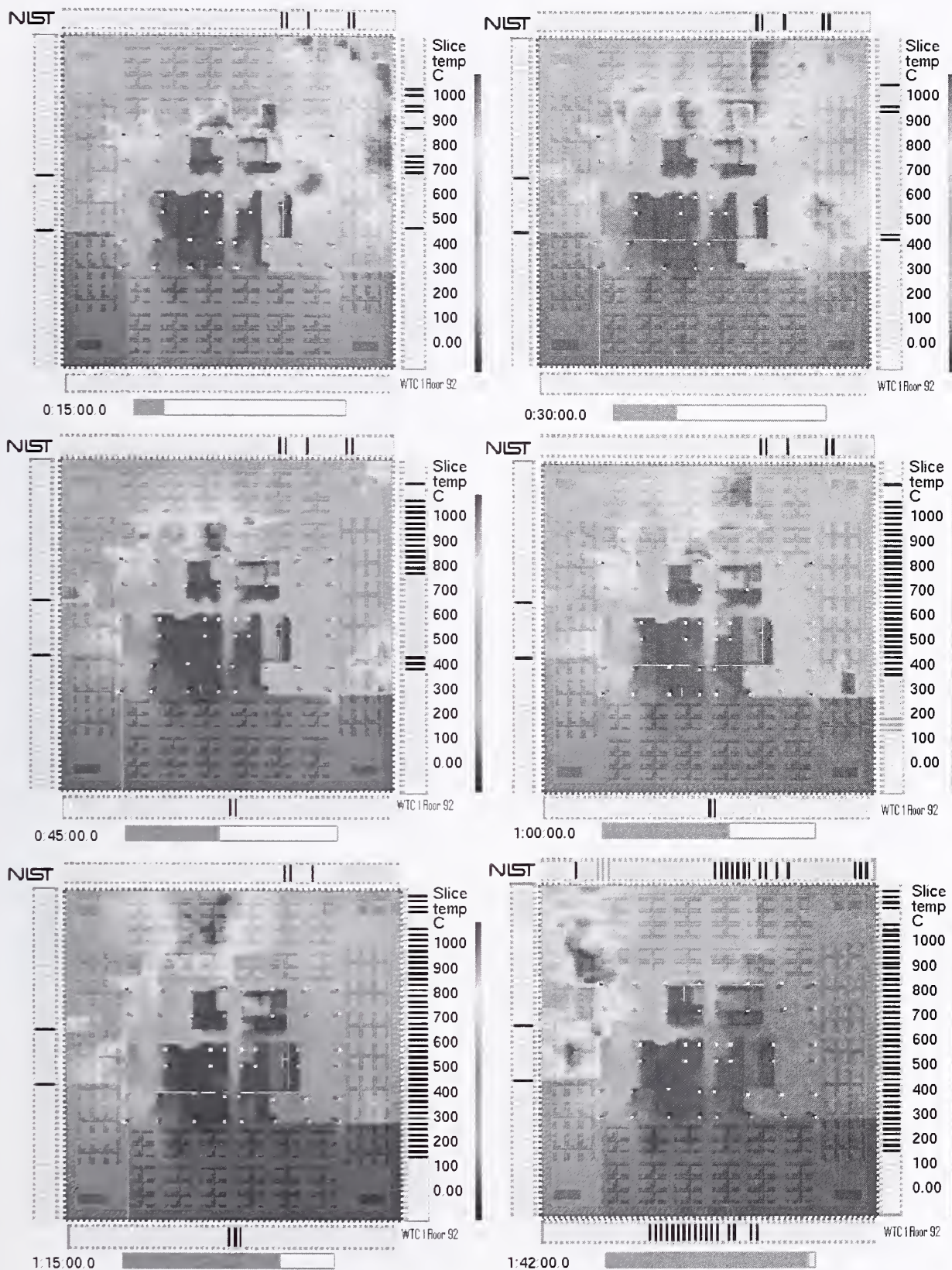


Figure 6–18. Simulation of WTC 1, floor 92, Case B, upper layer temperatures.

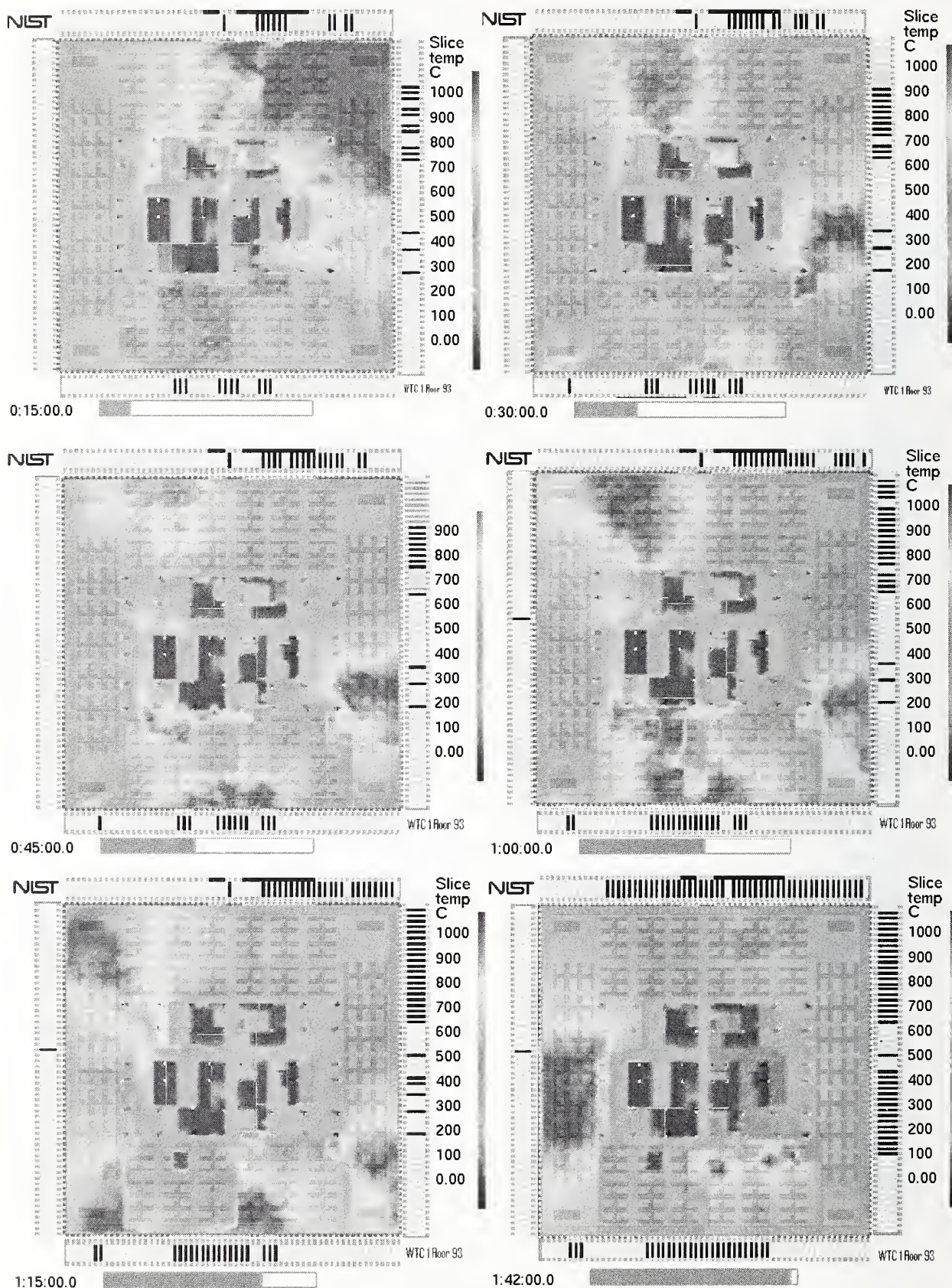


Figure 6-19. Simulation of WTC 1, floor 93, Case B, upper layer temperatures.

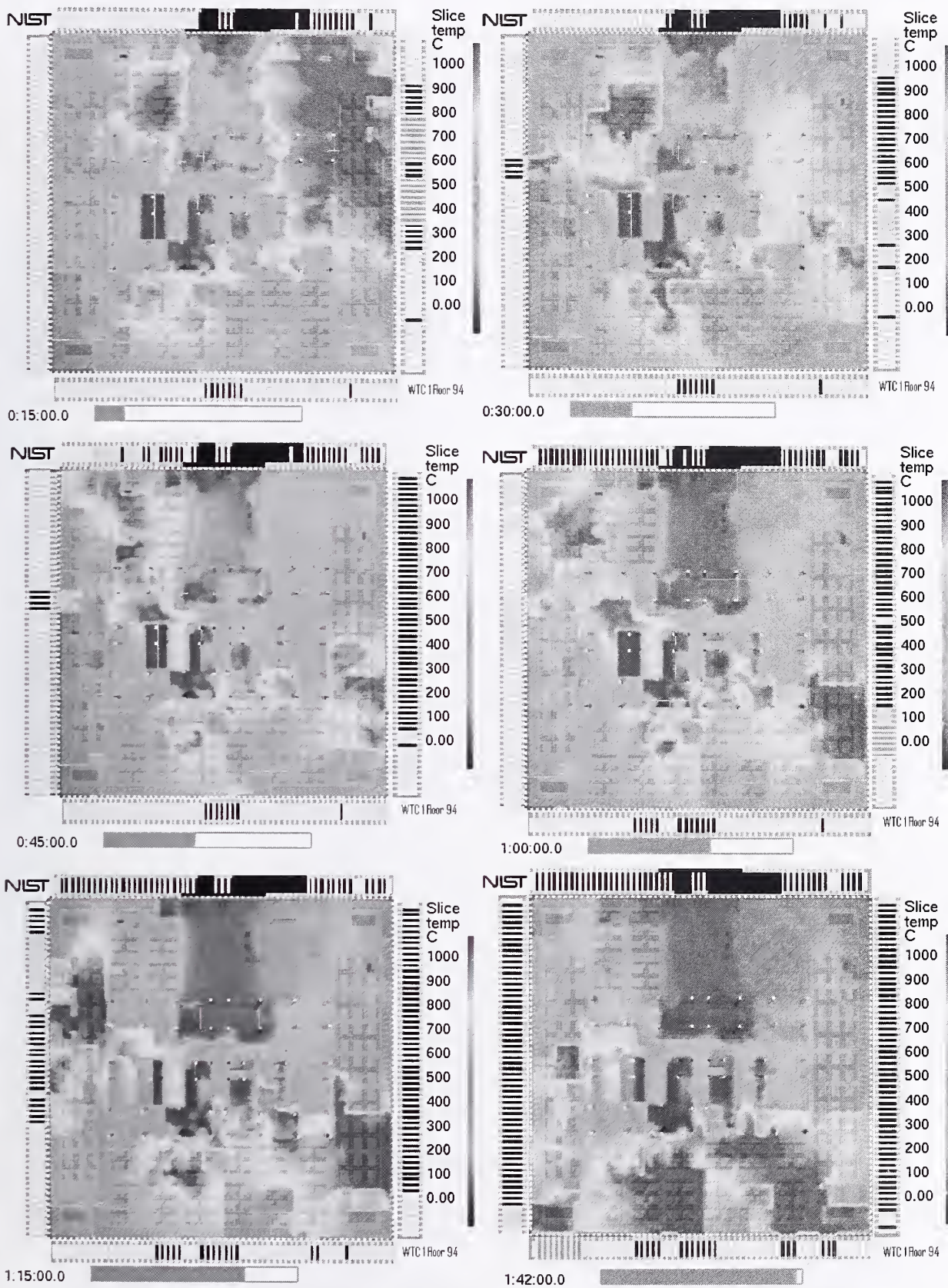


Figure 6–20. Simulation of WTC 1, floor 94, Case B, upper layer temperatures.

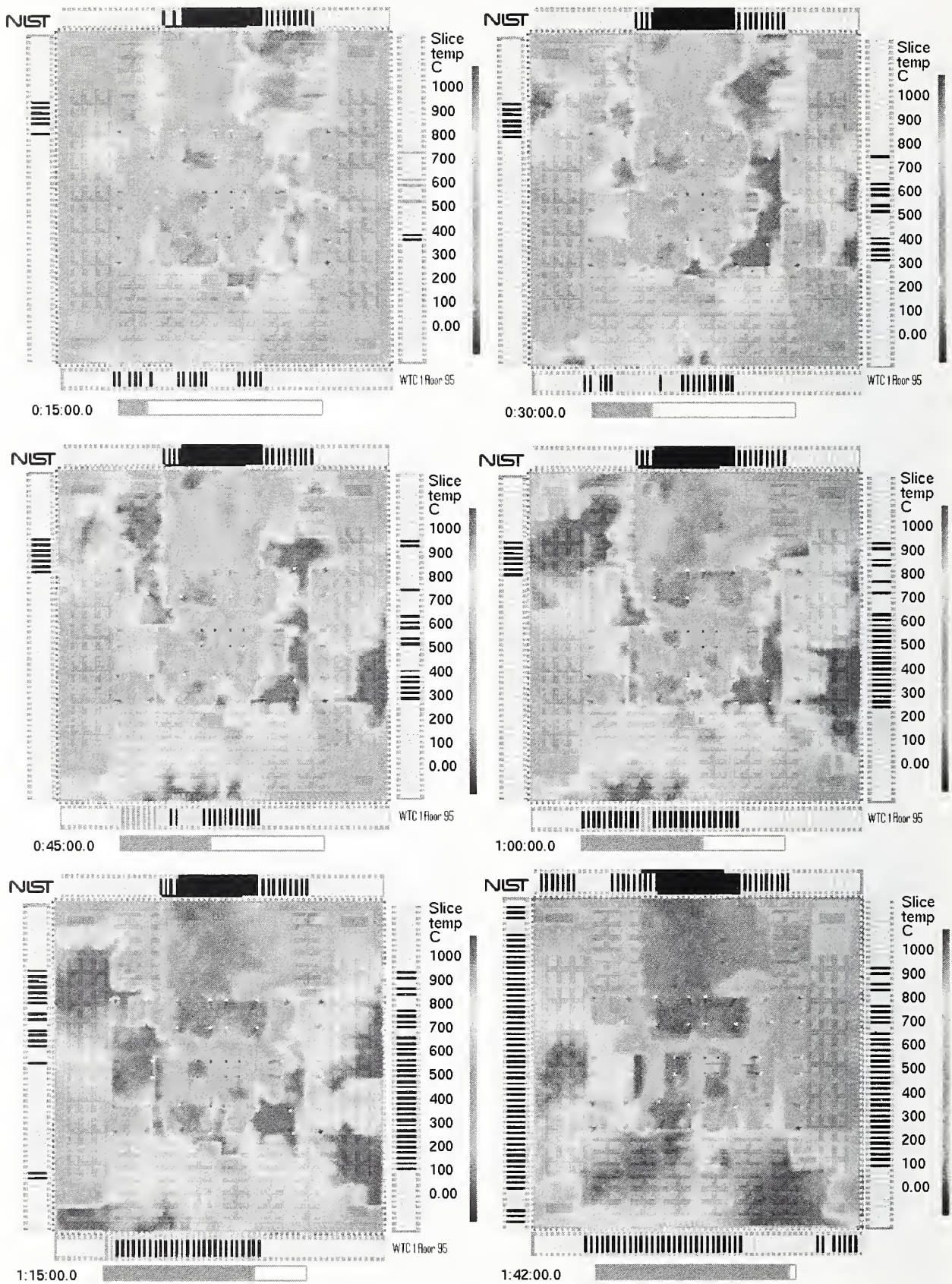


Figure 6–21. Simulation of WTC 1, floor 95, Case B, upper layer temperatures.

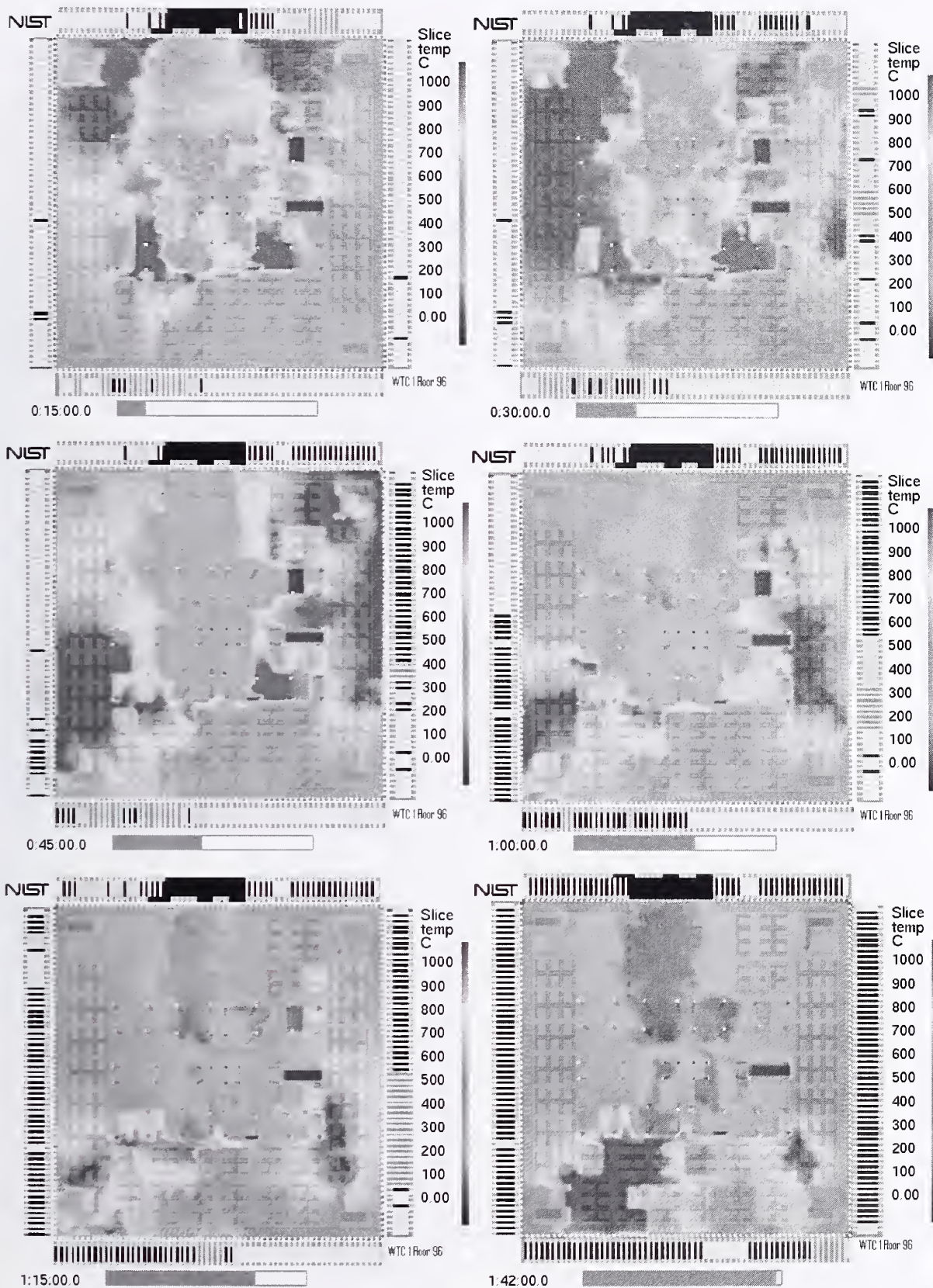


Figure 6-22. Simulation of WTC 1, floor 96, Case B, upper layer temperatures.

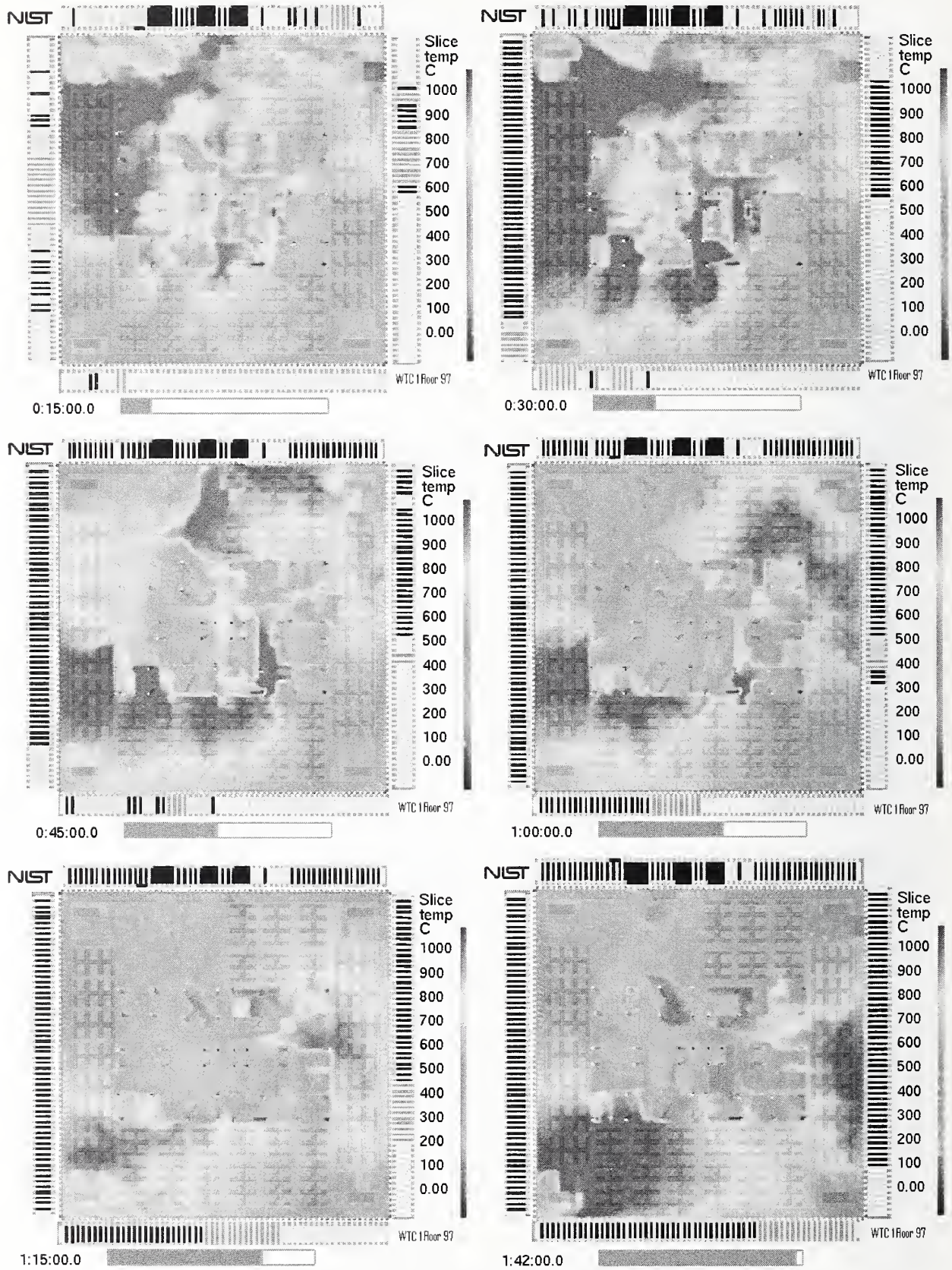


Figure 6–23. Simulation of WTC 1, floor 97, Case B, upper layer temperatures.

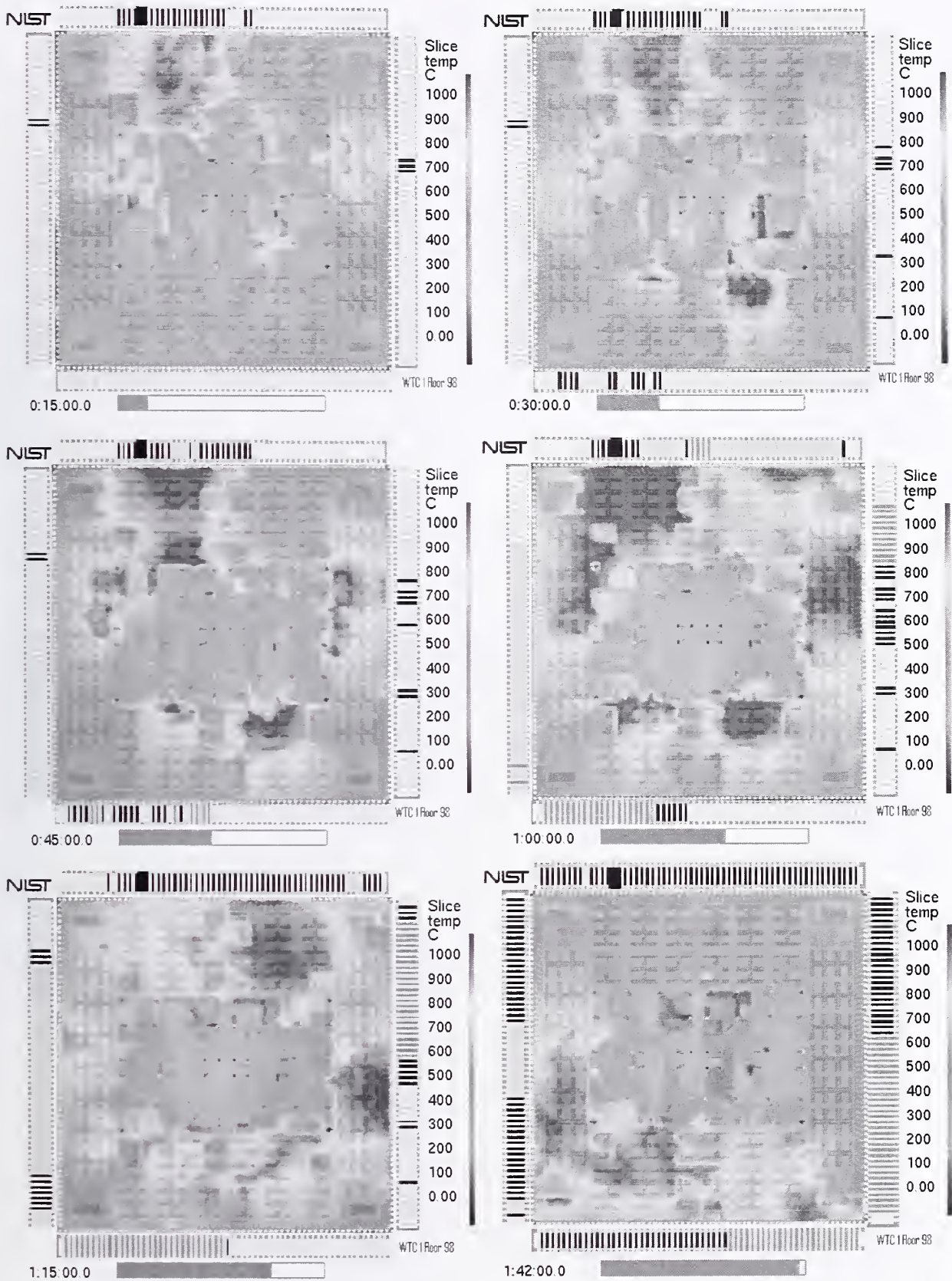


Figure 6–24. Simulation of WTC 1, floor 98, Case B, upper layer temperatures.

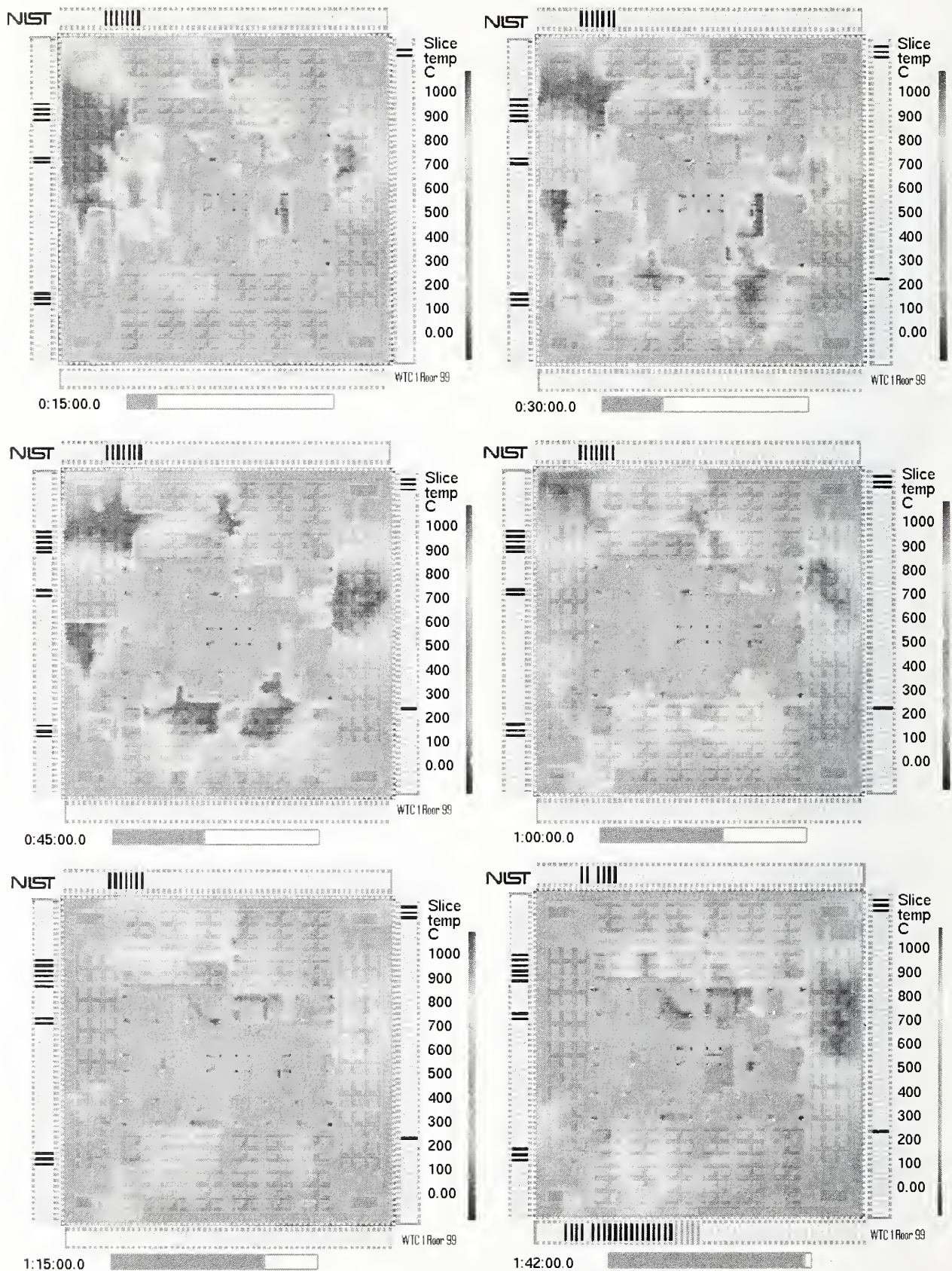


Figure 6–25. Simulation of WTC 1, floor 99, Case B, upper layer temperatures.

6.4 SIMULATION OF WTC 2, CASE C

Overall, the fire activity in WTC 2 was more difficult to simulate than that of WTC 1 for two reasons. First, the airplane swept across wide swaths of floor area exterior to the building core, simultaneously splintering much of the furnishings and plowing their mass towards the northeast corner of the building. Neither the impact study nor the validation experiments performed at NIST could be completely relied upon to predict the final distribution, condition and burning behavior of the demolished furnishings. Second, of the floors simulated, only the layout of the 78th floor was available to the Investigation, and the other floors were only roughly described by former occupants. This introduced uncertainties having to do with the spread, or lack of spread, of the observed fires on various floors.

The parameters for the simulation of WTC 2, Case C, were similar to those of WTC 1, Case A. However, unlike the simulation of WTC 1, the workstations were assumed to be damaged throughout most of the six floors that were included in the simulations. This was done to reduce the overall burning rate in the model that was judged to be inconsistent with the visual evidence in a number of preliminary calculations. In Case D, the furnishings were restored to their “undamaged” state, except in the immediate vicinity of the airplane impact, to create a more severe fire.

In both Cases C and D, the displaced furnishings in the impact areas on the east sides of floors 80, 81, and 82 were pushed toward the northeast corner of the building, where they along with the aircraft combustibles were represented by an equivalent mass of “rubble” (see Chapter 4 for a description of “rubble”). In Case C, the rubble was heavily concentrated in the corner (5 times the combustible load of 20 kg/m^2 over an area 15 m by 15 m), whereas, it was less concentrated in Case D (2.5 times over an area 30 m by 15 m). The heavy concentration of combustibles in the corner produced a fire that lasted an entire hour in that location, consistent with visual evidence.

In general, the observed fires in WTC 2, with the exception of the northeast corner, appeared to be less active, at least at the building exterior, than those of WTC 1. This was somewhat surprising, given that most of the windows on the east face from floor 80 to 82 and roughly a third of those on the north face were broken out upon impact. Fires appeared sporadically on the east face throughout the hour following impact. Eventually, toward collapse, fires appeared to be spreading westward on the north face in much the same way that the fires were observed to spread in WTC 1 on the east and west faces. Two of the questions that were not answered by the numerical simulation were why the fires took so long to spread along the north face, and why the fires did not reach the west face in sufficient quantity to break windows. The delays might have been due to barriers that were unknown to the Investigation.

6.4.1 Floor 78, Case C

There was only light fire activity observed on the 78th floor (Fig. 6–26), and this behavior is reflected in the numerical simulation. The impact analysis (NIST NCSTAR 1-2) predicted that a small amount of jet fuel was released on this floor. Given the modest number of window openings and the estimated light core damage, the numerical simulation of the fire (Fig. 6–27) did not predict any areas of significantly high temperature. Most of the observed broken windows were broken out upon impact.

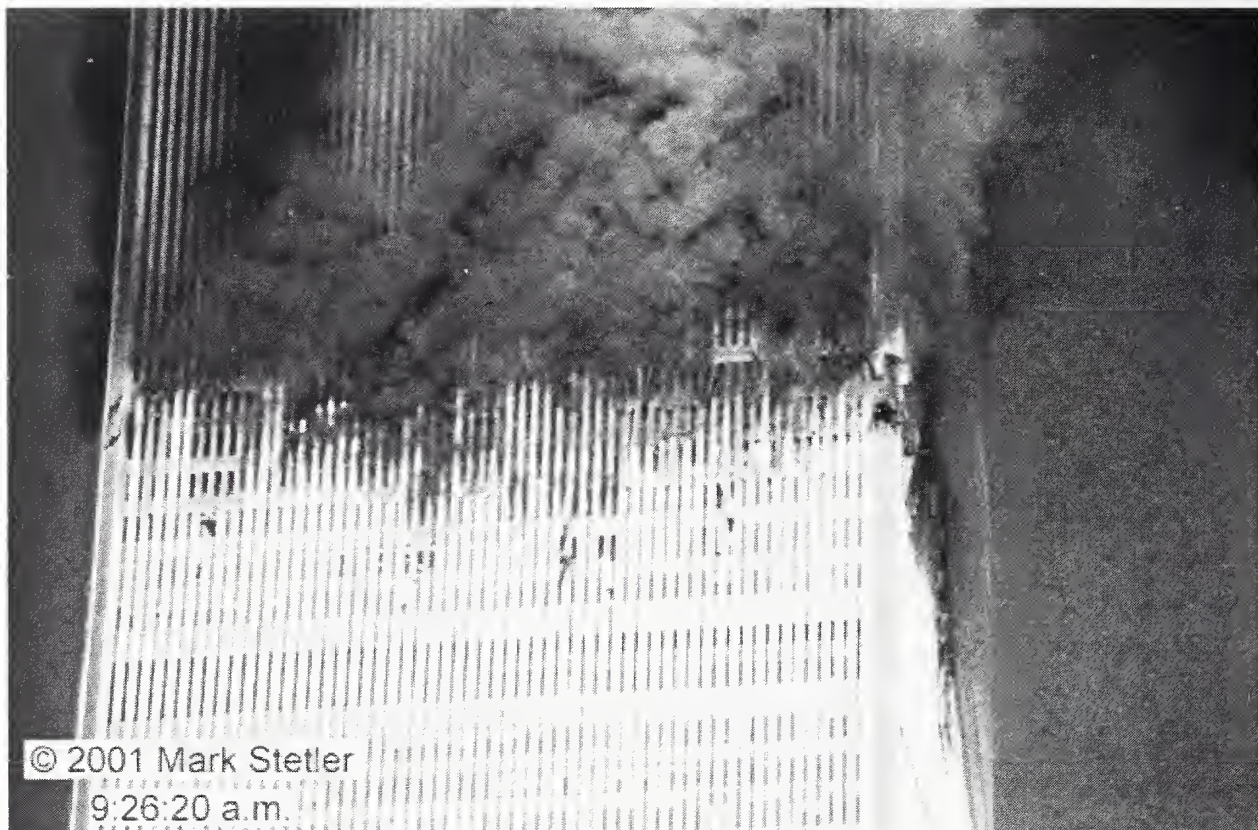


Figure 6–26. East face of WTC 2 at 9:26 a.m., 23 min after impact.

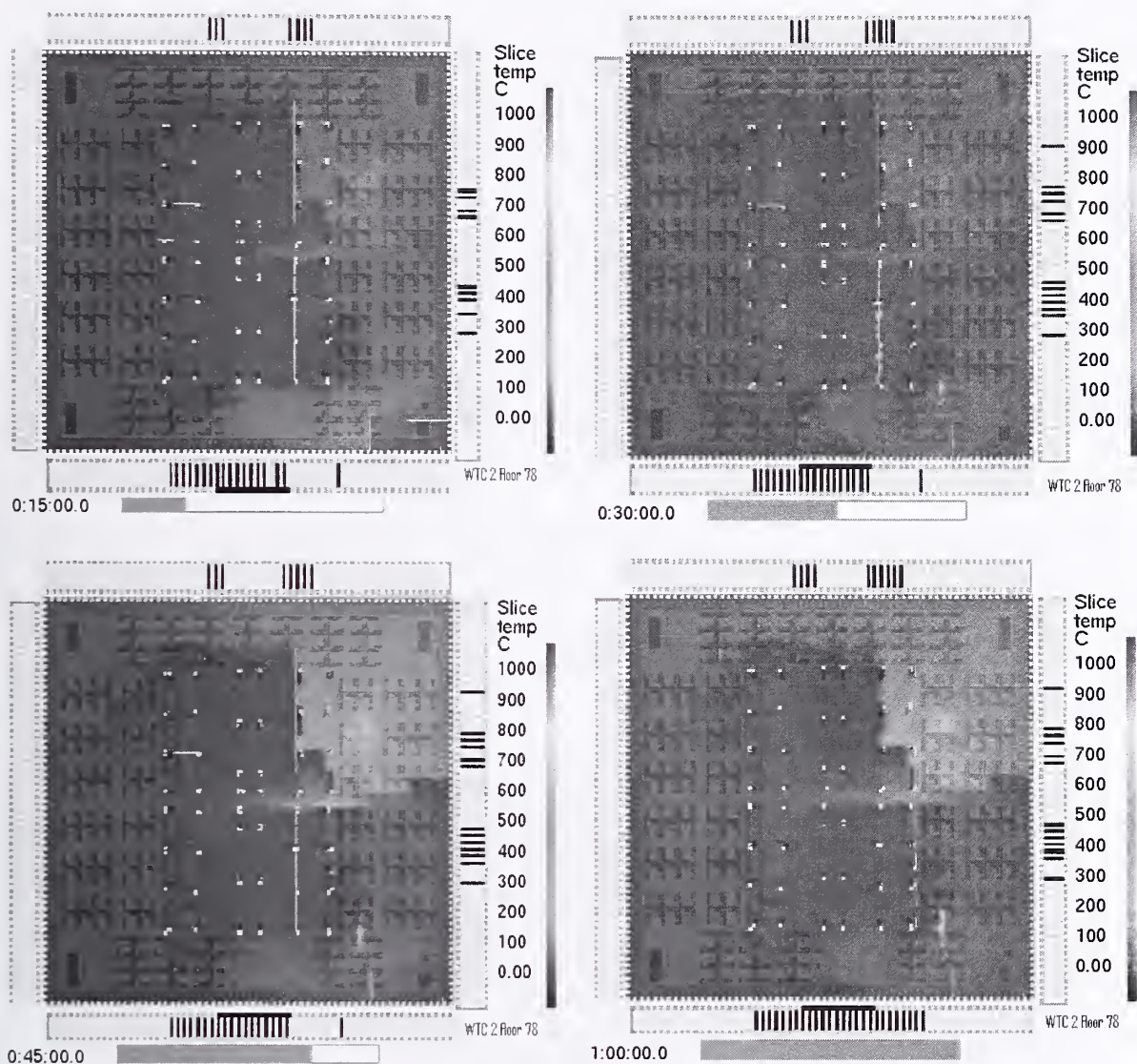


Figure 6-27. Upper layer temperatures of WTC 2, floor 78.

6.4.2 Floor 79, Case C

The left wing of the airplane struck the 79th floor near the center of the south face, starting fires there and at the opposite side of the floor on the north face (Fig. 6–28). Damage to the east face was modest initially, but after 57 min most of its windows were gone. Except for the steadily burning fires on the north face, there was only sporadic fire activity on the south and east faces, with a notable exception being a steady fire that burned on the east face 30 to 40 min after impact (not shown in the figures). There was no window breakage or fire activity observed on the west face.

The simulation (Fig. 6–29) predicted the fires on the north face, some activity on the east face, and some on the west. It is doubtful that this amount of fire activity could have occurred in the west part of the floor without any windows breaking out. The simulated west side fires were supported by air rising up through various openings in the floor slab.

The simulated fires burned more vigorously on the east side of the building than those that were observed. It was assumed in the model that the furnishings on the east side remained relatively intact, and numerous windows were broken out. Given that jet fuel was presumably spilled along a path from south to north through the middle of the floor, the model predicted that the initial fires spread from the core toward the open windows and combustibles of the east side. Even with an imposed 60 percent reduction in the nominal burning rate of the furnishings, the model still over-predicted the fire activity on the east side.

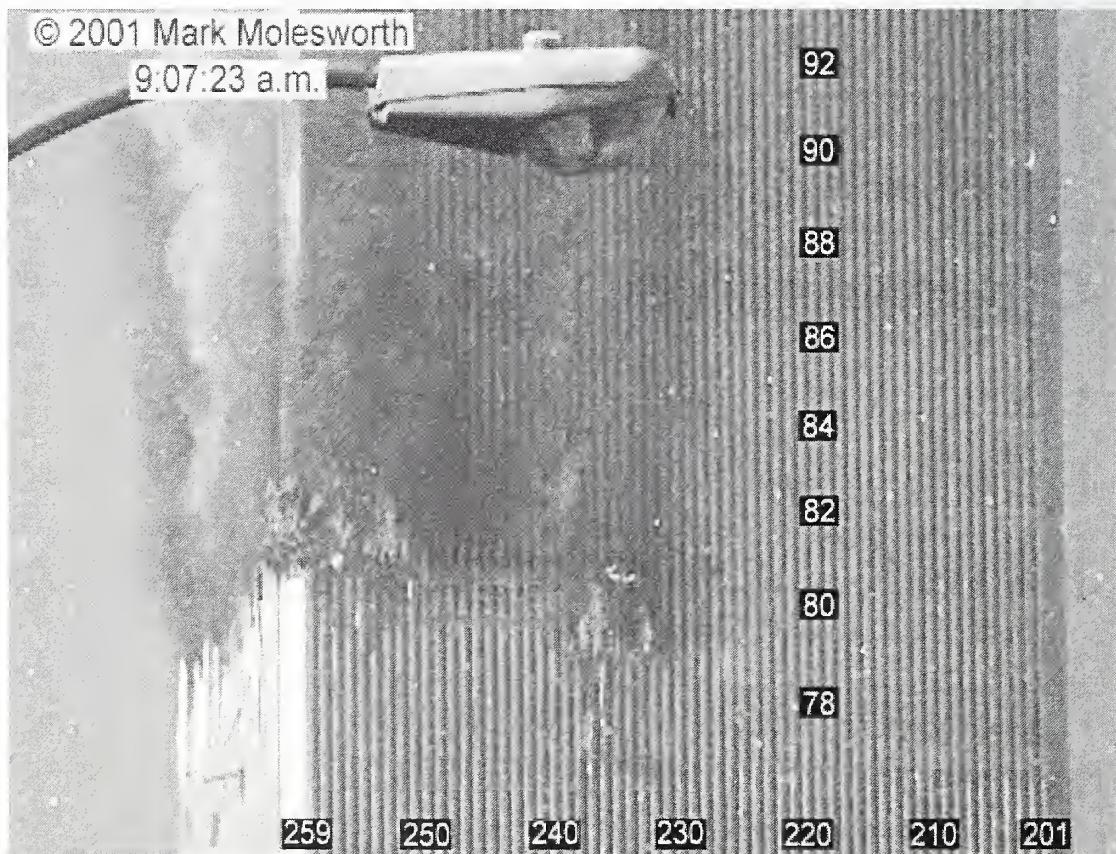


Figure 6–28. North face of WTC 2, with the fire on the 79th floor shown at center.

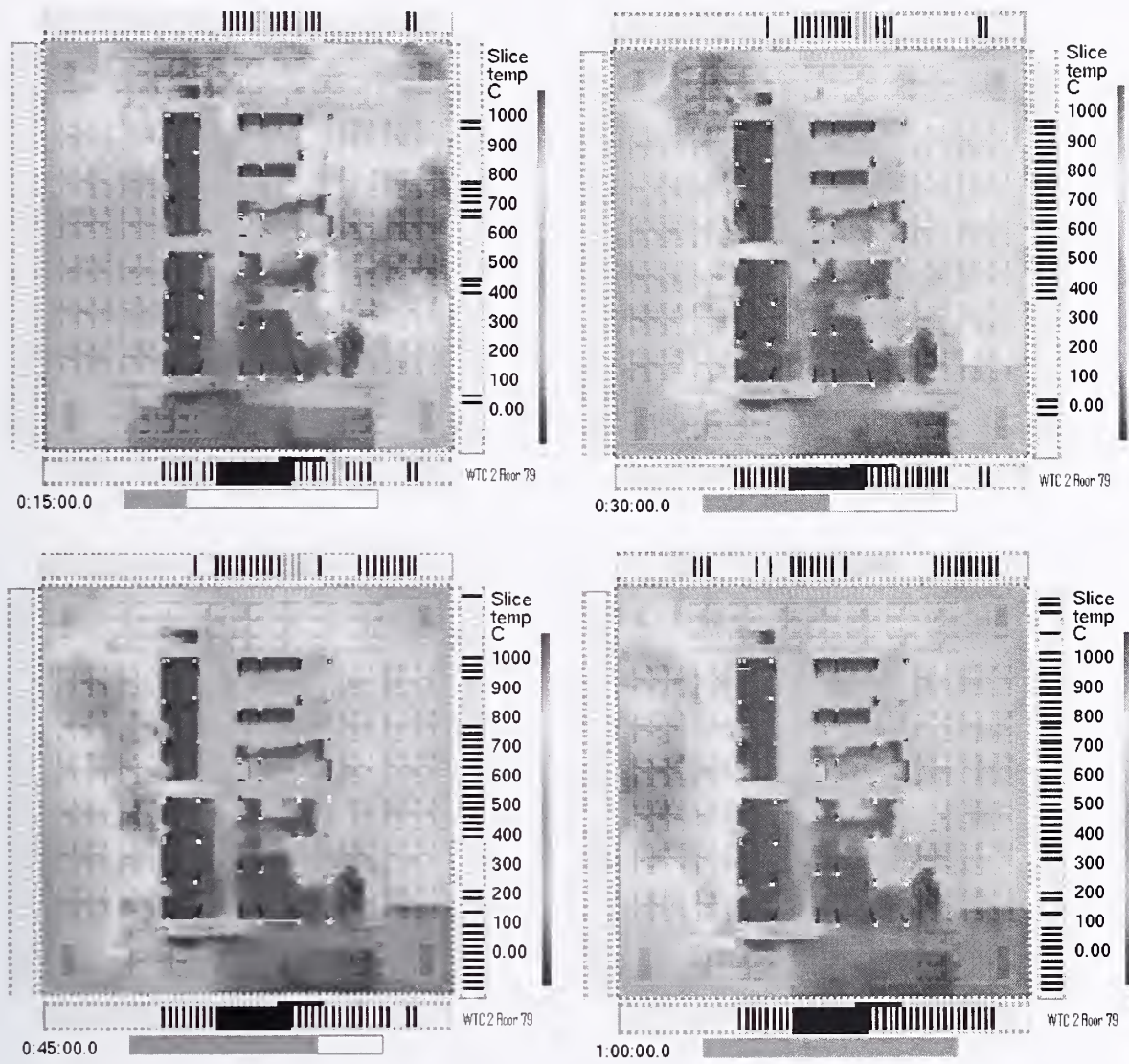


Figure 6–29. Upper layer temperatures of WTC 2, floor 79.

6.4.3 Floor 80, Case C

The lower half of the fuselage struck the 80th floor, causing considerable damage along a path from the south central to northeastern corner of the floor. Predictions of jet fuel distribution indicated less jet fuel was deposited on this floor, presumably because the main fuel tanks of the airplane struck the 79th and 81st floors. There was less fire activity in the northeast corner of the building compared to the 81st and 82nd floors (Fig. 6–30).

Preliminary simulations of WTC 2 showed far more fire activity on this floor than was observed. Consequently, the combustible load and the volatility of the furnishings were reduced to better match the observations. The only discernable trend in the simulation (Fig. 6–31) was the movement of fire westward on the north face at a rate greater than that of the observed fires. Fires that broke out on the south face close to the time of collapse were not captured in the simulation, probably because there were several barriers and an internal staircase on the south part of the floor that completely stopped the simulated fires.

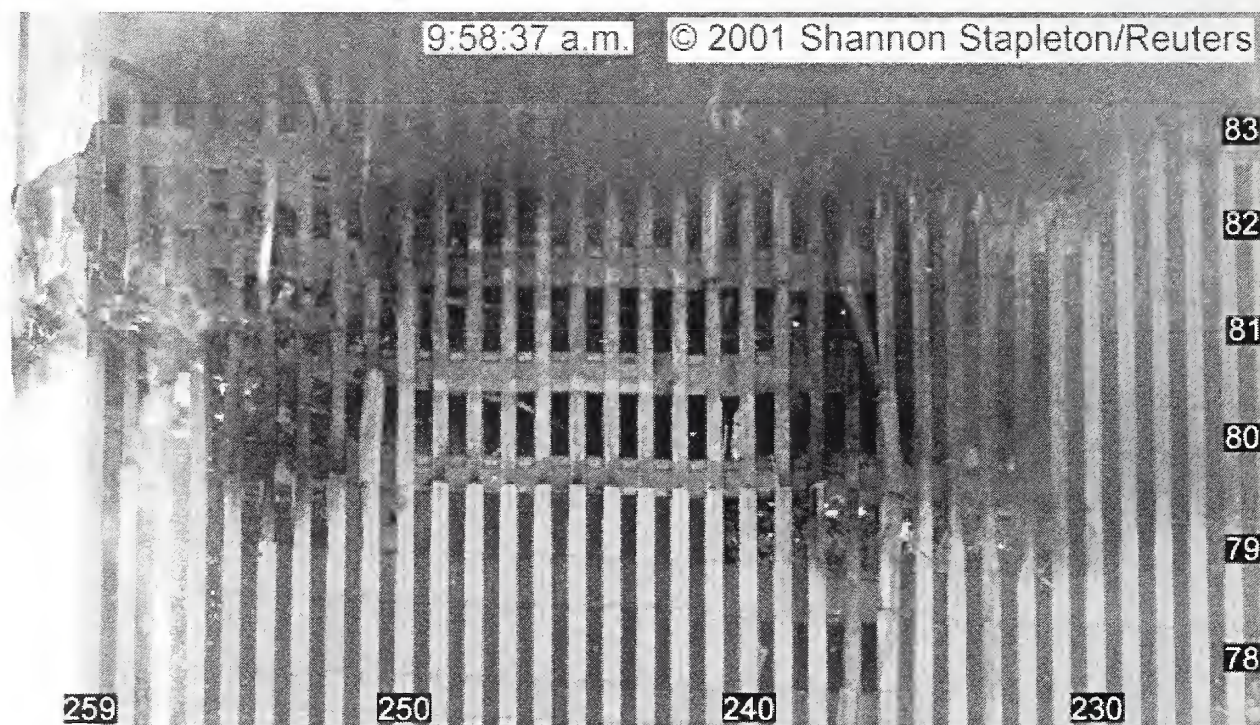


Figure 6–30. East side of north face, WTC 2, at 9:58 a.m., just before collapse.

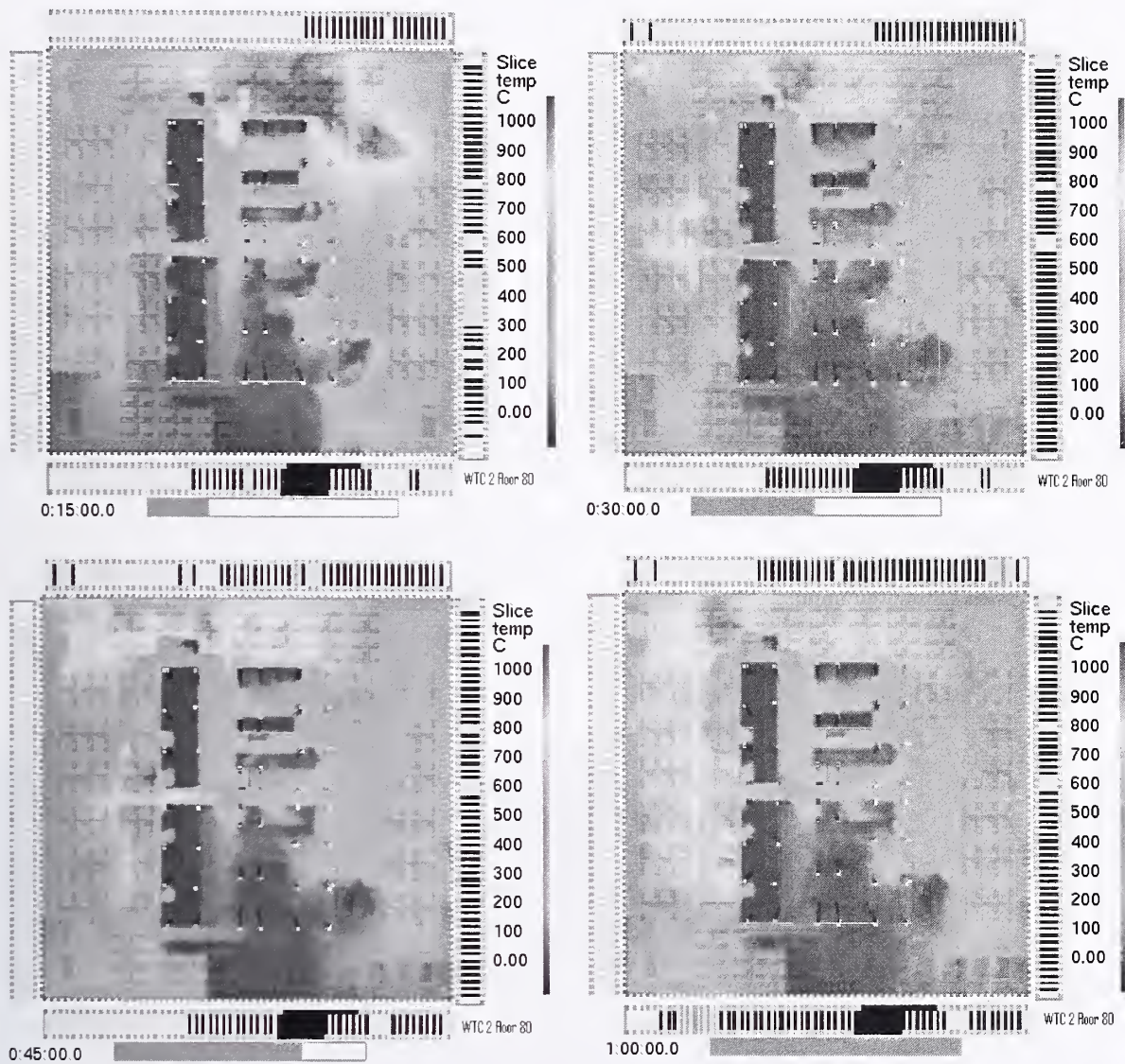


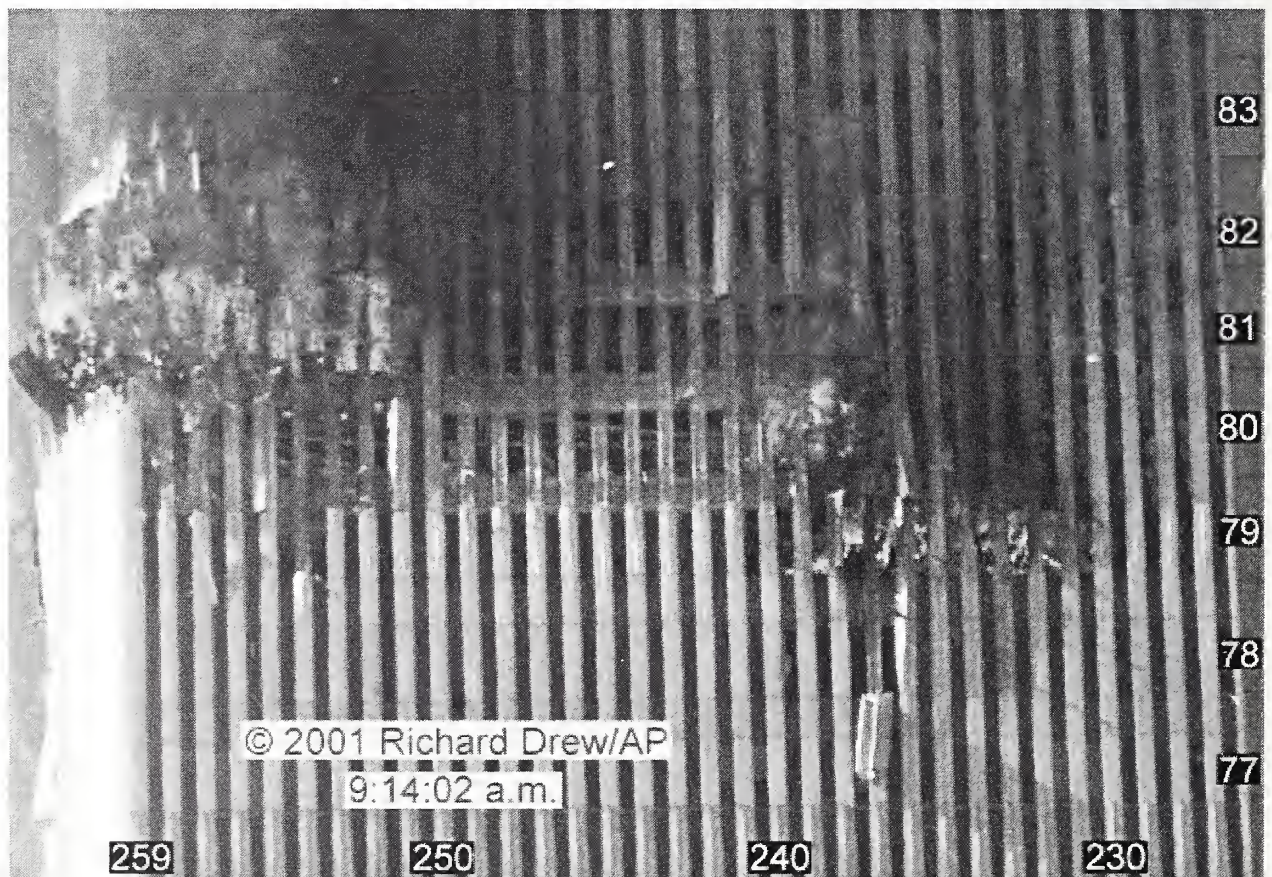
Figure 6-31. Upper layer temperatures of WTC 2, floor 80.

6.4.4 Floor 81, Case C

Floor 81 was notable primarily for the concentration of debris and fire in the northeast corner (Fig. 6–32). Fires were observed from the center of the east face to the northeast corner during the first 10 min, followed by steady burning mainly in that corner for the rest of the hour. There was little observed fire activity elsewhere on the floor, except for burning in the southeast corner initially, and spreading along the north face just prior to collapse.

To simulate the intense fires in the northeast corner (Fig. 6–33), a heavy concentration of combustibles was prescribed there under the assumption that the upper fuselage and right wing of the airplane plowed an appreciable amount of the combustible load of the east side of the floor into that corner. As expected, the predicted temperatures were highest in the northeast, with some fire activity predicted in the southwest (where none was observed) and some in the north central (where a light amount was observed).

Note that the abrupt change in temperature seen in the northeast corner in the temperature plots of Fig. 6–33 are due to a wall assumed in the floor plan. The coincidence of the wall and the observed window breakage for the first 30 min was merely fortuitous – the wall was put there based only on a rough sketch of the 81st floor by an occupant of the 80th. Nothing in the simulations explained the absence of fires just inside the ten window expanse on floors 80, 81, and 82 seen in the center of the photograph in Fig. 6–32. More discussion of this observation is in NIST NCSTAR 1-5A.



Note: The arrows point to hanging objects.

Figure 6–32. Northeast corner of WTC 2.

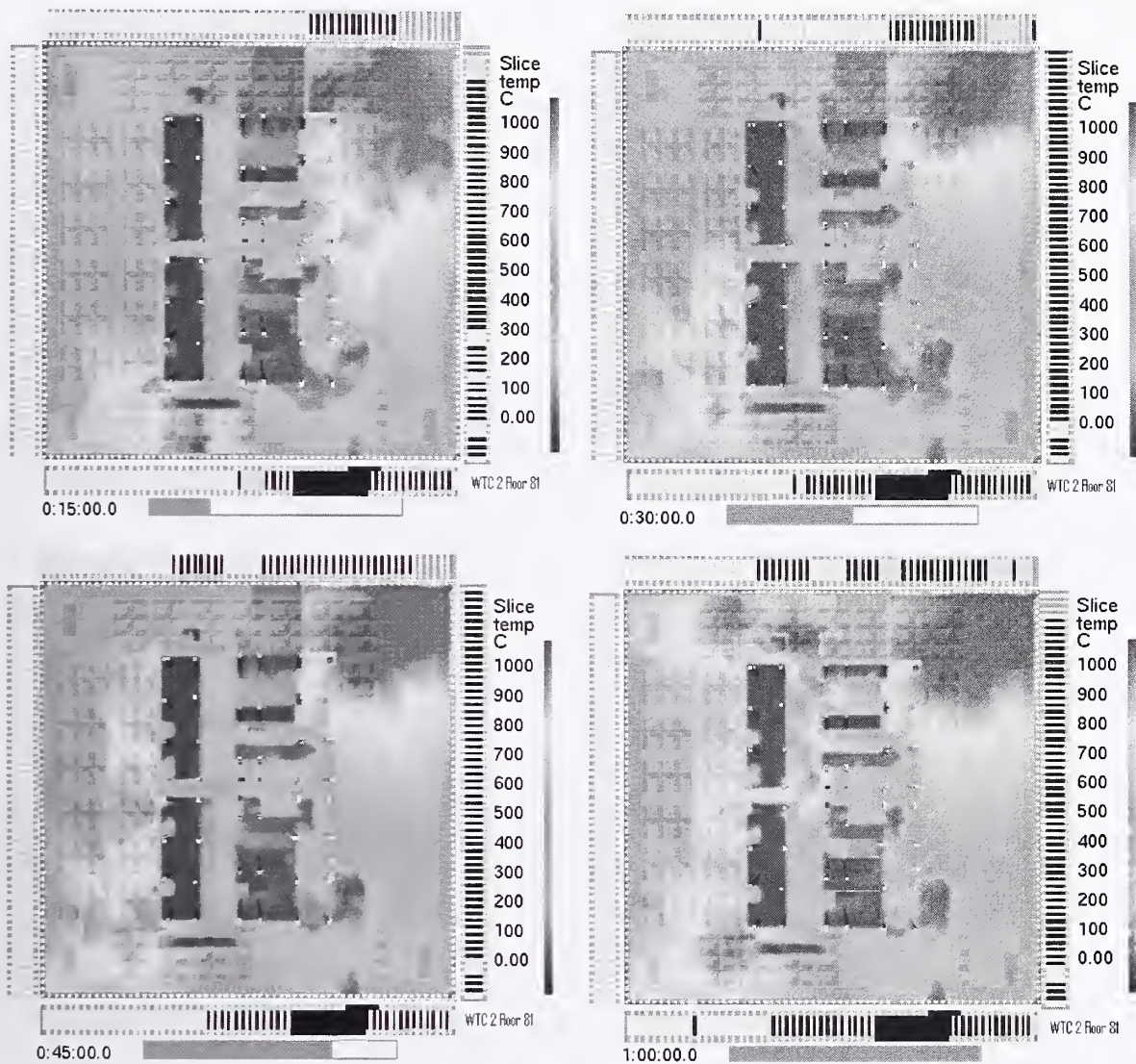


Figure 6-33. Upper layer temperatures of WTC 2, floor 81.

6.4.5 Floor 82, Case C

The 82nd floor was notable because upon impact a large fire ball emanated from its entire east face. After 10 min, fires were observed spreading from south to north along the east face, and burning continued throughout in the northeast corner, similar to the 81st floor. Figure 6–34 shows the south face, along with fire activity, in the southeast corner of the 82nd floor.

The simulated fires (Fig. 6–35) were similar to those of the 81st floor because of similar assumptions of combustible load, floor plan and initial jet fuel distribution.



Note: Fire at the right is on floor 82.

Figure 6–34. Impact area of south face of WTC 2.

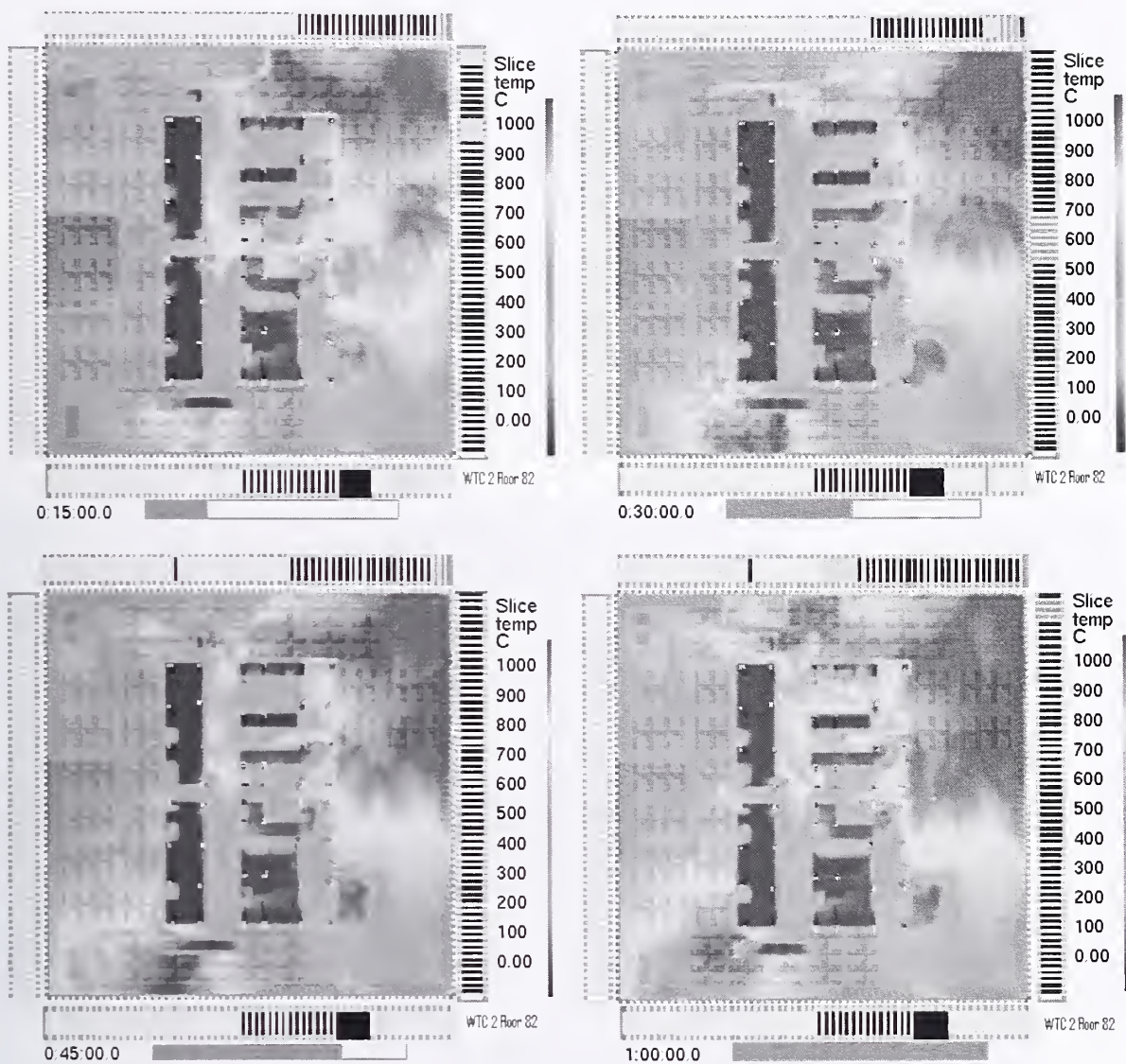


Figure 6-35. Upper layer temperatures of WTC 2, floor 82.

6.4.6 Floor 83, Case C

Floor 83 was impacted by the right wing of the airplane, and there was a modest amount of damage to the south side of the east face initially. The 83rd floor slab was also observed “sagging” along a considerable extent of the east face. Over the hour, the fire spread northward and then westward along the north face (Fig. 6–36).

This trend was captured in the simulation (Fig. 6–37), although the rate of spread was under-predicted. There was a barrier along the north side of the core that extended into the east part of the floor. There was no floor plan available, and this barrier was only a recollection by an occupant on the 80th floor. The barrier held the simulated fire back for about 15 extra minutes. Once the simulated fire moved around the barrier, it again followed the observed fire front as it moved toward the west side of the north face up until the time of collapse.

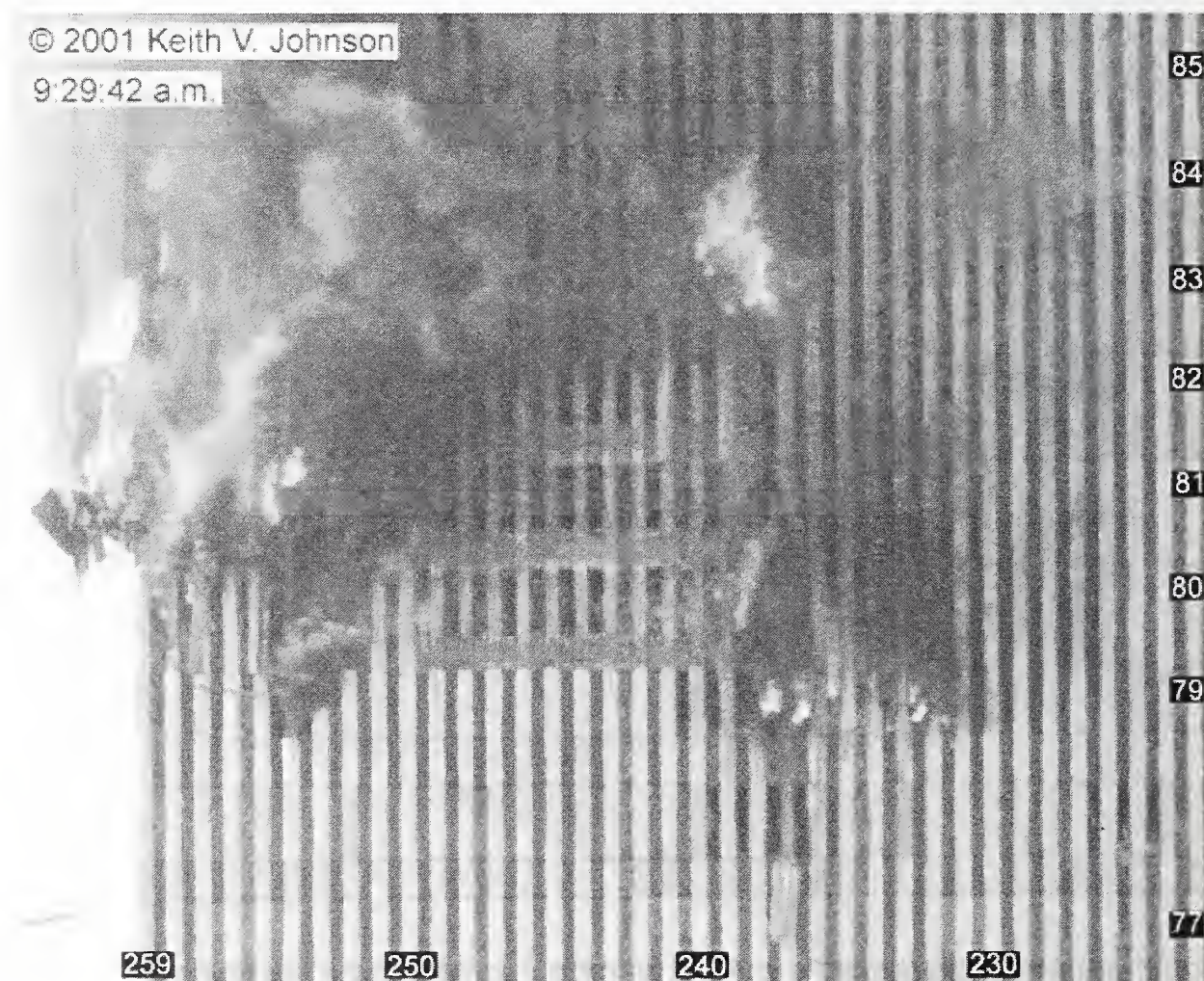


Figure 6–36. North face of WTC 2 at 9:29 a.m., 26 min after impact.

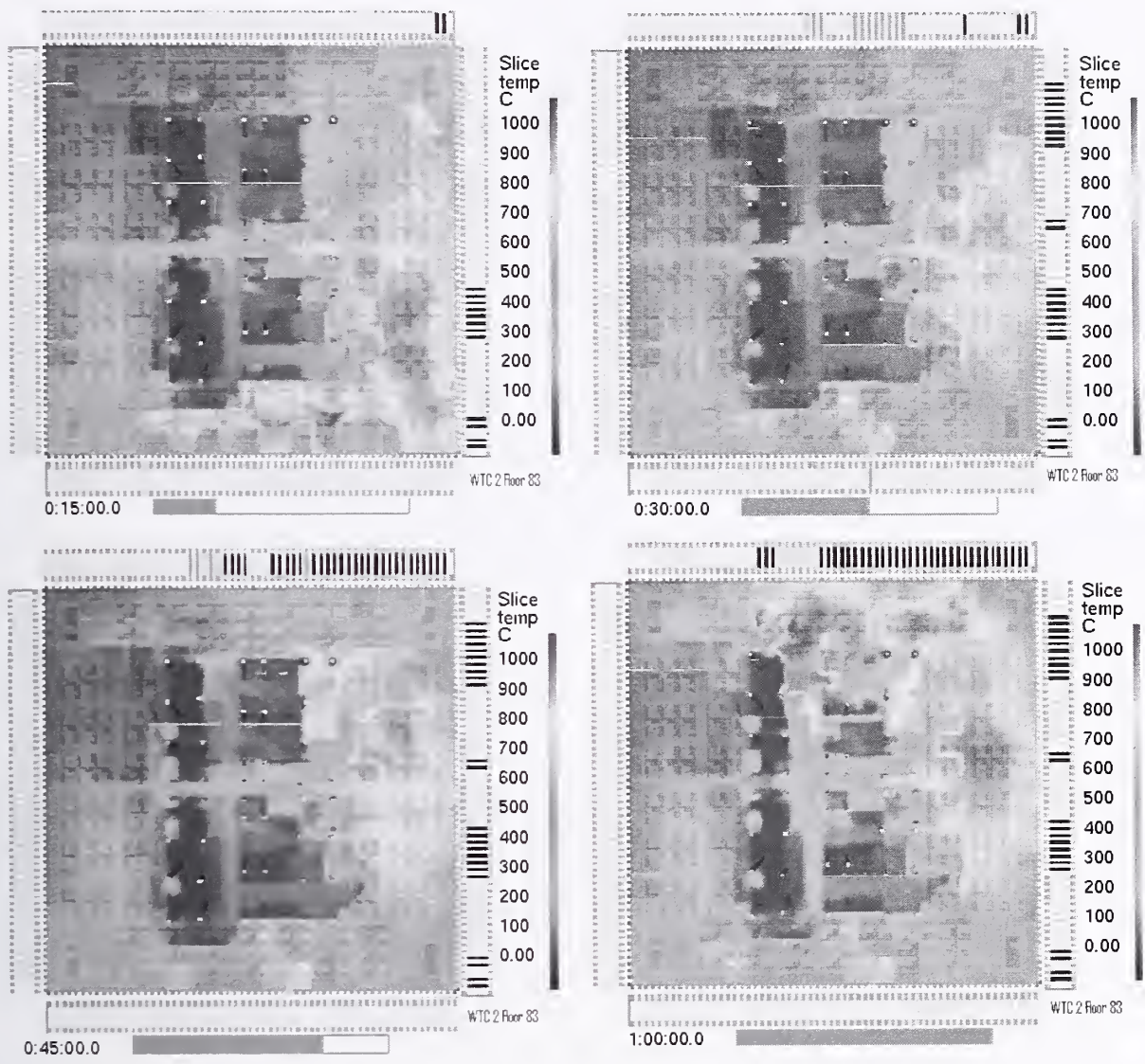


Figure 6-37. Upper layer temperatures of WTC 2, floor 83.

6.5 SIMULATION OF WTC 2, CASE D

Unlike WTC 1, the designated combustible load in WTC 2 had a noticeable effect on the outcome of the simulation. Because most of the windows on the impact floors were broken out by the airplane debris and the ensuing fireball, there was an adequate supply of air for the fires. In the Case D simulation of WTC 2, the combustible load was kept at 20 kg/m², the same as Case C, but the aircraft debris and “rubble” were spread out over a wider area. In Case C, the debris pile was concentrated in the northeast corner of the 80th, 81st, and 82nd floors, whereas in Case D, the pile was less concentrated. Also, in Case D, the furnishings away from the impact areas were assumed to be undamaged.

The Case D simulations of WTC 2 showed high temperatures extended over greater areas. The fires burning on the east side of WTC 2 were not believed to be oxygen-limited. A significant number of windows broke out on impact from floors 79 to 83, providing the fires with air. Increasing the burning rate of the furnishings, thus, led to increased fire activity and temperatures. The results shown on the following pages (Figs. 6–38 through 6–43) are, in some instances, significantly different than those of Case C, suggesting that the fires in WTC 2 were fuel, rather than oxygen, controlled.

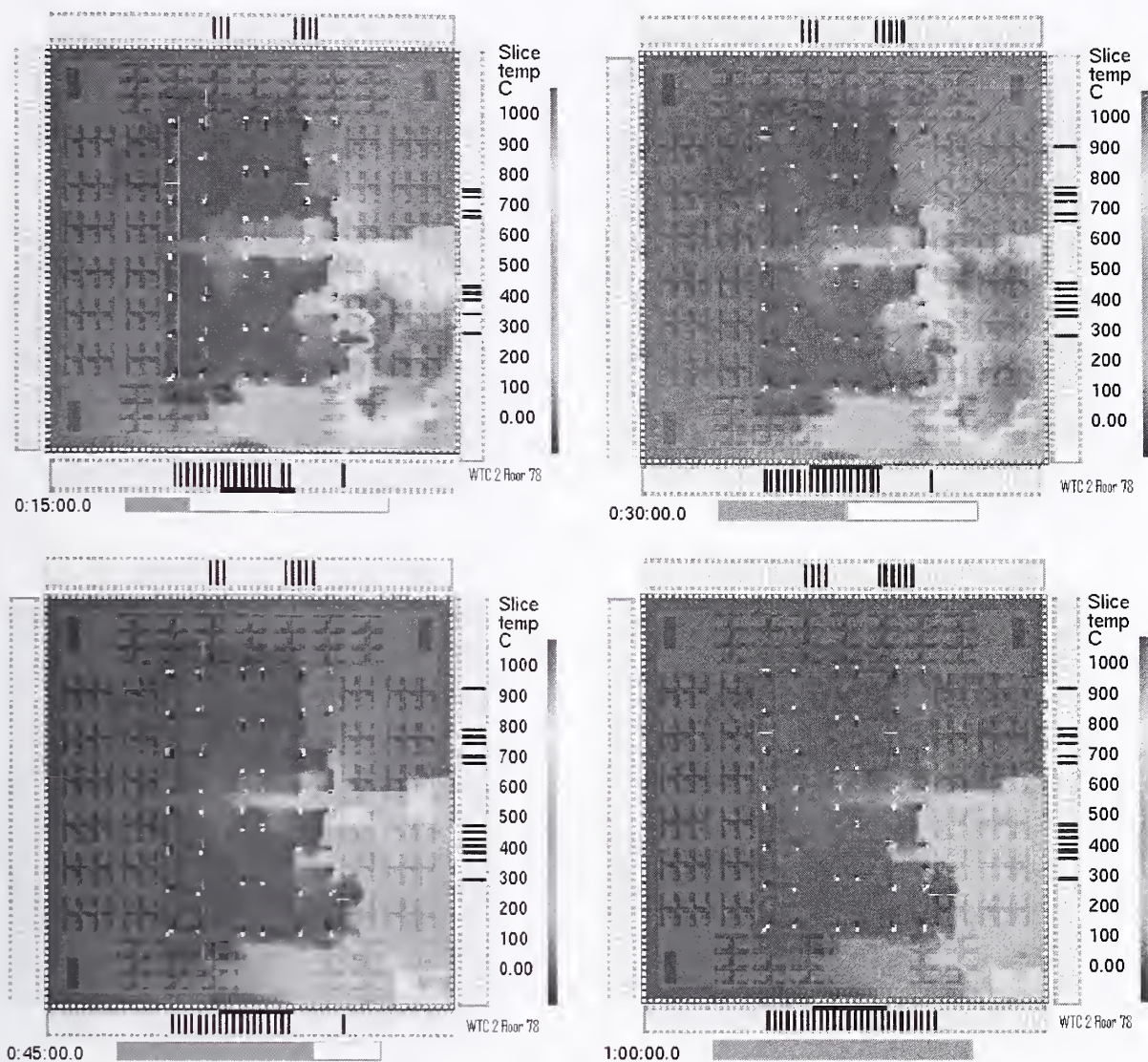


Figure 6–38. Simulation of WTC 2, floor 78, Case D, upper layer temperatures.

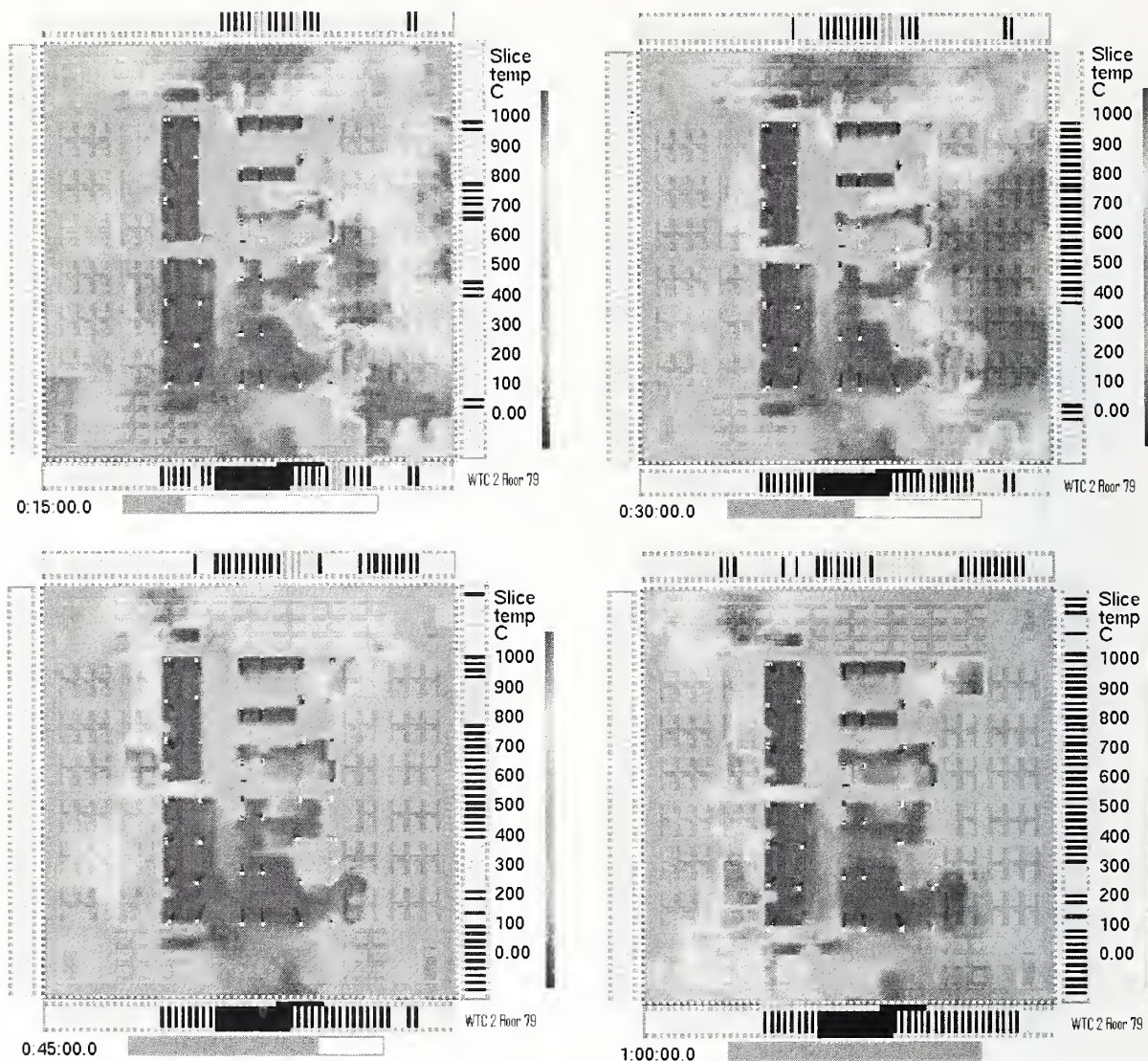


Figure 6–39. Simulation of WTC 2, floor 79, Case D, upper layer temperatures.

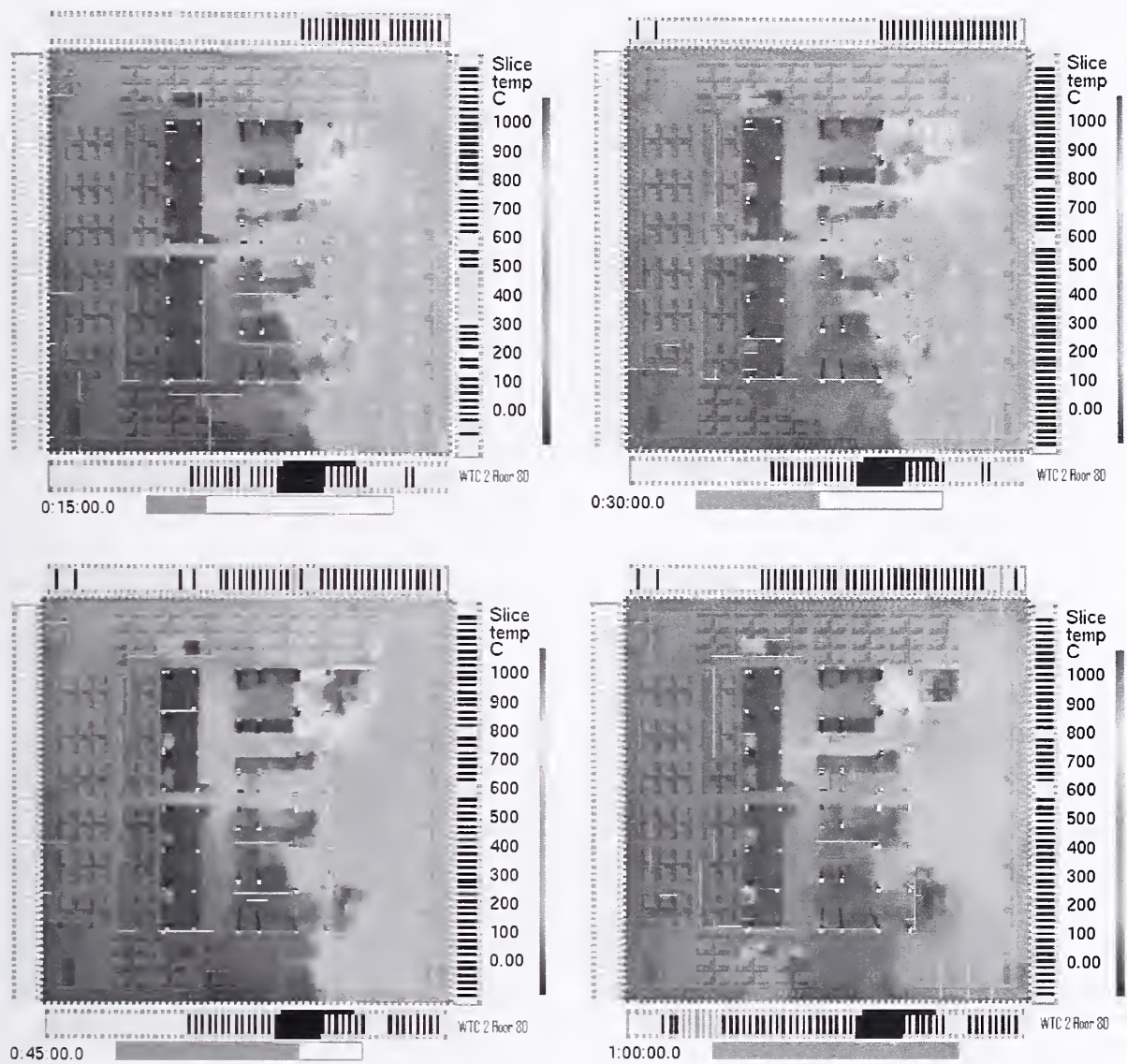


Figure 6-40. Simulation of WTC 2, floor 80, Case D, upper layer temperatures.

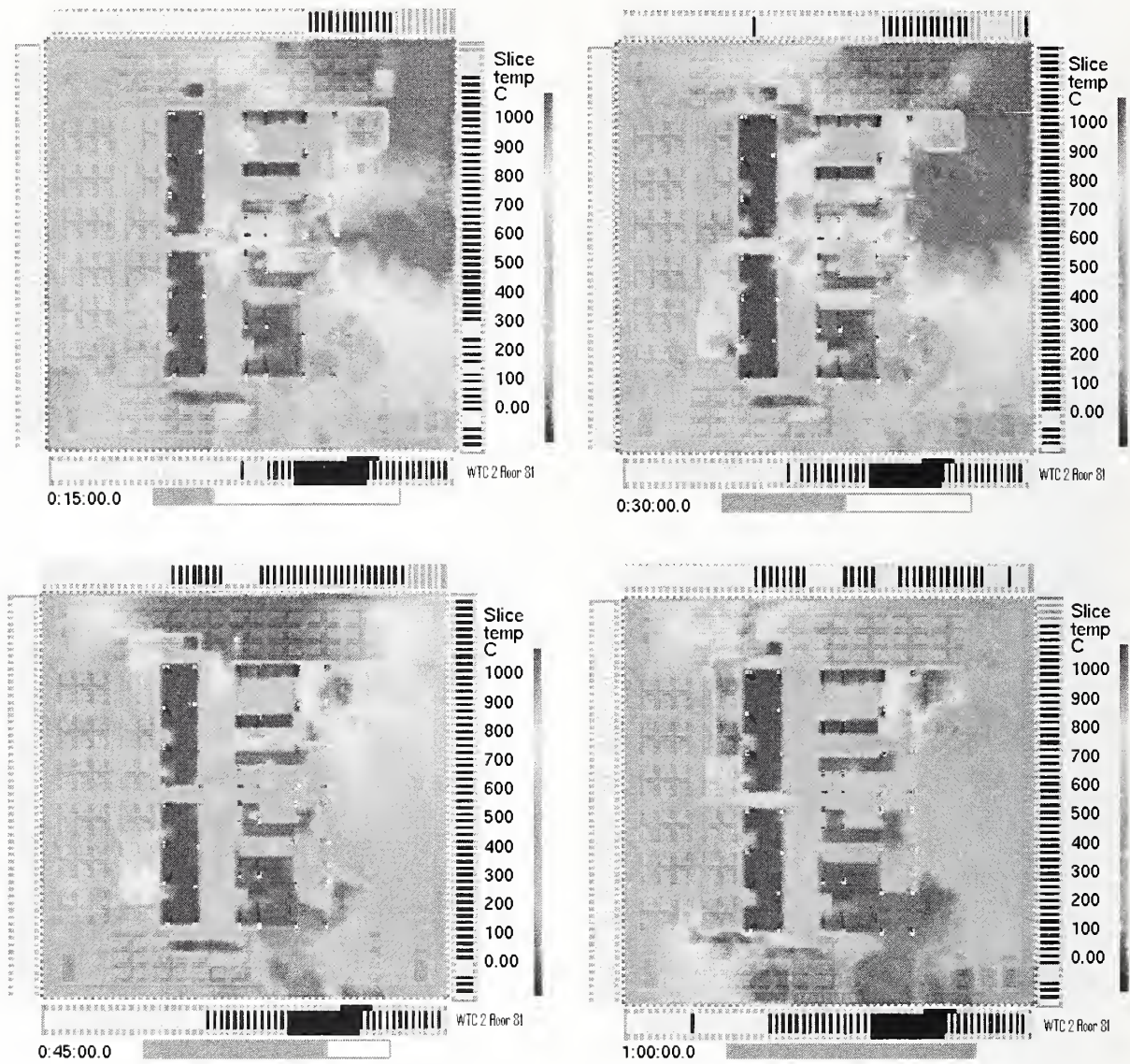


Figure 6-41. Simulation of WTC 2, floor 81, Case D, upper layer temperatures.

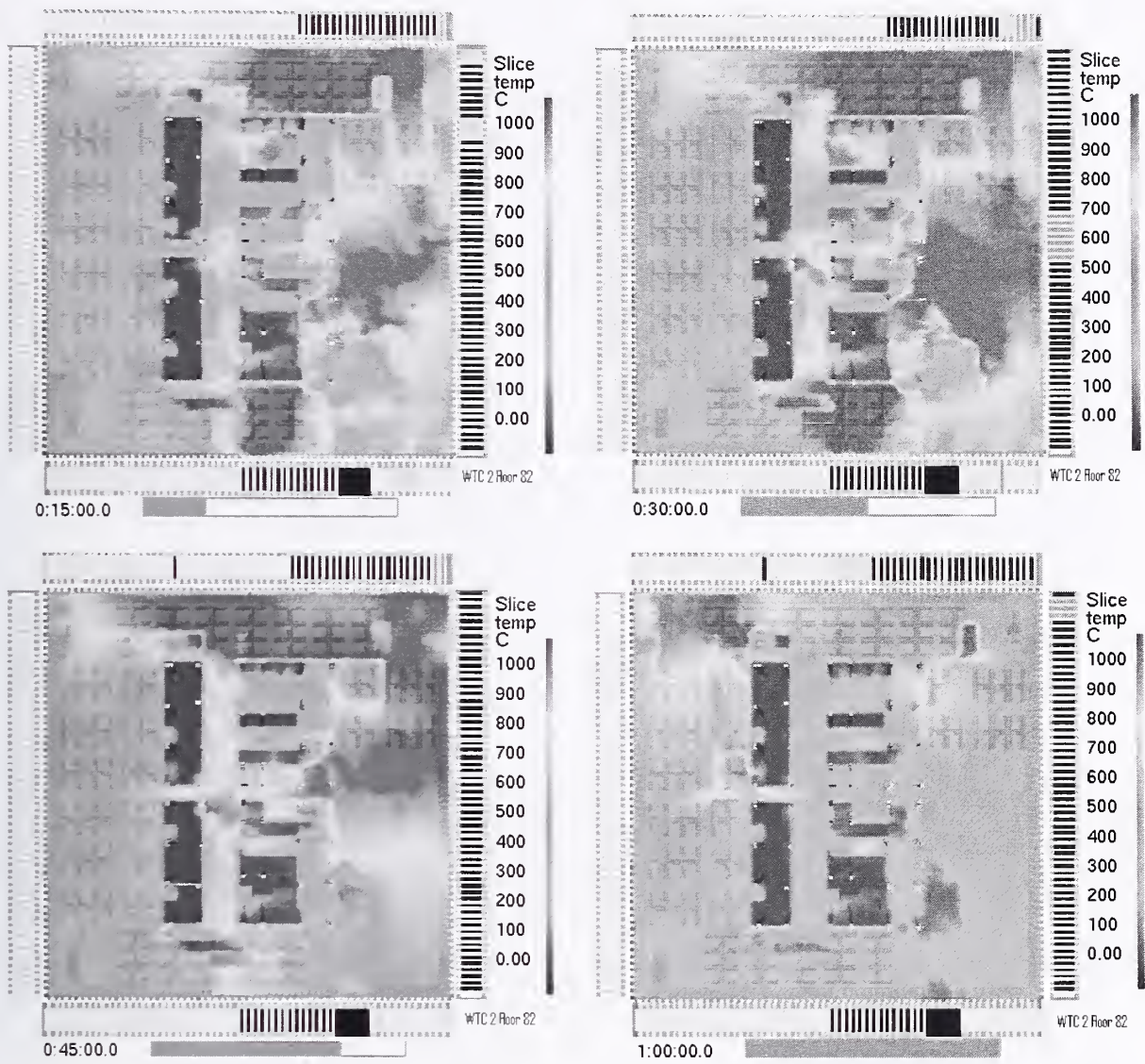


Figure 6-42. Simulation of WTC 2, floor 82, Case D, upper layer temperatures.

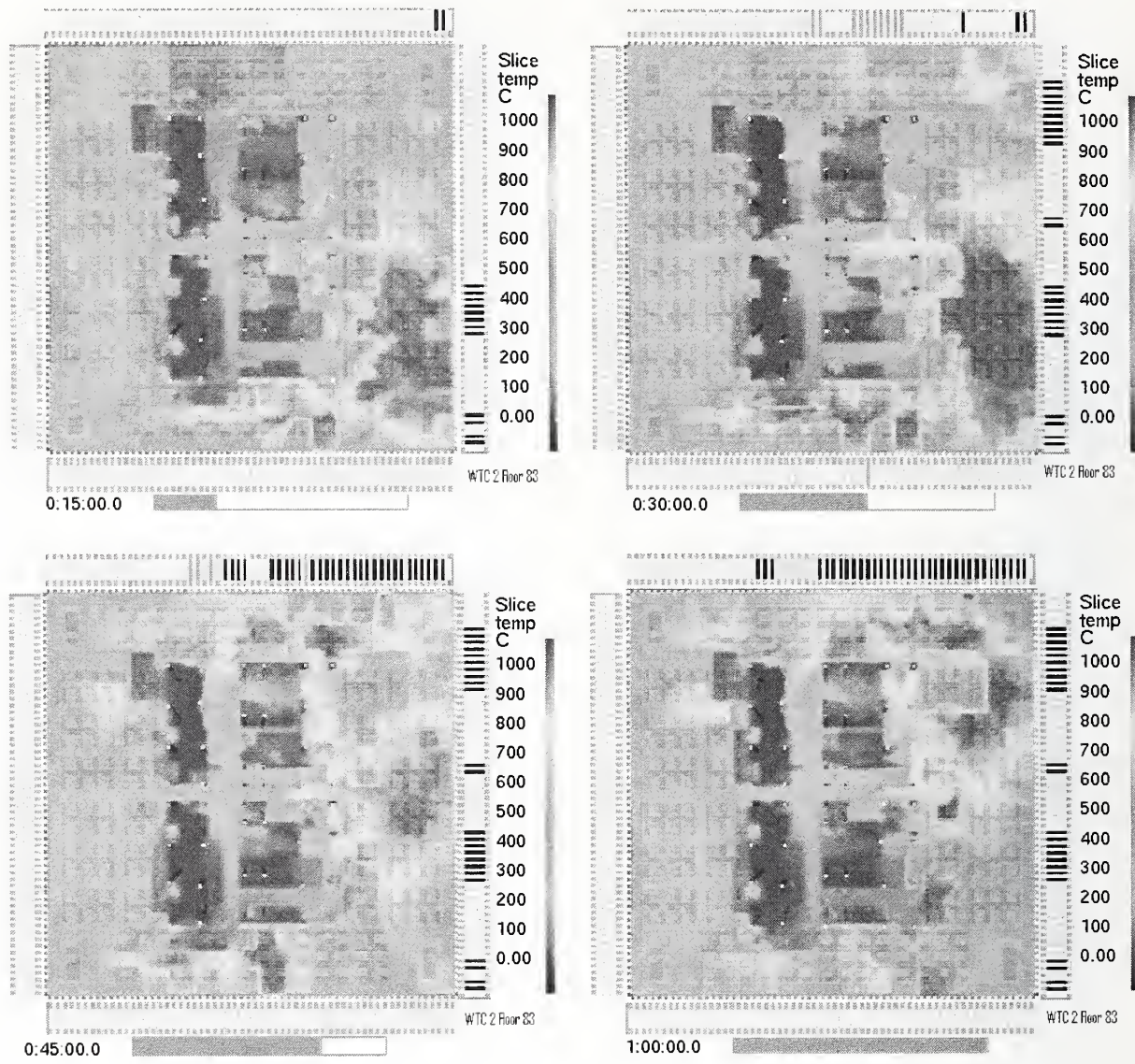


Figure 6-43. Simulation of WTC 2, floor 83, Case D, upper layer temperatures.

6.6 DISCUSSION

The purpose of the fire simulations presented in the previous sections was to recreate the thermal environment within WTC 1 and WTC 2 using the available information about the building contents and damage. The visual observations of the fire activity near the building exterior were the primary means of evaluating the accuracy of the numerical predictions. Although it was not possible to replicate all of the documented fire behavior (NIST NCSTAR 1-5A), the simulations captured the major trends of the fire activity in terms of spread and duration. In addition, the simulations produced estimates of the total heat release rate from the fires in both buildings. These estimates allow for some comparison of the two buildings and the nature of the fires within.

6.6.1 Fire Spread

In WTC 1, much of the fire activity was initially in the vicinity of the impact area in the north part of the building; then it spread around the east and west faces and was last observed to be concentrated in the south part of the building at the time of collapse. Figure 6-44 demonstrates the overall spread pattern of the fires, using the upper layer temperatures from an early and late time of the simulation for floors 94 and 97 of WTC 1 as an indication of the general path the fires followed from the north to the south part of the building. Figure 6-45 shows a photograph of the south face of WTC 1 shortly before collapse. In the photograph, intense fires can be seen on the 97th, 98th, and 99th floors in the southeast corner of the building. The same area had the least amount of damage caused by the airplane impact and remained free of fires for about 1 h. The simulations suggested that most of the combustible material in other areas of the impact floors was consumed during the course of 1 h to 1.5 h, with the furnishings in the southeast corner being the last to burn. The fact that the simulated fires encircled the building in roughly the same amount of time as the actual fires supported the estimate of the overall combustible load, 20 kg/m^2 (4 lb/ft^2). The simulated fires burned for roughly 20 min to 30 min in any one location, consistent with the visual evidence (NIST NCSTAR 1-5A) and the multiple workstation fire experiments performed at NIST (Chapter 4). Simulations performed with higher loads required a proportionately longer amount of time to bring the fires around to the southeast because the burn time was roughly proportional to the fuel mass in the oxygen-limited interior of the fire floors.

For WTC 2, it was more difficult to generalize the behavior of the fires. From the visual evidence, the fires did not appear to spread as rapidly nor burn as intensely as those in WTC 1. Because the airplane swept through a large expanse of the east side of the building, the fires were not as intense as would be expected along the east face, presumably because much of the furnishings were heavily damaged and a considerable mass was “plowed” into the northeast corner, where the fires burned most intensely for the entire hour before collapse. Whereas much of the fire behavior in WTC 1 could be characterized as “oxygen-controlled” or “oxygen-limited,” it appeared from the results of the simulations of WTC 2 that the fires there were controlled by the condition, mass and movement of the furnishings (fuel) more so than the availability of air (oxygen). To reproduce the observed behavior of the fires in WTC 2 required more speculation about the furnishings than was needed in WTC 1. The overall behavior of the fires in WTC 1 was relatively insensitive to the exact description of the furnishings, whereas, in WTC 2, the spread and duration of the fires in any given location was much more sensitive to the description of the combustibles.

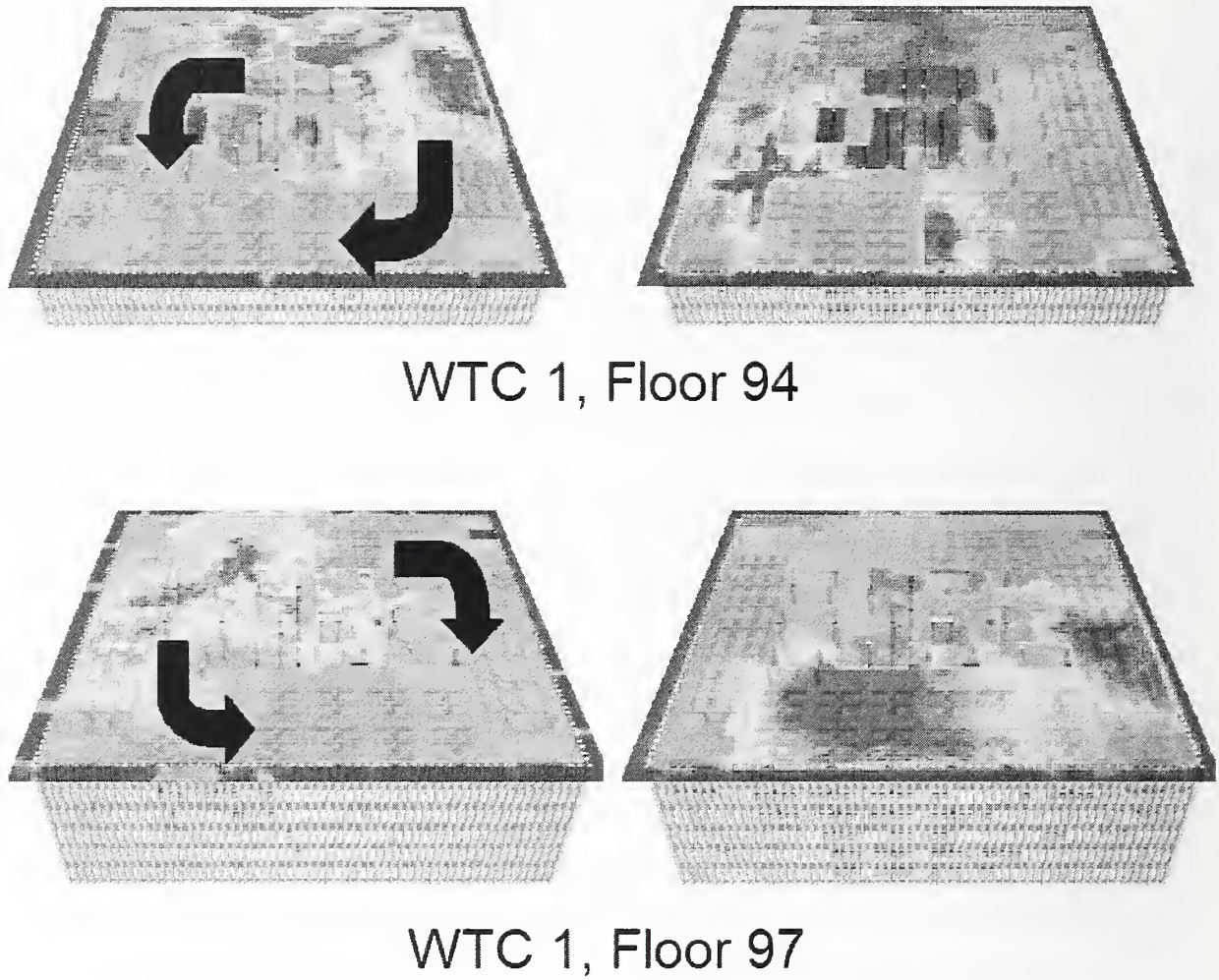


Figure 6–44. Simulated fire movement, floors 94 and 97, WTC 1.



Figure 6–45. Aerial view of the south face of WTC 1 shortly before collapse.

6.6.2 Fire Temperatures

It was clear from both the simulations and observations that the idea of computing some “average” gas temperature was not a satisfactory means of assessing the thermal environment of a building that was over 4,000 m² (1 acre) in plan. Not only would the assumption of an average temperature have been inconsistent with the visual evidence, but it would also have led to large errors in the subsequent thermal and structural analyses. The heat transferred to the structural components was largely by means of thermal radiation, a quantity that is roughly proportional to the fourth power of the gas temperature. It would not have been appropriate to assume that the thermal insult to the steel members was a function of the fourth power of the *average* temperature. The simulations and the visual evidence suggested that the duration of temperatures in the neighborhood of 1,000 °C at any given location on any given floor was about 15 min to 20 min. The rest of the time, temperatures were predicted to have been in the range of 400 °C to 800 °C on floors with active fires. To put this in perspective, the heat flux onto a truss surrounded by smoke-laden gases of 1,000 °C is approximately 150 kW/m², whereas it is 20 kW/m² for gases of 500 °C.

Figure 6–46 presents several time histories of the predicted upper layer gas temperature (Case A) on the 97th floor of WTC 1, along with two standard time-temperature curves, ASTM E119 (ASTM 2002) and UL 1709, referred to as the “Rapid-Rise Fire” (UL 1994). At each location, the predicted temperature peaked between 1,000 °C and 1,200 °C for periods of about 15 to 20 min, characteristic of intense fire activity. Neither the steady 1,100 °C “Rapid-Rise” curve, nor the gradually rising E119 curve are characteristic of the temperatures at any of these locations over the course of the 100 min.

In the past ten years, some experiments and modeling have been used to study the fire behavior in large, open-plan spaces. The results have brought into question the application of simple empirical rules to assess the burning rates within fully-engulfed compartments. It is often assumed that the burning rate within a compartment is controlled by a “ventilation factor,” $A\sqrt{h}$, where A is the area of the opening to the compartment, and h is the height of the opening. This correlation was developed using the results of numerous fire experiments in compartments representing single offices or rooms within houses. However, Thomas and Bennetts (2000) performed experiments in small scale compartments whose width to depth ratios were more typical of large open-plan office buildings. *Qualitatively*, the fire behavior they observed was similar to that of WTC 1 and WTC 2. The fires tended to move relatively quickly toward ventilation openings, remained there as long as the local fuel supply was adequate, and then moved steadily through the floors, consuming the remaining fuel along the way. The overall heat release rate was dependent on the geometry of the floors as well as the area and height of the openings. Thus, the simple $A\sqrt{h}$ dependence was not sufficient to predict the burning rate in long and/or wide enclosures.

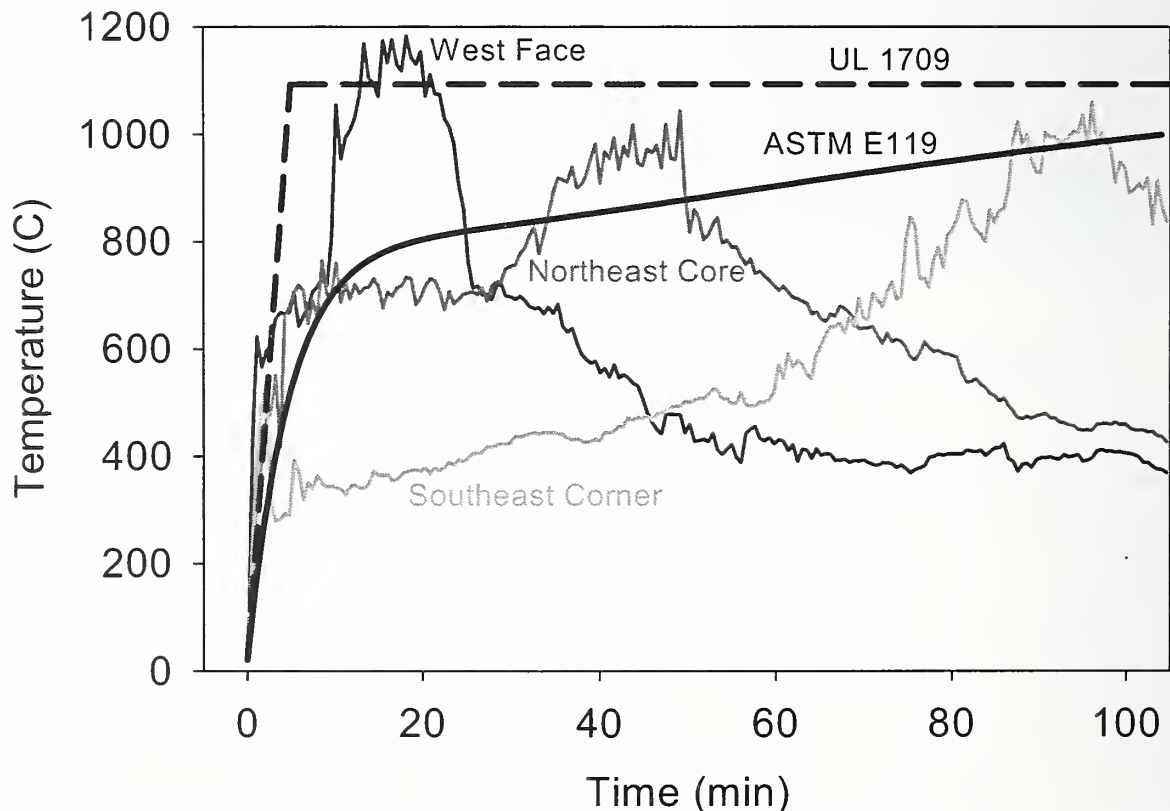


Figure 6–46. Predicted upper layer temperatures at various locations on the 97th floor.

6.6.3 Global Heat Release Rates

A very useful assessment of the fires in WTC 1 and WTC 2 came from the predictions of the total heat release rates (HRR). Preliminary estimates by Rehm et al. (2002) were between 1 GW and 1.5 GW for each tower. Shown in Fig. 6-47 are the heat release rates for the fires in WTC 1 and WTC 2. The rates were consistent with the preliminary estimates. The difference between the predicted HRR for WTC 1 and WTC 2 was another indication that the fires in WTC 1 were more extensive than those in WTC 2. The predicted HRR in WTC 1 was about 2 GW for the first 30 min, decreasing steadily to about 0.5 GW after 1 h 40 min. There was only a small change in the overall HRR as a result of the Case A and B parameter changes, consistent with the observation that the fires in WTC 1 were oxygen-controlled, and changes to the combustible load made little difference on the results.

The predicted HRR in WTC 2 was about half that of WTC 1, about 0.5 to 1 GW, depending on the choice of combustible loading/condition. For WTC 2, the increased burning rate of Case D did lead to a noticeably higher total HRR, consistent with the characterization of the WTC 2 fires as fuel-controlled.

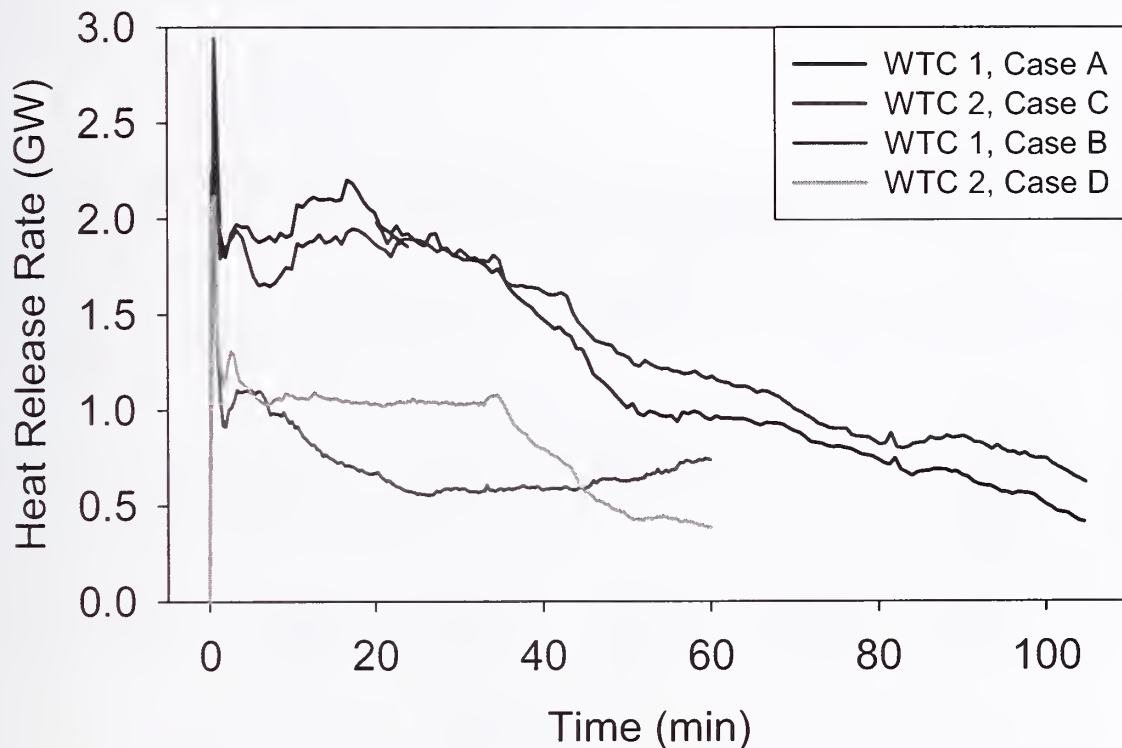


Figure 6-47. Predicted heat release rates for fires in WTC 1 and WTC 2.

Another useful result of the fire simulations was the global “energy budget.” Heat generated by a building fire will either flow out of the building via a smoke plume, or it will heat up the walls, ceilings, structural elements, etc. Figure 6–48 shows how the predicted HRR for WTC 1, Case A, could be decomposed into its convective and conductive components. The Conductive Loss was the rate at which energy was consumed heating up the building elements, while the Convective Loss was the rate at which energy flowed out the windows or up the vertical shafts to floors not included in the simulation. Initially, the Conductive Loss accounted for about two-thirds of the energy losses, and by the end of the simulation it only accounted for about one-third. As the building heated up, it absorbed less energy from the fire.

The energy budget emphasized the fact that the large width to height ratio of the floors within the towers meant that a substantial amount of the fires’ energy was absorbed by the buildings’ structural and non-structural components. In contrast, less of the energy was carried away by the smoke plume than would be expected from a fire in a more typical office or residential setting. Some refer to this effect as “energy trapping,” and it was an important consideration in the modeling. Indeed, the need for sophisticated modeling is partly justified by the difficulty in describing the global energy budget with conventional analytical or empirical techniques.

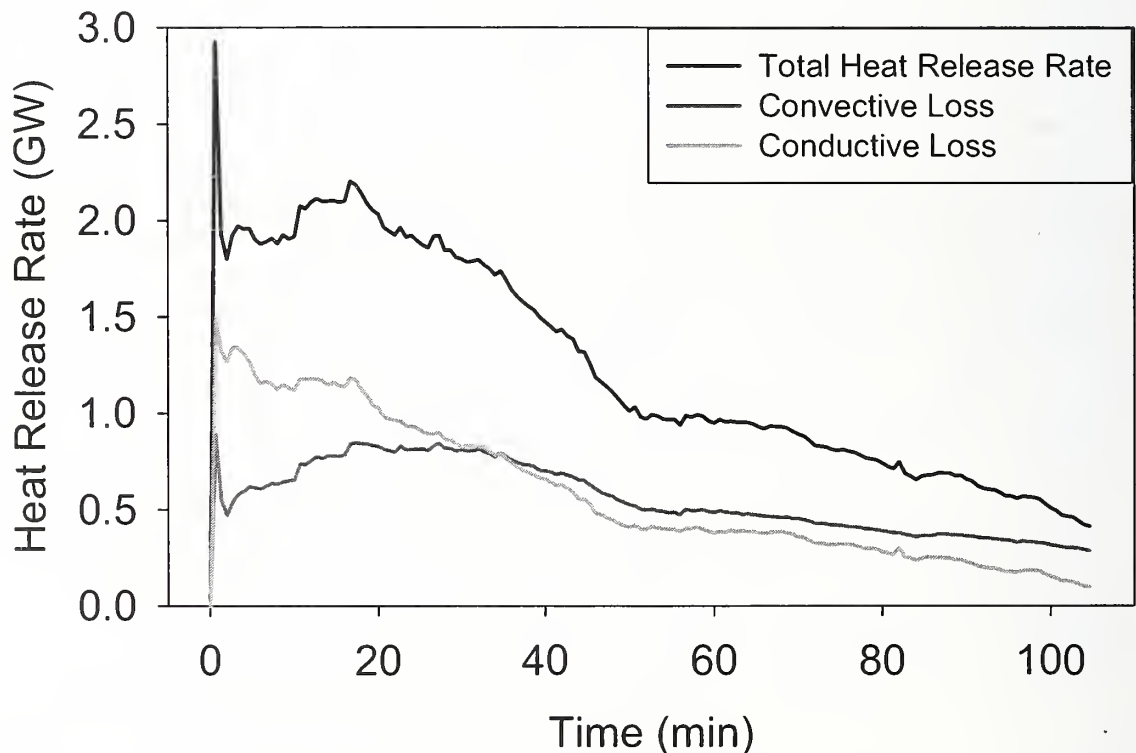


Figure 6–48. Energy budget for WTC 1 fire simulation, Case A.

6.7 DATA TRANSFER

The results of the simulations presented in this chapter were used in detailed calculations of the temperature histories of the structural components. The data from the FDS were processed and used as boundary conditions for the finite-element calculation of the structural temperatures. This process was termed the FSI (NIST NCSTAR 1-5G). Four quantities were transferred from FDS: the upper and lower layer gas temperatures, the depth of the smoke layer, and the absorption coefficient of the smoke layer. The upper layer gas temperatures were pictured in this chapter. The temperatures were time-averaged over 100 s and spatially-averaged over 1 m. The upper layer gas temperatures were taken 0.4 m (one grid cell) below the ceiling. The lower layer temperatures were taken 0.4 m above the floor. The absorption coefficient was taken 0.4 m below the ceiling. The depth of the smoke layer was estimated from the vertical temperature profile using a simple algorithm that is described in the FDS User's Guide.

All of the simulations described in this chapter were carried out for the time period between airplane impact and building collapse. However, one simulation (the more severe fire in WTC 2, or Case D) was extended two hours beyond the one hour that was presented above. The intent of this calculation was to allow the fires on the six floors under consideration to completely burn all of the specified furnishings, after which an assessment could be made of the peak temperatures in all of the major structural members. Details can be found in NIST NCSTAR 1-5G.

6.8 REFERENCES

- ASTM E 119. 2002. "Standard Test Methods for Fire Tests of Building Construction and Materials," American Society for Testing and Materials, West Conshohocken, PA.
- Rehm, R.G., W.A. Pitts, H.R. Baum, D.D. Evans, K. Prasad, K.B. McGrattan and G.P. Forney. 2002. *Initial Model for Fires in the World Trade Center*. NISTIR 6879. National Institute of Standards and Technology, Gaithersburg, MD, May.
- Thomas, I.R. and I.D. Bennetts. 2000. Fires in Enclosures with Single Ventilation Openings – Comparison of Long and Wide Enclosures. *Fire Safety Science – Proceedings of the Sixth International Symposium*. International Association for Fire Safety Science. University of Poitiers, France, July 5-9, 1999.
- UL 1709. 1994. "Standard for Rapid-Rise Fire Tests of Protection Materials for Structural Steel," Underwriters Laboratories, Northbrook, IL.

This page intentionally left blank.

Chapter 7

SUMMARY OF TECHNICAL RESULTS

The simulations of the fires in the World Trade Center (WTC) were part of a larger analysis that included the airplane impacts into WTC 1 and WTC 2, the subsequent fires, the heating of the structural elements, and the eventual collapse. The scale of these calculations and the interchange of information between them were unprecedented. Of concern from the outset was the propagation of uncertainty from one model to the next. The number of columns severed in the initial impacts, the temperature of the fires, the thickness of the thermal insulation on the columns and trusses, the strength of thousands of connections – each model passed along its uncertainties to the next. To increase the confidence in the fire simulations, the following steps were taken:

1. The National Institute of Standards and Technology (NIST) Fire Dynamics Simulator, a computational fluid dynamics model specifically designed for fire simulation, was made more powerful by making it run on multiple computers. With as many as 48 processors, calculations that would have required weeks were reduced to a few days. This allowed for dozens of full-scale, full-length calculations, plus hundreds of smaller, shorter calculations, to be performed to assess the sensitivity of the input parameters.
2. Large scale validation experiments were performed to test the accuracy of the model in predicting heat and smoke transport from controlled fires and the burning rate of real furnishings in an oxygen-limited environment. In the latter tests, conditions very similar to those in WTC 1 and WTC 2 were reproduced in the laboratory, and the model was shown to predict both the burning rate of the furnishings and the overall conditions within the test compartment.
3. Simulations of the fires in WTC 1 and WTC 2 were performed using as input the time history of window breakage, which was accurate to within 4 min. The importance of this information in the calculations cannot be over-stressed. The movement of the fires within the buildings would have been virtually impossible to predict were it not for the fact that a trail of broken windows was left in their wake. These broken windows were the pathways for air to reach the fires, an effect that was captured by the model. In essence, the observed pattern of window breakage guided the simulated fires to follow roughly the same path as the real fires.
4. In addition to the fire movement, the overall duration of fire on any given floor was matched in the simulations, owing mainly to the estimates made of the overall combustible load. In an oxygen-limited environment, the burn time is roughly proportional to the mass of fuel available.

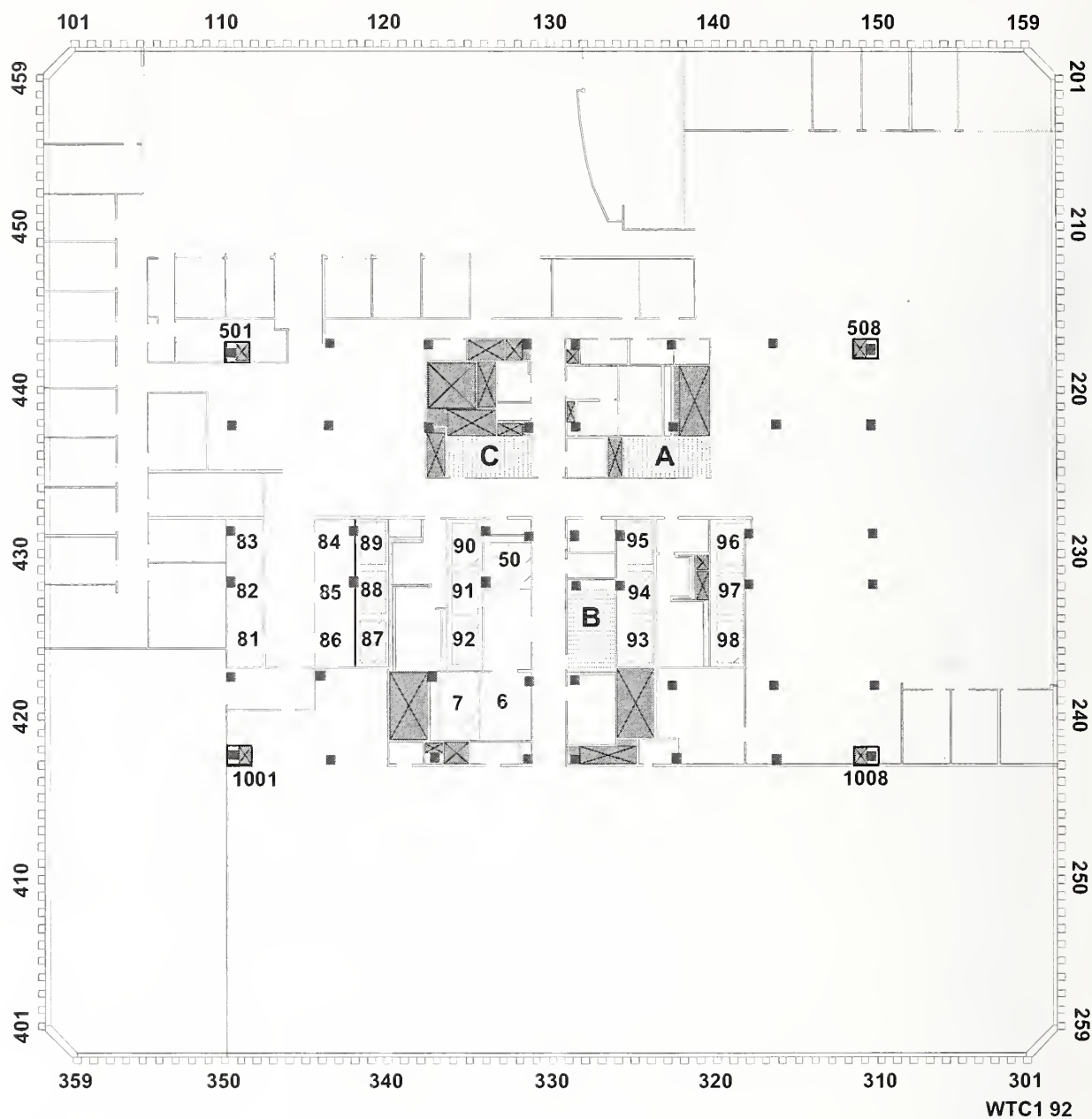
The simulated fires followed the same general paths, burned for about the same length of time, and as evidenced by the validation experiments, generated comparable temperatures to those of the real fires. This conclusion is not based on a single set of calculations, but rather on dozens performed during the second year of the two year Investigation. Certainly there were differences in the results as various parameters were exercised, but the overall patterns emerged again and again owing to the fact that fire, while appearing unpredictable and random, does obey the laws of physics that are codified within the numerical model.

APPENDIX A

FLOOR PLANS

The following pages contain the architectural plans for floors 92 through 99 of WTC 1 and 78 through 82 of WTC 2. The plans for WTC 1 were provided by Marsh & McLennan, and the drawings shown here are electronic renderings of the original plans. Only the 78th floor plan was available for WTC 2. The basic layout from the 78th floor was used for the higher floors with adjustments made to the elevators, vents and major partitions based on recollections of floor occupants.

In Figures A-1 through A-13, green lines denote glass partitions, red stripes denote stairwells, grayish-blue shading denotes ventilation ducts, yellow, pink and blue diagonal stripes denote elevators. The numbers 501, 508, 1001, and 1008 denote core columns (red squares). The numbers 101-159, 201-259, 301-359, and 401-459 denote exterior columns. The letters A, B, and C denote the major stairwells.



Note: North is at the top of the page.

Figure A-1. Floor plan of 92nd floor, WTC 1.



Note: North is at the top of the page.

Figure A-2. Floor plan of 93rd floor, WTC 1.



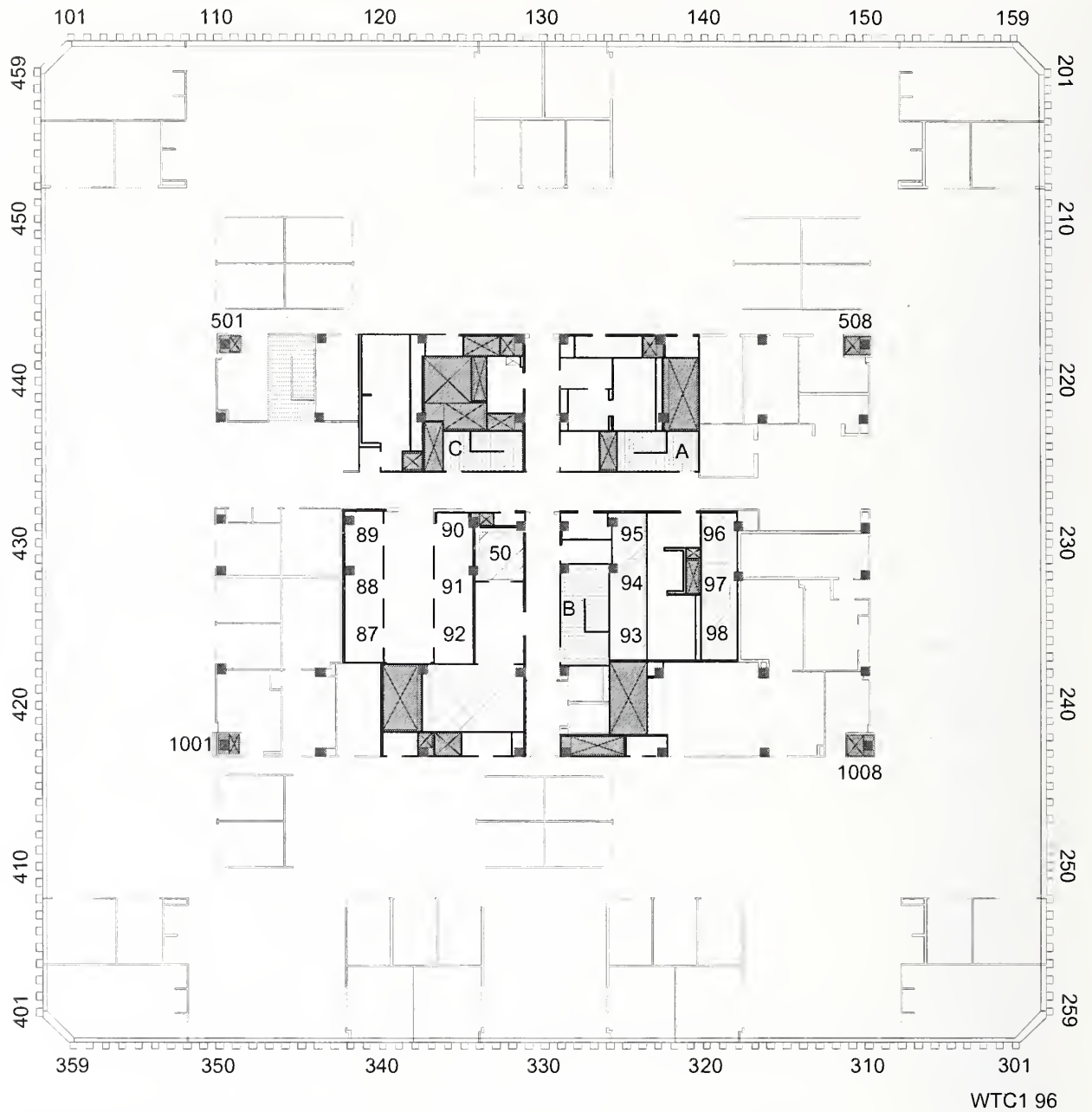
Note: North is at the top of the page.

Figure A-3. Floor plan of 94th floor, WTC 1.



Note: North is at the top of the page.

Figure A-4. Floor plan of 95th floor, WTC 1.



Note: North is at the top of the page.

Figure A-5. Floor plan of 96th floor, WTC 1.



Note: North is at the top of the page.

Figure A-6. Floor plan of 97th floor, WTC 1.



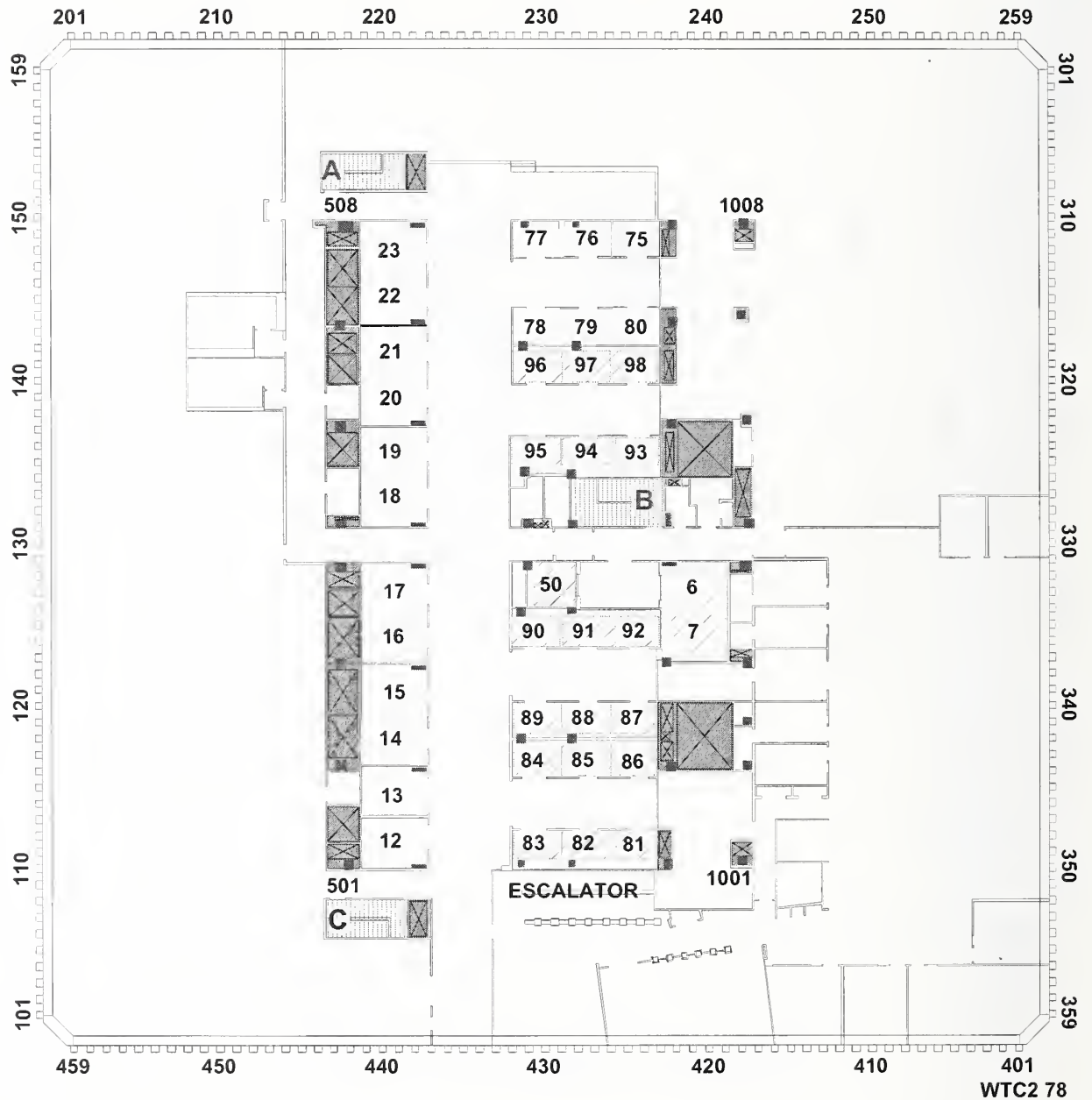
Note: North is at the top of the page.

Figure A-7. Floor plan of 98th floor, WTC 1.



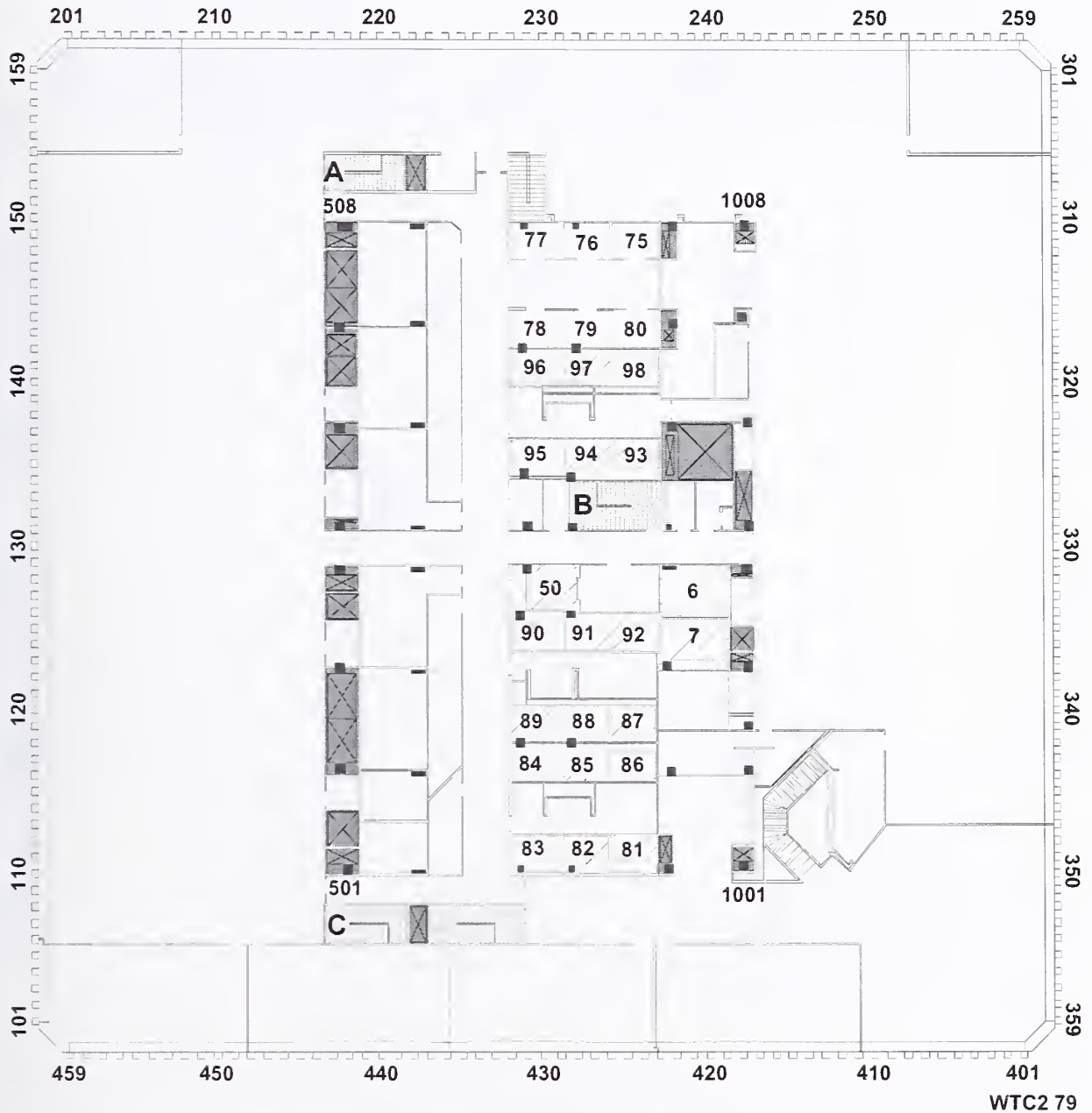
Note: North is at the top of the page.

Figure A-8. Floor plan of 99th floor, WTC 1.



Note: North is at the top of the page.

Figure A-9. Floor plan of 78th floor, WTC 2.



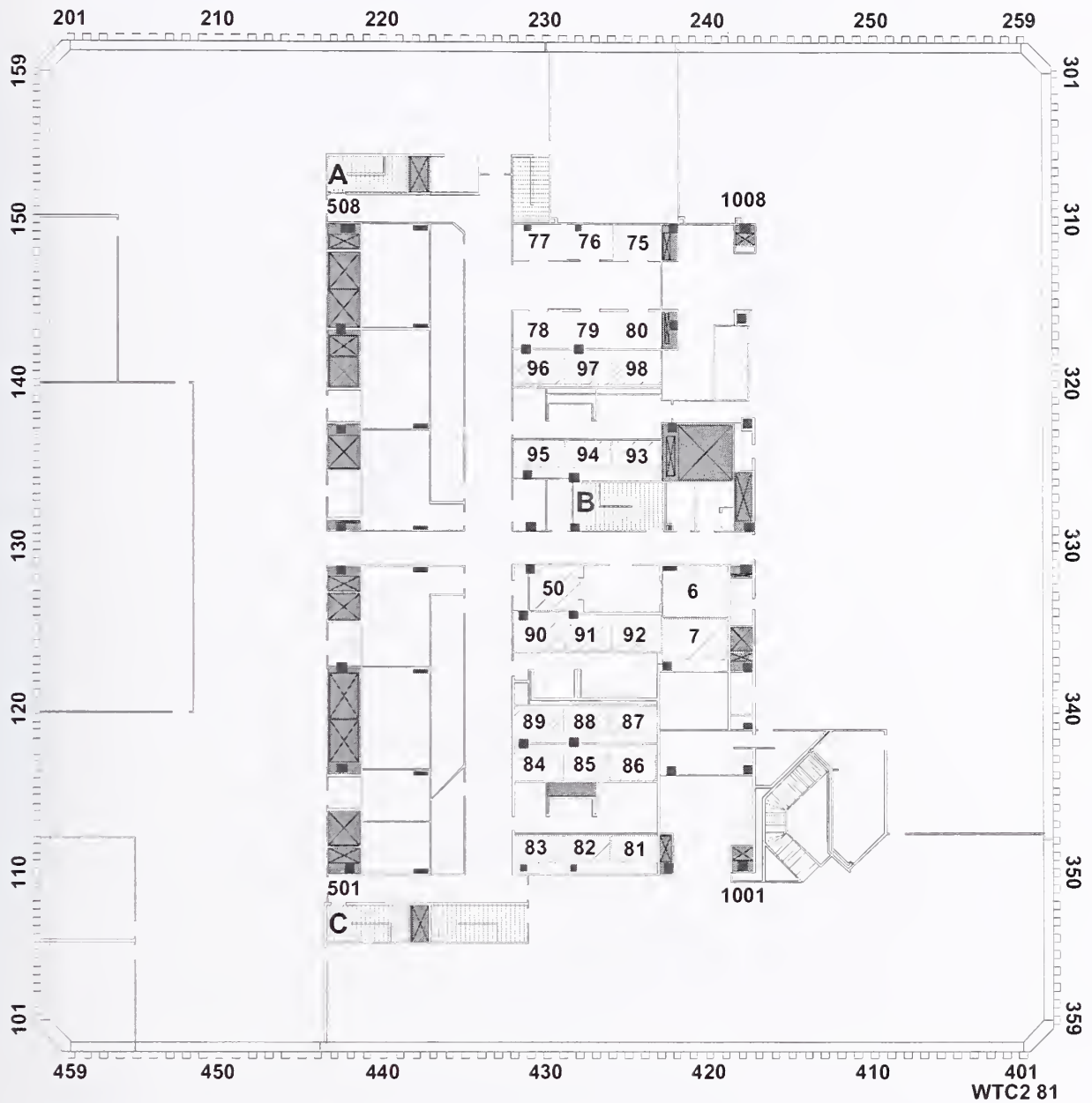
Note: North is at the top of the page.

Figure A-10. Floor plan of 79th floor, WTC 2.



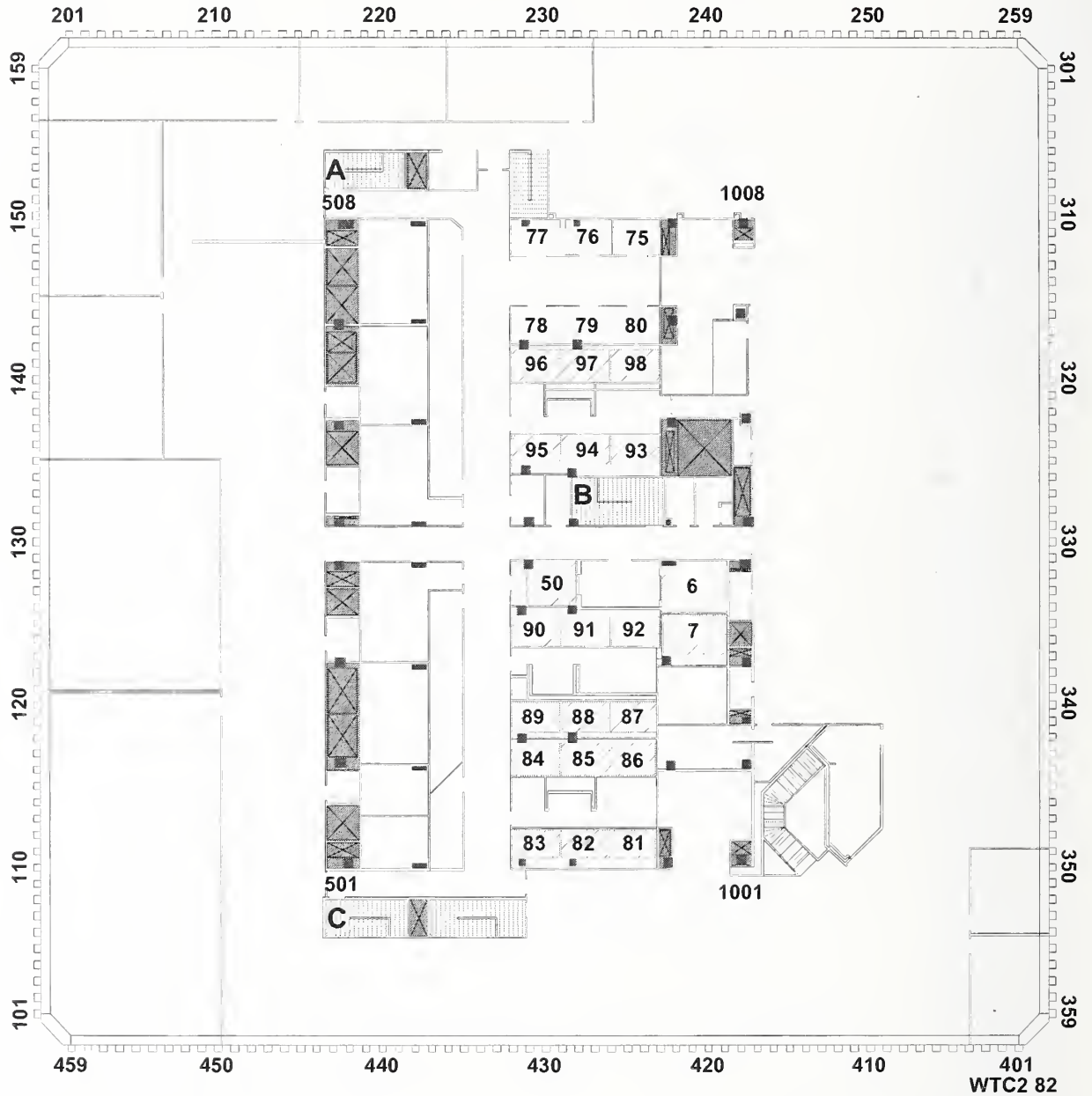
Note: North is at the top of the page.

Figure A-11. Floor plan of 80th floor, WTC 2.



Note: North is at the top of the page.

Figure A-12. Floor plan of 81st floor, WTC 2.



Note: The 83rd floor is assumed to be the same.

Figure A-13. Floor plan of 82nd floor, WTC 2.

